Imidazolium salts as convenient precursors to novel metal-carbene complexes

Richards, Stephen Paul

Award date:
2004

Awarding institution:
University of Bath

IMIDAZOLIUM SALTS AS CONVENIENT PRECURSORS TO NOVEL METAL-CARBENE COMPLEXES

Stephen Paul Richards

A thesis submitted for the degree of
Doctor of Philosophy

University of Bath
Department of Chemistry
September 2004

S.P. Richards

ProQuest LLC
789 East Eisenhower Parkway
P.O. Box 1346
Ann Arbor, MI 48106-1346

Acknowledgements

Firstly, I would like to thank Prof. Matthew Davidson and Dr Michael Whittlesey for all their guidance, assistance and support; and for giving me the opportunity to undertake this project. I would also like to acknowledge all the encouragement and understanding afforded me by Prof. Davidson, and thank him for his patience and for going out of his way to make writing this thesis as easy as possible.

I would also like to thank Dr Andrew Johnson for all his help, for performing the majority of the x-ray diffraction experiments discussed herein, and for being there to oversee my efforts in the laboratory. I must also acknowledge Prof. Davidson, Dr Mary Mahon and Cheryl Doherty for conducting x-ray diffraction experiments on my behalf. I would also like to thank Dr Steven Black, Jose Goicoechea, Dr Randolf Kohn, Rudolphe Jazzar and Dr Michael Whittlesey for all their help with NMR spectroscopy. I must thank Marie Brown, Gillian Eade and Prof. Matthew Davidson for all their assistance with the Gel Permeation Chromatography of the poly(caprolactone) samples. Chris Cryer is thanked for his Mass Spectrometry.

I would like to thank all the members of the Davidson and Whittlesey Research Groups past and present. Special mention must go to John Cowan, Sarah Lamb and Richard Price whose work provided the inspiration for much of the research conducted during the course of my studies. I am grateful to everyone within the Department of Chemistry who has made my time here so enjoyable. Thanks to all the people who have let me live with them over the years. I would also like to extend my thanks to Dr Mark Russell for his help with my computing problems.

I would like to thank all my family and friends in Cornwall, and indeed wherever, for their encouragement and support. I thank the University of Bath for funding my course of study.

Summary

Historically the *in situ* deprotonation of imidazolium salts by metallic reagents has represented a useful pathway to metal-*N*-heterocyclic carbene species. This thesis sets out to evaluate the extension of this well-documented synthetic methodology to the preparation of novel and catalytically relevant metal-*N*-heterocyclic carbene complexes from non-conventional imidazolium precursor salts.

Interesting hydrogen-bonding interactions arise in the products from the reaction of a strongly basic imidazol-2-ylidene with an acidic organic compound, such as a phenol or secondary amine. The deprotonation of a range of substituted phenols with strongly basic *N*-heterocyclic carbenes has provided a series of imidazolium phenoxide salts, which generally possess significant secondary hydrogen-bonding interactions in the solid state.

Chapter One is intended to place the work reported later in this thesis into context with the research previously conducted within the field of *N*-heterocyclic carbene chemistry. Other relevant concepts, that will either promote appreciation of the results arising from this study, or help to further explain the motivation behind the research carried out, will be introduced within the appropriate discussion chapters. Chapter Two will focus on the chemistry of the non-conventional imidazolium salts prepared during this investigation and briefly discuss the hydrogen-bonding exhibited by these systems.

Chapter Three will report on the chemistry of a series of *N*-heterocyclic carbene-copper(I) complexes prepared via the *in situ* deprotonation of non-conventional imidazolium salts. Chapter Four will concentrate on the chemistry of a range of zinc(II) phenoxides and alkoxides synthesised in the same manner as the copper(I) complexes discussed in Chapter Three, and their potential in the catalysis of bio-degradable polymer production via ring-opening polymerisations will be detailed. Finally, Chapter Five reports all the experimental procedures and characterisation data pertaining to this study.

Contents

Introduction

1.1: Preamble 1

1.2: Developments in *N*-heterocyclic carbene chemistry 1

1.3: Stability and Structure of *N*-heterocyclic carbenes 4

1.4: Synthetic routes to *N*-heterocyclic carbenes 9

1.5: Reactivity of *N*-heterocyclic carbenes 12

1.6: Metal-*N*-heterocyclic carbenes in catalysis 19

1.7: References 23

Hydrogen-Bonded Organic Precursors to Metal-*N*-Heterocyclic Carbene Complexes

2.1: Introduction 36

2.1.1: Background 37

2.1.2: Imidazol-2-ylidenes and Organic Acids 39

2.2: Imidazolium Phenoxide:Phenol Adducts 42

2.3: Imidazolium Phenoxide Salts 54

2.4: Other Hydrogen-Bonded Compounds 66

2.5: Conclusions 76

2.6: References 78

Copper-*N*-Heterocyclic Carbene Complexes

3.1: Introduction 81

3.1.1: Copper Compounds in Organic Transformations 81

3.1.2: Copper-*N*-Heterocyclic Carbene Complexes 86

3.2: Neutral Copper(I)-*N*-Heterocyclic Carbene Species 88

3.3: Copper-*N*-Heterocyclic Carbene Salt Complexes 109

3.4: Conclusions 121

3.5: References 122

Zinc-*N*-Heterocyclic Carbene Complexes

4.1: Introduction 125

4.1.1: Zinc Compounds in Polymerisation Catalysis 125

4.1.2: Zinc-*N*-Heterocyclic Carbene Complexes 128

4.2: Phenoxide and Amide Supported Zinc Species 130

4.3: ε-Caprolactone Polymerisation 143

4.4: Conclusions 148

4.5: References 149

Experimental Section

General Information 152

Characterisation Details 152

Solid-State Structure Determination 153

ε-Caprolactone Polymerisation 154

Compound Preparations 154

General ε-Caprolactone Polymerisation Procedure 174

References 175

Crystal Data and Diffraction Experiment Details

Compound **1** 176

Compound **2** 177

Compound **3** 178

Compound **4** 179

Compound **5** 180

Compound **8** 181

Compound **9** 182

Compound **11a** 183

Compound **15** 184

Compound **16** 185

Compound **17** 186

Compound **18** 187

Compound **19** 188

Compound **20** 189

Compound **21** 190

Compound **22** 191
Compound **23** 192
Compound **24** 193
Compound **25** 194
Compound **26** 195
Compound **27** 196
Compound **27a** 197
Compound **28 thf solvate** 198
Compound **28a** 199
Compound **29** 200
Compound **30** 201
Compound **31** 202

CD Data Disc

Tables of Structural Data CD

Introduction

1.1: Preamble

Since the isolation of the first stable *N*-heterocyclic carbene by Arduengo *et al.*[1] these species have generated considerable research interest, and have now been recognised as versatile ligands[2-6] for a number of catalytic processes.[7-10] Our interest in these remarkably strong neutral bases[11-13] stems from an investigation into their reaction with X-H acidic organic compounds.[14] The resulting products often exhibit interesting hydrogen-bonding, and are potential precursors to novel and catalytically relevant metal-*N*-heterocyclic carbene complexes.

This introduction is intended to outline the research previously conducted within the field of *N*-heterocyclic carbene chemistry that is pertinent to this investigation. A more comprehensive treatise of the area is provided by excellent review articles recently published by Arduengo,[15] Bertrand,[16] Crudden[17] and Herrmann.[18-21] Relevant concepts such as hydrogen-bonding, and metal-mediated transformations and polymerisations will be introduced in the appropriate discussion chapters.

1.2: Developments in *N*-heterocyclic carbene chemistry

To date, much of the research into stable carbenes has focused on five-membered heterocyclic diaminocarbenes with nitrogen atoms in the 1- and 3-positions of the ring (Figure 1.1).† The carbene centre of these *N*-heterocyclic carbenes occupies the 2-position (Figure 1.1) and is stabilised by the adjacent nitrogen heteroatoms, the origin and extent of this stabilisation will be discussed later in this chapter.

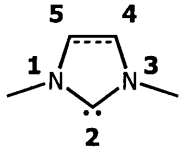

Figure 1.1: Numbering of imidazol-2-ylidene and imidazolin-2-ylidene ring positions

† By convention, the heteroatoms are assigned the lowest possible values when numbering the positions around a heterocyclic ring.[22]

N-heterocyclic carbenes of this type may be saturated in nature, or may possess C(4)=C(5) unsaturation (Figure 1.1). The unsaturated systems are accessible via the deprotonation of imidazolium precursor salts,[1, 2, 23, 24] and are often termed imidazol-2-ylidenes,§ which is how they will be classified throughout this thesis. In accordance with the nomenclature utilised by Arduengo,[24] the saturated analogues of the imidazol-2-ylidenes will be referred to as imidazolin-2-ylidenes,§ and their precursor salts will be termed imidazolinium salts in the interests of consistency.

The first metal-*N*-heterocyclic carbene complexes were prepared over thirty years ago by Öfele[25] and Wanzlick[26] via the *in situ* deprotonation of imidazolium salts. Öfele generated a chromium-*N*-heterocyclic carbene via the thermolysis of a related imidazolium metallate species,[25] whereas Wanzlick employed a basic metal source to effect the deprotonation of an imidazolium salt and produce the corresponding metal-*N*-heterocyclic carbene complex (Scheme 1.1).[26]

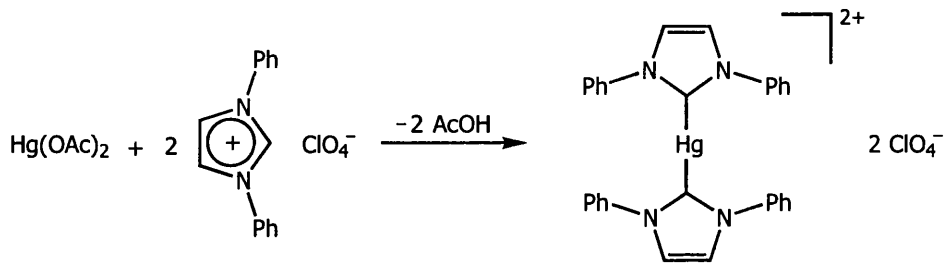

Scheme 1.1: Metal-*N*-heterocyclic carbene complex via imidazolium salt deprotonation

Palladium(II)-imidazol-2-ylidene complexes, utilised in the catalysis of a number of organic coupling reactions,[7, 27-33] have subsequently been prepared via the analogous deprotonation of imidazolium salts by palladium(II)-acetate.[2, 27, 34-36] Recent reports of the preparation of metal-*N*-heterocyclic carbene complexes via the *in situ* deprotonation of thiazolium[37, 38] and benzimidazolium[38-40] precursor salts further demonstrate the versatility of the synthetic methodology pioneered by Wanzlick.[26]

§ There is some controversy over the nomenclature of these *N*-heterocyclic carbenes and their precursors; Herrmann suggests that the unsaturated systems should be termed imidazolin-2-ylidenes and their saturated analogues should be referred to as imidazolidin-2-ylidenes.[18]

The imidazolin-2-ylidenes, the saturated analogues of the imidazol-2-ylidenes, were the focus of much of the early research into *N*-heterocyclic carbenes.[41, 42] Lappert investigated the chemistry of these species via the study of their metal complexes,[43, 44] generally prepared from the reaction of enetetraamines with coordinatively unsaturated metal centres.[45-71] Subsequent investigations into the reactivity of metal-imidazolin-2-ylidenes[49, 72-74] demonstrated that *N*-heterocyclic carbene ligands support metal centres in various oxidation states[54, 74, 75] and that their transition metal complexes may be utilised in homogeneous catalysis.[73]

N-heterocyclic carbenes became readily accessible following the isolation of the first stable crystalline imidazol-2-ylidene (Figure 1.2) by Arduengo *et al.*[1] over a decade ago. This breakthrough has opened up the field of *N*-heterocyclic carbene chemistry and subsequently allowed the detailed study of these species[11, 13, 76-106] and their metal complexes.[29, 84, 99, 107-124]

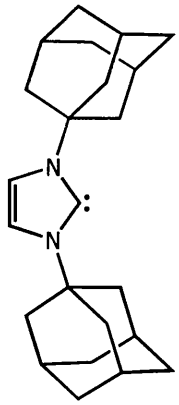

Figure 1.2: First stable crystalline *N*-heterocyclic carbene

Stable *N*-heterocyclic carbenes have also been prepared from triazolium[125, 126] and thiazolium[127] precursor salts. The fundamental and coordination chemistry of these species is underdeveloped compared to that of the imidazol-2-ylidenes and imidazolin-2-ylidenes. This is currently being addressed in the case of the triazolium-based systems; indeed, a number of publications concerned with the fundamental reactivity[128-130] and coordination chemistry[131-135] of these species have recently emerged in the scientific literature.

The versatility of *N*-heterocyclic carbene ligands in catalysis has initiated a study into their silylene, germylene, stannylene and plumbylene analogues.[136-149] The bond dissociation enthalpy of simple Group XI metal-*N*-heterocyclic silylene, germylene and stannylene complexes is quite significant,[143] suggesting that these species may also find utility as ligands in organometallic chemistry. Initial studies into the coordination chemistry of the *N*-heterocyclic carbene homologues seem to further demonstrate that this may be the case.[145, 146]

N-heterocyclic carbenes are currently the focus of considerable research interest and much is known of their stability,[77, 141, 150] fundamental reactivity[128, 151-164] and electronic properties,[83, 165-167] aspects of which will be discussed later on in this chapter. These species are now common ligands in organometallic chemistry and their metal complexes are widely used in the catalysis of a variety of different transformations and reactions.[27-32, 168-197]

1.3: Stability and Structure of *N*-heterocyclic carbenes

Carbenes are six-electron divalent carbon species possessing two non-bonding electrons and a formally uncharged C(II) centre,[16, 18, 77, 198, 199] and are generally classified in terms of their electronic configuration.[16, 18, 198, 199] The non-bonding electrons of a singlet state carbene have anti-parallel electronic spins and may be paired, in which case they occupy only one of the two orbitals available to them; whereas in a triplet state carbene the non-bonding electrons have spins parallel to each other and are, therefore, unpaired, singly occupying both of the orbitals not involved in bonding.[16, 18, 198, 199]

Hund's Rules suggest carbenes with a triplet electronic configuration are lower in energy than their singlet counterparts in which the two non-bonding electrons are paired in a single molecular orbital; since an unfavourable pairing energy arises as a result of the multiple occupation of a single orbital.[200] However, the orbitals available to the non-bonding electrons are not degenerate,[16] and, in the case of the *N*-heterocyclic carbenes, the stabilisation of the singlet state in relation to the triplet configuration is sufficient to offset this unfavourable pairing energy.

The relative stability of the imidazol-2-ylidenes essentially stems from their large singlet-triplet energy gap, calculated at approximately 330 kJ mol^{-1} for the unsubstituted model system.[165] It was initially believed sterically demanding substituents on the ring nitrogen atoms were required in order to impart kinetic stability.[77, 201] However, the subsequent isolation of less sterically demanding imidazol-2-ylidenes[77] (Figure 1.3) than that first reported by Arduengo *et al.*[1] has demonstrated that this is not necessarily the case.

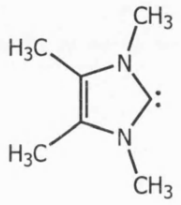

Figure 1.3: A sterically unhindered imidazol-2-ylidene

The stabilisation of the singlet state relative to the triplet configuration is effected by a combination of inductive effects, where relatively electronegative nitrogen atoms within the ring withdraw electron density from the carbene centre through the N-C(2) σ-bonds, and π-donation from the filled heteroatom p-orbitals into the vacant out-of-plane p_z orbital at the carbene centre (Figure 1.4).[1]

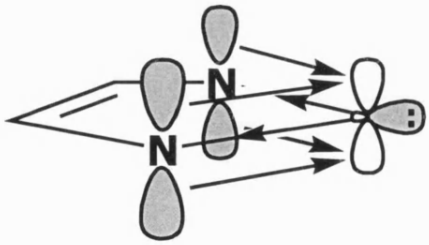

Figure 1.4: Synergic stabilisation of singlet carbene centre

Singlet carbenes are ambiphilic in nature, concomitantly displaying electrophilic and nucleophilic character.[77, 83] The nucleophilic reactivity of these systems is due to σ-donation of their lone pair of electrons, whereas their electrophilicity is a result of the vacant p-orbital perpendicular to the lone pair at the carbene centre.[83] The dimerisation of singlet carbenes arises as a direct result of this ambiphilic character.[83]

Computational studies suggest that the dimerisation of singlet carbenes proceeds via a non-least motion pathway[83, 151] (Figure 1.5), where one carbene molecule perpendicularly approaches another. The approaching carbene moiety initially acts as a nucleophile, donating its lone pair of electrons into the vacant out-of-plane p-orbital at the second carbene centre, and subsequently behaves as an electrophile, as electron density is transferred into its vacant p_z orbital by means of a retaliatory nucleophilic attack.[83, 151]

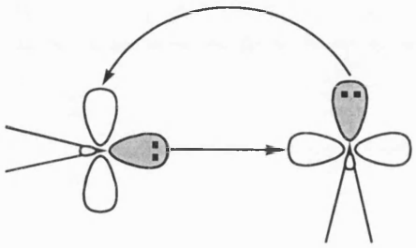

Figure 1.5: Non-least motion pathway for singlet carbene dimerisation

Reports of the irreversible dimerisation of imidazolin-2-ylidenes to yield electron-rich enetetraamines have recently emerged.[202-204] However, Wanzlick proposed the existence of an equilibrium between these *N*-heterocyclic carbene dimers and the corresponding monomeric species (Scheme 1.2).[205] Initial investigations into this claim involved monitoring mixed enetetraamine formation as a result of the scrambling of two distinct *N*-heterocyclic carbene dimers in solution. The expected mixed enetetraamine product was not observed, and hence it was argued that there was no equilibrium between these so-called Wanzlick dimers and *N*-heterocyclic carbenes.[206, 207] However, recent NMR studies have demonstrated that in the case of benzimidazol-2-ylidenes, the combination of the monomeric carbene species to form enetetraamines is in equilibrium with the dissociation of these dimers to yield *N*-heterocyclic carbenes.[208, 209]

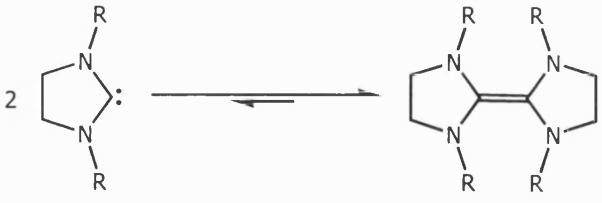

Scheme 1.2: The Wanzlick equilibrium

Enetetraamines react with coordinatively unsaturated transition metal centres to yield the corresponding metal-*N*-heterocyclic carbene complexes,[45-71] and with acids to form the respective carbene precursor salts.[205, 210, 211] Consequently, they are considered to be convenient precursors to *N*-heterocyclic carbenes.[42, 212]

A fundamental aspect of the chemistry of the imidazol-2-ylidenes, the unsaturated analogues of the imidazolin-2-ylidenes, is their apparent stability with respect to dimerisation.[18, 24, 88, 141] Although these singlet carbenes are highly nucleophilic, they do not exhibit the expected degree of electrophilicity.[77, 83] Even their metal adducts, which might be anticipated to demonstrate enhanced electrophilicity as a result of reduced electron density at the C(2) carbon, are generally not susceptible to nucleophilic attack at the carbene centre.[78, 83, 107, 110, 117, 213, 214] Consequently, these singlet carbenes do not exhibit significant ambiphilicity, and, therefore, the accepted non-least motion pathway for dimerisation is not accessible.

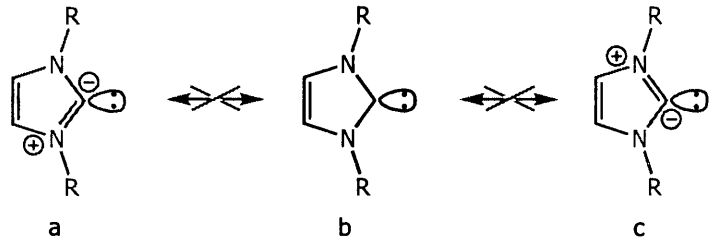

Figure 1.6: Delocalisation of π-system not prominent in imidazol-2-ylidenes

The enhanced stability of imidazol-2-ylidenes relative to their saturated analogues has been attributed to the presence of the C(4)=C(5) double bond.[141, 142, 150, 215] Indeed, since these systems possess 6π electrons and conform to Hückel's (4n+2) rule for aromaticity,[198, 199] it had long been postulated that a carbene centre in the C(2) position may potentially be stabilised via conjugation.[211] However, despite all the atoms within the planar heterocyclic core possessing a p-orbital suitable to constitute part of a delocalised π-system, the results of a charge density study performed by Arduengo *et al.* suggest that there is not significant delocalisation of π-electron density around the central five-membered ring.[83] Therefore, the ylidic character of imidazol-2-ylidenes is negligible and these species may be accurately described as carbenes, i.e. the canonical form **b** (Figure 1.6) is indeed an adequate representation of their electronic structure.[83, 165]

X-ray diffraction studies demonstrate that the delocalisation of π-electron density around the heterocyclic core in imidazol-2-ylidenes is much less significant than for their remarkably stable imidazolium precursor salts.[1, 155, 165, 216] The variation between the N-C(2) bond lengths of imidazolium salts and imidazol-2-ylidenes (Figure 1.7) may be used to validate the proposed synergic stabilisation of the carbene centre via π-donation and inductive effects.[1, 77, 216] The longer N-C(2) bonds in the imidazol-2-ylidenes may be attributed to a reduction in s-character, as a result of the inductive effects in operation, and an increase in their p-character due to π-donation into the vacant out-of-plane p_z orbital at the carbene centre.[165] Structural investigations also verify that imidazol-2-ylidenes are singlet carbenes, since they possess a N(1)-C(2)-N(3) angle of approximately 100° (Figure 1.7), which is consistent with the angle at a singlet carbene centre as predicted by theoretical calculations.[165]

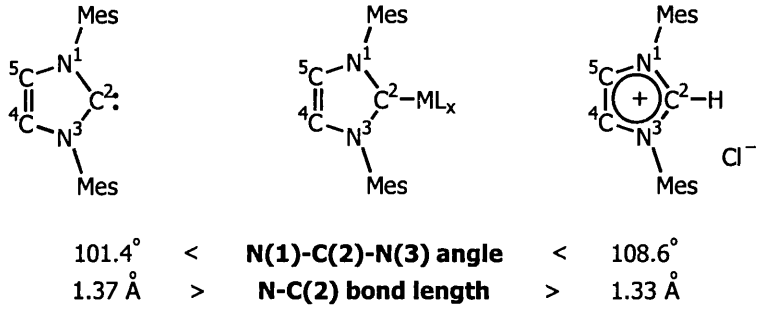

Figure 1.7: Key structural parameters of metal-imidazol-2-ylidene complexes relative to the related free *N*-heterocyclic carbene and imidazolium salt

Metal-imidazol-2-ylidenes generally possess N(1)-C(2)-N(3) angles and N-C(2) bond lengths between those of the corresponding free *N*-heterocyclic carbene and its imidazolium precursor salt (Figure 1.7).[83, 143, 213, 216] The observed reduction in the imidazol-2-ylidene N-C(2) bond length on coordination to a metal centre seems to suggest that π-electron density is delocalised around the heterocyclic core of metal-imidazol-2-ylidene species, albeit to a lesser extent than is evident within imidazolium salts (Figure 1.7).[83, 143, 213, 216] The stabilisation of metal-imidazol-2-ylidenes relative to the corresponding free *N*-heterocyclic carbenes can be attributed, at least in part, to this delocalisation of π-electron density, and provides the impetus for the coordination of imidazol-2-ylidenes to metal centres.

Comparison of the N(1)-C(2)-N(3) angle and N-C(2) bond lengths of a metal-imidazol-2-ylidene relative to that of the respective free *N*-heterocyclic carbene (Figure 1.7) provides an indication of the in-plane electron density at the 2-positon of the imidazol-2-ylidene ligand, which subsequently sheds some light on the strength of the metal-*N*-heterocyclic carbene bond.[143, 216] A complex with an extremely strong metal-imidazol-2-ylidene interaction may be better described as a metallo-imidazolium salt than a metal-*N*-heterocyclic carbene.[20]

1.4: Synthetic routes to *N*-heterocyclic carbenes

Arduengo *et al.* reported the preparation, isolation and structural characterisation of 1,3-di-(1-adamantyl)-imidazol-2-ylidene (Figure 1.2) in their seminal article on the chemistry of *N*-heterocyclic carbenes.[1] This exceptionally stable free carbene (Figure 1.2) was prepared by means of the deprotonation of a related imidazolium salt.[1] Subsequent reports of the preparation of various imidazol-2-ylidenes and imidazolin-2-ylidenes via the deprotonation of imidazolium[24, 77, 217] (Scheme 1.3) and imidazolinium[215] salts demonstrate the synthetic utility of this methodology in the preparation of free *N*-heterocyclic carbenes. Indeed, the most commonly employed strategy in the synthesis of imidazol-2-ylidenes is the exploitation of a basic reagent to effect the removal of the acidic C(2)-H proton of corresponding imidazolium precursor salts (Scheme 1.3).[2, 23, 167, 218-222]

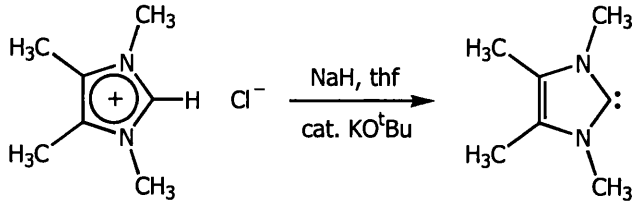

Scheme 1.3: Deprotonation of imidazolium precursor salt

The diversity of imidazol-2-ylidenes prepared via this deprotonation methodology depends upon the accessibility of the corresponding imidazolium precursor salts. The quaternisation of imidazole[223, 224] and commercially or synthetically readily available substituted imidazoles[19, 21, 225] by reaction with primary alkyl halides represents a facile route to alkyl substituted imidazolium salts (Scheme 1.4).

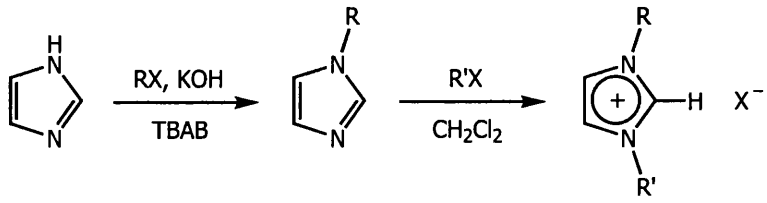

Scheme 1.4: Quaternisation of readily available imidazoles

1,3-dialkyl substituted imidazolium chloride species may also be prepared by the direct addition of two equivalents of the corresponding primary alkyl chloride to *N*-trimethylsilyl-imidazole (Scheme 1.5).[226] The advantage of this methodology is that the imidazolium *N*-heterocyclic carbene precursor is easily separated from the volatile trimethylsilyl chloride by-product.

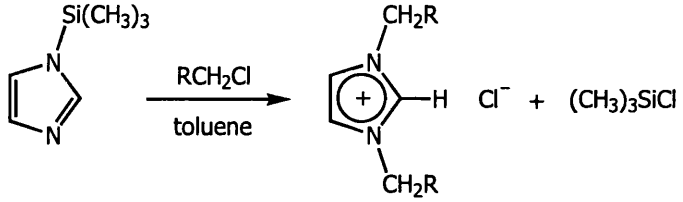

Scheme 1.5: One-step preparation of a 1,3-dialkyl-imidazolium salt

A convenient synthesis of highly substituted imidazolium salts possessing more sterically demanding substituents on the heteroatoms via a condensation reaction involving amines and carbonyl compounds (Scheme 1.6) has been developed by Arduengo *et al.*[227] This one-pot methodology has facilitated the preparation of significantly more diversely substituted imidazol-2-ylidenes.[77, 219]

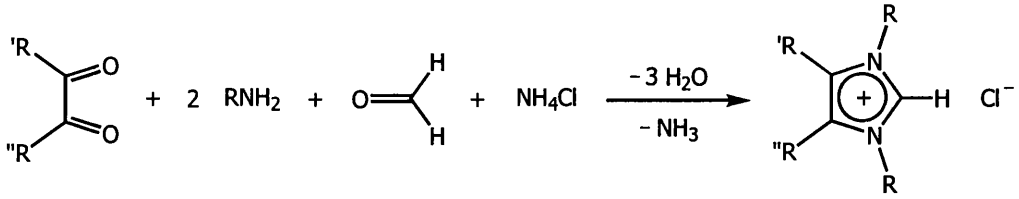

Scheme 1.6: One-pot synthesis of highly substituted imidazolium salts

Substituted imidazolium salts are generally prepared via a two-step variant of this one-pot methodology (Scheme 1.7).[24, 217] The first step being the reaction of an aqueous solution of glyoxal with two equivalents of a substituted amine to yield the corresponding 1,4-disubstituted diazabuta-1,3-diene (Scheme 1.7).[24, 217] The

imidazolium salt is subsequently obtained via the reaction of this diazabutadiene intermediate with paraformaldehyde and hydrogen chloride in dioxane (Scheme 1.7).[24, 217] This methodology may be extended to the preparation of substituted imidazolin-2-ylidenes. In this case, the diazabutadiene product is prepared in the same manner, but is then reduced with sodium borohydride prior to the formation of the heterocycle by reaction with triethyl orthoformate (Scheme 1.7).[24]

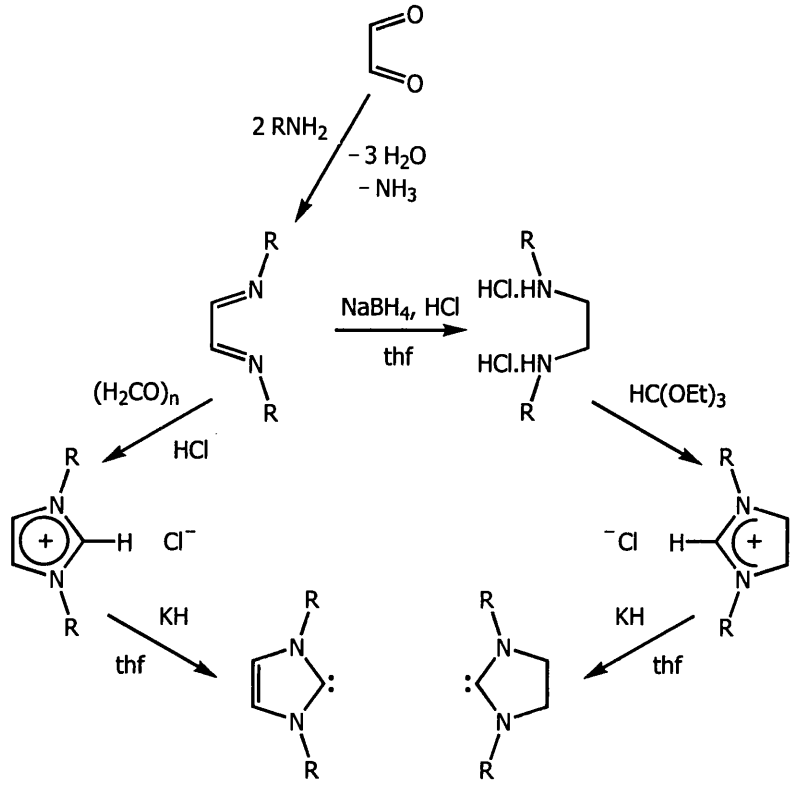

Scheme 1.7: Synthesis of imidazol-2-ylidenes and analogous imidazolin-2-ylidenes

Kühn has exploited an alternative synthetic approach to the imidazol-2-ylidenes, utilising an alkali metal to effect the reduction of the related thione compounds (Scheme 1.8).[228] However, the accessibility of imidazolium salts bearing highly varied substituents via the routes discussed earlier in this section has meant that this methodology has not received significant application.

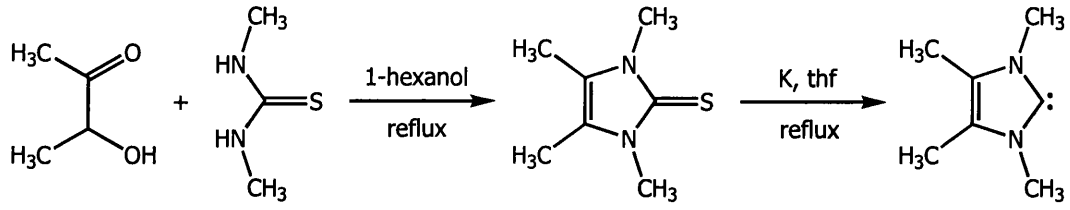

Scheme 1.8: Imidazol-2-ylidenes via reduction of related thiones

1.5: Reactivity of *N*-heterocyclic carbenes

N-heterocyclic carbenes coordinate to metal centres via σ-donation of their lone pair of electrons (Figure 1.4),[20, 143, 216, 229-231] and are generally considered to be phosphine mimics.[41, 42, 44, 230-239] However, it should be noted that these species differ significantly in terms of their electronic and steric properties.[124, 234, 238-240] Indeed, although they both act as two electron σ-donor ligands, compared to their phosphine counterparts, *N*-heterocyclic carbene ligands do not accept significant π-back donation of electron density from metal centres.[143, 216, 229] Consequently, *N*-heterocyclic carbene complexes of both early and late transition metal elements are readily formed.[79, 85, 91, 161-163, 219, 241-256] In addition, the steric requirements of a phosphine ligand can be described by a cone angle,[257-261] whereas the planarity of *N*-heterocyclic carbenes means that two different parameters need to be taken into account in order to describe the steric demands of these ligands.[240]

Despite differences in the steric and electronic characteristics of *N*-heterocyclic carbenes and phosphines, considerable research effort has been focused on the replacement of the phosphine ligands ubiquitous in catalysis with *N*-heterocyclic carbenes.[18, 20, 21, 30, 235] As a result, the reactivity of transition metal complexes of *N*-heterocyclic carbenes is quite well understood, in relation to the fundamental reactivity of these species in general.

Metal complexes of *N*-heterocyclic carbenes may be readily prepared by means of the displacement of more labile ligands at a metal centre. The substitution of phosphine ligands for imidazol-2-ylidenes (Scheme 1.9), in particular, represents a facile route to the imidazol-2-ylidene ligated analogues of catalytically active metal-phosphine complexes.[20, 180, 247, 248] This is exemplified by the replacement of the phosphine ligands in a ruthenium benzylidene olefin metathesis catalyst by more strongly σ-donating imidazol-2-ylidenes (Scheme 1.9).[246]

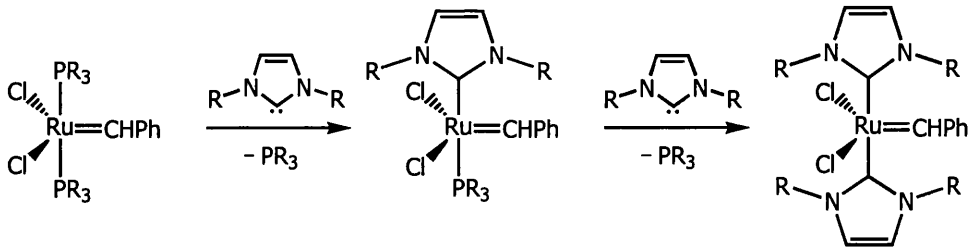

Scheme 1.9: Displacement of phosphine ligands by imidazol-2-ylidenes

In this case, a single phosphine ligand is exchanged for an imidazol-2-ylidene when the *N*-heterocyclic carbene moiety bears bulky *tert*-butyl or mesityl nitrogen substituents (Scheme 1.9).[246] On the other hand, sequential displacement of the phosphines results if the ring nitrogen atoms possess sterically less demanding isopropyl or cyclohexyl groups (Scheme 1.9).[246]

N-heterocyclic carbenes do not react with double bonds,[20, 125] and therefore the displacement of coordinated olefins represents an effective route to their transition metal complexes.[84, 170] The substitution of neutral donor solvent molecules is also a useful method for the preparation of metal coordination compounds bearing *N*-heterocyclic carbene ligands, and has been applied to the preparation of s-block metal-*N*-heterocyclic carbenes (Scheme 1.10).[262]

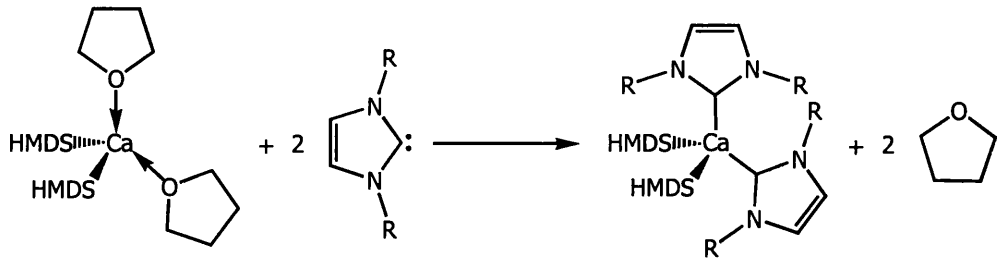

Scheme 1.10: Substitution of donor solvent molecules for imidazol-2-ylidene ligands

N-heterocyclic carbenes form adducts with coordinatively unsaturated main group metals, specifically Group II metal dialkyl species (Figure 1.8)[78] and Group III metal trialkyls[263] and trihydrides.[213, 264-266] The chemistry of the *N*-heterocyclic carbene main group metal adducts [78, 213, 263-266] (Scheme 1.10 and Figure 1.8) is underdeveloped in comparison to that of their transition metal complexes, which have received significantly more research attention by virtue of their perceived potential to catalyse a number of useful transformations.[18, 20, 21, 27, 180, 238]

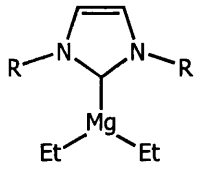

Figure 1.8: An s-block metal-imidazol-2-ylidene adduct

The coordination mode of *N*-heterocyclic carbenes is identical in their main group metal adducts and transition metal complexes, in that the *N*-heterocyclic carbene binds to the central metal atom via σ-donation of its in-plane lone pair of electrons (Figure 1.4).[78, 213, 229] The existence of main group metal adducts demonstrates that π-back donation from a metal centre is not a pre-requisite for *N*-heterocyclic carbene coordination.[18, 20, 267]

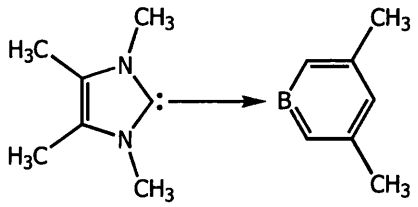

Figure 1.9: An imidazol-2-ylidene:borabenzene adduct

Imidazol-2-ylidenes are highly Lewis basic in nature, in fact, these *N*-heterocyclic carbenes are some of the strongest neutral organic bases known at present.[11, 13] The formation of a range of Lewis acid-Lewis base complexes[99, 155, 213, 263, 264, 268] as a result of the reaction of imidazol-2-ylidenes with electron-poor boron species (Figure 1.9)[81, 96, 269] provides further evidence for the strong σ-donor capacity of *N*-heterocyclic carbenes.

The exceptional Lewis basicity of the imidazol-2-ylidenes was demonstrated by Arduengo *et al.*, by means of an investigation into the reaction of 1,3-dimesityl-imidazol-2-ylidene with a related imidazolium salt (Scheme 1.11).[155] The NMR spectra of the product exhibit signals at intermediary chemical shifts to those of the imidazol-2-ylidene and imidazolium salt.[155] This suggests that the system is highly fluxional on the NMR timescale, with rapid proton exchange occurring in solution between the imidazolium salt and the *N*-heterocyclic carbene species.[155]

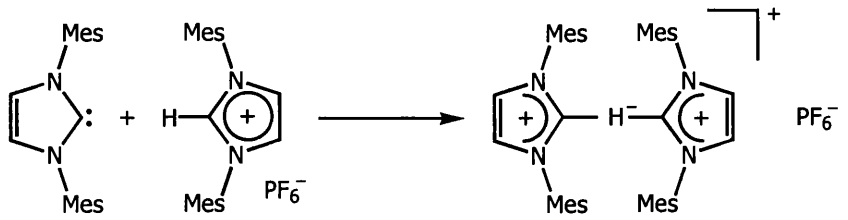

Scheme 1.11: Reaction of an imidazol-2-ylidene with a related imidazolium salt

A single crystal x-ray diffraction analysis of this imidazol-2-ylidene:imidazolium salt adduct prepared by Arduengo *et al.* (Scheme 1.11) revealed the presence of an unusual linear three-centre four-electron C·····H·····C bridging interaction between the two heterocyclic fragments.[155] This observation prompted speculation that *N*-heterocyclic carbenes may also form interesting hydrogen-bonding interactions with other X-H acidic compounds.[14]

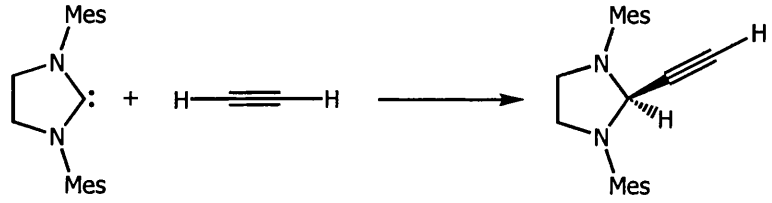

Scheme 1.12: Insertion of an imidazolin-2-ylidene into an acetylene C-H bond

Arduengo *et al.* have reported the insertion of imidazolin-2-ylidenes into the C-H bonds of acetylene (Scheme 1.12), acetonitrile and chloroform (Scheme 1.13),[12] demonstrating that, in addition to the formation of hydrogen-bonded salts, neutral organic compounds may result from the reaction of *N*-heterocyclic carbenes with C-H acidic organic molecules.[12]

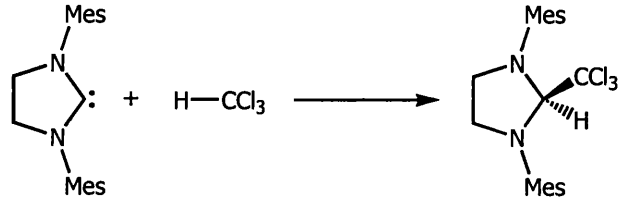

Scheme 1.13: Insertion of imidazolin-2-ylidene into chloroform C-H bond

The insertion of imidazolin-2-ylidenes into the C-H bond of chloroform (Scheme 1.13)[12] demonstrates a characteristic feature of the chemistry of *N*-heterocyclic carbenes, their reactivity towards chlorinated solvents. It is widely accepted that,

in such reactions, the nucleophilic *N*-heterocyclic carbene abstracts a proton from the C-H acidic species, generating a carbanion which subsequently attacks the former carbene centre.[12] Interestingly, imidazolin-2-ylidenes have been shown to react with carbon tetrachloride, which does not possess an acidic hydrogen atom, to yield a mixed-carbene dimer (Scheme 1.14).[12]

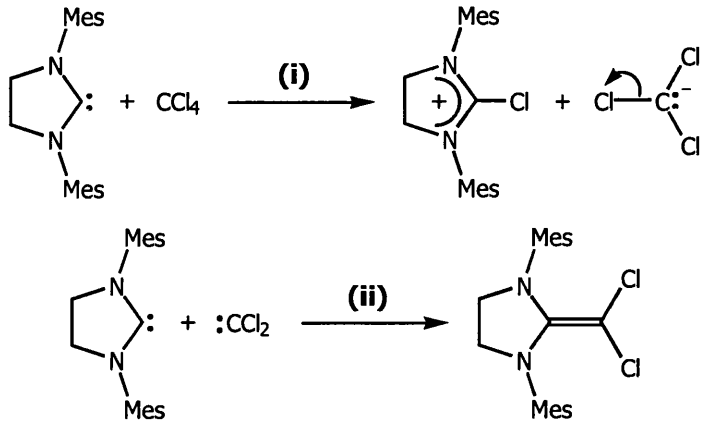

Scheme 1.14: Reaction between an imidazolin-2-ylidene and carbon tetrachloride
(i) Cl^+ abstraction from CCl_4 and α-elimination of Cl^- from resulting CCl_3^- anion;
(ii) mixed-carbene dimer formation via combination of imidazolin-2-ylidene and $:CCl_2$

The reaction of an imidazolin-2-ylidene with carbon tetrachloride initially results in the formation of the corresponding 2-chloro-imidazolinium trichloromethyl (CCl_3^-) salt (Scheme 1.14).[12] Dichlorocarbene is subsequently generated *in situ* via α-elimination of a chloride ion from the CCl_3^- anion, and the mixed-carbene dimer forms as a result of the combination of an imidazolin-2-ylidene moiety with the dichlorocarbene species (Scheme 1.14).[12]

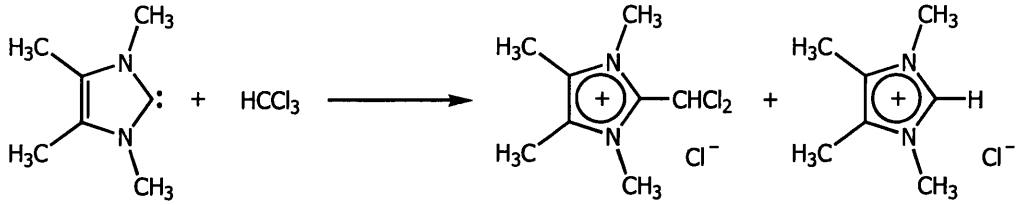

Scheme 1.15: Reaction of an imidazol-2-ylidene with chloroform

The reaction between an imidazol-2-ylidene and chloroform results in a mixture of the corresponding dichloromethyl-imidazolium and imidazolium chloride salts (Scheme 1.15).[12] However, although the acidic chloroform proton is abstracted

by the basic *N*-heterocyclic carbene, as in the reaction of imidazolin-2-ylidenes with chloroform (Scheme 1.13),[12] subsequent insertion of the imidazol-2-ylidene moiety into the chloroform C-H bond is not observed.[12] The formation of the dichloromethyl-imidazolium chloride is believed to proceed via a mixed-carbene dimer intermediate, similar to the species formed as a result of the reaction of imidazolin-2-ylidenes with carbon tetrachloride (Scheme 1.14).[12]

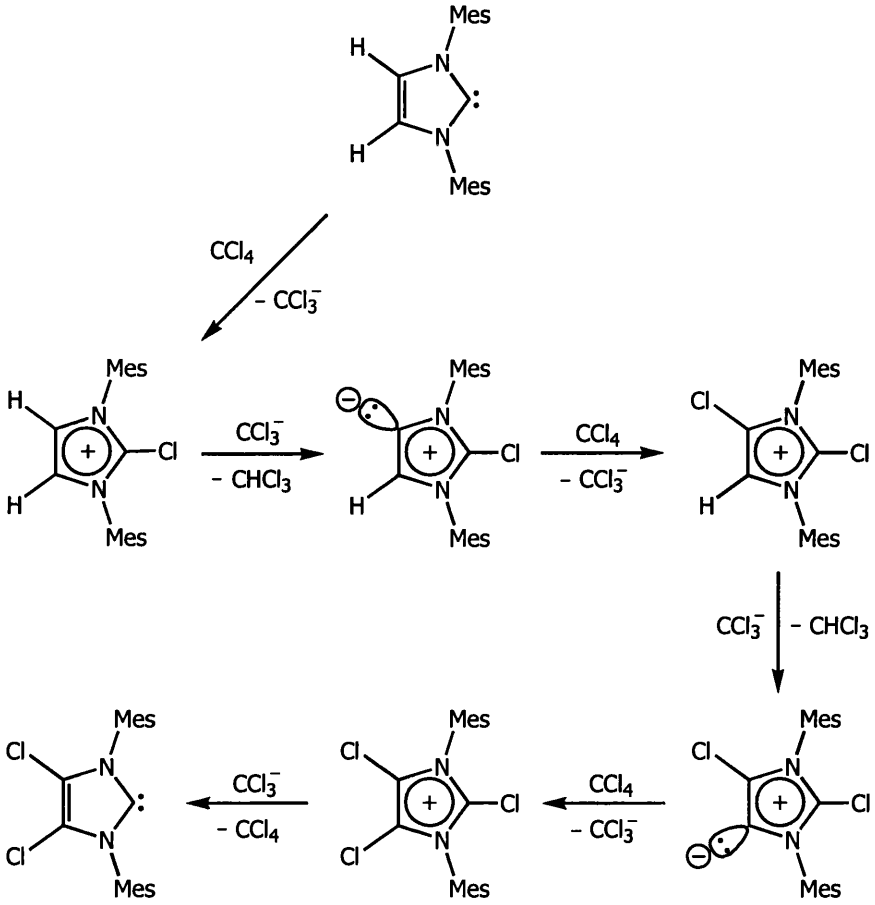

Scheme 1.16: Chlorine substitution of imidazol-2-ylidene C(4/5)-H hydrogen atoms

Arduengo *et al.* also demonstrated that rapid exchange of the C(4/5)-H hydrogen atoms for chlorine substituents occurs when an imidazol-2-ylidene is reacted with two equivalents of carbon tetrachloride (Scheme 1.16).[88] The first step of this substitution reaction is believed to be the generation of a 2-chloro-imidazolium salt analogous to the 2-chloro-imidazolinium species produced during the reaction of imidazolin-2-ylidenes with carbon tetrachloride (Scheme 1.14).[12] However, rather than undergoing α-elimination of a chloride ion to yield dichlorocarbene, the trichloromethyl anion in this case abstracts a proton from the C(4/5) position

of the imidazolium cation.[88] This results in the formation of a highly reactive intermediate possessing a carbene centre at C(4/5),[¥] which formally abstracts Cl^+ from a further equivalent of carbon tetrachloride, subsequently regenerating the CCl_3^- anion.[88] Ultimately, the remaining C(4/5)-H hydrogen atom is exchanged for a chlorine substituent in the same manner, yielding a remarkably air-stable 4,5-dichloro-imidazol-2-ylidene (Scheme 1.16).[88]

Further reaction of this 4,5-dichloro-imidazol-2-ylidene with carbon tetrachloride generates the corresponding 2,4,5-trichloro-imidazolium trichloromethyl salt.[88] However, over time, dichlorocarbene is generated due to the α-elimination of a chloride ion from the CCl_3^- anion, to yield the related 2,4,5-trichloro-imidazolium chloride (Scheme 1.17).[88] A mixed-carbene dimer (Scheme 1.17) then forms by means of the combination of the dichlorocarbene produced with an *N*-heterocyclic carbene moiety, in an analogous reaction to that depicted in Scheme 1.14.[88]

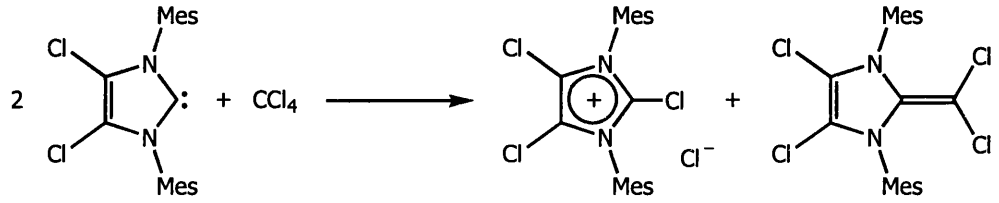

Scheme 1.17: Reaction of 4,5-dichloro-imidazol-2-ylidene with carbon tetrachloride

The air-sensitivity of *N*-heterocyclic carbenes, with the notable exception of the remarkably stable 4,5-dichloro-imidazol-2-ylidene prepared by Arduengo *et al.* (Scheme 1.16),[88] is well-documented,[1, 77, 88] even though it was relatively poorly understood until only quite recently. Denk *et al.* conducted an investigation into the reactivity of free imidazol-2-ylidenes and imidazolin-2-ylidenes towards small molecules such as oxygen and water and reported that *N*-heterocyclic carbenes are, in fact, inert towards oxygen but are hydrolysed by water (Scheme 1.18).[98] As a result, the observed air-sensitivity of these species has been attributed to the presence of water vapour in the air.[98]

[¥] Reports of abnormal *N*-heterocyclic carbene binding to metal centres[114, 121, 270] provide some evidence that a carbene centre can be supported in the C(4/5) position.

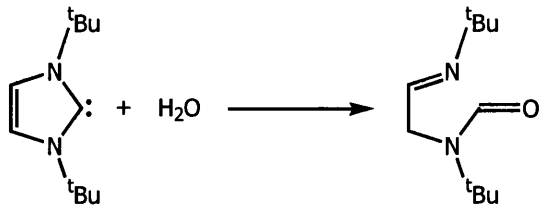

Scheme 1.18: Hydrolysis of an imidazol-2-ylidene

Hydrolysis of *N*-heterocyclic carbenes proceeds rapidly for imidazolin-2-ylidenes, but is slow in the case of the imidazol-2-ylidenes (Scheme 1.18).[98] The reaction is not catalysed by either acid or base, and Denk *et al.* suggest it occurs via the insertion of the *N*-heterocyclic carbene into a water O-H bond.[98]

1.6: Metal-*N*-heterocyclic carbenes in catalysis

N-heterocyclic carbenes are considered to be analogous to the phosphine ligands ubiquitous in catalysis,[230-239] as a result, significant research effort is focused on evaluating the catalytic potential of their transition metal complexes.[20, 21, 30, 235] However, phosphine ligands have been quite extensively developed, and tailored to provide highly specialised transition metal-phosphine catalysts.[258, 261, 271-280] Transition metal complexes of *N*-heterocyclic carbenes are unlikely to represent a viable alternative until specialisation available with these ligands approaches that of phosphine systems.[258, 261, 271-280] This challenge is now being addressed, and much of the innovation in phosphine ligand design has been successfully applied to *N*-heterocyclic carbenes; with donor-arm functionalised,[6, 23, 28, 232, 237, 281, 282] chiral,[67, 126, 222, 283-286] solid-supported[287-289] and chelating[2, 35, 38] *N*-heterocyclic carbenes recently reported in the chemical literature.

The enthalpy of dissociation of transition metal-*N*-heterocyclic carbene bonds is higher than that of transition metal-phosphine bonds.[143, 170, 287, 290] Consequently, the thermal stability of transition metal-*N*-heterocyclic carbene species is greater than that of their phosphine counterparts.[5, 30, 170, 238, 239] The increased strength of the transition metal-*N*-heterocyclic carbene bond, in comparison to a transition metal-phosphine bond, also has implications in solid-supported catalysis. The

immobilisation of a transition metal catalyst through an *N*-heterocyclic carbene, rather than via a phosphine ligand, is anticipated to result in reduced catalyst leaching, maintaining catalyst activity over the course of a number of runs.[20, 288]

Transition metal complexes that incorporate *N*-heterocyclic carbene ligands have been employed in the catalysis of a number of different organic transformations. Recent review articles[18, 20, 21] provide an excellent treatise of the implementation of these species in the catalysis of hydroformylation and hydrogenation reactions, and the hydrosilylation of alkenes, alkynes and ketones. However, it should be noted that the selectivity and activity of *N*-heterocyclic carbene catalysts is often inferior to that of their phosphine counterparts, although, only a limited number of *N*-heterocyclic carbene ligands have been evaluated to date.

The performance of transition metal-*N*-heterocyclic carbene complexes rivals that of more established transition metal-phosphines in the catalysis of ring-opening olefin metathesis polymerisations (Scheme 1.19).[8, 109, 112, 291, 292] Replacement of the phosphine ligands of the ruthenium phosphine alkylidene systems developed by Grubbs *et al.*[293-296] with *N*-heterocyclic carbenes provides a series of effective olefin metathesis catalysts.[180, 182, 246, 297, 298] The activity of bisimidazol-2-ylidene derivatives is comparable to that of the analogous bisphosphine systems.[238, 246] Superior catalytic activity is exhibited by complexes bearing imidazol-2-ylidenes (unsaturated *N*-heterocyclic carbenes) and phosphines,[180, 217, 238] the efficacy of these species is in turn surpassed by the analogous imidazolin-2-ylidene (saturated *N*-heterocyclic carbene) ligated systems.[8, 184, 299-308]

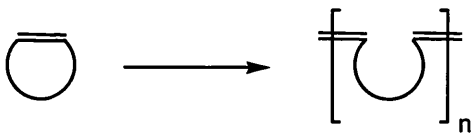

Scheme 1.19: Ring-opening metathesis polymerisation reaction

The phenomenal activity of ruthenium alkylidene species bearing *N*-heterocyclic carbenes and phosphine ligands is thought to verify that, when catalysts analogous to the phosphine systems developed by Grubbs *et al.*[293-296] are employed in olefin metathesis, a dissociative reaction mechanism is favoured.[20, 182, 309] Based on the

relative dissociation enthalpies of transition metal-*N*-heterocyclic carbene bonds and transition metal-phosphine bonds, decoordination of the phosphine ligand, rather than the *N*-heterocyclic carbene, occurs to facilitate the coordination of the substrate.[20, 309] The *N*-heterocyclic carbene stabilises the reactive metal fragment until the reaction reaches completion, and subsequent phosphine recoordination takes place.[20, 309]

N-heterocyclic carbenes stabilise metals in high and low oxidation states[2, 111, 153] and, therefore, constitute ideal ligands for transition metal complexes employed in the catalysis of carbon-carbon coupling reactions involving oxidative addition and reductive elimination steps. Transition metal-*N*-heterocyclic carbene complexes have indeed been successfully employed in the catalysis of the Heck reaction (Scheme 1.20)[20, 21, 170, 310] and other coupling reactions.[20, 21, 170, 310] Although, as is the case in olefin metathesis, catalysts in which *N*-heterocyclic carbene ligands are combined with phosphines tend to exhibit superior activity,[20, 21, 170, 310] which is further enhanced on increasing the steric bulk of the *N*-heterocyclic carbenes or phosphines coordinated to the metal centre.[20, 21, 170, 310]

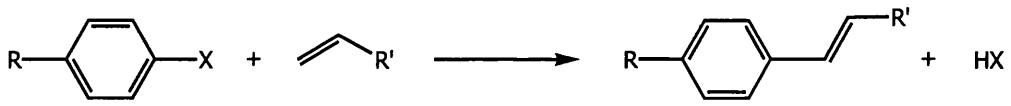

Scheme 1.20: Heck carbon-carbon bond forming reaction

Ionic liquids represent an alternative reaction medium to the hydrocarbon solvents that are extensively utilised in industrial processes, and significant recent research effort has been dedicated to the development and evaluation of systems based on imidazolium salts.[311-313] Many transition metal catalysed reactions, including the Heck coupling reaction (Scheme 1.20), have now been successfully conducted in an imidazolium salt ionic liquid medium.[314-319] Although these solvent systems are regarded as inert in nature, reports of the oxidative addition of imidazolium salts to metal fragments suggest that this is not necessarily the case.[117, 316, 320-322] Indeed, there is some evidence that the catalytically active species in transition metal catalysed transformations performed in imidazolium salt ionic liquids are, in fact, *in situ* generated transition metal-imidazol-2-ylidene species.[316, 320, 322]

N-heterocyclic carbenes are generally considered to be innocent spectator ligands, however, a number of reports to the contrary have been published in the chemical literature.[107, 110, 122] For instance, the *N*-heterocyclic carbene ligands within some ruthenium, rhodium and iridium coordination compounds have been shown to be susceptible to C-H and C-C bond activation.[57, 122, 250-252] Moreover, the reductive elimination of 2-substituted imidazolium salts from palladium-imidazol-2-ylidene complexes, which has implications for the use of transition metal-*N*-heterocyclic carbene species in metal-mediated catalysis, has also been observed.[107, 110, 117, 214] A better understanding of these processes would facilitate the design of transition metal-*N*-heterocyclic carbene catalyst systems in which such reactions are limited, or perhaps exploited in pre-catalyst activation. The reaction of non-conventional *N*-heterocyclic carbene precursor salts with basic metal source species is expected to represent a key synthetic strategy in the preparation of such highly specialised metal-*N*-heterocyclic carbene complexes.

A better understanding of the chemistry of imidazolium salts may provide an insight into the interaction of imidazolium salt ionic liquids with transition metal complexes, and various starting materials and reaction products. Consequently, in addition to highlighting the exploitation of non-conventional imidazolium salts as precursors to metal-imidazol-2-ylidene complexes with diverse ancillary ligation, this study may also be relevant in terms of the chemistry of imidazolium salt ionic liquids.

1.7: References

[1] A. J. Arduengo, R. L. Harlow, M. Kline, *J. Am. Chem. Soc.*, **1991**, *113*, 361.

[2] W. A. Herrmann, M. Elison, J. Fischer, C. Kocher, G. R. J. Artus, *Chem.-Eur. J.*, **1996**, *2*, 772.

[3] W. A. Herrmann, L. J. Goossen, G. R. J. Artus, C. Kocher, *Organometallics*, **1997**, *16*, 2472.

[4] D. S. Clyne, J. Jin, E. Genest, J. C. Gallucci, T. V. RajanBabu, *Org. Lett.*, **2000**, *2*, 1125.

[5] L. J. Xu, W. P. Chen, J. F. Bickley, A. Steiner, J. L. Xiao, *J. Organomet. Chem.*, **2000**, *598*, 409.

[6] A. A. Danopoulos, S. Winston, T. Gelbrich, M. B. Hursthouse, R. P. Tooze, *J. Chem. Soc.-Chem. Commun.*, **2002**, 482.

[7] C. M. Zhang, J. K. Huang, M. L. Trudell, S. P. Nolan, *J. Org. Chem.*, **1999**, *64*, 3804.

[8] C. W. Bielawski, R. H. Grubbs, *Angew. Chem.-Int. Ed. Engl.*, **2000**, *39*, 2903.

[9] H. M. Lee, T. Jiang, E. D. Stevens, S. P. Nolan, *Organometallics*, **2001**, *20*, 1255.

[10] F. Simal, S. Delfosse, A. Demonceau, A. F. Noels, K. Denk, F. I. Kohl, T. Weskamp, W. A. Herrmann, *Chem.-Eur. J.*, **2002**, *8*, 3047.

[11] R. W. Alder, P. R. Allen, S. J. Williams, *J. Chem. Soc.-Chem. Commun.*, **1995**, 1267.

[12] A. J. Arduengo, J. C. Calabrese, F. Davidson, H. V. R. Dias, J. R. Goerlich, R. Krafczyk, W. J. Marshall, M. Tamm, R. Schmutzler, *Helv. Chim. Acta*, **1999**, *82*, 2348.

[13] Y. J. Kim, A. Streitwieser, *J. Am. Chem. Soc.*, **2002**, *124*, 5757.

[14] J. A. Cowan, J. A. C. Clyburne, M. G. Davidson, R. L. W. Harris, J. A. K. Howard, P. Kupper, M. A. Leech, S. P. Richards, *Angew. Chem.-Int. Ed. Engl.*, **2002**, *41*, 1432.

[15] A. J. Arduengo, *Acc. Chem. Res.*, **1999**, *32*, 913.

[16] D. Bourissou, O. Guerret, F. P. Gabbai, G. Bertrand, *Chem. Rev.*, **2000**, *100*, 39.

[17] C. M. Crudden, D. P. Allen, *Coord. Chem. Rev.*, **2004**, *248*, 2247.

[18] W. A. Herrmann, C. Kocher, *Angew. Chem.-Int. Ed. Engl.*, **1997**, *36*, 2163.

[19] T. Weskamp, V. P. W. Bohm, W. A. Herrmann, *J. Organomet. Chem.*, **2000**, *600*, 12.

[20] W. A. Herrmann, T. Weskamp, V. P. W. Bohm, *"Metal complexes of stable carbenes"*, in *Advances in Organometallic Chemistry*, **2001**. 1-69.

[21] W. A. Herrmann, *Angew. Chem.-Int. Ed. Engl.*, **2002**, *41*, 1291.

[22] T. L. Gilchrist, *Heterocyclic Chemistry*, 3rd, Addison Wesley Longman Limited, Harlow, **1997**.

[23] W. A. Herrmann, C. Kocher, L. J. Goossen, G. R. J. Artus, *Chem.-Eur. J.*, **1996**, *2*, 1627.
[24] A. J. Arduengo, R. Krafczyk, R. Schmutzler, H. A. Craig, J. R. Goerlich, W. J. Marshall, M. Unverzagt, *Tetrahedron*, **1999**, *55*, 14523.
[25] K. Ofele, *J. Organomet. Chem.*, **1968**, *12*, P42.
[26] H. W. Wanzlick, H. J. Schonherr, *Angew. Chem.-Int. Ed. Engl.*, **1968**, *7*, 141.
[27] W. A. Herrmann, C. P. Reisinger, M. Spiegler, *J. Organomet. Chem.*, **1998**, *557*, 93.
[28] D. S. McGuinness, K. J. Cavell, *Organometallics*, **2000**, *19*, 741.
[29] G. A. Grasa, Z. Moore, K. L. Martin, E. D. Stevens, S. P. Nolan, V. Paquet, H. Lebel, *J. Organomet. Chem.*, **2002**, *658*, 126.
[30] A. C. Hillier, G. A. Grasa, M. S. Viciu, H. M. Lee, C. L. Yang, S. P. Nolan, *J. Organomet. Chem.*, **2002**, *653*, 69.
[31] M. S. Viciu, R. M. Kissling, E. D. Stevens, S. P. Nolan, *Org. Lett.*, **2002**, *4*, 2229.
[32] K. Melis, D. De Vos, P. Jacobs, F. Verpoort, *J. Organomet. Chem.*, **2003**, *671*, 131.
[33] M. S. Viciu, R. A. Kelly, E. D. Stevens, F. Naud, M. Studer, S. P. Nolan, *Org. Lett.*, **2003**, *5*, 1479.
[34] W. A. Herrmann, J. Schwarz, M. G. Gardiner, *Organometallics*, **1999**, *18*, 4082.
[35] M. G. Gardiner, W. A. Herrmann, C. P. Reisinger, J. Schwarz, M. Spiegler, *J. Organomet. Chem.*, **1999**, *572*, 239.
[36] G. Bertrand, E. Diez-Barra, J. Fernandez-Baeza, H. Gornitzka, A. Moreno, A. Otero, R. I. Rodriguez-Curiel, J. Tejeda, *Eur. J. Inorg. Chem.*, **1999**, 1965.
[37] W. A. Herrmann, J. Fischer, K. Ofele, G. R. J. Artus, *J. Organomet. Chem.*, **1997**, *530*, 259.
[38] W. A. Herrmann, J. Schwarz, M. G. Gardiner, M. Spiegler, *J. Organomet. Chem.*, **1999**, *575*, 80.
[39] B. Bildstein, M. Malaun, H. Kopacka, K. H. Ongania, K. Wurst, *J. Organomet. Chem.*, **1998**, *552*, 45.
[40] F. E. Hahn, M. Foth, *J. Organomet. Chem.*, **1999**, *585*, 241.
[41] M. F. Lappert, *J. Organomet. Chem.*, **1975**, *100*, 139.
[42] M. F. Lappert, *J. Organomet. Chem.*, **1988**, *358*, 185.
[43] D. J. Cardin, B. Cetinkaya, E. Cetinkaya, M. F. Lappert, E. W. Randall, E. Rosenberg, *J. Chem. Soc.-Dalton Trans.*, **1973**, 1982.
[44] D. J. Cardin, B. Cetinkaya, M. F. Lappert, *J. Organomet. Chem.*, **1974**, *72*, 139.
[45] D. J. Cardin, B. Cetinkaya, M. F. Lappert, L. J. Manojlovic-Muir, K. W. Muir, *J. Chem. Soc.-Chem. Commun.*, **1971**, 400.
[46] D. J. Cardin, B. Cetinkaya, E. Cetinkaya, M. F. Lappert, L. J. Manjolovic-Muir, K. W. Muir, *J. Organomet. Chem.*, **1972**, *44*, C59.

[47] D. J. Cardin, M. J. Doyle, M. F. Lappert, *J. Chem. Soc.-Chem. Commun.*, **1972**, 927.
[48] B. Cetinkaya, P. H. Dixneuf, M. F. Lappert, *J. Chem. Soc.-Chem. Commun.*, **1973**, 206.
[49] D. J. Cardin, B. Cetinkaya, E. Cetinkaya, M. F. Lappert, *J. Chem. Soc.-Dalton Trans.*, **1973**, 514.
[50] B. Cetinkaya, P. H. Dixneuf, M. F. Lappert, *J. Chem. Soc.-Dalton Trans.*, **1974**, 1827.
[51] M. J. Doyle, M. F. Lappert, G. M. McLaughlin, J. McMeeking, *J. Chem. Soc.-Dalton Trans.*, **1974**, 1494.
[52] B. Cetinkaya, P. B. Hitchcock, M. F. Lappert, P. L. Pye, *J. Chem. Soc.-Chem. Commun.*, **1975**, 683.
[53] P. B. Hitchcock, M. F. Lappert, P. L. Pye, *J. Chem. Soc.-Chem. Commun.*, **1976**, 644.
[54] M. F. Lappert, P. L. Pye, *J. Chem. Soc.-Dalton Trans.*, **1977**, 2172.
[55] P. B. Hitchcock, M. F. Lappert, P. L. Pye, *J. Chem. Soc.-Dalton Trans.*, **1977**, 2160.
[56] M. F. Lappert, P. L. Pye, G. M. McLaughlin, *J. Chem. Soc.-Dalton Trans.*, **1977**, 1272.
[57] P. B. Hitchcock, M. F. Lappert, P. L. Pye, *J. Chem. Soc.-Chem. Commun.*, **1977**, 196.
[58] M. F. Lappert, P. L. Pye, *J. Chem. Soc.-Dalton Trans.*, **1977**, 1283.
[59] P. B. Hitchcock, M. F. Lappert, P. L. Pye, *J. Chem. Soc.-Dalton Trans.*, **1978**, 826.
[60] M. F. Lappert, P. L. Pye, *J. Chem. Soc.-Dalton Trans.*, **1978**, 837.
[61] A. J. Carty, N. J. Taylor, W. F. Smith, M. F. Lappert, P. L. Pye, *J. Chem. Soc.-Chem. Commun.*, **1978**, 1017.
[62] A. J. Hartshorn, M. F. Lappert, K. Turner, *J. Chem. Soc.-Dalton Trans.*, **1978**, 348.
[63] P. B. Hitchcock, M. F. Lappert, P. L. Pye, S. Thomas, *J. Chem. Soc.-Dalton Trans.*, **1979**, 1929.
[64] M. F. Lappert, T. R. Martin, G. M. McLaughlin, *J. Chem. Soc.-Chem. Commun.*, **1980**, 635.
[65] P. B. Hitchcock, M. F. Lappert, P. Terreros, K. P. Wainwright, *J. Chem. Soc.-Chem. Commun.*, **1980**, 1180.
[66] P. B. Hitchcock, M. F. Lappert, P. Terreros, *J. Organomet. Chem.*, **1982**, *239*, C26.
[67] A. W. Coleman, P. B. Hitchcock, M. F. Lappert, R. K. Maskell, J. H. Muller, *J. Organomet. Chem.*, **1983**, *250*, C9.
[68] A. W. Coleman, P. B. Hitchcock, M. F. Lappert, R. K. Maskell, J. H. Muller, *J. Organomet. Chem.*, **1985**, *296*, 173.
[69] P. B. Hitchcock, M. F. Lappert, S. A. Thomas, A. J. Thorne, A. J. Carty, N. J. Taylor, *J. Organomet. Chem.*, **1986**, *315*, 27.
[70] B. Cetinkaya, P. B. Hitchcock, M. F. Lappert, D. B. Shaw, K. Spyropoulos, N. J. W. Warhurst, *J. Organomet. Chem.*, **1993**, *459*, 311.

[71] E. Cetinkaya, P. B. Hitchcock, H. Kucukbay, M. F. Lappert, S. Al-Juaid, *J. Organomet. Chem.*, **1994**, *481*, 89.
[72] M. J. Doyle, M. F. Lappert, P. L. Pye, P. Terreros, *J. Chem. Soc.-Dalton Trans.*, **1984**, 2355.
[73] M. F. Lappert, R. K. Maskell, *J. Organomet. Chem.*, **1984**, *264*, 217.
[74] M. F. Lappert, J. J. MacQuitty, P. L. Pye, *J. Chem. Soc.-Chem. Commun.*, **1977**, 411.
[75] M. F. Lappert, P. L. Pye, A. J. Rogers, G. M. McLaughlin, *J. Chem. Soc.-Dalton Trans.*, **1981**, 701.
[76] A. J. Arduengo, M. Kline, J. C. Calabrese, F. Davidson, *J. Am. Chem. Soc.*, **1991**, *113*, 9704.
[77] A. J. Arduengo, H. V. R. Dias, R. L. Harlow, M. Kline, *J. Am. Chem. Soc.*, **1992**, *114*, 5530.
[78] A. J. Arduengo, H. V. R. Dias, F. Davidson, R. L. Harlow, *J. Organomet. Chem.*, **1993**, *462*, 13.
[79] A. J. Arduengo, H. V. R. Dias, J. C. Calabrese, F. Davidson, *Organometallics*, **1993**, *12*, 3405.
[80] N. Kuhn, T. Kratz, G. Henkel, *J. Chem. Soc.-Chem. Commun.*, **1993**, 1778.
[81] N. Kuhn, G. Henkel, T. Kratz, J. Kreutzberg, R. Boese, A. H. Maulitz, *Chem. Ber.*, **1993**, *126*, 2041.
[82] N. Kuhn, G. Henkel, T. Kratz, *Chem. Ber.*, **1993**, *126*, 2047.
[83] A. J. Arduengo, H. V. R. Dias, D. A. Dixon, R. L. Harlow, W. T. Klooster, T. F. Koetzle, *J. Am. Chem. Soc.*, **1994**, *116*, 6812.
[84] A. J. Arduengo, S. F. Gamper, J. C. Calabrese, F. Davidson, *J. Am. Chem. Soc.*, **1994**, *116*, 4391.
[85] N. Kuhn, T. Kratz, R. Boese, D. Blaser, *J. Organomet. Chem.*, **1994**, *470*, C8.
[86] N. Kuhn, T. Kratz, D. Blaser, R. Boese, *Inorg. Chim. Acta*, **1995**, *238*, 179.
[87] A. Schafer, M. Weidenbruch, W. Saak, S. Pohl, *J. Chem. Soc.-Chem. Commun.*, **1995**, 1157.
[88] A. J. Arduengo, F. Davidson, H. V. R. Dias, J. R. Goerlich, D. Khasnis, W. J. Marshall, T. K. Prakasha, *J. Am. Chem. Soc.*, **1997**, *119*, 12742.
[89] W. A. Herrmann, F. C. Munck, G. R. J. Artus, O. Runte, R. Anwander, *Organometallics*, **1997**, *16*, 682.
[90] G. A. McGibbon, C. Heinemann, D. J. Lavorato, H. Schwarz, *Angew. Chem.-Int. Ed. Engl.*, **1997**, *36*, 1478.
[91] A. J. Arduengo, F. Davidson, R. Krafczyk, W. J. Marshall, M. Tamm, *Organometallics*, **1998**, *17*, 3375.
[92] D. E. Hibbs, M. B. Hursthouse, C. Jones, N. A. Smithies, *J. Chem. Soc.-Chem. Commun.*, **1998**, 869.
[93] R. W. Alder, M. E. Blake, C. Bortolotti, S. Bufali, C. P. Butts, E. Linehan, J. M. Oliva, A. G. Orpen, M. J. Quayle, *J. Chem. Soc.-Chem. Commun.*, **1999**, 241.

[94] F. Stabenow, W. Saak, M. Weidenbruch, *J. Chem. Soc.-Chem. Commun.*, **1999**, 1131.
[95] M. K. Denk, J. M. Rodezno, *J. Organomet. Chem.*, **2000**, *608*, 122.
[96] X. L. Zheng, G. E. Herberich, *Organometallics*, **2000**, *19*, 3751.
[97] C. D. Abernethy, A. H. Cowley, R. A. Jones, C. L. B. Macdonald, P. Shukla, L. K. Thompson, *Organometallics*, **2001**, *20*, 3629.
[98] M. K. Denk, J. M. Rodezno, S. Gupta, A. J. Lough, *J. Organomet. Chem.*, **2001**, *617*, 242.
[99] R. J. Baker, A. J. Davies, C. Jones, M. Kloth, *J. Organomet. Chem.*, **2002**, *656*, 203.
[100] M. L. Cole, C. Jones, P. C. Junk, *New J. Chem.*, **2002**, *26*, 1296.
[101] J. D. Gorden, C. L. B. Macdonald, A. H. Cowley, *J. Organomet. Chem.*, **2002**, *643*, 487.
[102] G. A. Grasa, R. M. Kissling, S. P. Nolan, *Org. Lett.*, **2002**, *4*, 3583.
[103] M. Niehues, G. Kehr, G. Erker, B. Wibbeling, R. Frohlich, O. Blacque, H. Berke, *J. Organomet. Chem.*, **2002**, *663*, 192.
[104] M. Niehues, G. Erker, G. Kehr, P. Schwab, R. Frohlich, O. Blacque, H. Berke, *Organometallics*, **2002**, *21*, 2905.
[105] M. K. Denk, K. Hatano, A. J. Lough, *Eur. J. Inorg. Chem.*, **2003**, 224.
[106] G. A. Grasa, T. Guveli, R. Singh, S. P. Nolan, *J. Org. Chem.*, **2003**, *68*, 2812.
[107] D. S. McGuinness, M. J. Green, K. J. Cavell, B. W. Skelton, A. H. White, *J. Organomet. Chem.*, **1998**, *565*, 165.
[108] H. M. J. Wang, I. J. B. Lin, *Organometallics*, **1998**, *17*, 972.
[109] U. Frenzel, T. Weskamp, F. J. Kohl, W. C. Schattenman, O. Nuyken, W. A. Herrmann, *J. Organomet. Chem.*, **1999**, *586*, 263.
[110] D. S. McGuinness, K. J. Cavell, B. W. Skelton, A. H. White, *Organometallics*, **1999**, *18*, 1596.
[111] V. P. W. Bohm, C. W. K. Gstottmayr, T. Weskamp, W. A. Herrmann, *J. Organomet. Chem.*, **2000**, *595*, 186.
[112] J. G. Hamilton, U. Frenzel, F. J. Kohl, T. Weskamp, J. J. Rooney, W. A. Herrmann, O. Nuyken, *J. Organomet. Chem.*, **2000**, *606*, 8.
[113] A. Furstner, L. Ackermann, B. Gabor, R. Goddard, C. W. Lehmann, R. Mynott, F. Stelzer, O. R. Thiel, *Chem.-Eur. J.*, **2001**, *7*, 3236.
[114] S. Grundemann, A. Kovacevic, M. Albrecht, J. W. Faller, R. H. Crabtree, *J. Chem. Soc.-Chem. Commun.*, **2001**, 2274.
[115] A. C. Hillier, H. M. Lee, E. D. Stevens, S. P. Nolan, *Organometallics*, **2001**, *20*, 4246.
[116] H. M. Lee, D. C. Smith, Z. J. He, E. D. Stevens, C. S. Yi, S. P. Nolan, *Organometallics*, **2001**, *20*, 794.
[117] D. S. McGuinness, N. Saendig, B. F. Yates, K. J. Cavell, *J. Am. Chem. Soc.*, **2001**, *123*, 4029.
[118] M. Albrecht, J. R. Miecznikowski, A. Samuel, J. W. Faller, R. H. Crabtree, *Organometallics*, **2002**, *21*, 3596.

[119] D. Bourgeois, A. Pancrazi, S. P. Nolan, J. Prunet, *J. Organomet. Chem.*, **2002**, *643*, 247.
[120] S. Caddick, F. G. N. Cloke, P. B. Hitchcock, J. Leonard, A. K. D. Lewis, D. McKerrecher, L. R. Titcomb, *Organometallics*, **2002**, *21*, 4318.
[121] S. Grundemann, A. Kovacevic, M. Albrecht, J. W. Faller, R. H. Crabtree, *J. Am. Chem. Soc.*, **2002**, *124*, 10473.
[122] R. F. R. Jazzar, S. A. Macgregor, M. F. Mahon, S. P. Richards, M. K. Whittlesey, *J. Am. Chem. Soc.*, **2002**, *124*, 4944.
[123] M. S. Viciu, R. F. Germaneau, O. Navarro-Fernandez, E. D. Stevens, S. P. Nolan, *Organometallics*, **2002**, *21*, 5470.
[124] R. F. R. Jazzar, P. H. Bhatia, M. F. Mahon, M. K. Whittlesey, *Organometallics*, **2003**, *22*, 670.
[125] D. Enders, K. Breuer, G. Raabe, J. Runsink, J. H. Teles, J. P. Melder, K. Ebel, S. Brode, *Angew. Chem.-Int. Ed. Engl.*, **1995**, *34*, 1021.
[126] D. Enders, H. Gielen, G. Raabe, J. Runsink, J. H. Teles, *Chem. Ber.*, **1996**, *129*, 1483.
[127] A. J. Arduengo, J. R. Goerlich, W. J. Marshall, *Liebigs Ann.-Recl.*, **1997**, 365.
[128] V. Nair, S. Bindu, V. Sreekumar, *Angew. Chem.-Int. Ed. Engl.*, **2004**, *43*, 5130.
[129] N. Kuhn, H. Bohnen, G. Henkel, *Z. Naturforsch. (B)*, **1994**, *49*, 1473.
[130] D. Enders, K. Breuer, J. Runsink, J. H. Teles, *Liebigs Ann.*, **1996**, 2019.
[131] D. Enders, H. Gielen, J. Runsink, K. Breuer, S. Brode, K. Boehn, *Eur. J. Inorg. Chem.*, **1998**, 913.
[132] O. Guerret, S. Sole, H. Gornitzka, G. Trinquier, G. Bertrand, *J. Organomet. Chem.*, **2000**, *600*, 112.
[133] D. Enders, H. Gielen, *J. Organomet. Chem.*, **2001**, *617*, 70.
[134] C. Buron, L. Stelzig, O. Guerret, H. Gornitzka, V. Romanenko, G. Bertrand, *J. Organomet. Chem.*, **2002**, *664*, 70.
[135] E. Diez-Barra, J. Guerra, R. I. Rodriguez-Curiel, S. Merino, J. Tejeda, *J. Organomet. Chem.*, **2002**, *660*, 50.
[136] W. A. Herrmann, M. Denk, J. Behm, W. Scherer, F. R. Klingan, H. Bock, B. Solouki, M. Wagner, *Angew. Chem.-Int. Ed. Engl.*, **1992**, *31*, 1485.
[137] M. Denk, R. Lennon, R. Hayashi, R. West, A. V. Belyakov, H. P. Verne, A. Haaland, M. Wagner, N. Metzler, *J. Am. Chem. Soc.*, **1994**, *116*, 2691.
[138] C. Heinemann, W. A. Herrmann, W. Thiel, *J. Organomet. Chem.*, **1994**, *475*, 73.
[139] B. Gehrhus, M. F. Lappert, J. Heinicke, R. Boese, D. Blaser, *J. Chem. Soc.-Chem. Commun.*, **1995**, 1931.
[140] B. Gehrhus, P. B. Hitchcock, M. F. Lappert, J. Heinicke, R. Boese, D. Blaser, *J. Organomet. Chem.*, **1996**, *521*, 211.
[141] C. Heinemann, T. Muller, Y. Apeloig, H. Schwarz, *J. Am. Chem. Soc.*, **1996**, *118*, 2023.
[142] C. Boehme, G. Frenking, *J. Am. Chem. Soc.*, **1996**, *118*, 2039.
[143] C. Boehme, G. Frenking, *Organometallics*, **1998**, *17*, 5801.

[144] M. K. Denk, K. Hatano, A. J. Lough, *Eur. J. Inorg. Chem.*, **1998**, 1067.
[145] A. Furstner, H. Krause, C. W. Lehmann, *J. Chem. Soc.-Chem. Commun.*, **2001**, 2372.
[146] B. Gehrhus, M. F. Lappert, *J. Organomet. Chem.*, **2001**, *617*, 209.
[147] L. Pause, M. Robert, J. Heinicke, O. Kuhl, *J. Chem. Soc.-Perkin Trans. 2*, **2001**, 1383.
[148] O. Kuhl, P. Lonnecke, J. Heinicke, *New J. Chem.*, **2002**, *26*, 1304.
[149] D. S. McGuinness, B. F. Yates, K. L. J. Cavell, *Organometallics*, **2002**, *21*, 5408.
[150] C. Heinemann, W. Thiel, *Chem. Phys. Lett.*, **1994**, *217*, 11.
[151] A. J. Arduengo, H. V. R. Dias, J. C. Calabrese, F. Davidson, *Inorg. Chem.*, **1993**, *32*, 1541.
[152] N. Kuhn, G. Henkel, T. Kratz, *Z. Naturforsch. (B)*, **1993**, *48*, 973.
[153] W. A. Herrmann, K. Ofele, M. Elison, F. E. Kuhn, P. W. Roesky, *J. Organomet. Chem.*, **1994**, *480*, C7.
[154] H. Schumann, M. Glanz, J. Winterfeld, H. Hemling, N. Kuhn, T. Kratz, *Chem. Ber.*, **1994**, *127*, 2369.
[155] A. J. Arduengo, S. F. Gamper, M. Tamm, J. C. Calabrese, F. Davidson, H. A. Craig, *J. Am. Chem. Soc.*, **1995**, *117*, 572.
[156] W. A. Herrmann, M. Elison, J. Fischer, C. Kocher, G. R. J. Artus, *Angew. Chem.-Int. Ed. Engl.*, **1995**, *34*, 2371.
[157] N. Kuhn, T. Kratz, D. Blaser, R. Boese, *Chem. Ber.*, **1995**, *128*, 245.
[158] W. A. Herrmann, G. M. Lobmaier, M. Elison, *J. Organomet. Chem.*, **1996**, *520*, 231.
[159] N. Kuhn, H. Bohnen, G. Henkel, J. Kreutzberg, *Z. Naturforsch. (B)*, **1996**, *51*, 1267.
[160] W. A. Herrmann, L. J. Goossen, M. Spiegler, *J. Organomet. Chem.*, **1997**, *547*, 357.
[161] W. A. Herrmann, G. Gerstberger, M. Spiegler, *Organometallics*, **1997**, *16*, 2209.
[162] M. J. Green, K. J. Cavell, B. W. Skelton, A. H. White, *J. Organomet. Chem.*, **1998**, *554*, 175.
[163] A. J. Arduengo, J. R. Goerlich, F. Davidson, W. J. Marshall, *Z. Naturforsch. (B)*, **1999**, *54*, 1350.
[164] W. J. Oldham, S. M. Oldham, B. L. Scott, K. D. Abney, W. H. Smith, D. A. Costa, *J. Chem. Soc.-Chem. Commun.*, **2001**, 1348.
[165] D. A. Dixon, A. J. Arduengo, *J. Phys. Chem.*, **1991**, *95*, 4180.
[166] A. J. Arduengo, D. A. Dixon, K. K. Kumashiro, C. Lee, W. P. Power, K. W. Zilm, *J. Am. Chem. Soc.*, **1994**, *116*, 6361.
[167] A. J. Arduengo, H. Bock, H. Chen, M. Denk, D. A. Dixon, J. C. Green, W. A. Herrmann, N. L. Jones, M. Wagner, R. West, *J. Am. Chem. Soc.*, **1994**, *116*, 6641.
[168] J. Huang, G. Grasa, S. P. Nolan, *Org. Lett.*, **1999**, *1*, 1307.
[169] F. Guillen, C. L. Winn, A. Alexakis, *Tetrahedron: Asymmetry*, **2001**, *12*, 2083.

[170] W. A. Herrmann, V. P. W. Bohm, C. W. K. Gstottmayr, M. Grosche, C. P. Reisinger, T. Weskamp, *J. Organomet. Chem.*, **2001**, *617*, 616.
[171] C. W. K. Gstottmayr, V. P. W. Bohm, E. Herdtweck, M. Grosche, W. A. Herrmann, *Angew. Chem.-Int. Ed. Engl.*, **2002**, *41*, 1363.
[172] G. W. Nyce, J. A. Lamboy, E. F. Connor, R. M. Waymouth, J. L. Hedrick, *Org. Lett.*, **2002**, *4*, 3587.
[173] C. W. Gao, X. C. Tao, Y. L. Qian, J. L. Huang, *J. Chem. Soc.-Chem. Commun.*, **2003**, 1444.
[174] Y. Sato, T. Yoshino, M. Mori, *Org. Lett.*, **2003**, *5*, 31.
[175] Y. H. Zhao, Y. Y. Zhou, D. D. Ma, J. P. Liu, L. Li, T. Y. Zhang, H. B. Zhang, *Org. Biomol. Chem.*, **2003**, *1*, 1643.
[176] L. D. Vazquez-Serrano, B. T. Owens, J. M. Buriak, *J. Chem. Soc.-Chem. Commun.*, **2002**, 2518.
[177] T. Y. Zhang, H. B. Zhang, *Tetrahedron Lett.*, **2002**, *43*, 193.
[178] M. Muehlhofer, T. Strassner, W. A. Herrmann, *Angew. Chem.-Int. Ed. Engl.*, **2002**, *41*, 1745.
[179] L. Ackermann, A. Furstner, T. Weskamp, F. J. Kohl, W. A. Herrmann, *Tetrahedron Lett.*, **1999**, *40*, 4787.
[180] J. K. Huang, E. D. Stevens, S. P. Nolan, J. L. Petersen, *J. Am. Chem. Soc.*, **1999**, *121*, 2674.
[181] L. Jafarpour, H. J. Schanz, E. D. Stevens, S. P. Nolan, *Organometallics*, **1999**, *18*, 5416.
[182] T. Weskamp, F. J. Kohl, W. Hieringer, D. Gleich, W. A. Herrmann, *Angew. Chem.-Int. Ed. Engl.*, **1999**, *38*, 2416.
[183] A. Furstner, M. Liebl, C. W. Lehmann, M. Picquet, R. Kunz, C. Bruneau, D. Touchard, P. H. Dixneuf, *Chem.-Eur. J.*, **2000**, *6*, 1847.
[184] S. B. Garber, J. S. Kingsbury, B. L. Gray, A. H. Hoveyda, *J. Am. Chem. Soc.*, **2000**, *122*, 8168.
[185] J. Cossy, S. BouzBouz, A. H. Hoveyda, *J. Organomet. Chem.*, **2001**, *624*, 327.
[186] S. W. Craig, J. A. Manzer, E. B. Coughlin, *Macromolecules*, **2001**, *34*, 7929.
[187] J. A. Smulik, S. T. Diver, *Tetrahedron Lett.*, **2001**, *42*, 171.
[188] M. S. M. Timmer, H. Ovaa, D. V. Filippov, G. A. van der Marel, J. H. van Boom, *Tetrahedron Lett.*, **2001**, *42*, 8231.
[189] B. De Clercq, F. Verpoort, *Tetrahedron Lett.*, **2002**, *43*, 9101.
[190] J. Louie, R. H. Grubbs, *Organometallics*, **2002**, *21*, 2153.
[191] G. Spagnol, M. P. Heck, S. P. Nolan, C. Mioskowski, *Org. Lett.*, **2002**, *4*, 1767.
[192] S. Demel, W. Schoefberger, C. Slugovc, F. Stelzer, *J. Mol. Catal. A-Chem.*, **2003**, *200*, 11.
[193] J. Guerra, *Synlett*, **2003**, 423.
[194] S. E. Lehman, J. E. Schwendeman, P. M. O'Donnell, K. B. Wagener, *Inorg. Chim. Acta*, **2003**, *345*, 190.

[195] C. Slugovc, S. Riegler, G. Hayn, R. Saf, F. Stelzer, *Macromol. Rapid Commun.*, **2003**, *24*, 435.
[196] B. De Clercq, F. Verpoort, *J. Organomet. Chem.*, **2003**, *672*, 11.
[197] L. Delaude, S. Delfosse, A. Richel, A. Demonceau, A. F. Noels, *J. Chem. Soc.-Chem. Commun.*, **2003**, 1526.
[198] J. McMurry, *Organic Chemistry*, 4th, Brooks/Cole, London, **1996**.
[199] M. B. Smith, J. March, *March's Advanced Organic Chemistry: Reactions, Mechanisms, and Structure*, 5th, John Wiley & Sons, Inc, Chichester, **2001**.
[200] D. F. Shriver, P. W. Atkins, C. H. Langford, *Inorganic Chemistry*, 2nd, Oxford University Press, Oxford, **1996**.
[201] M. Regitz, *Angew. Chem.-Int. Ed. Engl.*, **1991**, *30*, 674.
[202] R. W. Alder, M. E. Blake, *J. Chem. Soc.-Chem. Commun.*, **1997**, 1513.
[203] B. F. Bonini, M. Fochi, M. C. Franchini, G. Mazzanti, A. Ricci, J. P. Picard, J. Dunogues, J. M. Aizpurua, C. Palomo, *Synlett*, **1997**, 1321.
[204] M. K. Denk, A. Thadani, K. Hatano, A. J. Lough, *Angew. Chem.-Int. Ed. Engl.*, **1997**, *36*, 2607.
[205] H. W. Wanzlick, H. J. Kleiner, *Angew. Chem.*, **1961**, *73*, 493.
[206] D. M. Lemal, R. A. Lovald, K. I. Kawano, *J. Am. Chem. Soc.*, **1964**, *86*, 2518.
[207] H. E. Winberg, J. E. Carnahan, D. D. Coffman, M. Brown, *J. Am. Chem. Soc.*, **1965**, *87*, 2055.
[208] Y. F. Liu, P. E. Lindner, D. M. Lemal, *J. Am. Chem. Soc.*, **1999**, *121*, 10626.
[209] F. E. Hahn, L. Wittenbecher, D. Le Van, R. Frohlich, *Angew. Chem.-Int. Ed. Engl.*, **2000**, *39*, 541.
[210] H. W. Wanzlick, E. Schikora, *Angew. Chem.*, **1960**, *72*, 494.
[211] H. W. Wanzlick, *Angew. Chem.-Int. Ed. Engl.*, **1962**, *1*, 75.
[212] G. W. Nyce, T. Glauser, E. F. Connor, A. Mock, R. M. Waymouth, J. L. Hedrick, *J. Am. Chem. Soc.*, **2003**, *125*, 3046.
[213] A. J. Arduengo, H. V. R. Dias, J. C. Calabrese, F. Davidson, *J. Am. Chem. Soc.*, **1992**, *114*, 9724.
[214] D. S. McGuinness, K. J. Cavell, *Organometallics*, **2000**, *19*, 4918.
[215] A. J. Arduengo, J. R. Goerlich, W. J. Marshall, *J. Am. Chem. Soc.*, **1995**, *117*, 11027.
[216] M. Tafipolsky, W. Scherer, K. Ofele, G. Artus, B. Pedersen, W. A. Herrmann, G. S. McGrady, *J. Am. Chem. Soc.*, **2002**, *124*, 5865.
[217] L. Jafarpour, E. D. Stevens, S. P. Nolan, *J. Organomet. Chem.*, **2000**, *606*, 49.
[218] H. V. R. Dias, W. C. Jin, *Tetrahedron Lett.*, **1994**, *35*, 1365.
[219] W. A. Herrmann, L. J. Goossen, C. Kocher, G. R. J. Artus, *Angew. Chem.-Int. Ed. Engl.*, **1996**, *35*, 2805.
[220] A. A. Danopoulos, S. Winston, W. B. Motherwell, *J. Chem. Soc.-Chem. Commun.*, **2002**, 1376.
[221] V. Nair, S. Bindu, V. Sreekumar, N. P. Rath, *Org. Lett.*, **2003**, *5*, 665.

[222] M. C. Perry, K. Burgess, *Tetrahedron: Asymmetry*, **2003**, *14*, 951.
[223] S. Julia, P. Sala, J. del Mazo, M. Sancho, C. Ochoa, J. Elguero, J. P. Fayet, M. C. Vertut, *J. Heterocycl. Chem.*, **1982**, *19*, 1141.
[224] E. Diez-Barra, A. de la Hoz, A. Sanchez-Migallon, J. Tejeda, *Heterocycles*, **1992**, *34*, 1365.
[225] R. M. Claramunt, J. Elguero, T. Meco, *J. Heterocycl. Chem.*, **1983**, *20*, 1245.
[226] K. J. Harlow, A. F. Hill, T. Welton, *Synthesis*, **1996**, 697.
[227] A. J. Arduengo, US Patent No. 5077414, **1991**.
[228] N. Kuhn, T. Kratz, *Synthesis*, **1993**, 561.
[229] J. C. Green, R. G. Scurr, P. L. Arnold, F. G. N. Cloke, *J. Chem. Soc.-Chem. Commun.*, **1997**, 1963.
[230] S. Caddick, F. G. N. Cloke, G. K. B. Clentsmith, P. B. Hitchcock, D. McKerrecher, L. R. Titcomb, M. R. V. Williams, *J. Organomet. Chem.*, **2001**, *617*, 635.
[231] W. Baratta, E. Herdtweck, W. A. Herrmann, P. Rigo, J. D. Schwarz, *Organometallics*, **2002**, *21*, 2101.
[232] J. C. C. Chen, I. J. B. Lin, *Organometallics*, **2000**, *19*, 5113.
[233] A. A. D. Tulloch, A. A. Danopoulos, R. P. Tooze, S. M. Cafferkey, S. Kleinhenz, M. B. Hursthouse, *J. Chem. Soc.-Chem. Commun.*, **2000**, 1247.
[234] A. A. D. Tulloch, A. A. Danopoulos, S. Winston, S. Kleinhenz, G. Eastham, *J. Chem. Soc.-Dalton Trans.*, **2000**, 4499.
[235] T. Weskamp, V. P. W. Bohm, W. A. Herrmann, *J. Organomet. Chem.*, **2000**, *600*, 12.
[236] K. M. Lee, J. C. C. Chen, I. J. B. Lin, *J. Organomet. Chem.*, **2001**, *617*, 364.
[237] A. A. D. Tulloch, A. A. Danopoulos, S. Kleinhenz, M. E. Light, M. B. Hursthouse, G. Eastham, *Organometallics*, **2001**, *20*, 2027.
[238] L. Jafarpour, S. P. Nolan, *J. Organomet. Chem.*, **2001**, *617*, 17.
[239] A. M. Magill, D. S. McGuinness, K. J. Cavell, G. J. P. Britovsek, V. C. Gibson, A. J. P. White, D. J. Williams, A. H. White, B. W. Skelton, *J. Organomet. Chem.*, **2001**, *617*, 546.
[240] J. K. Huang, H. J. Schanz, E. D. Stevens, S. P. Nolan, *Organometallics*, **1999**, *18*, 2370.
[241] A. A. Danopoulos, D. M. Hankin, G. Wilkinson, S. M. Cafferkey, T. K. N. Sweet, M. B. Hursthouse, *Polyhedron*, **1997**, *16*, 3879.
[242] B. Bildstein, M. Malaun, H. Kopacka, K. H. Ongania, K. Wurst, *J. Organomet. Chem.*, **1999**, *572*, 177.
[243] A. Dohring, J. Gohre, P. W. Jolly, B. Kryger, J. Rust, G. P. J. Verhovnik, *Organometallics*, **2000**, *19*, 388.
[244] K. Ofele, W. A. Herrmann, D. Mihalios, M. Elison, E. Herdtweck, W. Scherer, J. Mink, *J. Organomet. Chem.*, **1993**, *459*, 177.
[245] N. Kuhn, T. Kratz, R. Boese, D. Blaser, *J. Organomet. Chem.*, **1994**, *479*, C32.

[246] T. Weskamp, W. C. Schattenman, W. C. Spiegler, W. A. Herrmann, *Angew. Chem.-Int. Ed. Engl.*, **1998**, *37*, 2490.
[247] T. Weskamp, F. J. Kohl, W. A. Herrmann, *J. Organomet. Chem.*, **1999**, *582*, 362.
[248] M. Scholl, T. M. Trnka, J. P. Morgan, R. H. Grubbs, *Tetrahedron Lett.*, **1999**, *40*, 2247.
[249] L. Jafarpour, J. K. Huang, E. D. Stevens, S. P. Nolan, *Organometallics*, **1999**, *18*, 3760.
[250] J. K. Huang, E. D. Stevens, S. P. Nolan, *Organometallics*, **2000**, *19*, 1194.
[251] N. M. Scott, R. Dorta, E. D. Stevens, A. Correa, L. Cavallo, S. P. Nolan, *J. Am. Chem. Soc.*, **2005**, *127*, 3516.
[252] M. Prinz, M. Grosche, E. Herdtweck, W. A. Herrmann, *Organometallics*, **2000**, *19*, 1692.
[253] J. Louie, R. H. Grubbs, *J. Chem. Soc.-Chem. Commun.*, **2000**, 1479.
[254] R. E. Douthwaite, D. Haussinger, M. L. H. Green, P. J. Silcock, P. T. Gomes, A. M. Martins, A. A. Danopoulos, *Organometallics*, **1999**, *18*, 4584.
[255] C. D. Abernethy, J. A. C. Clyburne, A. H. Cowley, R. A. Jones, *J. Am. Chem. Soc.*, **1999**, *121*, 2329.
[256] R. Faust, B. Gobelt, *J. Chem. Soc.-Chem. Commun.*, **2000**, 919.
[257] C. A. Tolman, *Chem. Rev.*, **1977**, *77*, 313.
[258] J. Bruckmann, C. Kruger, *J. Organomet. Chem.*, **1997**, *536*, 465.
[259] D. J. Darensbourg, M. S. Zimmer, P. Rainey, D. L. Larkins, *Inorg. Chem.*, **2000**, *39*, 1578.
[260] D. J. Darensbourg, P. Rainey, D. L. Larkins, J. H. Reibenspies, *Inorg. Chem.*, **2000**, *39*, 473.
[261] M. L. Clarke, A. M. Z. Slawin, J. D. Woollins, *Polyhedron*, **2003**, *22*, 19.
[262] W. A. Herrmann, C. Kocher, *Angew. Chem.-Int. Ed. Engl.*, **1997**, *36*, 1162.
[263] X. W. Li, J. Su, G. H. Robinson, *J. Chem. Soc.-Chem.Commun.*, **1996**, 2683.
[264] M. D. Francis, D. E. Hibbs, M. B. Hursthouse, C. Jones, N. A. Smithies, *J. Chem. Soc.-Dalton Trans.*, **1998**, 3249.
[265] R. J. Baker, M. L. Cole, C. Jones, M. F. Mahon, *J. Chem. Soc.-Dalton Trans.*, **2002**, 1992.
[266] C. D. Abernethy, R. J. Baker, M. L. Cole, A. J. Davies, C. Jones, *Transit. Met. Chem.*, **2003**, *28*, 296.
[267] C. J. Carmalt, A. H. Cowley, *"The reactions of stable nucleophilic carbenes with main group compounds"*, in *Advances in Inorganic Chemistry*, **2000**. 1-32.
[268] S. J. Black, D. E. Hibbs, M. B. Hursthouse, C. Jones, K. M. A. Malik, N. A. Smithies, *J. Chem. Soc.-Dalton Trans.*, **1997**, 4313.
[269] L. Weber, E. Dobbert, H. G. Stammler, B. Neumann, R. Boese, D. Blaser, *Chem. Ber.*, **1997**, *130*, 705.

[270] A. Kovacevic, S. Grundemann, J. R. Miecznikowski, E. Clot, O. Eisenstein, R. H. Crabtree, *J. Chem. Soc.-Chem. Commun.*, **2002**, 2580.
[271] S. Wingerter, M. Pfeiffer, A. Murso, C. Lustig, T. Stey, V. Chandrasekhar, D. Stalke, *J. Am. Chem. Soc.*, **2001**, *123*, 1381.
[272] A. Miyashita, A. Yasuda, H. Takaya, K. Toriumi, T. Ito, T. Souchi, R. Noyori, *J. Am. Chem. Soc.*, **1980**, *102*, 7932.
[273] G. Parrinello, J. K. Stille, *J. Am. Chem. Soc.*, **1987**, *109*, 7122.
[274] T. R. Ward, L. M. Venanzi, A. Albinati, F. Lianza, T. Gerfin, V. Gramlich, G. M. R. Tombo, *Helv. Chim. Acta*, **1991**, *74*, 983.
[275] U. Matteoli, V. Beghetto, C. Schiavon, A. Scrivanti, G. Menchi, *Tetrahedron: Asymmetry*, **1997**, *8*, 1403.
[276] S. D. de Paule, S. Jeulin, V. Ratovelomanana-Vidal, J. P. Genet, N. Champion, P. Dellis, *Tetrahedron Lett.*, **2003**, *44*, 823.
[277] E. Lindner, M. Kemmler, H. A. Mayer, P. Wegner, *J. Am. Chem. Soc.*, **1994**, *116*, 348.
[278] G. Y. Li, P. J. Fagan, P. L. Watson, *Angew. Chem.-Int. Ed. Engl.*, **2001**, *40*, 1106.
[279] M. A. O. Volland, B. F. Straub, I. Gruber, F. Rominger, P. Hofmann, *J. Organomet. Chem.*, **2001**, *617*, 288.
[280] K. Kromm, F. Hampel, J. A. Gladysz, *Organometallics*, **2002**, *21*, 4264.
[281] V. Cesar, S. Bellemin-Laponnaz, L. H. Gade, *Organometallics*, **2002**, *21*, 5204.
[282] P. L. Arnold, A. C. Scarisbrick, A. J. Blake, C. Wilson, *J. Chem. Soc.-Chem. Commun.*, **2001**, 2340.
[283] W. A. Herrmann, L. J. Goossen, M. Spiegler, *Organometallics*, **1998**, *17*, 2162.
[284] M. Scholl, S. Ding, C. W. Lee, R. H. Grubbs, *Org. Lett.*, **1999**, *1*, 953.
[285] C. Bolm, M. Kesselgruber, G. Raabe, *Organometallics*, **2002**, *21*, 707.
[286] M. C. Perry, X. H. Cui, M. T. Powell, D. R. Hou, J. H. Reibenspies, K. Burgess, *J. Am. Chem. Soc.*, **2003**, *125*, 113.
[287] J. Schwarz, V. P. W. Bohm, M. G. Gardiner, M. Grosche, W. A. Herrmann, W. Hieringer, G. Raudaschl-Sieber, *Chem.-Eur. J.*, **2000**, *6*, 1773.
[288] S. C. Schurer, S. Gessler, N. Buschmann, S. Blechert, *Angew. Chem.-Int. Ed. Engl.*, **2000**, *39*, 3898.
[289] S. Varray, R. Lazaro, J. Martinez, F. Lamaty, *Organometallics*, **2003**, *22*, 2426.
[290] L. Jafarpour, S. P. Nolan, *"Transition-metal systems bearing a nucleophilic carbene ancillary ligand: From thermochemistry to catalysis"*, in *Advances in Organometallic Chemistry*, **2001**. 181-222.
[291] L. Delaude, M. Szypa, A. Demonceau, A. F. Noels, *Adv. Synth. Catal.*, **2002**, *344*, 749.
[292] T. M. Trnka, J. P. Morgan, M. S. Sanford, T. E. Wilhelm, M. Scholl, T. L. Choi, S. Ding, M. W. Day, R. H. Grubbs, *J. Am. Chem. Soc.*, **2003**, *125*, 2546.

[293] S. T. Nguyen, L. K. Johnson, R. H. Grubbs, *J. Am. Chem. Soc.*, **1992**, *114*, 3974.
[294] S. T. Nguyen, R. H. Grubbs, J. W. Ziller, *J. Am. Chem. Soc.*, **1993**, *115*, 9858.
[295] P. Schwab, M. B. France, J. W. Ziller, R. H. Grubbs, *Angew. Chem.-Int. Ed. Engl.*, **1995**, *34*, 2039.
[296] P. Schwab, R. H. Grubbs, J. W. Ziller, *J. Am. Chem. Soc.*, **1996**, *118*, 100.
[297] M. Scholl, T. M. Trnka, J. P. Morgan, R. H. Grubbs, *Tetrahedron Lett.*, **1999**, *40*, 2247.
[298] T. Weskamp, W. C. Schattenman, M. Spiegler, W. A. Herrmann, *Angew. Chem.-Int. Ed. Engl.*, **1999**, *38*, 262.
[299] A. K. Chatterjee, R. H. Grubbs, *Org. Lett.*, **1999**, *1*, 1751.
[300] A. K. Chatterjee, J. P. Morgan, M. Scholl, R. H. Grubbs, *J. Am. Chem. Soc.*, **2000**, *122*, 3783.
[301] A. Furstner, O. R. Thiel, G. Blanda, *Org. Lett.*, **2000**, *2*, 3731.
[302] C. W. Lee, R. H. Grubbs, *Org. Lett.*, **2000**, *2*, 2145.
[303] L. Hyldtoft, R. Madsen, *J. Am. Chem. Soc.*, **2000**, *122*, 8444.
[304] I. Efremov, L. A. Paquette, *J. Am. Chem. Soc.*, **2000**, 9324.
[305] J. Limanto, M. L. Snapper, *J. Am. Chem. Soc.*, **2000**, *122*, 8071.
[306] H. D. Maynard, S. Y. Okada, R. H. Grubbs, *Macromolecules*, **2000**, *33*, 6239.
[307] J. A. Smulik, S. T. Diver, *Org. Lett.*, **2000**, *2*, 2271.
[308] D. L. Wright, J. P. Schulte, M. A. Page, *Org. Lett.*, **2000**, *2*, 1847.
[309] E. L. Dias, S. T. Nguyen, R. H. Grubbs, *J. Am. Soc. Chem.*, **1997**, *119*, 3887.
[310] T. Weskamp, V. P. W. Bohm, W. A. Herrmann, *J. Organomet. Chem.*, **1999**, *585*, 348.
[311] T. Welton, *Chem. Rev.*, **1999**, *99*, 2071.
[312] P. Wasserscheid, W. Keim, *Angew. Chem.-Int. Ed. Engl.*, **2000**, *39*, 3772.
[313] J. Dupont, R. F. de Souza, P. A. Z. Suarez, *Chem. Rev.*, **2002**, *102*, 3667.
[314] A. J. Carmichael, M. J. Earle, J. D. Holbrey, P. B. McCormac, K. R. Seddon, *Org. Lett.*, **1999**, *1*, 997.
[315] J. Howarth, A. Dallas, *Molecules*, **2000**, *5*, 851.
[316] L. J. Xu, W. P. Chen, J. L. Xiao, *Organometallics*, **2000**, *19*, 1123.
[317] C. L. Yang, H. M. Lee, S. P. Nolan, *Org. Lett.*, **2001**, *3*, 1511.
[318] C. L. Yang, S. P. Nolan, *Synlett*, **2001**, 1539.
[319] K. Selvakumar, A. Zapf, M. Beller, *Org. Lett.*, **2002**, *4*, 3031.
[320] D. S. McGuinness, K. J. Cavell, B. F. Yates, *J. Chem. Soc.-Chem. Commun.*, **2001**, 355.
[321] D. S. McGuinness, K. J. Cavell, B. F. Yates, B. W. Skelton, A. H. White, *J. Am. Chem. Soc.*, **2001**, *123*, 8317.
[322] D. S. McGuinness, W. Mueller, P. Wasserscheid, K. J. Cavell, B. W. Skelton, A. H. White, U. Englert, *Organometallics*, **2002**, *21*, 175.

Hydrogen-Bonded Organic Precursors to Metal-*N*-Heterocyclic Carbene Complexes

2.1: Introduction

This chapter reports the preparation and characterisation of a series of hydrogen-bonded organic metal-*N*-heterocyclic carbene precursors. Before reviewing some of the reports within the literature that are more specifically related to this study, a brief introduction to the concept of hydrogen-bonding would perhaps be useful.

A hydrogen bond, [$^{\delta-}$A–H$^{\delta+}$·····B$^{\delta-}$], may be described as an electrostatic interaction between the partially deshielded Lewis acidic hydrogen atom of a hydrogen bond donor group (A-H), and the lone-pair or polarisable π-electron cloud of a Lewis basic hydrogen bond acceptor group (B) (Figure 2.1).[1] Evidence for hydrogen-bonding within a given system may be provided by IR or ^{1}H-NMR spectroscopy, by means of a shift in ν(A-H) or δ(A-H).[1] Single crystal diffraction experiments are perhaps more useful as they provide precise information of molecular structure in the solid state, which facilitates comparison of hydrogen-bonding interactions. The atom or group (A) bearing the Lewis acidic hydrogen and the hydrogen bond acceptor group (B) may be located by x-ray diffraction, although precise hydrogen atom positions can only be determined through neutron diffraction studies.

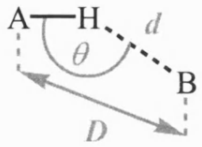

Figure 2.1: Convention for the description of hydrogen-bonding interactions

In line with convention, throughout this thesis hydrogen-bonding interactions in the solid state will be compared in terms of the parameters *D*, *d* and *θ*; where *D* is the distance between the atom or group (A) bearing the Lewis acidic hydrogen atom and the Lewis basic hydrogen bond acceptor group (B), *d* corresponds to the H·····B separation, and *θ* represents the A–H·····B angle (Figure 2.1).[1]

2.1.1: Background

Remarkably stable *N*-heterocyclic carbenes have been the focus of considerable research interest ever since Arduengo *et al.* reported the isolation of the first stable crystalline imidazol-2-ylidene.[2] They are generally regarded as analogues to the phosphine ligands ubiquitous in organometallic chemistry,[3] and as a result their coordination chemistry has been extensively studied.[3-5] Indeed, transition metal-*N*-heterocyclic carbenes are now finding utility in the catalysis of carbon-carbon bond forming reactions[6-10] and olefin metathesis.[11-17]

Metal-*N*-heterocyclic carbenes are often prepared via the *in situ* deprotonation of azolium precursor salts by metal source compounds possessing basic ligands (Scheme 2.1).[18-30] This methodology is quite well developed in terms of the diversity of *N*-heterocyclic carbene that can be incorporated into the resulting metal complex. Indeed, this synthetic strategy has been applied to the preparation of imidazolium, benzimidazolium, imidazolinium, and triazolium derived metal-*N*-heterocyclic carbene complexes.[25-29]

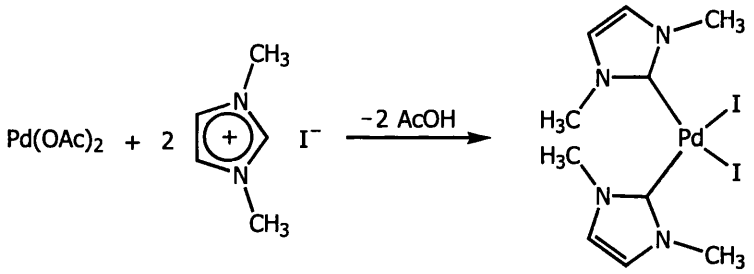

Scheme 2.1: A metal-*N*-heterocyclic carbene complex via imidazolium salt deprotonation

However, variation of the azolium salt anion has attracted only limited attention in comparison. The *in situ* deprotonation of an azolium halide with a suitable metal source generates the corresponding neutral, halide ligated, metal-*N*-heterocyclic carbene complex (Scheme 2.1).[24] Exchange of the azolium halide salt anion via salt metathesis[29] allows the preparation of cationic metal-*N*-heterocyclic carbene species possessing non-coordinating anions by means of this *in situ* deprotonation methodology (Scheme 2.2).[29, 30]

The azolium salt anion affects the binding mode of pyridyl-sidearm functionalised chelating *N*-heterocyclic carbene ligands in cationic metal fragments prepared via this *in situ* deprotonation methodology. Subtle variation of the anion in otherwise identical azolium salts allows metal complexes with both conventional C(2)- and unusual C(4/5)-bound (Scheme 2.2) *N*-heterocyclic carbenes to be accessed by means of this synthetic strategy.[31] Since the non-coordinating anion can have such an impact on the chemistry of cationic metal-*N*-heterocyclic carbene species, variation of the azolium salt anion provides an opportunity to tailor the properties of such metal complexes that, to date, has been under-exploited in comparison to modification of the azolium salt cation.

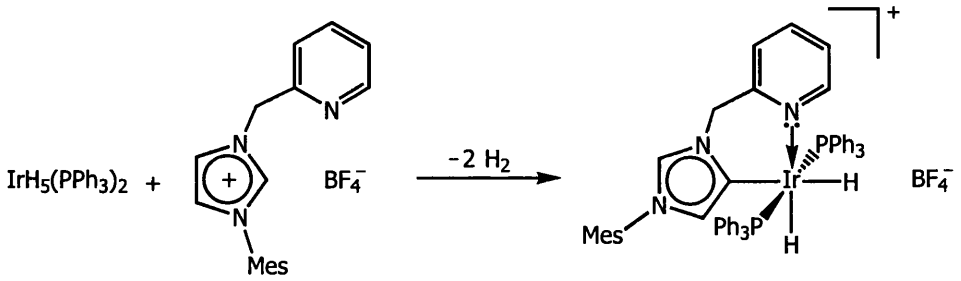

Scheme 2.2: A cationic metal-*N*-heterocyclic carbene via imidazolium salt deprotonation

The *in situ* deprotonation methodology is not only a convenient strategy for the synthesis of metal species bearing *N*-heterocyclic carbene ligation, but, since the azolium precursor salt anion may be incorporated into the resulting metal complex as an ancillary ligand (Scheme 2.1), it also represents a useful approach to the preparation of metal complexes possessing reactive substituents such as amide and alkoxide functionalities. Conceivably, the properties of these species could be tailored to provide catalytically active metal-*N*-heterocyclic carbenes by fine-tuning the reactive functionality via systematic variation of the azolium salt anion.

In addition to representing convenient precursors to metal-*N*-heterocyclic carbene complexes; azolium salts are also utilised as room temperature ionic liquids.[32, 33] Systematic variation of the anion should facilitate optimisation of the molten-salt solvent system for any given application, which may subsequently lead to these non-volatile, non-flammable, organic salts being considered viable alternatives to hydrocarbon solvents.

2.1.2: Imidazol-2-ylidenes and Organic Acids

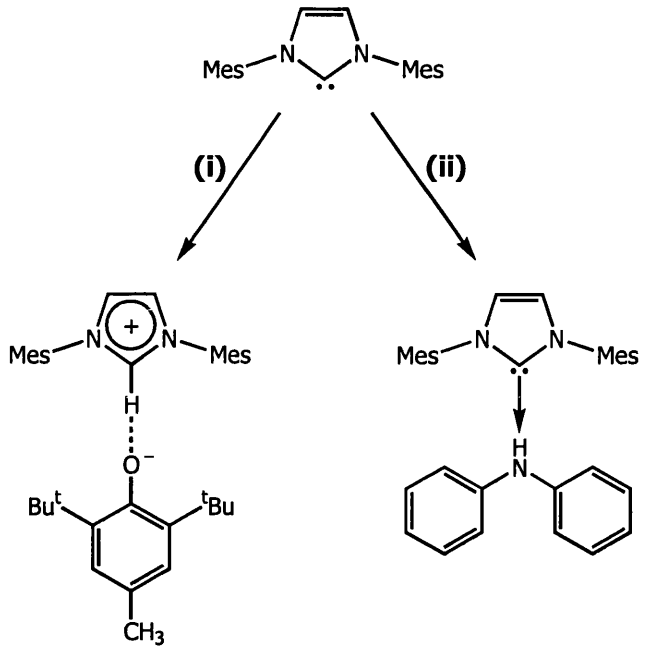

Scheme 2.3: Reaction of an imidazol-2-ylidene with acidic organic compounds **(i)** 2,6-di-*tert*-butyl-4-methylphenol, toluene; **(ii)** diphenylamine, toluene

The biscarbene-proton complex reported by Arduengo *et al.*[34] demonstrates that strongly basic imidazol-2-ylidenes[35, 36] may behave as hydrogen bond acceptors and that imidazolium cations are C(2)-H hydrogen bond donors. Furthermore, the less acidic C(4/5)-H backbone hydrogen atoms of imidazolium cations have also been observed to participate in hydrogen-bonding interactions;[37, 38] indeed, the polymeric supramolecular extended structure of simple imidazolium halide salts is the result of intramolecular and intermolecular hydrogen-bonding between the halide anions and imidazolium cations through C(2)–H·····X^- and C(4/5)–H·····X^- contacts, respectively.[34]

Our recent report on the reaction of an imidazol-2-ylidene with acidic organic compounds[39] demonstrates that azolium salts with non-conventional anions may be prepared by exploiting the basicity of these *N*-heterocyclic carbenes.[34-36, 39-41] Specifically, the direct reaction of a substituted phenol with an imidazol-2-ylidene was shown to yield the related imidazolium phenoxide salt (Scheme 2.3).[39] The

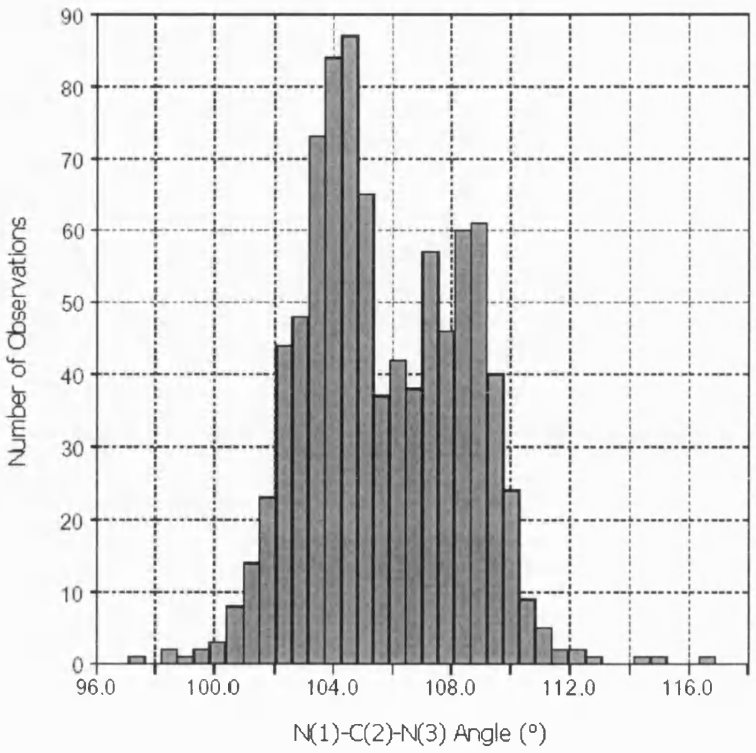

Figure 2.2: N(1)-C(2)-N(3) angle within the heterocyclic core of imidazolium salts and imidazol-2-ylidene species

analogous reaction of a secondary amine with the imidazol-2-ylidene formed a neutral imidazol-2-ylidene:amine adduct rather than an imidazolium amide salt (Scheme 2.3).[39] Although not an azolium salt, the *in situ* deprotonation of this adduct would still facilitate the incorporation of a reactive amide ligand into a metal-*N*-heterocyclic carbene complex.

The structural differences observed in the heterocyclic cores of imidazolium salts and imidazol-2-ylidenes allow the differentiation of these species on the basis of data obtained by single crystal x-ray diffraction. Indeed, the results from a search of the Cambridge Structural Database (Version 5.25, January 2004 Update)[42] clearly show that the heterocyclic core metrical parameters of imidazolium salts and imidazol-2-ylidene species are quite different (Figures 2.2 and 2.3).

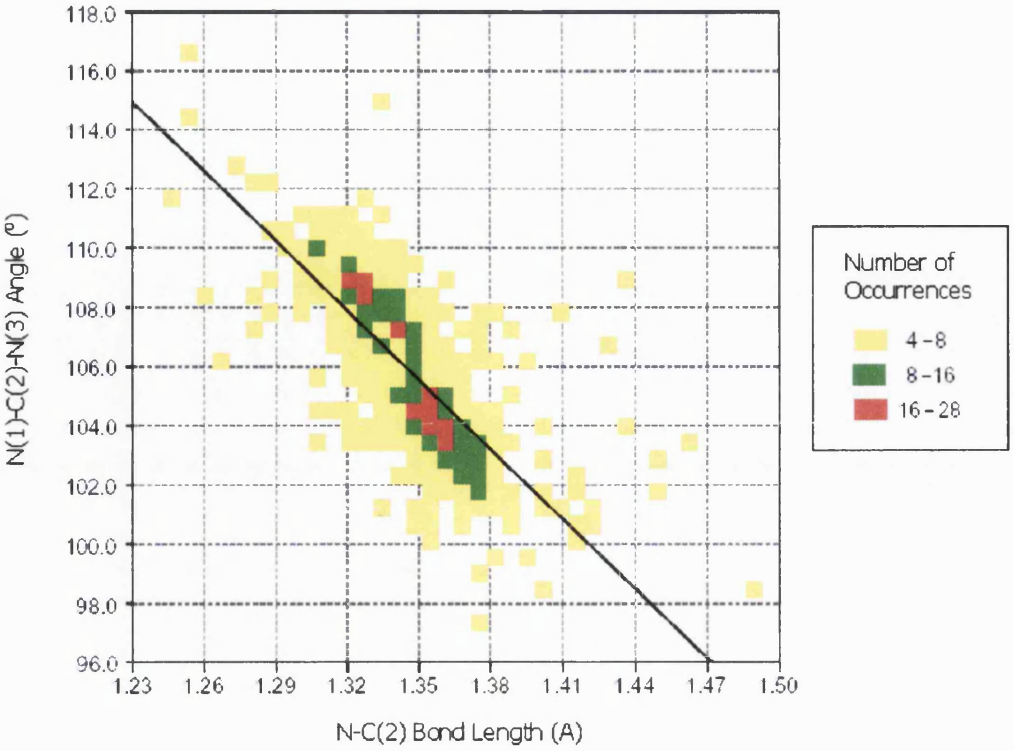

Figure 2.3: Correlation between N(1)-C(2)-N(3) angle and N-C(2) bond length in imidazolium salts and imidazol-2-ylidene species

Imidazol-2-ylidenes possess more acute N(1)-C(2)-N(3) angles than imidazolium salts (Figure 2.2); for instance, the N(1)-C(2)-N(3) angles within the heterocyclic cores of the neutral compound 1,3-bis-(2,4,6-trimethylphenyl)-imidazol-2-ylidene (IMes) and the cation of the related organic salt 1,3-bis-(2,4,6-trimethylphenyl)-imidazolium chloride ([IMesH][Cl]) are reported as 101.4(2)°[43] and 108.7(4)°,[34] respectively. Additionally, the significantly shorter N-C(2) bond lengths observed within imidazolium cations compared to those of imidazol-2-ylidenes (1.326(5) Å within the heterocyclic core of the 1,3-bis-(2,4,6-trimethylphenyl)-imidazolium chloride salt ([IMesH][Cl])[34] versus 1.368(4) Å observed within the Lewis basic neutral organic compound 1,3-bis-(2,4,6-trimethylphenyl)-imidazol-2-ylidene[43]) demonstrate that the delocalisation of electronic charge around the heterocyclic ring of these systems is more pronounced than is the case in imidazol-2-ylidenes (Figure 2.3).

2.2: Imidazolium Phenoxide:Phenol Adducts

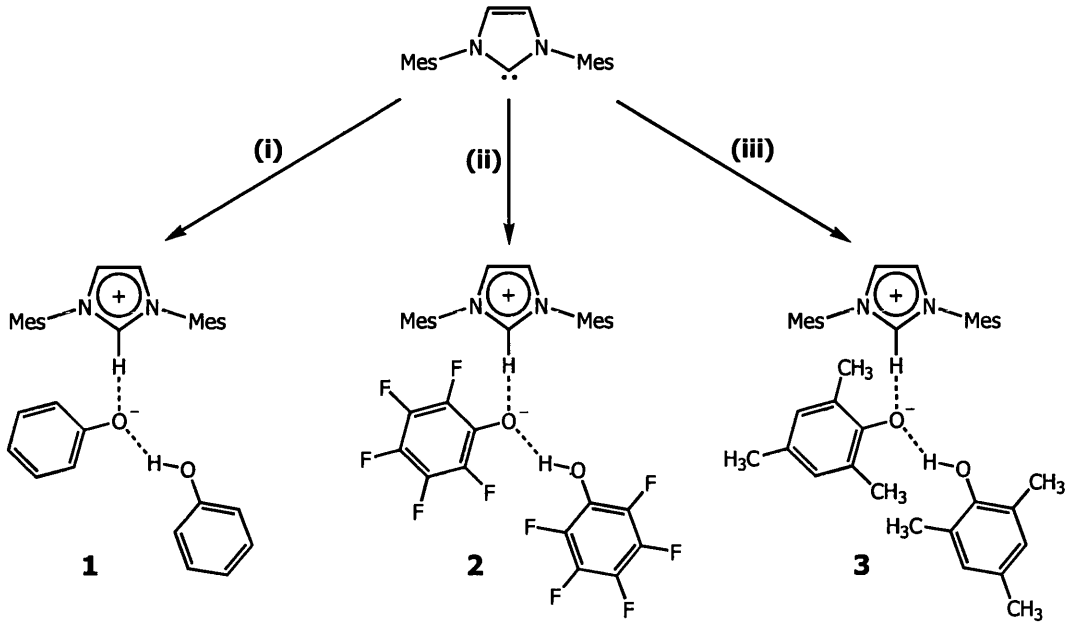

Scheme 2.4: Reaction of an imidazol-2-ylidene with acidic organic compounds **(i)** phenol, toluene; **(ii)** pentafluorophenol, toluene; **(iii)** 2,4,6-trimethylphenol, toluene

The reaction of 1,3-bis-(2,4,6-trimethylphenyl)-imidazol-2-ylidene (IMes) with two equivalents of phenol (PhOH), pentafluorophenol, or 2,4,6-trimethylphenol (MesOH), results in the formation of imidazolium phenoxide:phenol adducts **1**, **2** and **3** (Scheme 2.4), respectively. Attempts to prepare the imidazolium phenoxide salts [IMesH][OPh] and [IMesH][OMes] from dilute toluene solution, via the stoichiometric reaction of 1,3-bis-(2,4,6-trimethylphenyl)-imidazol-2-ylidene with one equivalent of phenol or 2,4,6-trimethylphenol, once again yield **1** and **3** as the only crystalline products (Scheme 2.4).[¥] Reetz *et al.* have recently reported the preparation of a tetra-*n*-butylammonium phenoxide:phenol species, and, similarly, were unable to isolate the related tetra-*n*-butylammonium phenoxide salt.[44]

Imidazolium phenoxide:phenol adducts **1**, **2** and **3** (Scheme 2.4) readily crystallise from cooling toluene solution, but do not redissolve in toluene on gentle warming.

[¥] ^{1}H-NMR spectroscopy suggests that the reaction of 1,3-bis-(2,4,6-trimethylphenyl)-imidazol-2-ylidene with one equivalent of 2,4,6-trimethylphenol in dilute tetrahydrofuran solution yields a mixture of [IMesH][OMes] and compound **3**; subsequent separation of these two species could not be achieved and, therefore, no further characterisation carried out.

These species are, however, soluble in dichloromethane and chloroform, although significant decomposition is observed over the course of half an hour in such solvents. Characterisation of **1** and **3** by ^{1}H- and ^{13}C{^{1}H}-NMR spectroscopy was undertaken in d_6-DMSO solution, since decomposition is less pronounced in this solvent. Unfortunately, compound **2** is not sufficiently soluble in d_6-DMSO to facilitate the acquisition of NMR data; ^{1}H- and ^{13}C{^{1}H}-NMR spectra for this species were, therefore, recorded in CD_2Cl_2 solution. The NMR data for **1**, **2** and **3** is consistent with these species being hydrogen-bonded imidazolium phenoxides (Scheme 2.4). In light of their similarities, the ^{1}H-NMR spectra of compounds **1** and **3** recorded in d_6-DMSO solution will be discussed together, and, likewise, the data from **2** and **3** in CD_2Cl_2 will be examined concurrently.

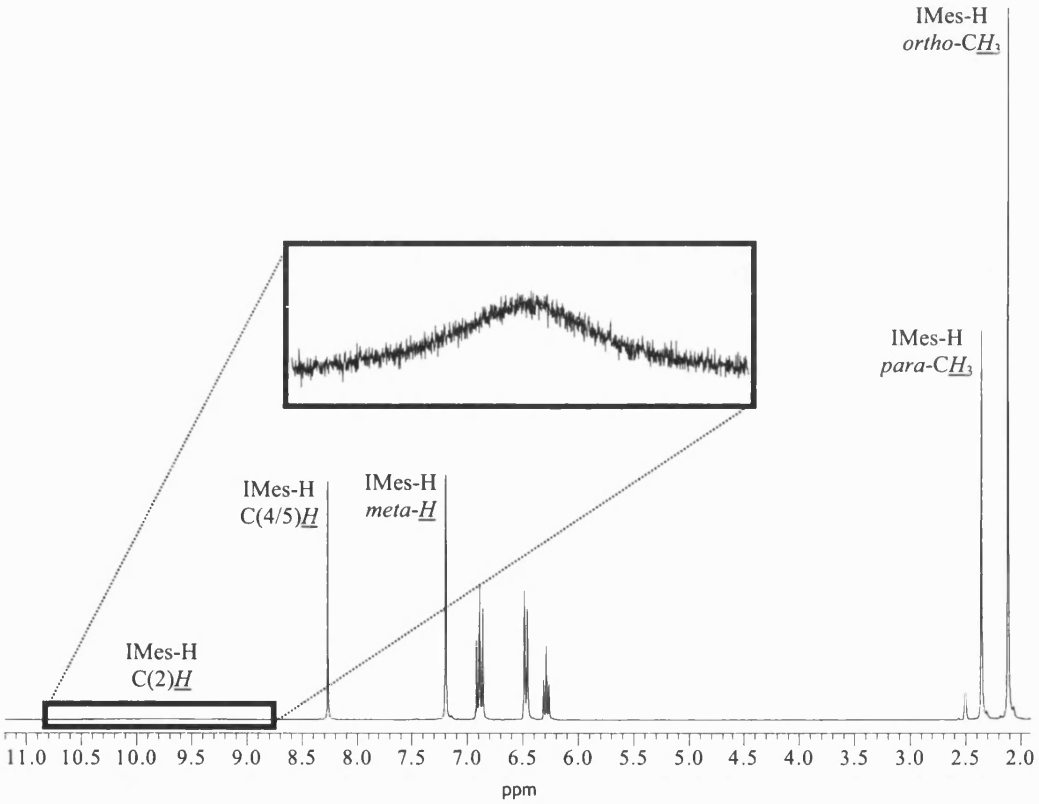

Figure 2.4: ^{1}H-NMR spectrum of **1** in d_6-DMSO recorded at 300 MHz

Integration of the ^{1}H-NMR data acquired from d_6-DMSO solutions of compounds **1** (Figure 2.4) and **3** reveals that these species are composed of one imidazol-2-ylidene-derived moiety and two units related to the phenol (Scheme 2.4). The acidic imidazolium C(2)-H and phenolic protons are not fully accounted for in the ^{1}H-NMR spectra of **1** (Figure 2.4) and **3**, which suggests that exchange processes,

consistent with the existence of hydrogen-bonding interactions in solution, are in operation. The ^{1}H-NMR spectra of these imidazolium phenoxide:phenol adducts provide no evidence that exchange of the less acidic C(4/5)-H backbone hydrogen atoms, as reported by Denk *et al.*,[45] occurs in solution. The existence of only one set of resonances corresponding to both the phenoxide anion and phenol moiety in the ^{1}H-NMR spectra of these species (Figure 2.4) confirms that phenoxide-phenol exchange is occurring and is rapid on the NMR timescale.

A broad low-field resonance attributed to the imidazolium proton is apparent in the ^{1}H-NMR spectrum of **1** at a chemical shift of 9.75 ppm (Figure 2.4), however, the absence of such a signal in the ^{1}H-NMR spectrum of **3** does not preclude this species being described as an imidazolium salt. Indeed, since the degree of charge delocalisation around the heterocyclic core is different in imidazol-2-ylidenes and imidazolium salts,[2, 46-48] the chemical shift of the C(4/5)-H backbone hydrogens provides a good indication of whether a given system is more *N*-heterocyclic carbene-like or azolium salt-like. The ^{1}H-NMR spectra of **1** (Figure 2.4) and **3** both exhibit a singlet corresponding to the C(4/5)-H backbone hydrogens of an imidazolium cation in d_6-DMSO solution (8.26 and 8.22 ppm, respectively),[49] rather than that of an imidazol-2-ylidene species (7.38 ppm in the ^{1}H-NMR spectrum of **15** in d_6-DMSO (Figure 2.24)).

The ^{1}H-NMR spectra of **2** and **3** in CD_2Cl_2 solution (Figure 2.5) exhibit a single broad low-field resonance corresponding to the acidic imidazolium C(2)-H and the phenolic protons at 10.32 ppm and 11.32 ppm, respectively. The C(4/5)-H backbone hydrogens are observed at a chemical shift of 7.47 ppm in the ^{1}H-NMR spectrum of **2**, and 7.21 ppm in that of compound **3** (Figure 2.5). The existence of only one set of resonances corresponding to the phenoxide anion and phenol moiety in the ^{1}H-NMR spectrum of **3** (Figure 2.5) and the ^{19}F-NMR spectrum of **2**, suggests that phenoxide-phenol exchange is occurring in solution and is rapid on the NMR timescale.

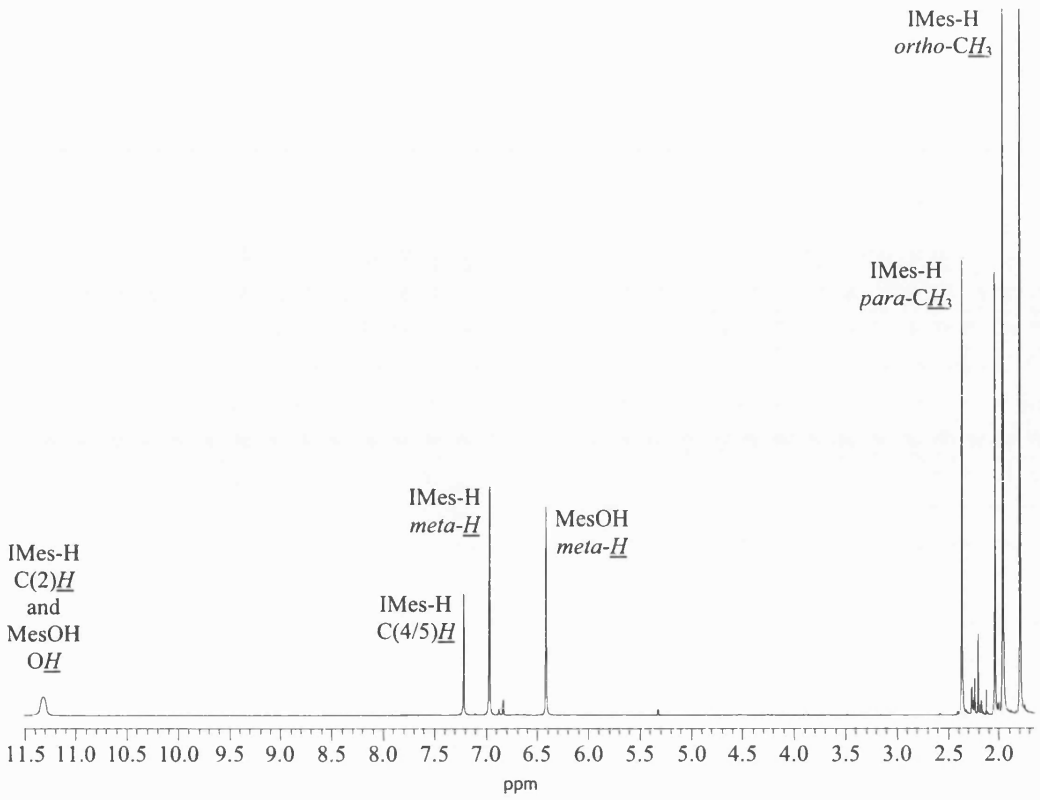

Figure 2.5: ^{1}H-NMR spectrum of **3** in CD_2Cl_2 recorded at 300 MHz

The $^{13}C\{^{1}H\}$-NMR data available for **2** and **3** in CD_2Cl_2 solution compares well with that acquired from samples of **1** and **3** in d_6-DMSO, in terms of the chemical shift of the imidazolium cation resonances. The $^{13}C\{^{1}H\}$-NMR spectrum of **1** in d_6-DMSO solution (Figure 2.6) illustrates all the features that will be examined during the discussion of the $^{13}C\{^{1}H\}$-NMR data of adducts **1**, **2** and **3**, and, from this point of view, is representative of that of all these imidazolium species.

The absence of a resonance corresponding to a protonated C(2) carbon atom in the $^{13}C\{^{1}H\}$-NMR spectra of **1** (Figure 2.6), **2** and **3**, does not preclude these products being characterised as imidazolium species by means of their $^{13}C\{^{1}H\}$-NMR data. Indeed, since the degree of delocalisation of charge around the heterocyclic core of imidazolium salts and imidazol-2-ylidenes is different,[2, 46-48] the chemical shift of the C(4/5) carbon atom resonance facilitates differentiation between these two extremes. The $^{13}C\{^{1}H\}$-NMR spectra of **1** recorded in d_6-DMSO (Figure 2.6), **2** in CD_2Cl_2 solution, and **3** in both d_6-DMSO and CD_2Cl_2, exhibit a resonance characteristic of the C(4/5) carbon atoms of a cationic imidazolium heterocyclic

core, at, respectively, 124.7 ppm, 124.5 ppm and 124.4 ppm. The fact that the $^{13}C\{^{1}H\}$-NMR spectra of **1** in d_6-DMSO (Figure 2.6) and **3** in both d_6-DMSO and CD_2Cl_2 solution are not more complicated verifies that rapid exchange, on the NMR timescale, occurs between the phenoxide anion and phenol moiety.

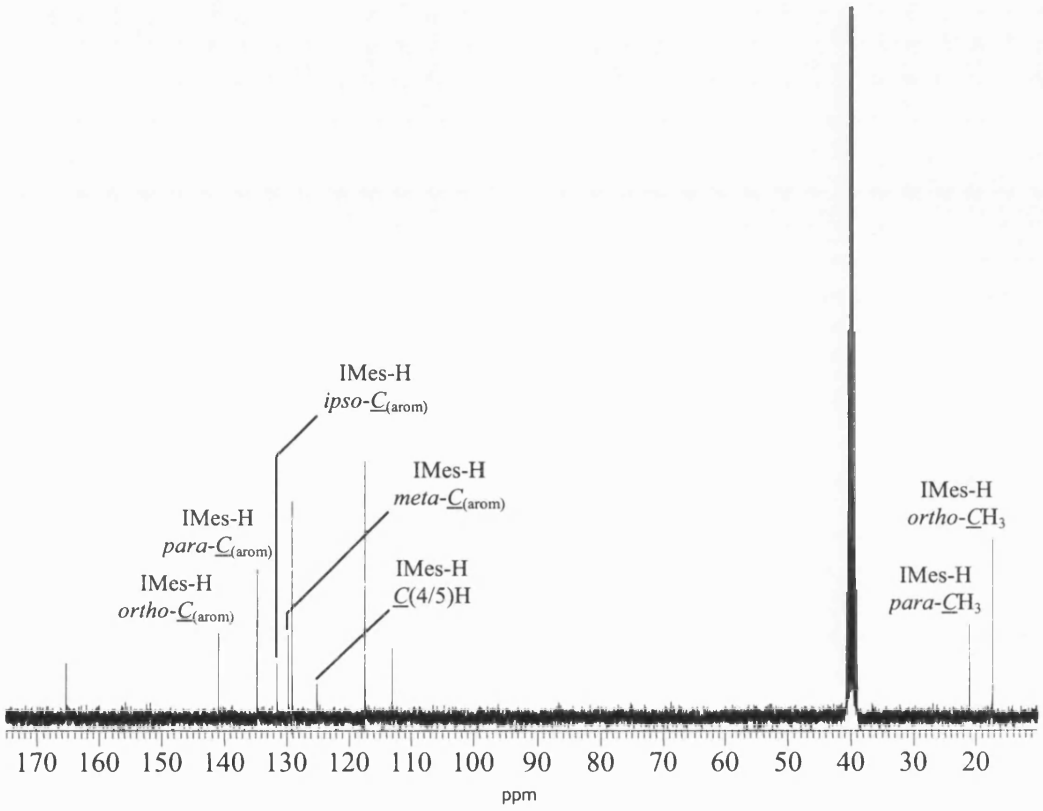

Figure 2.6: $^{13}C\{^{1}H\}$-NMR spectrum of **1** in d_6-DMSO recorded at 75.5 MHz

In line with the NMR spectroscopic evidence, analysis of suitable single crystals of **1**, **2** and **3** by x-ray diffraction reveals that these species are hydrogen-bonded imidazolium phenoxide:phenol adducts (Scheme 2.4). The asymmetric units are, in all cases, composed of a single imidazolium cation, a phenoxide anion and a molecule of phenol (Figure 2.7); the metrical parameters of which are consistent with those previously reported in the literature for imidazolium cations, phenoxide anions and phenols. The N(1)–C(2)–N(3) angle within **1**, **2** and **3**, at 107.9(1)°, 108.3(2)° and 107.4(2)°, respectively, correlates well with that observed for 1,3-bis-(2,4,6-trimethylphenyl)-imidazolium chloride (108.7(4)°),[34] which provides compelling evidence that the imidazol-2-ylidene moiety is protonated in the C(2)-position on reaction with two equivalents of phenol, pentafluorophenol or 2,4,6-

trimethylphenol (Scheme 2.4). The average N–C(2) bond lengths in adducts **1** and **3** (1.335(2) Å and 1.335(2) Å, respectively) are shorter than that of the parent imidazol-2-ylidene (1.368(4) Å),[43] which is again indicative of an imidazolium heterocyclic core. At 1.361(2) Å, the average N–C(2) bond length within **2** is significantly longer than in **1** and **3**, and, in fact, compares well with that of 1,3-bis-(2,4,6-trimethylphenyl)-imidazol-2-ylidene (1.368(4) Å). As in the analogous tetra-*n*-butylammonium phenoxide:phenol adduct prepared by Reetz *et al.*,[44] the O–C(ipso) bond length of the phenoxide anion is shorter than that in the phenol unit (1.321(2) Å versus 1.350(2) Å in **1**; 1.340(2) Å versus 1.357(3) Å in **2**; and 1.332(2) Å versus 1.360(2) Å in **3**); due either to the donation of electron-density into the π-cloud of the aromatic ring, or, to the fact that the phenoxide participates in C–H·····O^- hydrogen-bonding solely as a hydrogen bond acceptor - whereas the phenol behaves as both a donor and acceptor in different C–H·····O interactions.

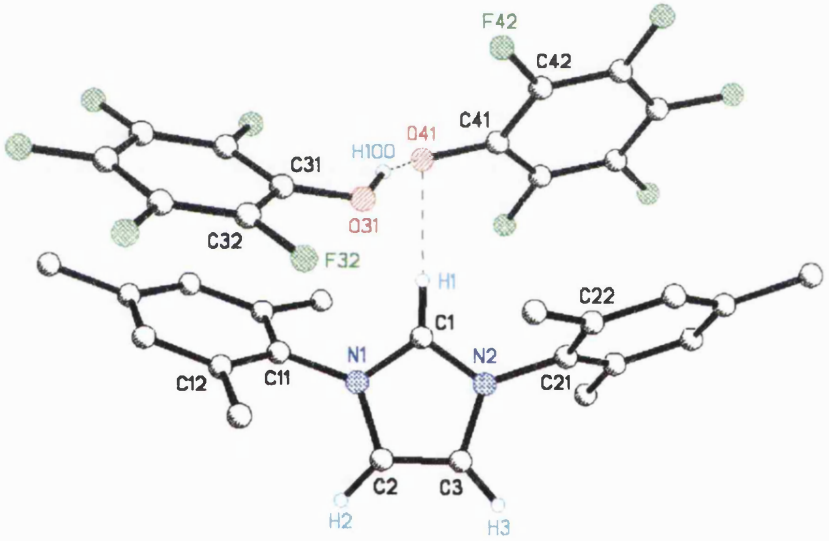

Figure 2.7: Graphical representation of the molecular structure of **2**

Determination of the solid state structure of **1**, **2** and **3** by single crystal x-ray diffraction allows the elucidation and complete characterisation of the hydrogen-bonding interactions within these species. The intramolecular hydrogen-bonding motifs observed in compounds **1**, **2** (Figure 2.7) and **3** are remarkably similar (Scheme 2.4), and shall, therefore, be discussed together. Subtle differences, however, exist in the intermolecular interactions exhibited in these imidazolium phenoxide:phenol systems, which shall subsequently be examined individually.

In all cases, the imidazolium cation and phenoxide anion represent a contact ion pair associated through C–H·····O^- interactions (D = 2.837(2) Å, d = 1.86(2) Å and θ = 168(2)° in **1**; D = 3.121(2) Å, d = 2.13(2) Å and θ = 178(2)° in **2**; and D = 2.911(2) Å, d = 1.98(2) Å and θ = 168(2)° in **3**), which exhibit minimum C·····O separations (D) at the short end of the range for such hydrogen bonds.[50] Indeed, the intramolecular C–H·····O^- interactions in **1** and **3** are shorter than some of the shortest structurally characterised C–H·····O contacts reported to date; shorter, in fact, than in the neutral adducts [$((NO_2)_3CH)_2$.dioxane] (D = 2.94 Å, d = 2.01 Å and θ = 146° (C–H corrected to 1.07 Å))[51] and [$Ph_3SiC{\equiv}CH.OPPh_3$] (D = 3.02 Å, d = 2.01 Å and θ = 155°),[52] the chiral bisoxazoline-derived imidazolium triflate salt isolated by Glorius *et al.* (D = 3.00 Å, d = 2.01 Å and θ = 165°),[53] and [$(Ph_3PCH_3)^+(2,6\text{-}Ph_2C_6H_3O)^-$] ($D$ = 3.02 Å, d = 1.94 Å and θ = 167°).[54]

The heavy-atom separation (D) within C–H·····O hydrogen bonds is related to the acidity of the C-H donor and the basicity of the oxygen acceptor;[55-58] however, the effect of crystal packing forces upon this weak electrostatic interaction should not be underestimated. The similar relative orientation of the three components (the imidazolium cation, the phenoxide anion, and the phenol moiety) in **2** (Figure 2.7) and **3** allows the effect of the phenoxide anion basicity on the intramolecular C–H·····O^- interaction to be explored. At 3.121(2) Å and 2.911(2) Å, the C·····O separations (D) observed within the intramolecular C–H·····O^- interactions in **2** and **3**, respectively, suggest that the more basic the phenoxide anion the shorter the intramolecular C–H·····O^- contact. The pK_a values of 2,4,6-trimethylphenol and pentachlorophenol in water are 10.39 and 4.75,[59] respectively; demonstrating that pentachlorophenol is more acidic than 2,4,6-trimethylphenol (pentafluorophenol is expected to be even more acidic than pentachlorophenol). The 2,4,6-trimethyl-substituted phenoxide anion is therefore more basic than the conjugate base of pentachlorophenol (which by analogy should be more basic than the pentafluoro-substituted phenoxide anion). However, although phenol is more acidic than 2,4,6-trimethylphenol (pK_a values in water of 9.92 and 10.39, respectively),[59] the

C–H·····O^- interaction in **1** is shorter than that in **3**; crystal packing effects may account for this disparity.

Further to the short intramolecular C–H·····O^- interaction, the imidazolium cation and phenoxide anion in compound **2** are held in intimate contact by a pairwise π(arene)·····π(haloarene) stack, which involves one of the mesityl substituents of the cation and the π-system of the phenoxide anion (centroid-centroid: 3.831(1) Å; shortest perpendicular distance: 3.525(2) Å) (Figure 2.8); the intercentroid distance between the arene and haloarene rings within this short stack is

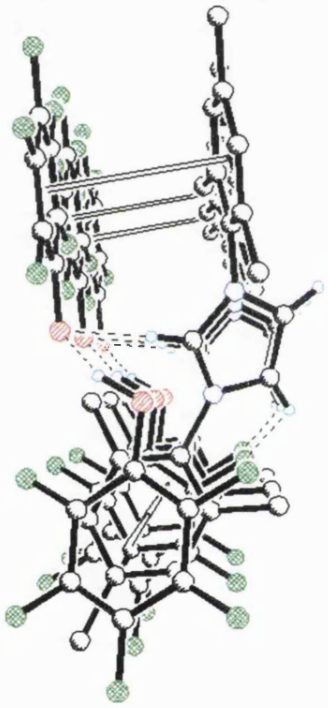

Figure 2.8: Pairwise and infinite π(arene)·····π(haloarene) stacking in the solid state structure of **2** determined by single crystal x-ray diffraction analysis

comparable to those recently reported by Nangia *et al.*[60] In the same vein, the cationic and anionic components within the asymmetric unit of **3** associate via a π(arene)·····π(arene) interaction involving a mesityl substituent of the imidazolium cation and the π-system of the phenoxide anion (centroid-centroid: 3.823(2) Å; shortest perpendicular distance: 3.476(2) Å). The phenol moiety in compound **2** is also held in place by an intramolecular π(arene)·····π(haloarene) interaction that

involves the second mesityl substituent of the imidazolium cation and possesses an arene-haloarene ring separation comparable to those within polyfluorinated tolans, as reported in a recent paper[61] (centroid-centroid: 4.117(1) Å; shortest perpendicular distance: 3.589(2) Å); which extends into an infinite stack to link molecules of **2** together in polymeric chains (Figure 2.8).

The phenoxide anion and phenol moiety in products **1**, **2** and **3** are, in all cases, associated by means of O–H·····O$^-$ hydrogen-bonded contacts (D = 2.486(2) Å, d = 1.44(3) Å and θ = 176(3)° in **1**; D = 2.487(2) Å, d = 1.43(4) Å and θ = 163(3)° in **2**; and D = 2.506(2) Å, d = 1.34(3) Å and θ = 173(3)° in **3**); Reetz *et al.* have reported a comparable interaction within an analogous tetra-*n*-butylammonium phenoxide:phenol adduct.[44] The phenol unit acts as a hydrogen bond acceptor in the intermolecular interactions that link individual molecules of **1**, **2** and **3** into the extended supramolecular arrays observed in the solid state; a detailed discussion of the intermolecular interactions within each of these species follows below.

Although the C(4/5)-H backbone hydrogens are less acidic than the imidazolium C(2)-H proton, hydrogen-bonding interactions involving these atoms often govern the supramolecular structure of imidazolium salts, imidazol-2-ylidene adducts and metal-*N*-heterocyclic carbene complexes;[34, 62, 63] implying that they are still good hydrogen bond donors. Both C(4/5)-H hydrogen atoms in **1** and **3** are involved in the formation of the one-dimensional polymeric chains connecting each molecule of the imidazolium phenoxide:phenol adduct to the next. However, in the solid state structure of **2**, two different polymer chains intersect at each imidazolium cation, leading to the formation of a molecular grid in which any given molecule of **2** is linked to two neighbouring molecules via its two C(4/5)-H substituents.

The polymeric extended structure of **1** (Figure 2.9) is the result of cooperative intermolecular C–H·····π(arene) (D = 3.577(2) Å, d = 2.81(3) Å and θ = 139(3)°), [C2–H2·····centroid(C101-C106)], and C–H·····O interactions (D = 3.264(2) Å, d = 2.53(3) Å and θ = 135(3)°), [C3–H3·····O1]; in which the C(4/5)-H hydrogen atoms of the imidazolium cation act as hydrogen bond donors, and the phenol unit

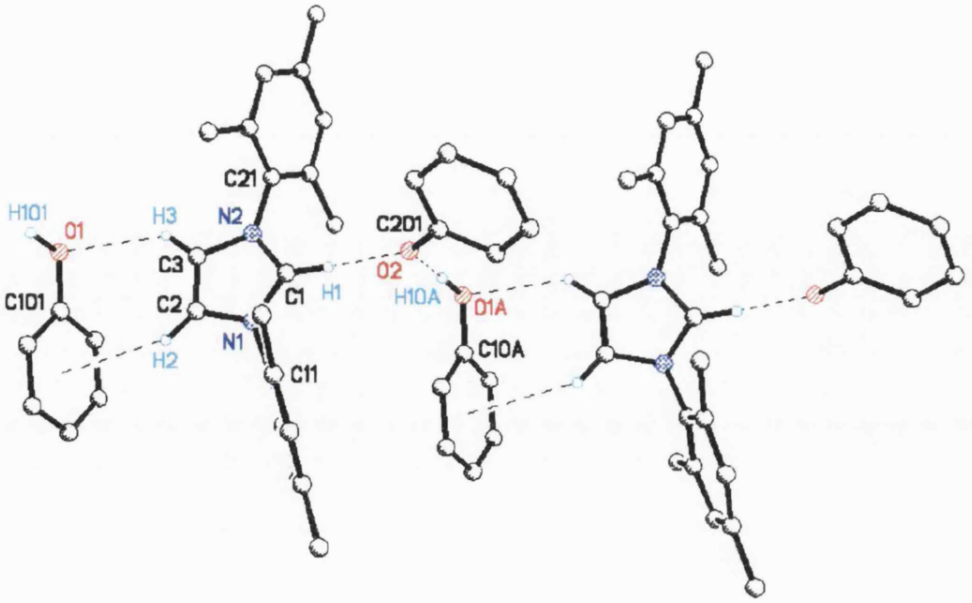

Figure 2.9: Supramolecular structure of imidazolium phenoxide:phenol adduct **1**

behaves as a hydrogen bond acceptor. Similar intermolecular C–H·····π(arene) and C–H·····O interactions are exhibited in the solid state supramolecular structure of **3** (Figure 2.10); in this case the C–H·····O interaction (D = 3.174(2) Å, d = 2.25 Å and θ = 164°), [C2–H2·····O1], once again involves the oxygen atom of the phenol moiety, although it is the π-system of the phenoxide anion that participates

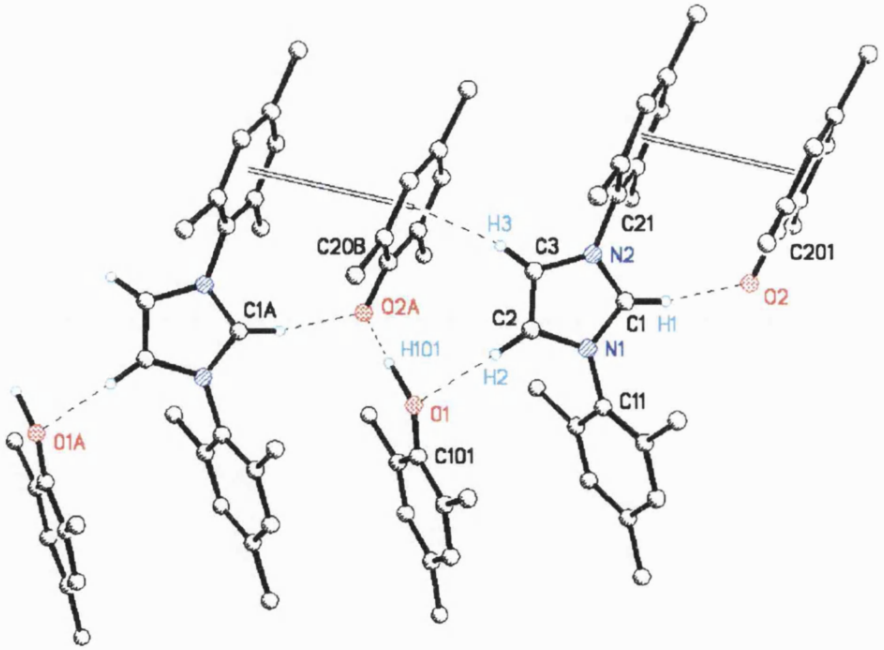

Figure 2.10: Polymeric extended structure of imidazolium phenoxide:phenol adduct **3**

in the C–H·····π(arene) interaction (D = 3.206(2) Å, d = 2.45(3) Å and θ = 136(3)°), [C3–H3·····centroid(C20B-C25B)] (Figure 2.10). The geometric parameters of these intermolecular interactions are quite representative of C–H·····π(arene) and C–H·····O hydrogen-bonding interactions.[50, 64]

The hydrogen-bonding interactions comprising the two polymeric chains observed in the solid state structure of compound **2** involve distinctly different electrostatic interactions. C–H·····O^- contacts (D = 3.162(2) Å, d = 2.57(2) Å and θ = 118(2)°), [C3A–H3A·····O41$^-$], between one of the imidazolium cation C(4/5)-H backbone

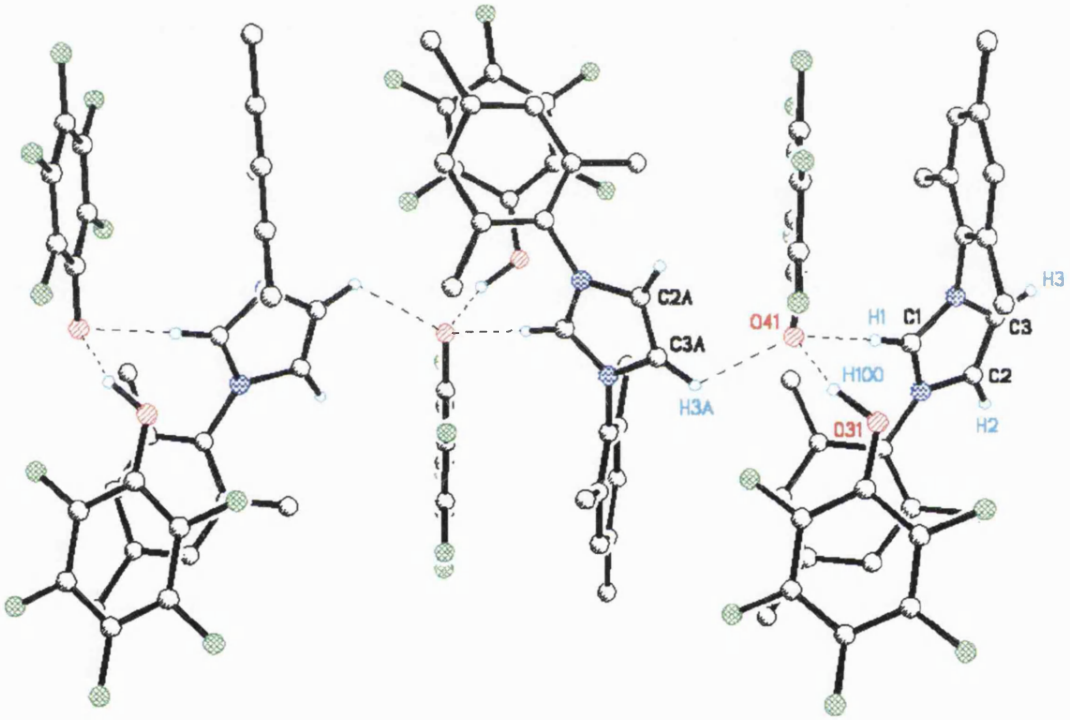

Figure 2.11: C–H·····O^- interactions and intramolecular O–H·····O^- contacts in the solid state structure of **2** determined by single crystal x-ray diffraction

hydrogens of one molecule of **2** and the phenoxide anion of a neighbouring molecule, are responsible for the formation of one polymeric chain (Figure 2.11). As might be expected on the basis of the relative acidities of the C-H hydrogen bond donor groups; this intermolecular hydrogen-bond (D = 3.162(2) Å, d = 2.57(2) Å and θ = 118(2)°), [C3A–H3A·····O41$^-$] (Figure 2.11), is longer than the

intramolecular C–H·····O^- contact (D = 3.121(2) Å, d = 2.13(2) Å and θ = 178(2)°), [C1–H1·····O41$^-$] (Figures 2.7 and 2.11).[55-58]

In the second polymeric chain, the imidazolium cation of one molecule of **2** and the phenol unit of a neighbouring molecule associate through an intermolecular π(arene)·····π(haloarene) interaction; involving the delocalised π-systems of one of the imidazolium cation mesityl substituents and the phenol moiety of the adjacent molecule of **2** (centroid-centroid: 4.087(2) Å; shortest perpendicular distance:

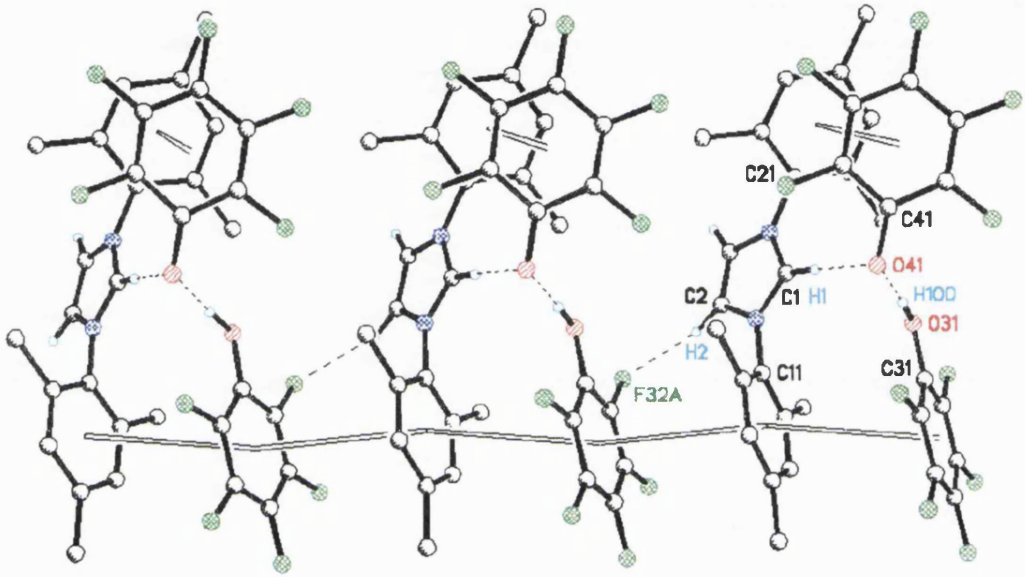

Figure 2.12: π(arene)·····π(haloarene) stacking in the solid state structure of imidazolium phenoxide:phenol adduct **2**

3.511(2) Å). This extends the intramolecular π(arene)·····π(haloarene) interaction (centroid-centroid: 4.117(2) Å; shortest perpendicular distance: 3.589(2) Å) between the imidazolium cation mesityl ring and the phenol moiety of the same molecule of **2** into an infinite π-stack (Figures 2.8 and 2.12). This intermolecular π(arene)·····π(haloarene) interaction is accompanied by an intermolecular C–H·····F (D = 3.168(3) Å, d = 2.45(2) Å and θ = 128(2)°) contact, [C2–H2·····F32A], between the other C(4/5)-H hydrogen substituent of the imidazolium heterocyclic core and an *ortho*-fluorine substituent of the phenol moiety.

2.3: Imidazolium Phenoxide Salts

In addition to imidazolium phenoxide:phenol adducts **1**, **2** and **3** (Scheme 2.4), we have isolated and characterised imidazolium phenoxide salts **4-10** (Scheme 2.5). Compounds **4-9** are accessible via the reaction of 1,3-bis-(2,4,6-trimethylphenyl)-imidazol-2-ylidene with one equivalent of the corresponding substituted phenol (Scheme 2.5). The reaction of 4,4'-methylene-bis-(2,6-di-*tert*-butylphenol) with two equivalents of 1,3-bis-(2,4,6-trimethylphenyl)-imidazol-2-ylidene results in the formation of the bisimidazolium diphenoxide salt **10** (Scheme 2.5).

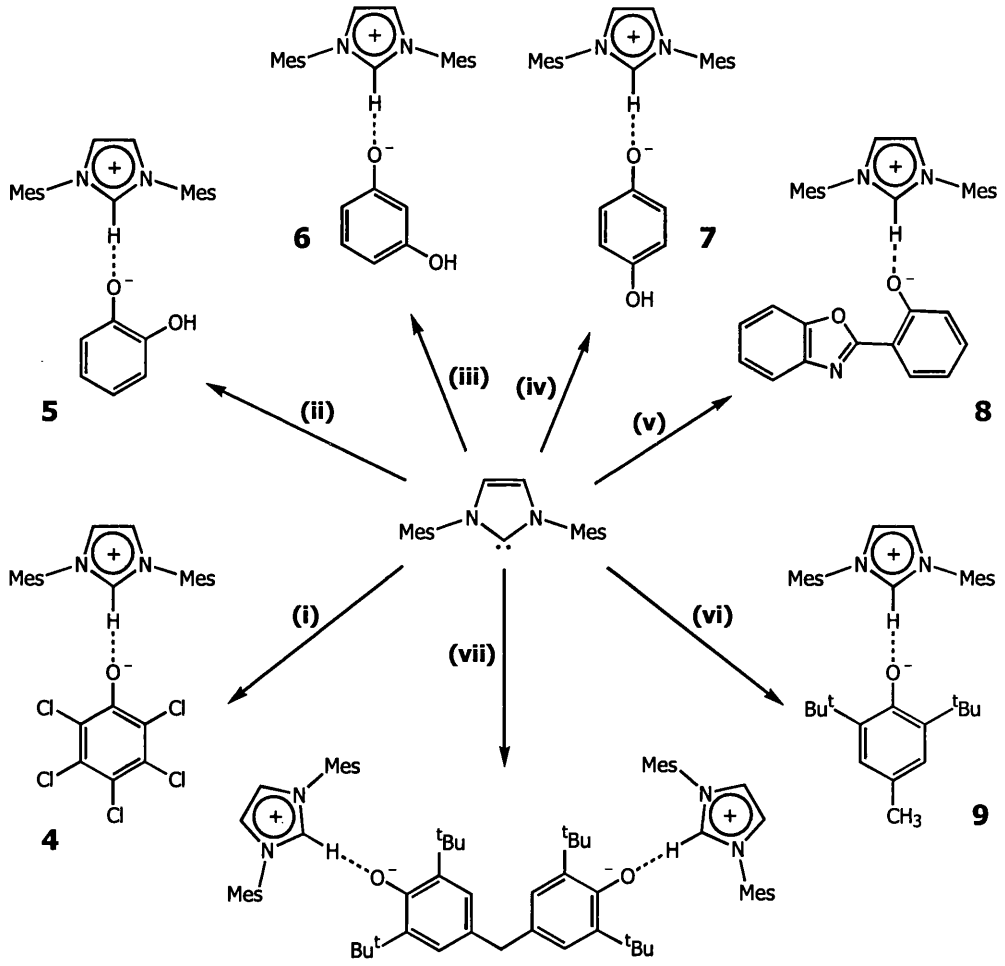

Scheme 2.5: Reaction of an imidazol-2-ylidene with acidic organic compounds
(i) pentachlorophenol, toluene/tetrahydrofuran; **(ii)** catechol, tetrahydrofuran;
(iii) resorcinol, tetrahydrofuran; **(iv)** hydroquinone, toluene;
(v) 2-(2-hydroxyphenyl)benzoxazole, toluene;
(vi) 2,6-di-*tert*-butyl-4-methylphenol, toluene;
(vii) 4,4'-methylene-bis-(2,6-di-*tert*-butylphenol), toluene

The imidazolium phenoxide salt **4** is isolated as a white microcrystalline solid from toluene solution, or colourless needles suitable for study by x-ray diffraction from tetrahydrofuran. Compounds **5**, **8** and **9** are crystalline materials; **6** and **10** are microcrystalline solids; and **7** is a white powder. Recrystallisation of **8** from acetonitrile provides crystals suitable for study by x-ray diffraction. Compounds **4-10** are readily soluble in dichloromethane, dimethyl sulphoxide and chloroform solution, although decomposition is often observed over time.

Analysis of **4-10** by NMR spectroscopy reveals that these compounds are discrete imidazolium phenoxide salts (Scheme 2.5), rather than imidazol-2-ylidene:phenol adducts. Integration of the ^{1}H-NMR data obtained from samples of these species in d_6-DMSO solution demonstrates that their composition is consistent with the reaction stoichiometry (Scheme 2.5). The ^{1}H-NMR spectra of **4**, **5** (Figure 2.13), **6** (Figure 2.14) and **8** exhibit a broad low-field resonance corresponding to the acidic imidazolium C(2)-H at a chemical shift of 9.69 ppm, 8.73 ppm, 9.94 ppm and 9.91 ppm, respectively (Table 2.1). The broad nature of these peaks suggests that these protons are involved in exchange processes in solution; this is perhaps best illustrated in the ^{1}H-NMR spectrum of the imidazolium phenoxide salt **5** (Figure 2.13), where a single resonance at 8.73 ppm is observed for both the imidazolium C(2)-H and phenolic protons. Exchange in solution is prominent in the ^{1}H-NMR spectrum of **7**, such that a single broad resonance corresponding to the acidic imidazolium C(2)-H and phenolic protons, and hydroquinone aromatic hydrogen atoms, is observed at a chemical shift of 6.34 ppm (Table 2.1). The absence of a resonance corresponding to the imidazolium C(2)-H proton in the ^{1}H-NMR spectra of compounds **9** and **10** (Table 2.1) indicates that exchange in solution also occurs in these systems.

The dearth of a resonance corresponding to the acidic imidazolium C(2)-H proton in the ^{1}H-NMR spectra of compounds **9** and **10**, complicates, but does not prevent, the characterisation of these species as imidazolium salts on the basis of their ^{1}H-NMR data. Moreover, at 6.34 ppm in the ^{1}H-NMR spectrum of **7**, the chemical shift of the acidic C(2)-H proton resonance (Table 2.1) alone does not provide convincing evidence that this species is an imidazolium phenoxide. However, the

C(4/5)-H backbone hydrogen atoms are observed in the ^{1}H-NMR spectra of **4-10**, recorded in d_6-DMSO solution, at a chemical shift ranging between 8.21 ppm and 8.28 ppm (Table 2.1), which is indicative of a cationic imidazolium heterocyclic core.

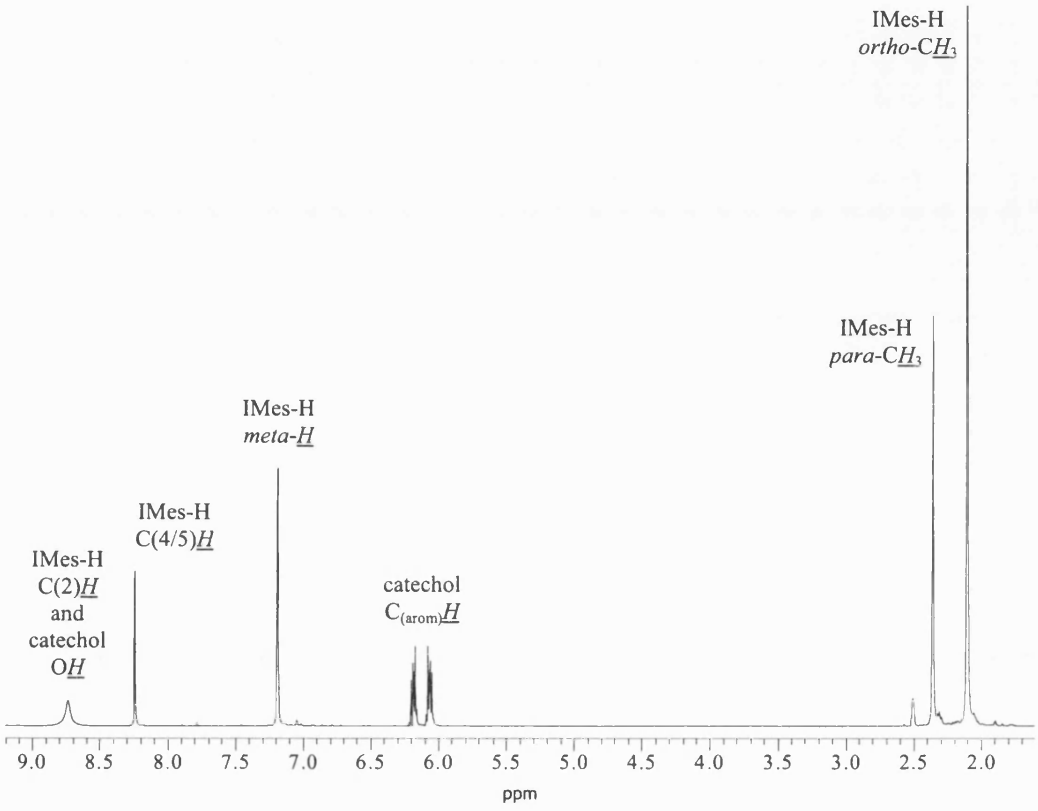

Figure 2.13: ^{1}H-NMR spectrum of **5** in d_6-DMSO recorded at 300 MHz

The imidazolium cation resonances remain reasonably static within the ^{1}H-NMR spectra of compounds **4-10** recorded in d_6-DMSO (Table 2.1), and therefore, the ^{1}H-NMR spectrum of **5** (Figure 2.13) may be considered representative of that of all these imidazolium phenoxide species. Indeed, comparison of the ^{1}H-NMR spectrum of **5** (Figure 2.13) with that of compound **6** (Figure 2.14) provides a good illustration of this fact. Closer inspection of the ^{1}H-NMR spectrum of **6** (Figure 2.14) reveals that the resorcinol resonances are "shadowed" by smaller peaks at a higher chemical shift (0.04–0.08 ppm), which suggests that two different resorcinol-derived species are present in solution. The origin of this minor component is not known and the apparent absence of exchange between these two species in solution is surprising.

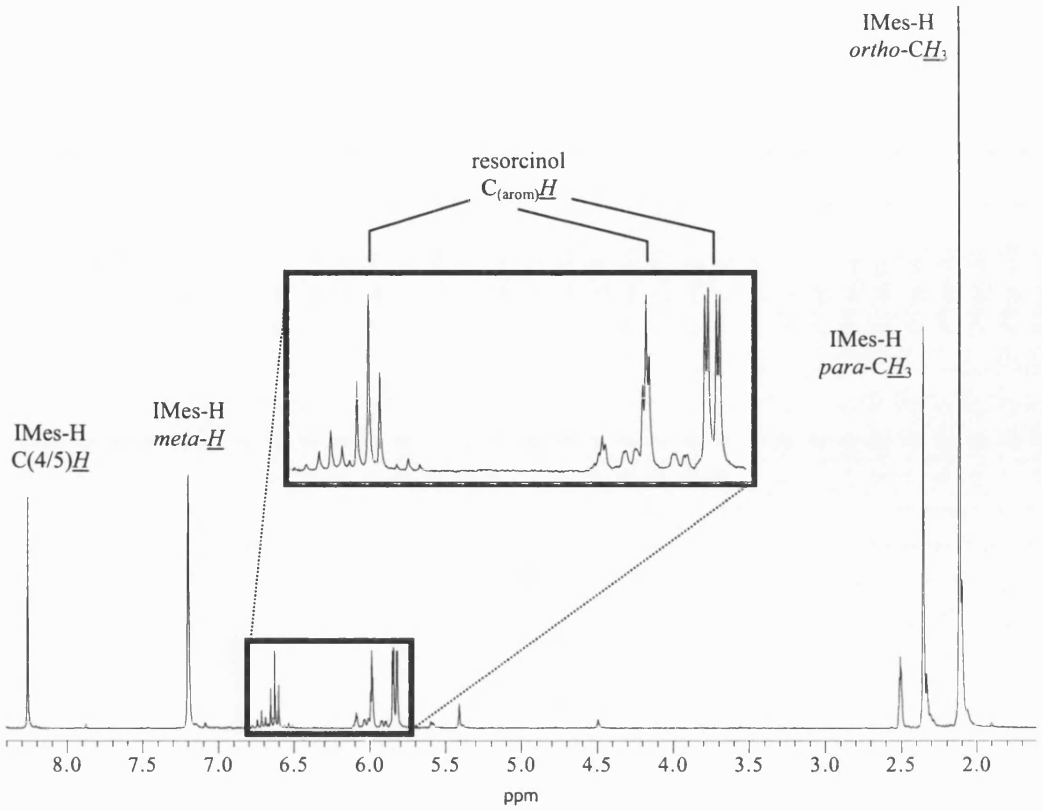

Figure 2.14: ^{1}H-NMR spectrum of **6** in d_6-DMSO recorded at 300 MHz

The $^{13}C\{^{1}H\}$-NMR spectra of samples of compounds **4-10** in d_6-DMSO solution provide further evidence that the imidazol-2-ylidene moiety is protonated at C(2) on reaction with pentachlorophenol, catechol, resorcinol, hydroquinone, 2-(2-hydroxyphenyl)benzoxazole, 2,6-di-*tert*-butyl-4-methylphenol or 4,4'-methylene-bis-(2,6-di-*tert*-butylphenol) (Scheme 2.5). Indeed, a resonance consistent with the imidazolium C(2) carbon atom is observed at a chemical shift of 138.4 ppm, 139.2 ppm and 139.1 ppm, in the $^{13}C\{^{1}H\}$-NMR spectra of compounds **4**, **7** and **8**, respectively (Table 2.1). The absence of such a peak in the $^{13}C\{^{1}H\}$-NMR spectra of **5** (Figure 2.15), **6**, **9** and **10**, is believed to be a facet of the exchange processes in operation in solution. The classification of these compounds as imidazolium species may, once again, be achieved with reference to the chemical shift of the C(4/5) backbone carbon atoms.

		4	5	6	7	8	9	10
^{1}H-NMR	C(2)-*H*	9.69	8.73	9.94	6.34	9.91	——	——
(d_6-DMSO)	C(4/5)-*H*	8.28	8.24	8.26	8.23	8.27	8.22	8.21
^{13}C-NMR	*C*(2)	138.4	——	——	139.2	139.1	——	——
(d_6-DMSO)	*C*(4/5)	124.6	124.6	124.5	124.5	124.7	124.6	124.6

Table 2.1: Significant chemical shifts in the ^{1}H- and ^{13}C{^{1}H}-NMR spectra of **4-10** recorded in d_6-DMSO at 298 K and quoted in units of ppm downfield of TMS

The olefinic C(4/5) carbons are observed at between 124.5 ppm and 124.7 ppm in the ^{13}C{^{1}H}-NMR spectra of **4-10** recorded in d_6-DMSO (Table 2.1), indicative of a delocalised cationic imidazolium heterocyclic core. The degree of variation in the chemical shift of the imidazolium cation resonances is slight, and, from this point of view, the ^{13}C{^{1}H}-NMR spectrum of **5** (Figure 2.15) can be considered representative of that of imidazolium phenoxide salts **4-10**.

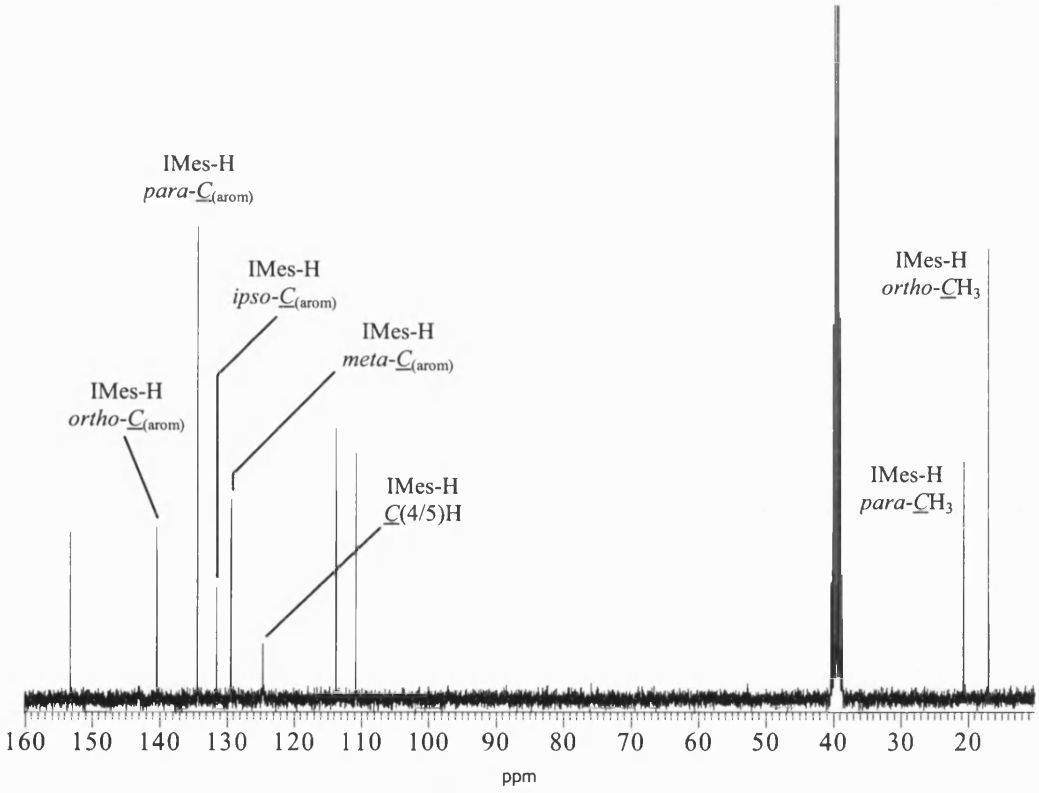

Figure 2.15: ^{13}C{^{1}H}-NMR spectrum of **5** in d_6-DMSO recorded at 75.5 MHz

In accordance with the proposed structures of **4**, **5**, **8** and **9** in solution, analysis of suitable single crystals of these products by x-ray diffraction reveals that they are hydrogen-bonded imidazolium phenoxide salts (Scheme 2.5) in the solid state. The asymmetric units of **4**, **5** and **8** contain a single imidazolium cation and a phenoxide anion; the metrical parameters of the cation are consistent with those reported for other imidazolium salts. For instance, the N(1)–C(2)–N(3) angles in compounds **4**, **5** and **8** (at 108.0(3)°, 107.8(1)° and 107.8(1)°, respectively) correlate well with that of 1,3-bis-(2,4,6-trimethylphenyl)-imidazolium chloride (108.7(4)°).[34] The average N–C(2) bond lengths in **4**, **5** and **8** (at 1.339(4) Å, 1.335(2) Å and 1.336(2) Å, respectively) are shorter than that observed in the parent imidazol-2-ylidene (1.368(4) Å).[43] The asymmetric unit of compound **9** contains two crystallographically independent molecules, each composed of an imidazolium cation and a phenoxide anion; the average N–C(2) bond lengths within the two independent molecules are 1.337(3) Å and 1.338(3) Å, and the N(1)–C(2)–N(3) angle within both cations is 107.3(2)°. These structural features provide compelling evidence to support the protonation of the imidazol-2-ylidene moiety in the C(2)-position on reaction with one equivalent of pentachlorophenol, catechol, 2-(2-hydroxyphenyl)benzoxazole, and, 2,6-di-*tert*-butyl-4-methylphenol (Scheme 2.5).

Organic salts incorporating the pentachlorophenoxide anion have previously been reported by Sobczyk[65] and Szafran;[66] more recently, thermally induced partial proton transfer from pentachlorophenol to 4-methylpyridine within an O–H·····N hydrogen-bonded adduct has been studied by neutron diffraction.[67] Compounds **5** and **8** are, to our knowledge, the first structurally characterised ion pairs that incorporate the conjugate bases of catechol and 2-(2-hydroxyphenyl)benzoxazole as the anionic component. The 2,6-di-*tert*-butyl-4-methylphenoxide anion in **9** has previously been crystallographically characterised in a related phosphonium phenoxide species.[54] The metrical parameters of the anions in compounds **4** and **9** are consistent with those reported in the literature for these analogous systems.

The intramolecular hydrogen-bonding in compounds **4**, **5**, **8** and **9** is remarkably similar; the imidazolium cation and the phenoxide anion, in all cases, represent a

contact ion pair associated through short C–H·····O^- interactions (D = 2.914(4) Å, d = 2.029 Å and θ = 154.2° in **4**; D = 2.838(2) Å, d = 1.90(2) Å and θ = 162(1)° in **5**; D = 2.896(2) Å, d = 2.00(2) Å and θ = 153(2)° in **8**; and D = 2.801(3) Å, 2.842(3) Å; d = 1.87(3) Å, 1.88(3) Å; and θ = 175(2)°, 169(2)° in **9**). These interactions are shorter than those in adducts [$((NO_2)_3CH)_2$.dioxane] (D = 2.94 Å, d = 2.01 Å and θ = 146° (C–H corrected to 1.07 Å))[51] and [$Ph_3SiC{\equiv}CH.OPPh_3$] (D = 3.02 Å, d = 2.01 Å and θ = 155°),[52] the bisoxazoline-derived imidazolium triflate salt isolated by Glorius *et al.* (D = 3.00 Å, d = 2.01 Å and θ = 165°),[53] and [$(Ph_3PCH_3)^+(2,6\text{-}Ph_2C_6H_3O)^-$] ($D$ = 3.02 Å, d = 1.94 Å and θ = 167°);[54] which represent some of the shortest C–H·····O interactions reported to date.

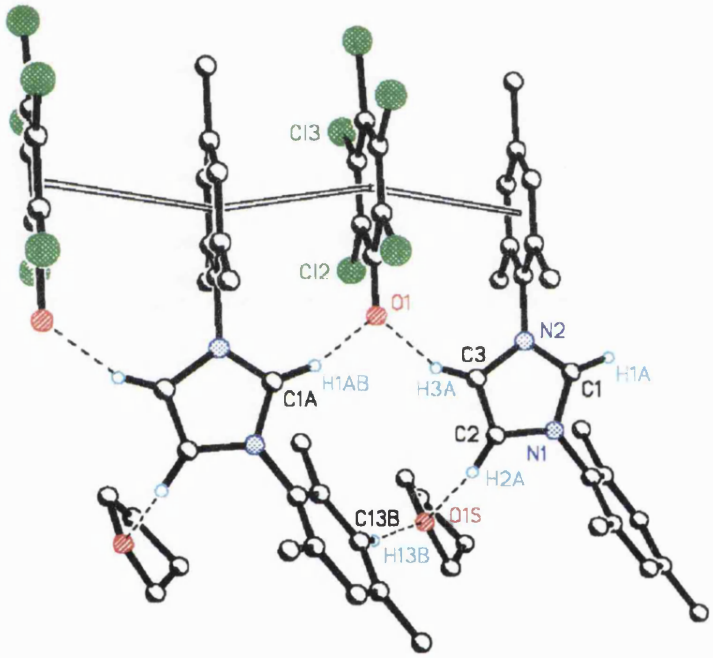

Figure 2.16: Hydrogen-bonding in the solid state structure of **4** determined by single crystal x-ray diffraction

The phenoxide anion and a mesityl substituent of the imidazolium cation in compound **4** lie virtually co-planar, facilitating the augmentation of the dominant C–H·····O^- interaction, [C1A–H1AB·····$O1^-$] (Figure 2.16), with an intramolecular π(arene)·····π(haloarene) interaction (centroid-centroid: 3.800(1) Å; shortest perpendicular distance: 3.403(3) Å); the intercentroid distance here is not dissimilar to the shortest observed within the solid state structure of the hydrogen-

dissimilar to the shortest observed within the solid state structure of the hydrogen-bonded adduct $C_6H_5COOH:HOOCC_6F_5$.[60] This interaction is extended into an infinite stack in the supramolecular structure of **4** (Figure 2.16) by intermolecular π(arene)·····π(haloarene) interactions. Likewise, the C–H·····O^- contact in the solid state structure of **8** is found to be accompanied by a π·····π interaction (centroid-centroid: 3.522(1) Å; shortest perpendicular distance: 3.476(1) Å) (Figure 2.19) lying towards the short end of the range for such interactions.[68] The intramolecular hydrogen-bonding in compound **5** is completed by a strong constrained geometry O–H·····O^- hydrogen bond (D = 2.605(2) Å, d = 1.63(4) Å and θ = 133(3)°), [O1A–H10A·····O2A$^-$], between the phenoxide oxygen and the *ortho*-hydroxy substituent of the catechol moiety (Figure 2.18); reminiscent of the intramolecular O–H·····O^- hydrogen-bonding exhibited within **1** (Figure 2.9) and the analogous tetra-*n*-butylammonium phenoxide:phenol species.[44]

Compounds **4**, **5**, **8** and **9** (Scheme 2.5) are two component systems (imidazolium cation and phenoxide anion), whereas adducts **1**, **2** and **3** (Scheme 2.4) are three component systems (imidazolium cation, phenoxide anion and phenol molecule). The supramolecular hydrogen-bonded array observed in the solid state structures of **4**, **5**, **8** and **9** is, as might be expected, simplified in comparison to that of **1**, **2** and **3** in terms of the number of interactions present. Once again, the C(4/5)-H hydrogen atoms play a significant role in the formation of the polymeric extended structure of these imidazolium phenoxides. For instance, the imidazolium cation of one molecule of **4** and the phenoxide anion of another molecule are associated by a C–H·····O^- hydrogen bond (D = 3.031(2) Å, d = 2.154 Å and θ = 153.0°), [C3–H3A·····O1$^-$] (Figure 2.16), involving one of these C(4/5)-H backbone hydrogen substituents, reminiscent of the intermolecular C–H·····O^- contact within one of the polymeric chains in the solid state structure of the imidazolium phenoxide:phenol adduct **2** (Figure 2.11). This interaction is augmented by a molecule of tetrahydrofuran bridging the other imidazolium C(4/5)-H hydrogen atom and the *meta*-hydrogen substituent of a mesityl ring belonging to the neighbouring cation (Figure 2.16).

The hydrogen-bonding network in compound **4** is completed by an intermolecular π(arene)·····π(haloarene) interaction between the π-system of the phenoxide anion of one molecule of **4** and the mesityl substituent of a proximal imidazolium cation (centroid-centroid: 3.708(1) Å; shortest perpendicular distance: 3.435(2) Å) participating in an intramolecular π(arene)·····π(haloarene) interaction (centroid-centroid: 3.800(1) Å; shortest perpendicular distance: 3.403(3) Å) (Figure 2.16), which leads to the formation of an infinite stack (Figure 2.17). The aromatic ring separation within this intermolecular π-stack is similar to that recently reported in polyfluorinated tolans,[61] and smaller than the shortest observed in the hydrogen-bonded adduct $C_6H_5COOH{:}HOOCC_6F_5$.[60]

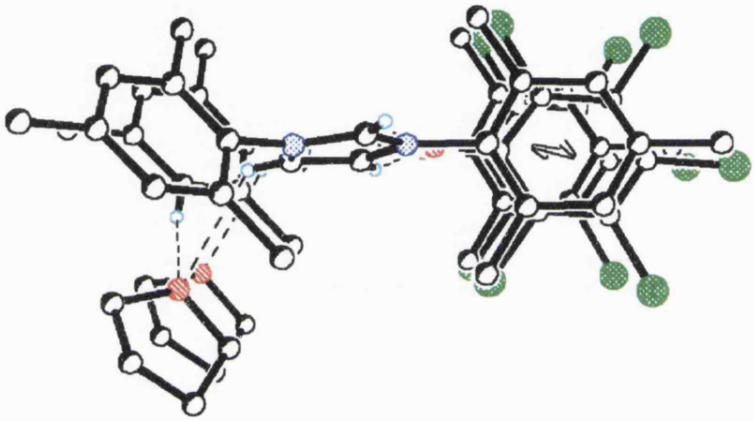

Figure 2.17: View down the infinite π(arene)·····π(haloarene) stack in the solid state structure of imidazolium phenoxide **4**

The polymeric extended structure of compound **5** is formed by virtue of C–H·····O^- contacts involving one of the C(4/5)-H backbone hydrogens of one molecule of **5** and the deprotonated oxygen atom of the catecholate anion (D = 3.10(2) Å, d = 2.288 Å and θ = 143.2°) of a neighbouring molecule, [C3–H3·····$O2^-$] (Figure 2.18); which is reminiscent of the intermolecular C–H·····O^- contacts observed within one of the polymeric chains in the solid state structure of **2** (Figure 2.11), and in **4** (Figure 2.16). This is accompanied by a C–H·····π(arene) interaction (D = 4.014 Å, d = 3.07 Å and θ = 177°), [C2A–H2A·····centroid(C21-C26)], between the other C(4/5)-H hydrogen atom and one of the mesityl rings of the cation of the proximal molecule (Figure 2.18), that is significantly longer than those exhibited

in the solid state structures of **1** (D = 3.577(2) Å, d = 2.81(3) Å and θ = 139(3)°) (Figure 2.9) and **3** (D = 3.206(2) Å, d = 2.45(3) Å and θ = 136(3)°) (Figure 2.10).

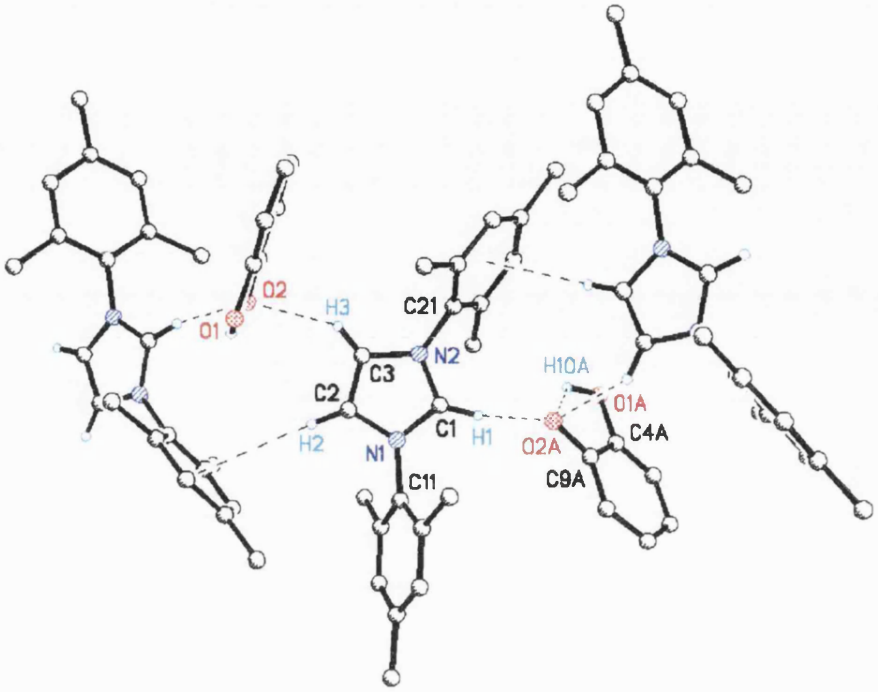

Figure 2.18: Polymeric extended solid state structure of compound **5**

An intermolecular C–H·····O$^-$ interaction, [C2–H2·····O1A$^-$] (D = 3.132(2) Å, d = 2.39(2) Å and θ = 134(1)°) (Figure 2.19), similar to those in the supramolecular arrays of imidazolium phenoxide:phenol adduct **2** (Figure 2.11) and imidazolium phenoxide salts **4** (Figure 2.16) and **5** (Figure 2.18), is observed in the extended solid state structure of the imidazolium phenoxide **8**; in which one of the C(4/5)-H substituents of the cation in one molecule of **8** acts as a hydrogen bond donor and the phenoxide anion oxygen atom of a neighbouring molecule behaves as a hydrogen bond acceptor. Intermolecular π·····π interactions (centroid-centroid: 3.428(4) Å; shortest perpendicular distance: 3.405(6) Å), between the π-system of the phenoxide anion in one molecule of **8** and one of the mesityl rings of the imidazolium cation in a neighbouring molecule (Figures 2.19 and 2.20), extend the intramolecular π·····π interactions (centroid-centroid: 3.522(1) Å; shortest perpendicular distance: 3.476(1) Å) into an infinite π-stack.

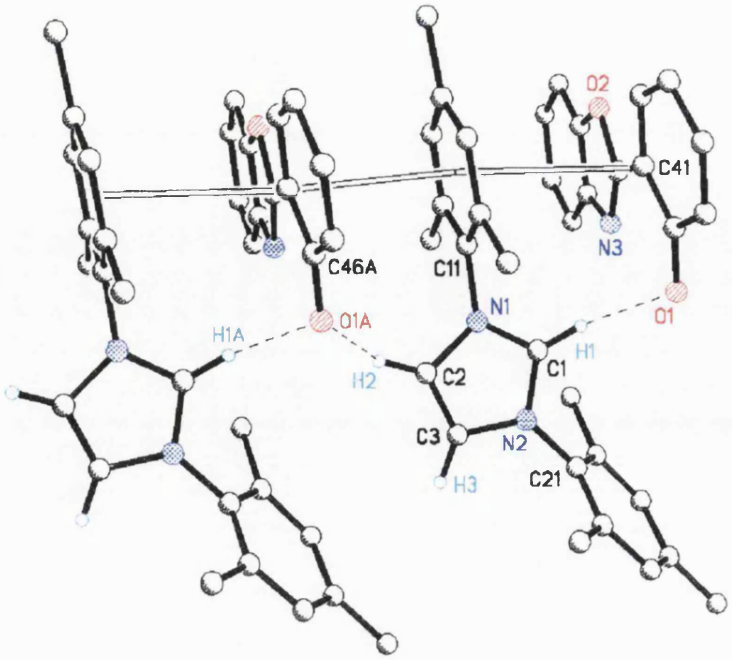

Figure 2.19: Infinite π-stacking and intermolecular C–H·····O^- interactions in the solid state structure of compound **8**

The intermolecular hydrogen-bonding interactions observed in the supramolecular structure of **9** (Figure 2.21) bear a remarkable similarity to those observed in the extended array of imidazolium phenoxide:phenol adduct **1** (Figure 2.9). Indeed, the imidazolium cation of one molecule of **9** associates with the phenoxide anion of a neighbouring ion pair by a C–H·····π(arene) interaction (D = 3.041(2) Å,

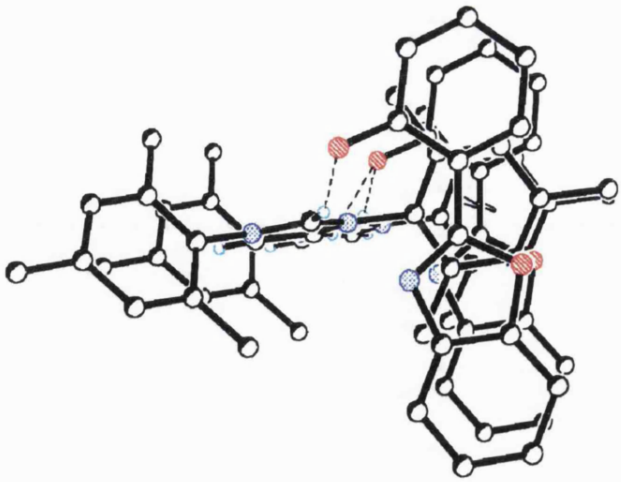

Figure 2.20: View down the infinite π-stack in the solid state structure of compound **8**

3.185(2) Å; d = 2.19 Å, 2.31 Å; and θ = 151°, 156°), which involves one of the C(4/5)-H backbone hydrogens of the cation and the π-system of the anion, and a C–H·····O$^-$ contact (D = 3.544(3) Å, 3.658(3) Å; d = 2.82 Å, 2.98 Å; and θ = 136°, 131°) between the other C(4/5)-H hydrogen and the oxygen atom of the same phenoxide anion. However, the intermolecular C–H·····π(arene) interaction, partly responsible for the association of the crystallographically independent molecules in the solid state structure of **9**, is significantly shorter than its contemporary in **1** (D = 3.577(2) Å, d = 2.81(3) Å and θ = 139(3)°). Additionally, the intermolecular C–H·····O$^-$ contact in **9** is longer than the intermolecular C–H·····O hydrogen bond within imidazolium phenoxide:phenol adduct **1** (D = 3.264(2) Å, d = 2.53(3) Å and θ = 135(3)°). This is attributed to the steric bulk of the *tert*-butyl substituents protecting the phenoxide anion oxygen atom from the neighbouring molecule of imidazolium salt **9** since the reverse would be anticipated on the basis of the relative basicities of the hydrogen-bond acceptors.

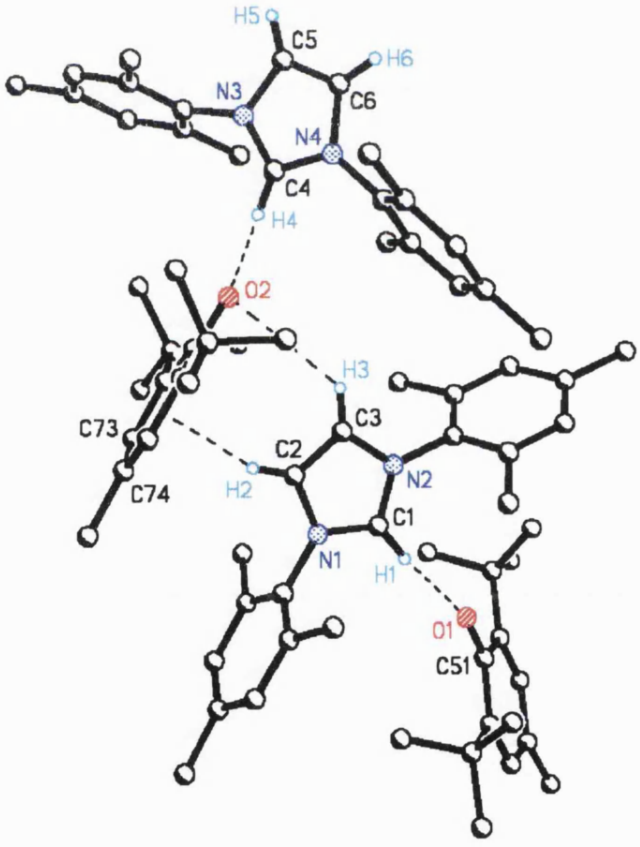

Figure 2.21: Association of crystallographically independent molecules in the solid state structure of imidazolium phenoxide **9**

2.4: Other Hydrogen-Bonded Compounds

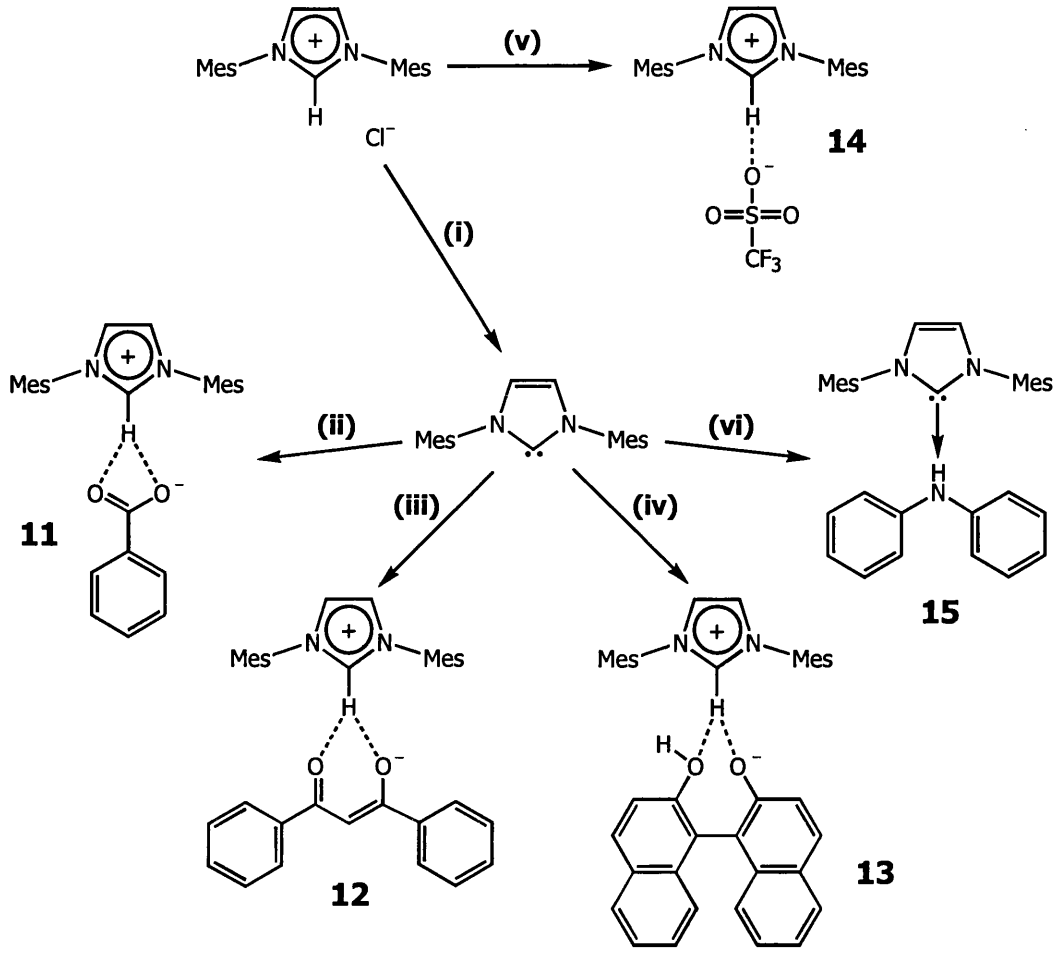

Scheme 2.6: *N*-heterocyclic carbene precursors via the reaction of an imidazol-2-ylidene with acidic organic compounds and salt metathesis
(i) potassium *tert*-butoxide, tetrahydrofuran; **(ii)** benzoic acid, toluene; **(iii)** dibenzoylmethane, toluene; **(iv)** binaphthol, tetrahydrofuran; **(v)** silver(I) triflate, dichloromethane; **(vi)** diphenylamine, toluene

In order to evaluate the versatility of simple acid-base reactions in the preparation of non-conventional imidazolium salts, we have also investigated the protonation of imidazol-2-ylidenes with acidic organic compounds other than phenols. In addition, a preliminary examination of the preparation of imidazolium precursors to chiral metal-*N*-heterocyclic carbene complexes via this synthetic strategy has been performed; by means of the study of the reaction of racemic binaphthol with 1,3-bis-(2,4,6-trimethylphenyl)-imidazol-2-ylidene. The results of these studies demonstrate that the direct reaction of *N*-heterocyclic carbenes with acidic organic

compounds, as a means by which to vary the anion of the *N*-heterocyclic carbene precursor salt, is a useful addition to the salt metathesis reaction. Furthermore, the co-crystallisation of imidazol-2-ylidenes with less acidic organic compounds also allows the preparation of neutral *N*-heterocyclic carbene adducts by means of simple acid-base reactions.

The imidazolium salts **11**,[ψ] **12** and **13** are accessible by means of the reaction of 1,3-bis-(2,4,6-trimethylphenyl)-imidazol-2-ylidene with one equivalent of benzoic acid (pK_a of 11.1 in DMSO),[71] dibenzoylmethane (pK_a of 13.35 in DMSO)[71] and binaphthol, respectively (Scheme 2.6). Compound **14** may be prepared via a salt metathesis methodology; the reaction of 1,3-bis-(2,4,6-trimethylphenyl)-imidazolium chloride with silver(I) triflate results in the precipitation of silver(I) chloride and the formation of the imidazolium triflate **14** (Scheme 2.6). However, the treatment of 1,3-bis-(2,4,6-trimethylphenyl)-imidazol-2-ylidene with one equivalent of diphenylamine (pK_a of 24.95 in DMSO)[71] yields the imidazol-2-ylidene:amine adduct **15** (Scheme 2.6), rather than an imidazolium amide salt.

NMR spectroscopic analysis of compounds **11-15** reveals that **11-14** are indeed imidazolium salts and that product **15** is an imidazol-2-ylidene:diphenylamine adduct (Scheme 2.6). Integration of the ^{1}H-NMR data obtained from samples of these species in d_6-DMSO solution confirms their composition is consistent with the reaction stoichiometry (Scheme 2.6). The ^{1}H-NMR spectra of **11-14** exhibit broad low-field resonances corresponding to the acidic imidazolium C(2)-H at 9.78 ppm (**11**) (Figure 2.23), 10.14 ppm (**12**), 9.64 ppm (**13**) and 9.64 ppm (**14**) (Table 2.2). In addition, the C(4/5)-H backbone hydrogen atoms are observed at

[ψ] An analogous 1:1 reaction between 1,3-bis-(2,6-diisopropylphenyl)-imidazol-2-ylidene[69] and dibenzoylmethane in toluene solution yielded a number of single crystals of **11a** (an imidazolium benzoate species akin to **11**) of a suitable quality for analysis by x-ray diffraction. This product is thought to be the result of the crystallographic trapping, by the imidazol-2-ylidene, of benzoic acid produced *in situ* by the hydrolysis of dibenzoylmethane in the presence of adventitious water.[70] ^{1}H-NMR spectroscopic analysis of the bulk material suggested that this was composed of both **11a** and the anticipated product **12a** (related to compound **12**) in approximately equal molar ratios, subsequent separation of these two compounds could not be achieved.

chemical shifts of 8.29 ppm (**11**) (Figure 2.23), 8.25 ppm (**12**), 8.27 ppm (**13**) and 8.28 ppm (**14**) (Table 2.2), which is indicative of a delocalised imidazolium heterocyclic core. The imidazolium cation resonances remain reasonably static within the ^{1}H-NMR spectra of compounds **11-14** (Table 2.2), and therefore, the ^{1}H-NMR spectrum of **11** (Figure 2.23) may be considered representative of that of all these imidazolium salts. However, in line with an imidazol-2-ylidene species, the C(4/5)-H backbone hydrogen atoms in the ^{1}H-NMR spectrum of a sample of compound **15** in d_6-DMSO solution (Figure 2.24) are observed at a chemical shift of 7.38 ppm (Table 2.2).

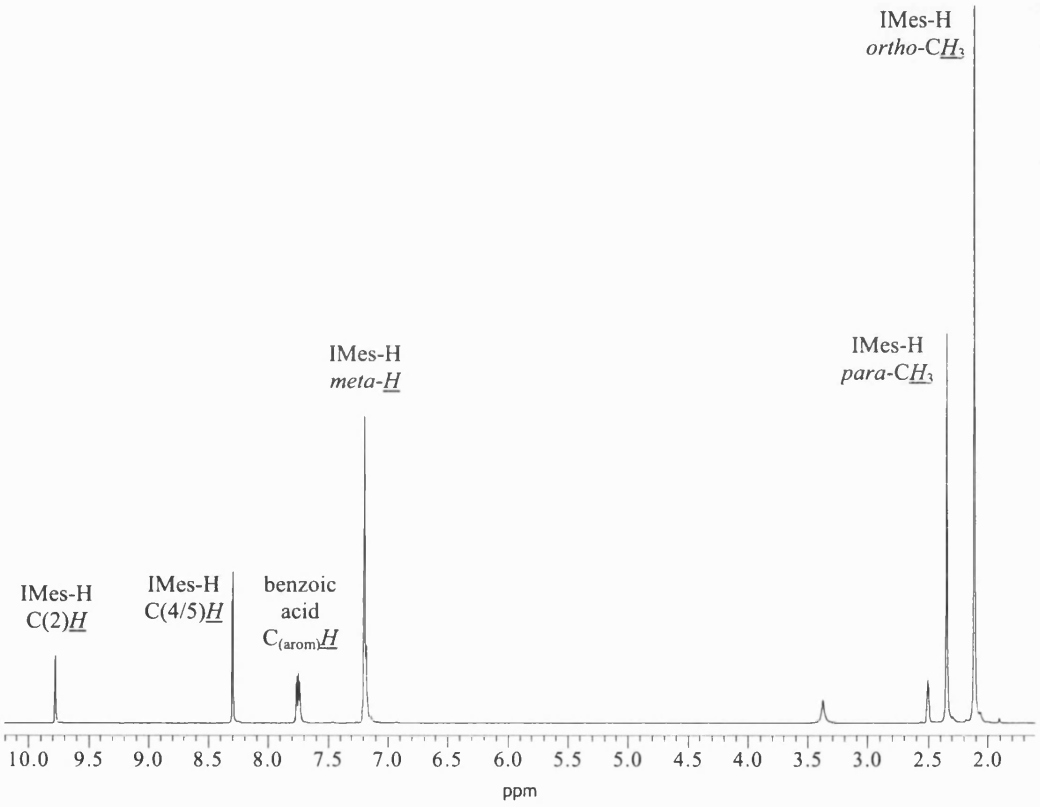

Figure 2.23: ^{1}H-NMR spectrum of **11** in d_6-DMSO recorded at 300 MHz

The ^{13}C{^{1}H}-NMR spectra acquired from samples of **11-13** in d_6-DMSO solution provide further evidence that the imidazol-2-ylidene moiety is protonated in the C(2)-position on reaction with benzoic acid, dibenzoylmethane and binaphthol (Scheme 2.6). Indeed, in all cases, the chemical shift of the imidazolium C(2) carbon atom resonance compares well with that observed in the ^{13}C{^{1}H}-NMR spectrum of imidazolium triflate **14** (138.5 ppm); 138.4 ppm (**11**), 139.3 ppm (**12**)

		11	12	13	14	15
^{1}H-NMR	**C(2)-*H***	9.78	10.14	9.64	9.64	——
(d_6-DMSO)	**C(4/5)-*H***	8.29	8.25	8.27	8.28	7.38
^{13}C-NMR	***C*(2)**	138.4	139.3	138.3	138.5	——
(d_6-DMSO)	***C*(4/5)**	124.6	124.4	124.6	124.8	121.5

Table 2.2: Significant chemical shifts in the ^{1}H- and ^{13}C{^{1}H}-NMR spectra of **11-15** recorded in d_6-DMSO at 298 K and quoted in units of ppm downfield of TMS

and, 138.3 ppm (**13**) (Table 2.2). Furthermore, the olefinic C(4/5) carbon atoms are observed at 124.6 ppm (**11**), 124.4 ppm (**12**) and 124.6 ppm (**13**); consistent with an imidazolium heterocyclic core as, for example, in imidazolium triflate **14** (124.8 ppm) (Table 2.2).

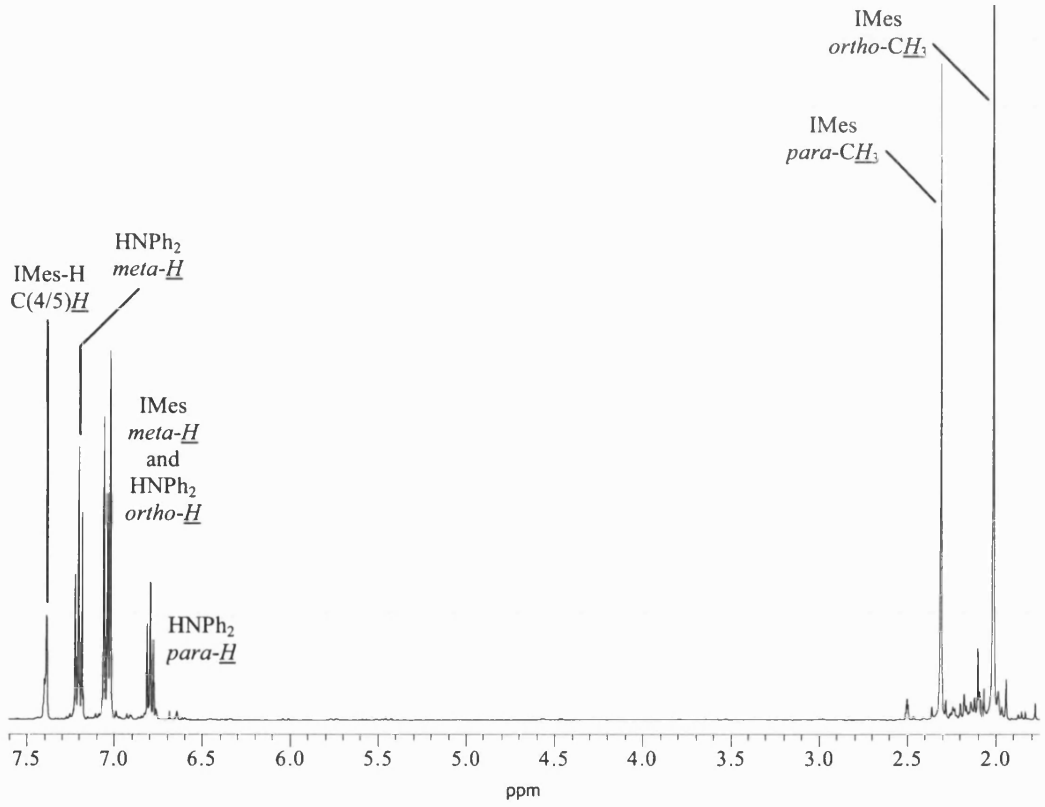

Figure 2.24: ^{1}H-NMR spectrum of **15** in d_6-DMSO recorded at 400 MHz

Since the degree of variation in the chemical shift of the imidazolium cation resonances is only slight, the $^{13}C\{^{1}H\}$-NMR spectrum of **11** (Figure 2.25) can be considered to be representative of that of the imidazolium salts **11-14**. $^{13}C\{^{1}H\}$-NMR spectroscopy also provides compelling evidence that **15** is indeed an imidazol-2-ylidene:amine adduct, since the C(4/5) carbon atoms are observed at a chemical shift (121.5 ppm) indicative of an imidazol-2-ylidene heterocyclic core.

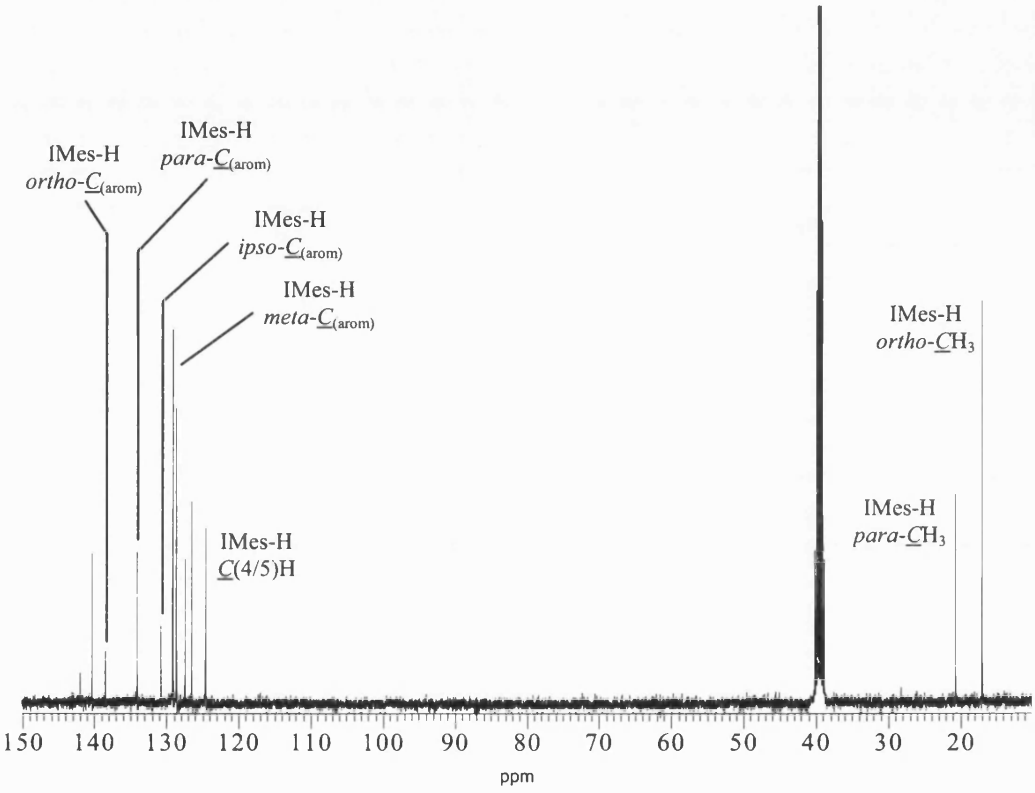

Figure 2.25: ^{13}C-NMR spectrum of **11** in d_6-DMSO recorded at 100 MHz

Single crystals of **11** suitable for x-ray diffraction analysis could not be obtained; however, the stoichiometric reaction of 1,3-bis-(2,6-diisopropylphenyl)-imidazol-2-ylidene with one equivalent of dibenzoylmethane yielded crystals of a related imidazolium benzoate species, **11a**, which were subsequently studied by means of x-ray diffractometry. The N(1)–C(2)–N(3) angle observed in **11a** is 109.3(1)°, which is in good agreement with that reported for 1,3-bis-(2,4,6-trimethylphenyl)-imidazolium chloride (108.7(4)°),[34] and, at 1.341(2) Å, the average N–C(2) bond length is shorter than that of 1,3-bis-(2,4,6-trimethylphenyl)-imidazol-2-ylidene (1.368(4) Å);[43] providing compelling evidence that this product is indeed an imidazolium salt and not a neutral imidazol-2-ylidene:benzoic acid adduct.

The imidazolium cation and benzoate anion in **11a** are associated through a short C–H·····O^- hydrogen-bonding interaction (D = 2.897 Å, d = 1.96 Å and θ = 176°), [C1–H1·····$O1^-$] (Figure 2.26); shorter in fact than those within the neutral adducts [$((NO_2)_3CH)_2$.dioxane] (D = 2.94 Å, d = 2.01 Å and θ = 146° (C–H corrected to 1.07 Å))[51] and [$Ph_3SiC{\equiv}CH.OPPh_3$] (D = 3.02 Å, d = 2.01 Å and θ = 155°),[52] the bisoxazoline-derived imidazolium triflate recently reported by Glorius *et al.* (D = 3.00 Å, d = 2.01 Å and θ = 165°),[53] and [$(Ph_3PCH_3)^+(2,6\text{-}Ph_2C_6H_3O)^-$] ($D$ = 3.02 Å, d = 1.94 Å and θ = 167°).[54] A molecule of water trapped in the lattice

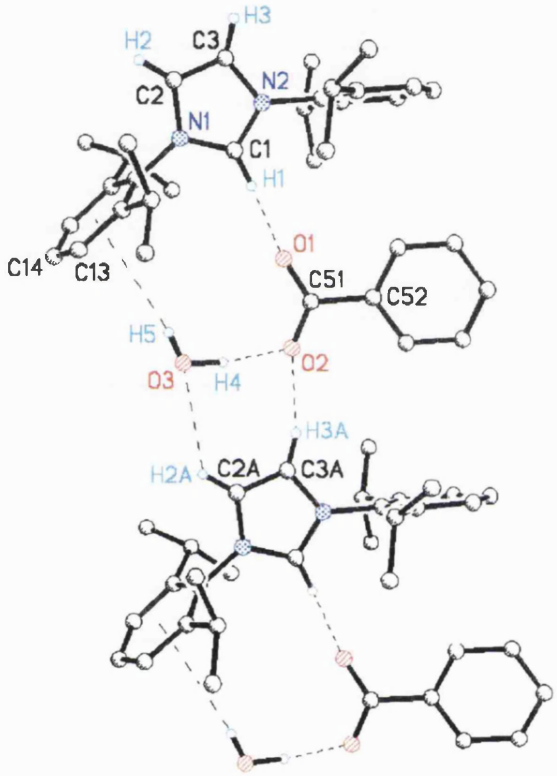

Figure 2.26: Supramolecular solid state structure of imidazolium benzoate **11a**

also bridges the cation and anion via O–H·····π(arene), [O3–H5·····centroid(C11-C16)] (D = 4.106 Å, d = 3.29 Å and θ = 171°), and O–H·····O, [O3–H4·····O2] (D = 2.739 Å, d = 1.72 Å and θ = 157°), interactions (Figure 2.26); lending support to the proposed hydrolysis reaction.[70] This interaction is significantly longer than the charge assisted O–H·····O^- contacts within **1** (D = 2.486(2) Å, d = 1.44(3) Å and θ = 176(3)°), **2** (D = 2.487(2) Å, d = 1.43(4) Å and θ = 163(3)°) and **3** (D =

2.506(2) Å, d = 1.34(3) Å and θ = 173(3)°). The supramolecular hydrogen-bonded network is formed by means of intermolecular C–H·····O hydrogen bonds between the imidazolium cation C(4/5)-H hydrogen atoms and the oxygen atoms of the benzoate anion, [C3A–H3A·····O2] (D = 3.012 Å, d = 2.11 Å and θ = 158°), and the molecule of water in the lattice (D = 3.456 Å, d = 2.77 Å and θ = 130°), [C2A–H2A·····O3] (Figure 2.26).

Slow cooling to room temperature of a hot toluene solution of imidazolium triflate **14** results in the formation of single crystals of this species that are suitable for study by x-ray diffraction. A room temperature x-ray diffraction experiment was subsequently performed, and the asymmetric unit found to contain an equal number of imidazolium cations and triflate anions; presumably associated through C–H·····O^- interactions (Figure 2.27). Unfortunately the data could not be refined sufficiently for any meaningful discussion of the metrical parameters of the

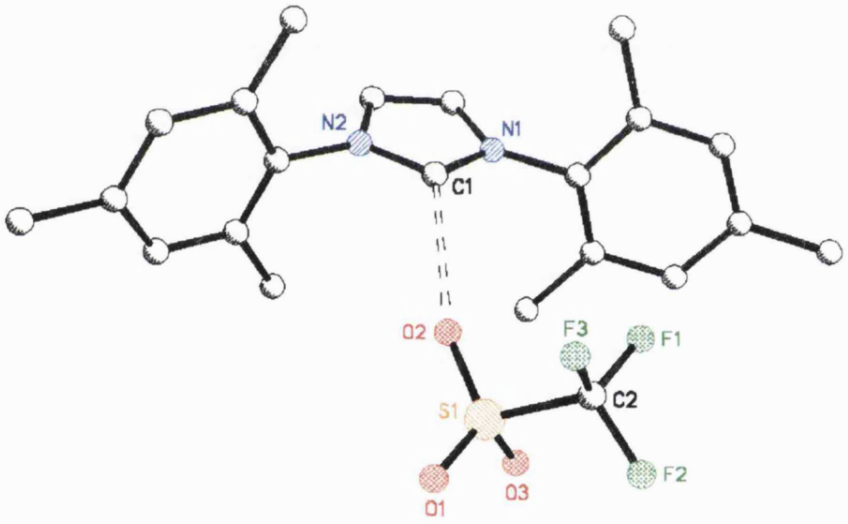

Figure 2.27: Imidazolium cation and triflate anion as a contact ion pair in compound **14**

cationic or anionic components, or the hydrogen-bonding present, to be entered into. However, it should be noted that, in addition to the NMR spectroscopic evidence, support for the classification of this species as an imidazolium triflate salt, as opposed to an imidazol-2-ylidene:triflic acid adduct, is provided by the relative acidities of triflic acid and the imidazolium cation (pK_a values in DMSO

solution of 0.3,[71] and 24,[35] respectively). Moreover, Glorius *et al.* have recently structurally characterised an analogous species as an imidazolium triflate salt.[53]

In line with the available NMR spectroscopic evidence, x-ray diffraction analysis of a suitable single crystal of compound **15** reveals that this species is indeed a neutral imidazol-2-ylidene:amine adduct (Scheme 2.6). The asymmetric unit contains a single unprotonated imidazol-2-ylidene moiety and a molecule of diphenylamine; the metrical parameters of the five-membered heterocyclic ring compare well with those of 1,3-bis-(2,4,6-trimethylphenyl)-imidazol-2-ylidene. For instance, the N(1)–C(2)–N(3) angle and the average N–C(2) bond length are

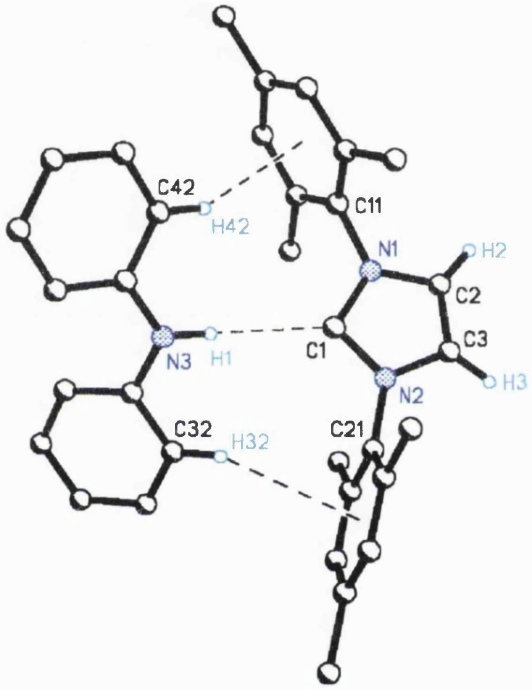

Figure 2.28: Intramolecular hydrogen-bonding in the solid state structure of **15**

101.7(1)° and 1.372(2) Å in **15**, and 101.4(2)° and 1.368(4) Å in 1,3-bis-(2,4,6-trimethylphenyl)-imidazol-2-ylidene.[43] The relative acidities of the imidazolium cation and diphenylamine (pK_a values in DMSO solution of 24,[35] and 24.95,[71] respectively) are consistent with the 1,3-bis-(2,4,6-trimethylphenyl)-imidazol-2-ylidene moiety remaining unprotonated on treatment with diphenylamine.

The intramolecular hydrogen-bonding within **15** consists of an N–H·····C contact, [N3–H1·····C1] (D = 3.196(2) Å, d = 2.30(1) Å and θ = 179(2)°), accompanied by a representative C–H·····π(arene) interaction, [C32–H32·····centroid(C21-C26)] (D = 3.437(4) Å, d = 2.52(2) Å and θ = 156(2)°),[50, 64] and a long C–H·····π(arene) contact [C42–H42·····centroid(C11-C16)] (D = 3.808(4) Å, d = 2.90(2) Å and θ = 156(2)°) (Figure 2.28). Of these intramolecular interactions, the N–H·····C contact in which the imidazol-2-ylidene acts as a hydrogen bond acceptor would seem to be the dominant electrostatic interaction, since it is significantly shorter than the two out-rigging C–H·····π(arene) contacts. It should be noted that, a C–H·····C hydrogen bond, in which an imidazol-2-ylidene moiety acts as a hydrogen bond acceptor, has recently been structurally characterised by Arduengo *et al.*[34]

The x-ray diffraction data collection was performed at 30 K (Oxford Cryosystems HELIX) to allow the best possible dataset to be acquired. The electron density within the plane of the imidazol-2-ylidene heterocyclic core is depicted in the

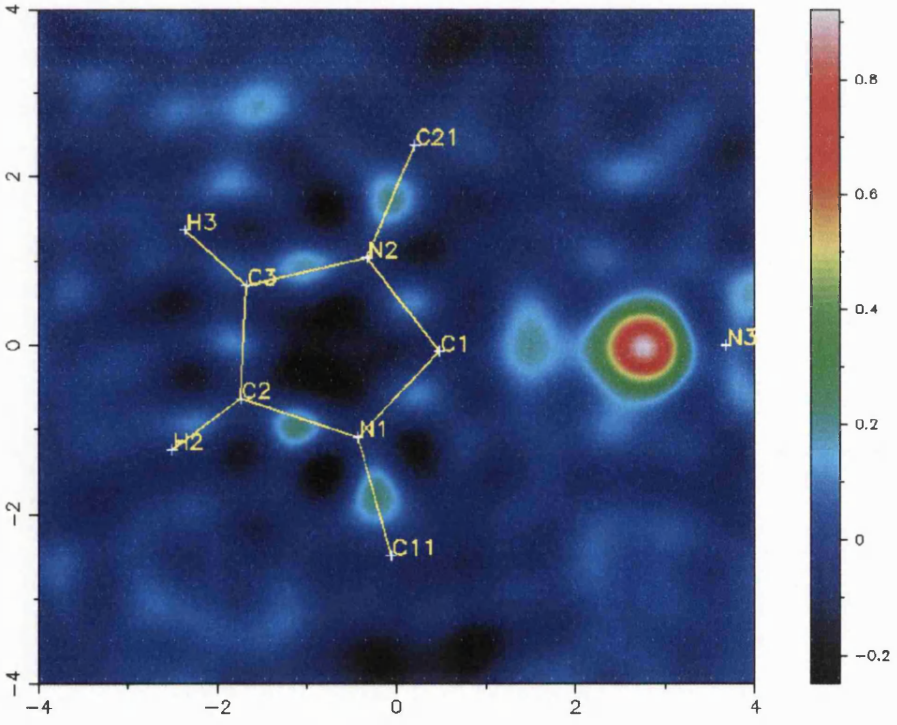

Figure 2.29: Electron density difference map within the plane of the heterocyclic core in imidazol-2-ylidene:diphenylamine adduct **15**

difference map above (Figure 2.29); which clearly shows the hydrogen atom at 0.90 Å from N3 along the N3-C1 vector. The electron density at 1.00 Å from C1 (along the C1-N3 vector) corresponds to the imidazol-2-ylidene lone pair; the fact that this spot is not more intense is perhaps a reflection of the stabilisation of the singlet carbene centre by way of inductive effects and π-donation.[2] Disorder of the hydrogen atom over these two positions along the C1-N3 vector (consistent with the double minima on the potential energy surface of strong hydrogen bonds) does not seem to account for the two islands of electron density since there is not any significant disorder within the heterocyclic core itself; especially within the N1–C1–N2 angle, and, N1–C1 and N2–C1 bond lengths. The electron density difference map (Figure 2.29) illustrates that the imidazol-2-ylidene lone pair is polarised by the Lewis acidic hydrogen atom, confirming that the N3–H1·····C1 contact (Figure 2.28) is a genuine electrostatic interaction.

The C(4/5)-H backbone hydrogen substituents are involved in the intermolecular interactions responsible for the extended polymeric array observed in the solid state structure of imidazol-2-ylidene:amine adduct **15**; as is the case in all of the

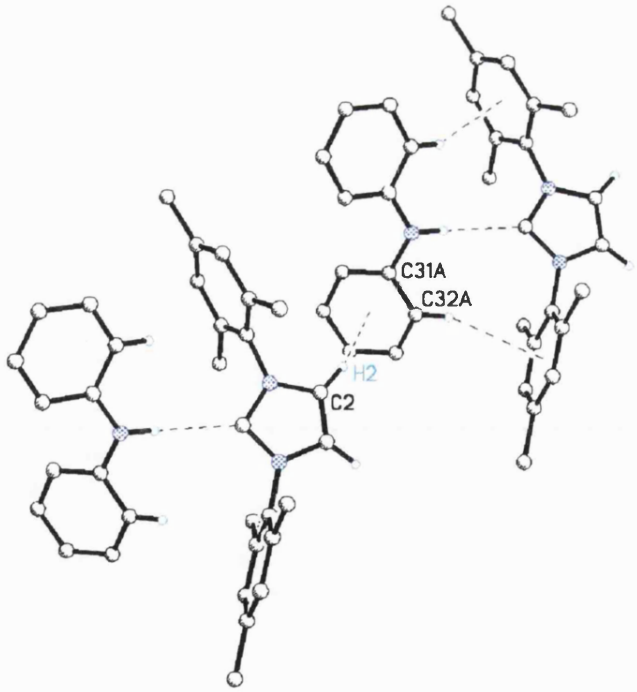

Figure 2.30: Intermolecular C–H·····π(arene) interactions in the extended solid state structure of **15**

imidazolium species that have been structurally characterised in this study. Indeed, the individual molecules of **15** associate by means of C–H·····π(arene) interactions, [C2–H2·····centroid(C31A-C36A)] (D = 3.725(4) Å, d = 2.95(2) Å and θ = 140(2)°), involving an imidazol-2-ylidene C(4/5)-H backbone hydrogen atom of one molecule of **15** and the π-system of a phenyl ring substituent of the diphenylamine moiety within a neighbouring molecule (Figure 2.30).

2.5: Conclusions

Reaction of 1,3-bis-(2,4,6-trimethylphenyl)-imidazol-2-ylidene with O-H acidic organic compounds results in the abstraction of the acidic proton by the basic imidazol-2-ylidene to yield the corresponding imidazolium salt. A number of imidazolium salts have been prepared in this manner; many of which have been structurally characterised by single crystal x-ray diffraction. The imidazolium cation and the organic anion are, in all cases, associated via exceptionally short C–H·····O^- hydrogen bonds; indeed, compounds **1**, **3**, **4**, **5**, **8**, **9**, and **11a** feature the shortest C–H·····O contacts reported to date. The ^{1}H- and ^{13}C{^{1}H}-NMR spectra of all the imidazolium salts prepared in this study suggest that exchange of the acidic protons occurs in solution; these imidazolium salts may therefore be considered to be activated towards *in situ* deprotonation.

The neutral imidazol-2-ylidene:amine adduct **15** forms as a result of the treatment of 1,3-bis-(2,4,6-trimethylphenyl)-imidazol-2-ylidene with diphenylamine; in this case, the imidazol-2-ylidene is not basic enough to deprotonate the N-H acid, and participates in an unprecedented N–H·····C hydrogen-bonding interaction instead (the *N*-heterocyclic carbene acting as the hydrogen bond acceptor group). The electron density difference map constructed from the data collection obtained from a low temperature x-ray diffraction experiment (30 K) shows that there is an electrostatic interaction between the amine hydrogen atom and the imidazol-2-ylidene lone pair. This compound represents an imidazol-2-ylidene stabilised by hydrogen-bonding.

The results of this study demonstrate that the reaction of imidazol-2-ylidenes with sufficiently acidic organic compounds represents an effective route to hydrogen-bonded imidazolium salts, which possess non-conventional anionic components; neutral hydrogen-bonded imidazol-2-ylidene adducts may also be prepared if the organic compound is less acidic than the conjugate acid of the imidazol-2-ylidene. This suggests that a wider range of organic precursors to metal-*N*-heterocyclic carbenes may be accessible by means of this simple acid-base approach than by the more established salt metathesis methodology. Further study of the reaction of imidazol-2-ylidenes with O-H, N-H, and even C-H acidic organic compounds is required in order to determine the full scope of organic metal-*N*-heterocyclic carbene precursors accessible in this manner.

A discussion of the exploitation of the hydrogen-bonded imidazolium salts and neutral imidazol-2-ylidene:amine adduct reported here as convenient organic precursor compounds to copper(I)- and zinc(II)-*N*-heterocyclic carbene complexes bearing phenoxide and amide functionalities as ancillary ligands is subsequently reported in Chapter Three and Chapter Four, respectively.

2.6: References

[1] G. A. Jeffrey, *An Introduction to Hydrogen Bonding*, Oxford University Press, Oxford, **1997**.

[2] A. J. Arduengo, R. L. Harlow, M. Kline, *J. Am. Chem. Soc.*, **1991**, *113*, 361.

[3] W. A. Herrmann, C. Kocher, *Angew. Chem.-Int. Ed. Engl.*, **1997**, *36*, 2163.

[4] W. A. Herrmann, T. Weskamp, V. P. W. Bohm, *"Metal complexes of stable carbenes"*, in *Advances in Organometallic Chemistry*, **2001**. 1-69.

[5] W. A. Herrmann, *Angew. Chem.-Int. Ed. Engl.*, **2002**, *41*, 1291.

[6] C. M. Zhang, J. K. Huang, M. L. Trudell, S. P. Nolan, *J. Org. Chem.*, **1999**, *64*, 3804.

[7] T. Weskamp, W. A. Herrmann, *Abstr. Pap. Am. Chem. Soc.*, **1999**, *218*, 43.

[8] J. Schwarz, V. P. W. Bohm, M. G. Gardiner, M. Grosche, W. A. Herrmann, W. Hieringer, G. Raudaschl-Sieber, *Chem.-Eur. J.*, **2000**, *6*, 1773.

[9] C. W. K. Gstottmayr, V. P. W. Bohm, E. Herdtweck, M. Grosche, W. A. Herrmann, *Angew. Chem.-Int. Ed. Engl.*, **2002**, *41*, 1363.

[10] A. C. Hillier, G. A. Grasa, M. S. Viciu, H. M. Lee, C. L. Yang, S. P. Nolan, *J. Organomet. Chem.*, **2002**, *653*, 69.

[11] T. Weskamp, F. J. Kohl, W. Hieringer, D. Gleich, W. A. Herrmann, *Angew. Chem.-Int. Ed. Engl.*, **1999**, *38*, 2416.

[12] C. W. Bielawski, R. H. Grubbs, *Angew. Chem.-Int. Ed. Engl.*, **2000**, *39*, 2903.

[13] L. Jafarpour, S. P. Nolan, *Org. Lett.*, **2000**, *2*, 4075.

[14] J. G. Hamilton, U. Frenzel, F. J. Kohl, T. Weskamp, J. J. Rooney, W. A. Herrmann, O. Nuyken, *J. Organomet. Chem.*, **2000**, *606*, 8.

[15] L. Jafarpour, S. P. Nolan, *J. Organomet. Chem.*, **2001**, *617*, 17.

[16] M. S. Sanford, J. A. Love, R. H. Grubbs, *Organometallics*, **2001**, *20*, 5314.

[17] W. Baratta, E. Herdtweck, W. A. Herrmann, P. Rigo, J. D. Schwarz, *Organometallics*, **2002**, *21*, 2101.

[18] W. A. Herrmann, M. Elison, J. Fischer, C. Kocher, G. R. J. Artus, *Chem.-Eur. J.*, **1996**, *2*, 772.

[19] H. W. Wanzlick, H. J. Schonherr, *Angew. Chem.-Int. Ed. Engl.*, **1968**, *7*, 141.

[20] W. A. Herrmann, C. P. Reisinger, M. Spiegler, *J. Organomet. Chem.*, **1998**, *557*, 93.

[21] W. A. Herrmann, J. Schwarz, M. G. Gardiner, *Organometallics*, **1999**, *18*, 4082.

[22] M. G. Gardiner, W. A. Herrmann, C. P. Reisinger, J. Schwarz, M. Spiegler, *J. Organomet. Chem.*, **1999**, *572*, 239.

[23] G. Bertrand, E. Diez-Barra, J. Fernandez-Baeza, H. Gornitzka, A. Moreno, A. Otero, R. I. Rodriguez-Curiel, J. Tejeda, *Eur. J. Inorg. Chem.*, **1999**, 1965.
[24] W. A. Herrmann, M. Elison, J. Fischer, C. Kocher, G. R. J. Artus, *Angew. Chem.-Int. Ed. Engl.*, **1995**, *34*, 2371.
[25] D. Enders, H. Gielen, G. Raabe, J. Runsink, J. H. Teles, *Chem. Ber.*, **1996**, *129*, 1483.
[26] W. A. Herrmann, G. Gerstberger, M. Spiegler, *Organometallics*, **1997**, *16*, 2209.
[27] O. Guerret, S. Sole, H. Gornitzka, G. Trinquier, G. Bertrand, *J. Organomet. Chem.*, **2000**, *600*, 112.
[28] C. Buron, L. Stelzig, O. Guerret, H. Gornitzka, V. Romanenko, G. Bertrand, *J. Organomet. Chem.*, **2002**, *664*, 70.
[29] S. Grundemann, A. Kovacevic, M. Albrecht, J. W. Faller, R. H. Crabtree, *J. Am. Chem. Soc.*, **2002**, *124*, 10473.
[30] S. Grundemann, A. Kovacevic, M. Albrecht, J. W. Faller, R. H. Crabtree, *J. Chem. Soc.-Chem. Commun.*, **2001**, 2274.
[31] A. Kovacevic, S. Grundemann, J. R. Miecznikowski, E. Clot, O. Eisenstein, R. H. Crabtree, *J. Chem. Soc.-Chem. Commun.*, **2002**, 2580.
[32] J. Dupont, R. F. de Souza, P. A. Z. Suarez, *Chem. Rev.*, **2002**, *102*, 3667.
[33] S. V. Dzyuba, R. A. Bartsch, *Angew. Chem.-Int. Ed. Engl.*, **2003**, *42*, 148.
[34] A. J. Arduengo, S. F. Gamper, M. Tamm, J. C. Calabrese, F. Davidson, H. A. Craig, *J. Am. Chem. Soc.*, **1995**, *117*, 572.
[35] R. W. Alder, P. R. Allen, S. J. Williams, *J. Chem. Soc.-Chem. Commun.*, **1995**, 1267.
[36] Y. J. Kim, A. Streitwieser, *J. Am. Chem. Soc.*, **2002**, *124*, 5757.
[37] A. G. Avent, P. A. Chaloner, M. P. Day, K. R. Seddon, T. Welton, *J. Chem. Soc.-Dalton Trans.*, **1994**, 3405.
[38] A. Elaiwi, P. B. Hitchcock, K. R. Seddon, N. Srinivasan, Y. M. Tan, T. Welton, J. A. Zora, *J. Chem. Soc.-Dalton Trans.*, **1995**, 3467.
[39] J. A. Cowan, J. A. C. Clyburne, M. G. Davidson, R. L. W. Harris, J. A. K. Howard, P. Kupper, M. A. Leech, S. P. Richards, *Angew. Chem.-Int. Ed. Engl.*, **2002**, *41*, 1432.
[40] D. A. Dixon, A. J. Arduengo, *J. Phys. Chem.*, **1991**, *95*, 4180.
[41] A. J. Arduengo, J. C. Calabrese, F. Davidson, H. V. R. Dias, J. R. Goerlich, R. Krafczyk, W. J. Marshall, M. Tamm, R. Schmutzler, *Helv. Chim. Acta*, **1999**, *82*, 2348.
[42] F. H. Allen, O. Kennard, *Chem. Des. Autom. News*, **1993**, *8*, 31.
[43] A. J. Arduengo, H. V. R. Dias, R. L. Harlow, M. Kline, *J. Am. Chem. Soc.*, **1992**, *114*, 5530.
[44] R. Goddard, H. M. Herzog, M. T. Reetz, *Tetrahedron*, **2002**, *58*, 7847.
[45] M. K. Denk, J. M. Rodezno, *J. Organomet. Chem.*, **2000**, *608*, 122.
[46] A. J. Arduengo, H. V. R. Dias, D. A. Dixon, R. L. Harlow, W. T. Klooster, T. F. Koetzle, *J. Am. Chem. Soc.*, **1994**, *116*, 6812.

[47] C. Heinemann, T. Muller, Y. Apeloig, H. Schwarz, *J. Am. Chem. Soc.*, **1996**, *118*, 2023.
[48] M. Tafipolsky, W. Scherer, K. Ofele, G. Artus, B. Pedersen, W. A. Herrmann, G. S. McGrady, *J. Am. Chem. Soc.*, **2002**, *124*, 5865.
[49] A. J. Arduengo, R. Krafczyk, R. Schmutzler, H. A. Craig, J. R. Goerlich, W. J. Marshall, M. Unverzagt, *Tetrahedron*, **1999**, *55*, 14523.
[50] G. R. Desiraju, T. Steiner, *The Weak Hydrogen Bond: In Structural Chemistry and Biology*, Oxford University Press, Oxford, **1999**.
[51] H. Bock, R. Dienelt, H. Schodel, Z. Havlas, *J. Chem. Soc.-Chem. Commun.*, **1993**, 1792.
[52] T. Steiner, J. van der Maas, B. Lutz, *J. Chem. Soc.-Perkin Trans. 2*, **1997**, 1287.
[53] F. Glorius, G. Altenhoff, R. Goddard, C. Lehmann, *J. Chem. Soc.-Chem. Commun.*, **2002**, 2704.
[54] M. G. Davidson, A. E. Goeta, J. A. K. Howard, S. Lamb, S. A. Mason, *New J. Chem.*, **2000**, *24*, 477.
[55] G. R. Desiraju, *J. Chem. Soc.-Chem. Commun.*, **1989**, 179.
[56] G. R. Desiraju, *Acc. Chem. Res.*, **1991**, *24*, 290.
[57] V. R. Pedireddi, G. R. Desiraju, *J. Chem. Soc.-Chem. Commun.*, **1992**, 988.
[58] G. R. Desiraju, *Acc. Chem. Res.*, **1996**, *29*, 441.
[59] www.colorado.edu/ceae/environmental/ryan/cven5424/lect12acidbase.ppt.
[60] L. S. Reddy, A. Nangia, V. M. Lynch, *Cryst. Growth Des.*, **2004**, *4*, 89.
[61] C. E. Smith, P. S. Smith, R. L. Thomas, E. G. Robins, J. C. Collings, C. Dai, A. J. Scott, S. Borwick, A. S. Batsanov, S. W. Watt, S. J. Clark, C. Viney, J. A. K. Howard, W. Clegg, T. B. Marder, *J. Mater. Chem.*, **2004**, *14*, 413.
[62] T. Ramnial, C. D. Abernethy, M. D. Spicer, I. D. McKenzie, I. D. Gay, J. A. C. Clyburne, *Inorg. Chem.*, **2003**, *42*, 1391.
[63] T. Ramnial, H. Jong, I. D. McKenzie, M. Jennings, J. A. C. Clyburne, *J. Chem. Soc.-Chem. Commun.*, **2003**, 1722.
[64] C. K. Broder, M. G. Davidson, V. T. Forsyth, J. A. K. Howard, S. Lamb, S. A. Mason, *Cryst. Growth Des.*, **2002**, *2*, 163.
[65] W. Sawka-Dobrowolska, E. Grech, B. Brzezinski, Z. Malarski, L. Sobczyk, *J. Mol. Struct.*, **1995**, *356*, 117.
[66] E. Tykarska, Z. Dega-Szafran, M. Szafran, *J. Mol. Struct.*, **1999**, *477*, 49.
[67] T. Steiner, I. Majerz, C. C. Wilson, *Angew. Chem.-Int. Ed. Engl.*, **2001**, *40*, 2651.
[68] N. W. Alcock, P. R. Barker, J. M. Haider, M. J. Hannon, C. L. Painting, Z. Pikramenou, E. A. Plummer, K. Rissanen, P. Saarenketo, *J. Chem. Soc.-Dalton Trans.*, **2000**, 1447.
[69] L. Jafarpour, E. D. Stevens, S. P. Nolan, *J. Organomet. Chem.*, **2000**, *606*, 49.
[70] R. Connor, H. Adkins, *J. Am. Chem. Soc.*, **1932**, *54*, 3420.
[71] F. G. Bordwell, *Acc. Chem. Res.*, **1988**, *21*, 456.

Copper-*N*-Heterocyclic Carbene Complexes

3.1: Introduction

This chapter investigates the preparation of *N*-heterocyclic carbene ligated copper species that may potentially be utilised as catalysts or group-transfer reagents, via the *in situ* deprotonation of organic precursors discussed in Chapter Two. This introduction highlights the use of copper species as catalysts and stoichiometric reagents in a variety of organic transformations, and provides a brief overview of previous work involving copper-*N*-heterocyclic carbene complexes.

3.1.1: Copper Compounds in Organic Transformations

Copper reagents are employed in a number of organic transformations, examples that will be briefly described here include: the oxidation of alkanes, alkenes and alcohols; oxidative coupling reactions; the Aldol reaction; Diels Alder reactions; the reduction of organic carbonyl compounds; 1,4-conjugate additions to enones; cyclopropanations; and polymerisation reactions.

Active catalysts for the homogeneous aerobic oxidation of alkanes, alkenes and alcohols may be prepared *in situ* from simple copper salts.[1] Indeed, Murahashi *et al.* have recently reported that copper(II) chloride combined with crown ethers represents an efficient catalytic system for the aerobic oxidation of alkanes with acetaldehyde (Scheme 3.1); oxidation of cyclohexane in this manner results in formation of cyclohexanone and cyclohexanol in yields based on acetaldehyde of 61% and 10%, respectively.[2] The mechanism has not yet been elucidated, but it has been postulated that the reaction of acetaldehyde with molecular oxygen in the presence of the copper salt generates a peroxy acid,[3] which subsequently reacts with the copper centre to form the catalytically active species - believed to be a Cu(III)–O$^{\cdot}$ or Cu(IV)=O complex.[4] It is thought that this highly reactive copper centre abstracts a hydrogen atom from the alkane substrate leading to formation of the related alcohol following electron-transfer; the alcohol can be further oxidised to the ketone under the reaction conditions (Scheme 3.1).[1]

An earlier publication from Murahashi *et al.* reported the homogeneous aerobic oxidation of alkenes to epoxides (Scheme 3.1) under similar conditions; catalysed by a copper species generated *in situ* from copper(II) hydroxide.[5] The catalytic oxidation of alcohols to the respective aldehydes utilising *in situ* generated copper catalysts has also been recorded in the chemical literature;[6] indeed, most notably, Knochel *et al.* have developed a fluorous biphasic system in which the fluorous soluble catalytically active copper species is generated from $[CuBr][S(CH_3)_2]$, a fluoroalkylated 2,2'-bipyridyl ligand, and the TEMPO radical (Scheme 3.1).[7]

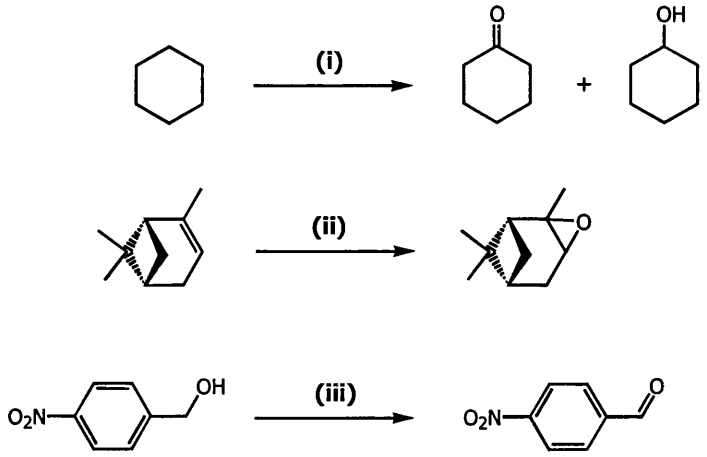

Scheme 3.1: Aerobic oxidation of alkanes, alkenes and alcohols under mild conditions catalysed by *in situ* generated copper species
(i) acetaldehyde, O_2 (1 atm), $CuCl_2$, 18-crown-6, dichloromethane, 70 °C;[2]
(ii) cyclohexanecarbaldehyde, O_2 (1 atm), $Cu(OH)_2$, dichloromethane, room temperature;[5] **(iii)** O_2, $[CuBr][S(CH_3)_2]$, fluorous soluble 2,2'-bipyridyl ligand, TEMPO, C_8F_{18}/C_6H_5Cl, 90 °C[7]

Dinuclear copper complexes have been shown to catalyse the oxidative coupling of phenols that are unsubstituted in the *para*-position but possess two bulky *ortho*-substituents; and, similarly, *para*-substituted phenols in which one of the *ortho*-positions is occupied by a bulky substituent while the other remains unsubstituted (Scheme 3.2). Indeed, Mukherjee has recently demonstrated that, in the presence of molecular oxygen, a dicopper(I) complex bearing the α,α'-bis-((*N*-methyl-2-pyridyl)-ethylamino)-2-fluoro-*meta*-xylene ligand catalyses the conversion of 2,4-di-*tert*-butylphenol into the C-C coupled bisphenol product.[8]

An *in situ* generated copper(I) species has been implicated as the active catalyst in the copper catalysed Aldol reaction reported by Carreira (Scheme 3.2).[9, 10] The catalytically active species was initially reported to be a copper(II) complex, ((*S*)-Tol-BINAP)CuF_2; however, subsequent work has demonstrated that the copper(I) phosphine species ((*S*)-Tol-BINAP)-CuF is, in fact, an equally effective catalyst for this reaction.[10] Furthermore, this latter report interestingly suggests that the copper(I) alkoxide complex ((*S*)-Tol-BINAP)-CuO^tBu also represents a practical catalyst for Aldol reactions - such as that depicted below in Scheme 3.2.

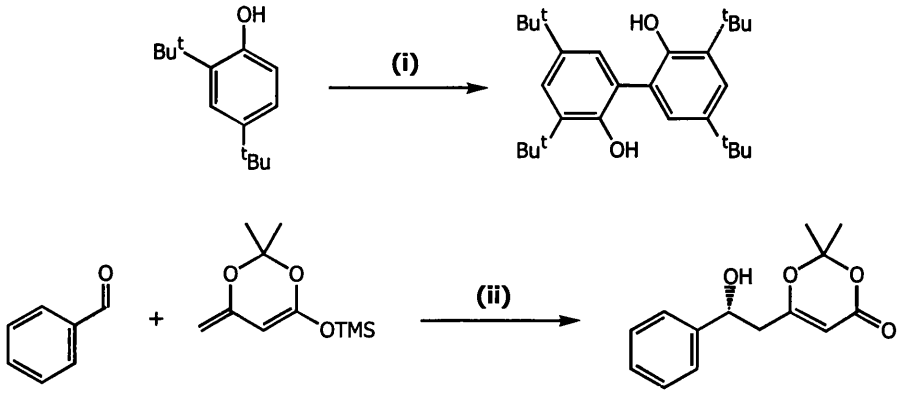

Scheme 3.2: Copper catalysed oxidative aryl-aryl couplings and Aldol reactions
(i) O_2, [(α,α'-bis-((*N*-methyl-2-pyridyl)-ethylamino)-2-fluoro-*meta*-xylene)$Cu_2(NCCH_3)_2][ClO_4]_2$, dichloromethane, room temperature;[8]
(ii) $Cu(OTf)_2$, (*S*)-Tol-BINAP, $[Bu_4N][Ph_3SiF_2]$, tetrahydrofuran, -78 °C[9]

Copper(II) coordination compounds possessing non-coordinating anions, such as $CF_3SO_3^-$ and SbF_6^-, have been shown to constitute effective Lewis acid catalysts for Diels Alder reactions, Michael reactions, and Ene reactions. A comprehensive treatise of the use of cationic copper(II) species as Lewis acid catalysts in these and other such reactions is provided within a review article, examining copper(I) and copper(II) catalysed asymmetric organic transformations, recently published by Rovis and Evans.[11]

In addition to catalysing both oxidative couplings of phenols and Aldol reactions (Scheme 3.2), copper(I) complexes have been reported to catalyse the reduction of organic carbonyl compounds.[12, 13] Indeed, Buchwald and Sadighi have recently demonstrated that conjugate reduction of α,β-unsaturated carbonyl compounds

(Scheme 3.3) is catalysed by a copper(I) hydride generated *in situ* as a result of the reaction between the related copper(I) *tert*-butoxide reactive intermediate and polymethylhydrosiloxane.[12] Interestingly, Nolan *et al.* have subsequently used the same copper(I) hydride species as a catalyst for the reductive silylation of ketones; in which the catalytically active species is formed *in situ* as a result of the reaction of the highly reactive copper(I) *tert*-butoxide intermediate with silane.[13]

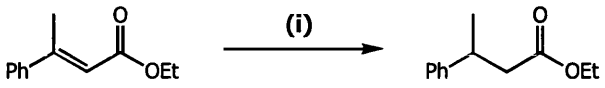

Scheme 3.3: Conjugate reduction of α,β-unsaturated carbonyl compounds
(i) (IPr)CuCl, NaO^{t}Bu, polymethylhydrosiloxane, ^{t}BuOH, toluene, room temperature

Organocuprates - organometallic copper reagents of the type R_2CuLi - are utilised as stoichiometric group-transfer reagents in organic synthesis.[11] Treatment of an enone substrate with the organocuprate reagent $(CH_2{=}CH)_2CuLi$[14] results in the 1,4-conjugate addition (Michael addition) of the organometallic to the substrate; the substituted cyclohexanone product (Scheme 3.4) is then isolated following an acidic aqueous work-up. There is evidence to suggest that the reactivity of these organocuprates is affected by the degree of aggregation in solution; indeed, the presence of phosphite ligands is reported to enhance organocuprate reactivity.[14]

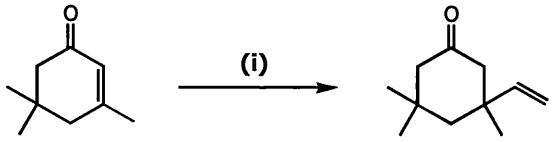

Scheme 3.4: Conjugate addition to enones
(i) $(P(OCH_3)_3)CuBr$, $CH_2{=}CHLi$, diethyl ether, -60 °C[14]

Copper complexes are also effective catalysts for the cyclopropanation of alkenes; a carbene-transfer reaction in which the carbene species is generated *in situ* from a diazo compound and trapped by the copper centre, and subsequently transferred to the alkene substrate. Analogous copper nitrenoids have been shown to transfer a nitrene in the aziridination of alkenes.[15, 16] A comprehensive review of the use of copper species in these organic transformations is provided by the recent articles published by Rovis and Evans[11] and Kirmse.[17]

Copper coordination compounds have also been reported to constitute effective catalysts for polymerisation reactions. Indeed, copper-phenoxide complexes have been proposed to be the catalytically active species in the polymerisation of 2,6-dimethylphenol to provide poly-(2,6-dimethyl-1,4-phenylene ether).[1] However, the most promising application of copper complexes in homogeneous catalysis is, perhaps, in controlled radical polymerisations. Control of the molecular weight of polymers obtained from radical polymerisations effected by persistent radicals is notoriously difficult to achieve;[18] Atom Transfer Radical Polymerisation (ATRP) provides low polydispersity polymers with molecular weights dependent solely on the number of molecules of monomer present per molecule of catalyst.[19-27] The propagating radicals are generated via a reversible activation step - abstraction of the halogen atom from a dormant polymer chain by the copper catalyst, homolytic fission of the carbon-halogen bond, and oxidation of the copper centre - and may potentially react with a vinyl monomer molecule before undergoing deactivation (Scheme 3.5). The equilibrium between the dormant chains and the propagating radicals lies well towards the halogen-terminated macromolecule. Consequently the steady-state concentration of the organic radicals is low, limiting irreversible termination steps such as the combination of propagating radicals.

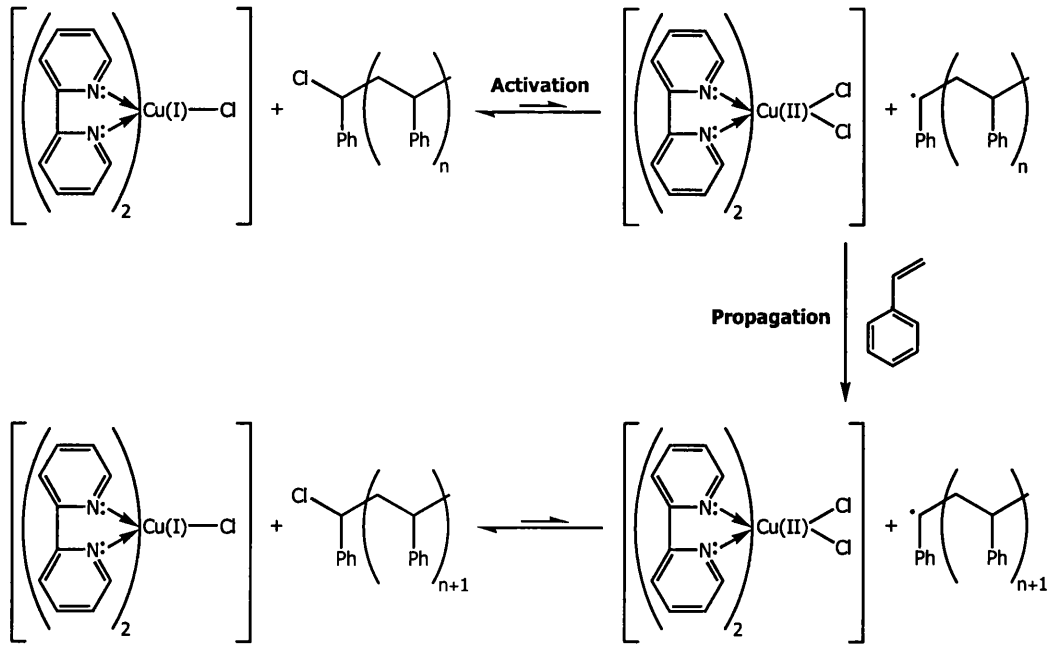

Scheme 3.5: Reversible activation of halogen-terminated dormant macromolecular chains and addition of monomer to propagating radicals in copper catalysed ATRP of styrene

3.1.2: Copper-*N*-Heterocyclic Carbene Complexes

Only a few copper-*N*-heterocyclic carbene complexes have been reported to date. Arduengo *et al.* synthesised and isolated the very first of these; a bis-(imidazol-2-ylidene)-copper(I) triflate salt prepared via the reaction of two equivalents of the corresponding free *N*-heterocyclic carbene with a single equivalent of copper(I) triflate.[28] Interestingly, this compound is isostructural with a biscarbene-proton complex subsequently reported by the same group.[29]

Raubenheimer *et al.* reported the preparation, isolation, and subsequent structural characterisation, of a (thiazol-2-ylidene)-copper(I) chloride adduct;[30, 31] the first copper species with mono-(*N*-heterocyclic carbene)-substitution to emerge in the chemical literature. The analogous (1,3-bis-(2,6-diisopropylphenyl)-imidazol-2-ylidene)-copper(I) chloride has recently been employed in the catalysis of the reduction of organic carbonyl compounds. Buchwald and Sadighi, and also more recently Nolan *et al.*, have utilised this *N*-heterocyclic carbene-copper(I) chloride adduct to generate the corresponding (imidazol-2-ylidene)-copper(I) *tert*-butoxide complex *in situ* (Scheme 3.6); which is, under the reaction conditions, converted to the catalytically active *N*-heterocyclic carbene-copper(I) hydride species.[12, 13]

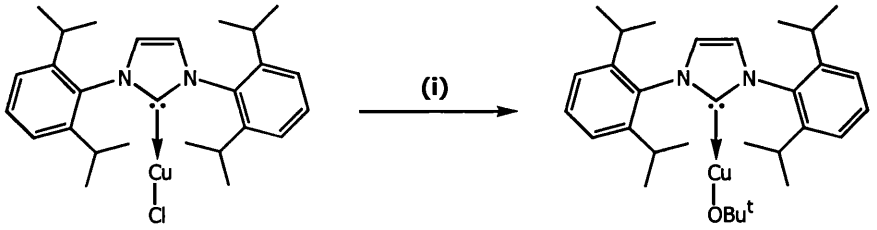

Scheme 3.6: Generation of *N*-heterocyclic carbene-copper(I) *tert*-butoxide complex from related chloride species
(i) NaO^{t}Bu, toluene/tetrahydrofuran, room temperature[12, 13]

Sadighi has also recently reported the reversible preparation of an *N*-heterocyclic carbene-copper(I) methyl complex, (1,3-bis-(2,6-diisopropylphenyl)-imidazol-2-ylidene)-copper(I) methyl, from the related (imidazol-2-ylidene)-copper(I) acetate (Scheme 3.7).[32] The copper(I) acetate species may be prepared via the treatment of one equivalent of copper(I) acetate with a single equivalent of the imidazol-2-ylidene; subsequent reaction of this acetate complex with $Al(CH_3)_2OEt$ affords the

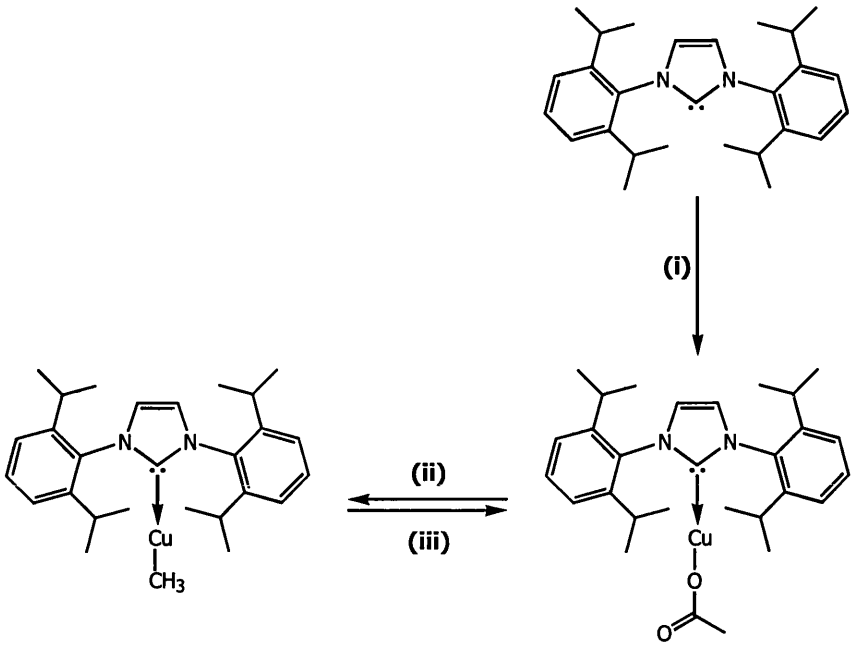

Scheme 3.7: Reversible preparation of an imidazol-2-ylidene-copper(I) methyl complex from a related *N*-heterocyclic carbene-copper(I) acetate species **(i)** Cu(OAc), toluene, room temperature; **(ii)** $Al(CH_3)_2OEt$, diethyl ether, -45 °C; **(iii)** CO_2 (1 atm), benzene, room temperature

corresponding copper(I) methyl compound (Scheme 3.7).[32] In benzene solution under a 1 atm pressure of carbon dioxide, the copper(I) methyl complex, (1,3-bis-(2,6-diisopropylphenyl)-imidazol-2-ylidene)-copper(I) methyl, reverts back to the corresponding copper(I) acetate species via insertion of a molecule of CO_2 into the Cu-CH_3 bond (Scheme 3.7).[32] This *N*-heterocyclic carbene-copper(I) methyl complex is currently being evaluated as a catalyst for carbonylation reactions.

Danopoulos *et al.* have recently structurally characterised monomeric, dimeric, and polymeric *N*-heterocyclic carbene-copper(I) bromide species; prepared via the *in situ* deprotonation of imidazolium salts bearing pyridyl-sidearms by reaction with copper(I) oxide.[33] The bidentate ligand in the monomeric example chelates a single metal centre; whereas in the dimeric and polymeric (imidazol-2-ylidene)-copper(I) bromide complexes, which are in fact structural isomers of each other, the ligand bridges two different metal atoms.

Arnold *et al.* have also structurally characterised a dimeric copper(I) complex of a donor functionalised *N*-heterocyclic carbene ligand; in which two anionic alkoxy-biscarbene ligands bridge the two metal centres.[34] In addition, it should be noted that Meyer *et al.* have recently reported the preparation and isolation of cationic monomeric copper(I) species in which the central metal ions are coordinated by tripodal triscarbene ligands.[35]

3.2: Neutral Copper(I)-*N*-Heterocyclic Carbene Species

We decided to evaluate oligomeric 2,4,6-trimethylphenyl-copper(I) (CuMes)[36, 37] as a basic metal source compound for the preparation of copper(I)-*N*-heterocyclic carbene complexes via the *in situ* deprotonation of organic precursors described in Chapter Two (Scheme 3.8).[Ψ] Our initial investigations focused on the reaction of CuMes with one equivalent of 1,3-bis-(2,4,6-trimethylphenyl)-imidazol-2-ylidene (IMes) and 1,3-bis-(2,4,6-trimethylphenyl)-imidazolium chloride ([IMesH][Cl]) (Scheme 3.8). The reaction of CuMes with a single equivalent of IMes results in the coordination of the imidazol-2-ylidene ligand and complete deaggregation of the basic organometallic reagent to yield the monomeric *N*-heterocyclic carbene-copper(I)-aryl species **16** (Scheme 3.8).[æ] The stoichiometric reaction of CuMes with one equivalent of [IMesH][Cl] provides the *N*-heterocyclic carbene-copper(I) chloride complex **17** (Scheme 3.8);[ϒ] which suggests that CuMes is indeed basic enough to deprotonate the more acidic hydrogen-bonded precursors to metal-*N*-heterocyclic carbenes reported in Chapter Two. The encouraging nature of these preliminary results led us to further evaluate the suitability of CuMes in the direct metallation of the organic precursors to metal-*N*-heterocyclic carbene complexes discussed in Chapter Two (Scheme 3.8).

[Ψ] Precedent for the exploitation of Group XI metal-aryl species as stoichiometric reagents for the direct metallation of acidic organic compounds does exist in the scientific literature.[38, 39]

[æ] Floriani *et al.* have previously observed a reduction in the aggregation state of the analogous silver(I)- and gold(I)-aryl species as a result of bidentate phosphine ligand coordination.[36]

[ϒ] We have also isolated single crystals of *N*-heterocyclic carbene-copper(I) chloride **17** suitable for study by x-ray diffraction from the reaction of IMes with copper(I) chloride; and, the reaction of lithiated 2,4,6-trimethylphenol with one equivalent of copper(I) chloride in the presence of IMes.

The reaction of CuMes with one equivalent of 1,3-bis-(2,4,6-trimethylphenyl)-imidazolium 2,4,6-trimethylphenoxide ([IMesH][OMes]), generated *in situ* via the treatment of the imidazolium phenoxide:phenol adduct **3** with IMes, results in the monomeric *N*-heterocyclic carbene-copper(I)-phenoxide species **18** (Scheme 3.8). Similarly, the reaction of CuMes with a single equivalent of the hydrogen-bonded metal-*N*-heterocyclic carbene precursor species **3**, **9** and **15**, yields compounds **19**, **20** and **21**, respectively, as the only crystalline products (Scheme 3.8). Initially,

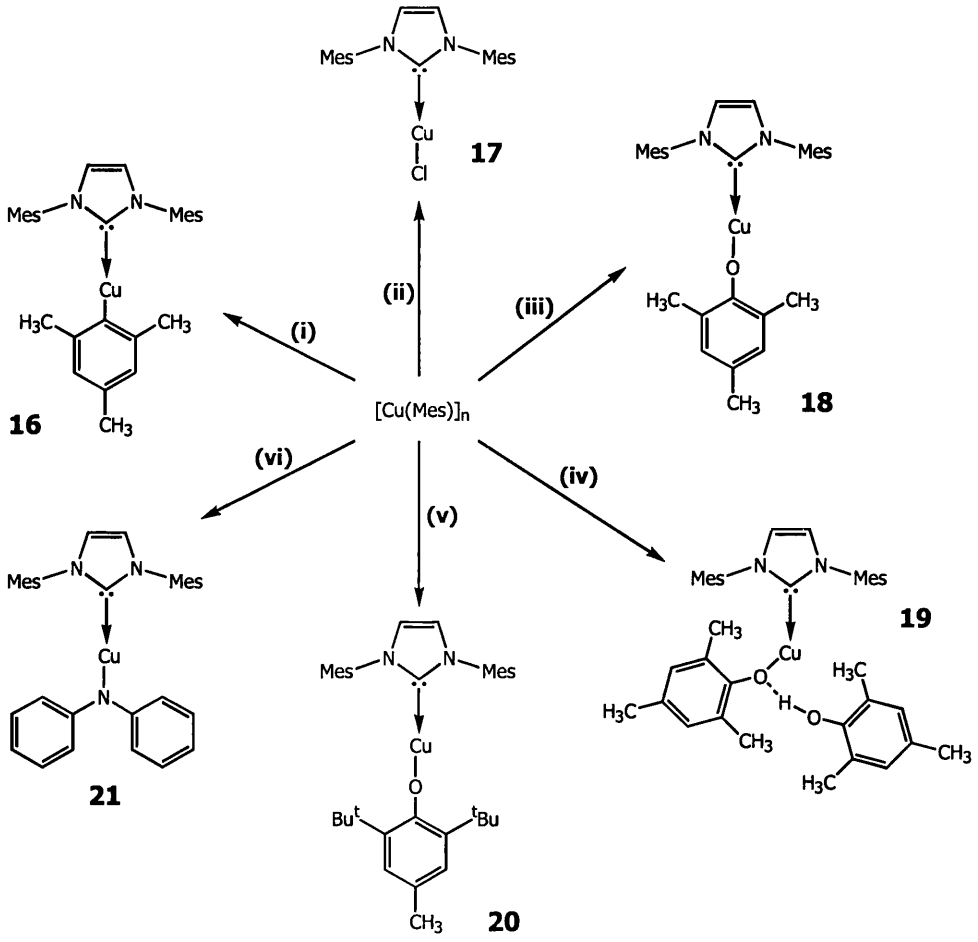

Scheme 3.8: Reaction of 2,4,6-trimethylphenyl-copper(I) with 1,3-bis-(2,4,6-trimethylphenyl)-imidazol-2-ylidene, 1,3-bis-(2,4,6-trimethylphenyl)-imidazolium chloride and related organic precursors to metal-*N*-heterocyclic carbene complexes

(i) 1,3-bis-(2,4,6-trimethylphenyl)-imidazol-2-ylidene, toluene;

(ii) 1,3-bis-(2,4,6-trimethylphenyl)-imidazolium chloride, toluene;

(iii) 1,3-bis-(2,4,6-trimethylphenyl)-imidazol-2-ylidene and imidazolium phenoxide:phenol adduct **3**, toluene; **(iv)** imidazolium phenoxide:phenol adduct **3**, toluene; **(v)** imidazolium phenoxide salt **9**, toluene;

(vi) imidazol-2-ylidene:amine adduct **15**, toluene

crystals of **18** and **19** were not forthcoming from their deep red toluene solutions; a fine suspension of what is presumed to be copper(0) metal formed on standing and crystal growth was not observed until the reaction mixture had been filtered through Celite for a second time, in order to remove the suspended material.

NMR spectroscopic analysis of samples of compounds **16**, **18**, **19** and **20** in C_6D_6 solution, and **17** in $CDCl_3$ solution, establishes these species as imidazol-2-ylidene ligated metal complexes (Scheme 3.8). The olefinic C(4/5)-H backbone hydrogen atom resonance within the ^{1}H-NMR spectra of metal-imidazol-2-ylidene species is generally observed downfield of that of the free carbene, and upfield of that of the imidazolium cation within related organic precursor salts; since the degree of delocalisation of charge about the heterocyclic core of imidazol-2-ylidene adducts is enhanced relative to that of the free carbene, but reduced in comparison to that of related imidazolium salts.[40-42] However, this is not reflected in the ^{1}H-NMR spectra of **16**, **18**, **19** (Figure 3.1) and **20** recorded in C_6D_6 solution; which exhibit resonances corresponding to the C(4/5)-H backbone hydrogens at chemical shifts

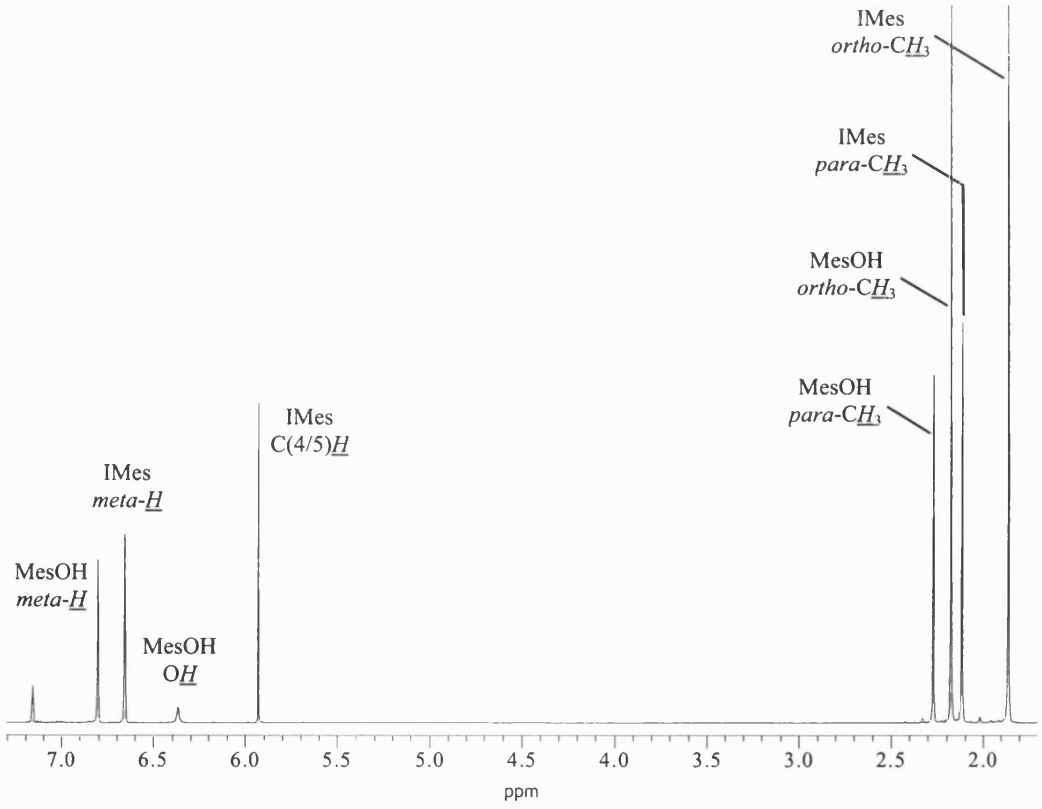

Figure 3.1: ^{1}H-NMR spectrum of compound **19** in C_6D_6 solution recorded at 400 MHz

Compound	C(4/5)-*H*
[IMesH][Cl]	7.62,[a] 8.07[b]
IMes	6.48[c]
16	6.02[c]
17	7.05[a]
18	5.93[c]
19	5.93[c]
20	5.95[c]
21	7.28,[b] 7.40[b]

Table 3.1: Chemical shifts of the C(4/5)-H backbone hydrogen atoms in the ^{1}H-NMR spectra of [IMesH][Cl], IMes, and compounds **16-21**, in various solvents (a = $CDCl_3$, b = CD_3OD and c = C_6D_6) recorded at 298 K and quoted in units of ppm downfield of TMS

upfield of that observed within the ^{1}H-NMR spectrum of IMes.[ℵ] The fact that the resonance corresponding to the C(4/5)-H backbone hydrogen atoms is located at a lower than anticipated chemical shift within the ^{1}H-NMR spectra of products **16**, **18**, **19** (Figure 3.1) and **20** (Table 3.1) is presumably a result of the participation of these substituents in hydrogen-bonding or C–H·····π(arene) interactions such as those described in Chapter Two. However, at 7.05 ppm, the chemical shift of the C(4/5)-H backbone hydrogen atom resonance within the ^{1}H-NMR spectrum of **17** recorded in $CDCl_3$ solution is upfield of that of [IMesH][Cl] recorded in the same solvent[ℭ] (Table 3.1); as would be expected from a consideration of the degree of delocalisation of charge around the heterocyclic core of metal-imidazol-2-ylidene complexes relative to imidazolium salts.[40-42] ^{13}C-NMR spectroscopic analysis of

[ℵ] ^{1}H-NMR (300 MHz, C_6D_6): δ 2.17 (18H, s, IMes *ortho*-C*H*$_3$ and IMes *para*-C*H*$_3$), 6.48 (2H, s, IMes C(4/5)*H*), 6.81 (4H, s, IMes *meta*-*H*).

[ℭ] ^{1}H-NMR (300 MHz, $CDCl_3$): δ 2.15 (12H, s, IMes-H *ortho*-C*H*$_3$), 2.33 (6H, s, IMes-H *para*-C*H*$_3$), 7.01 (4H, s, IMes-H *meta*-*H*), 7.62 (2H, s, IMes-H C(4/5)*H*), 10.63 (1H, s, IMes-H C(2)*H*).

Compound	C(4/5)	C(2)
[IMesH][Cl]	124.6,[a] 126.5[b]	139.4,[a] 139.9[b]
IMes	120.5[c]	219.2[c]
16	121.1[c]	——
17	122.2[a]	178.8[a]
18	121.5[c]	——
19	121.5[c]	——
20	121.6[c]	——
21	124.1,[b] 124.2[b]	136.0,[b] 136.7[b]

Table 3.2: Chemical shifts of the C(2) and C(4/5) carbon atoms in the ^{13}C-NMR spectra of [IMesH][Cl], IMes, and compounds **16-21**, in various solvents (a = $CDCl_3$, b = CD_3OD and c = C_6D_6) recorded at 298 K and quoted in units of ppm downfield of TMS

solutions of compounds **16**, **18**, **19** and **20** in C_6D_6, and **17** in $CDCl_3$, confirm that these species are indeed imidazol-2-ylidene ligated metal complexes; since their respective $^{13}C\{^1H\}$-NMR spectra exhibit resonances corresponding to the C(4/5) carbon atoms of the heterocyclic core that are upfield of those observed for the [IMesH][Cl] salt and downfield of those observed for free IMes (Table 3.2).

In the presence of water and molecular oxygen, compound **16** reacts with excess CD_3OD generating one equivalent of 1,3,5-trimethylbenzene and [IMesH][OCD_3] (Scheme 3.9), which were identified via ^{1}H-NMR spectroscopy (Figure 3.2). The signals at 2.14 ppm, 2.35 ppm, 7.07 ppm and 7.42 ppm (Figure 3.2) are confirmed as imidazolium cation resonances by comparison with the ^{1}H-NMR spectrum of [IMesH][Cl].[§] The reaction of IMes with methanol also results in the protonation

[§] ^{1}H-NMR (300 MHz, CD_3OD): δ 2.20 (12H, s, IMes-H *ortho*-C*H*$_3$), 2.40 (6H, s, IMes-H *para*-C*H*$_3$), 7.20 (4H, s, IMes-H *meta*-*H*), 8.07 (2H, s, IMes-H C(4/5)*H*), 9.53 (1H, s, IMes-H C(2)*H*).

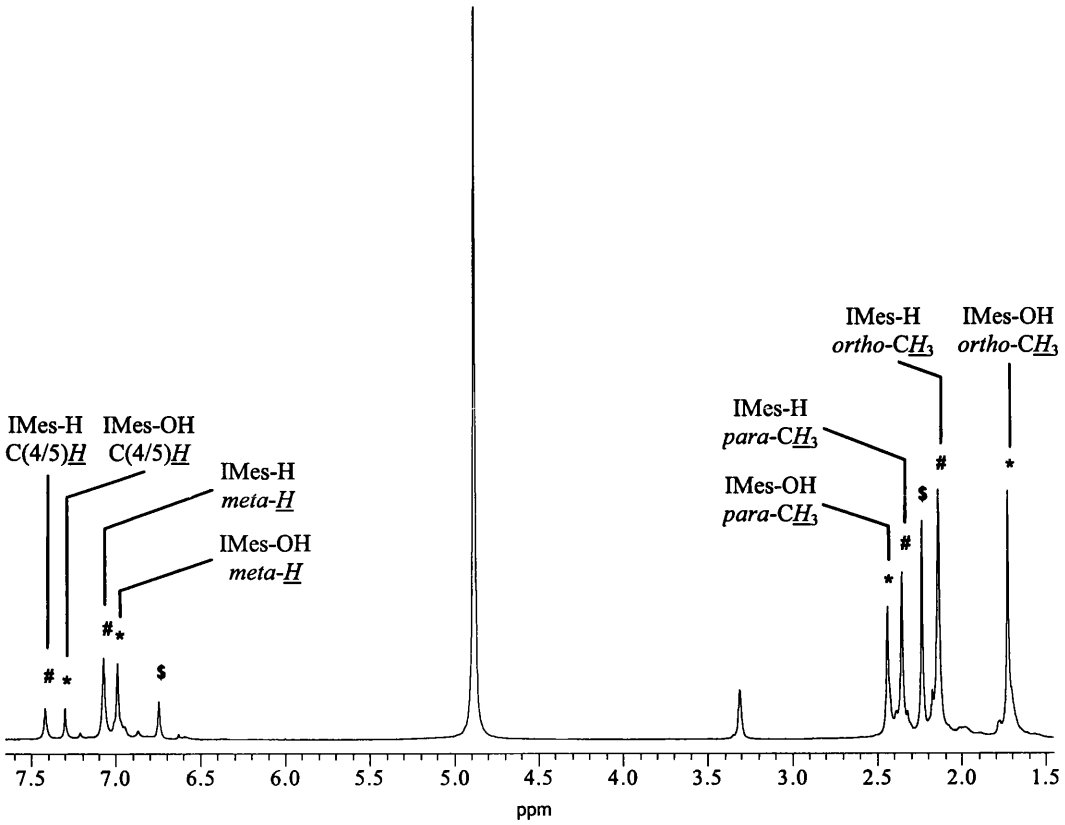

Figure 3.2: ^{1}H-NMR spectrum recorded at 400 MHz during the course of the reaction of compound **16** with CD_3OD showing the three components: **(s)** 1,3,5-trimethylbenzene; **(#)** 1,3-bis-(2,4,6-trimethylphenyl)-imidazolium methoxide; **(*)** 1,3-bis-(2,4,6-trimethylphenyl)-2-hydroxy-imidazolium methoxide

of the *N*-heterocyclic carbene,[¥] which is not surprising considering the basicity of imidazol-2-ylidenes[43, 44] and in the light of the results reported in Chapter Two; however, it does suggest that protonation of the *N*-heterocyclic carbene moiety on the reaction of **16** with an excess of CD_3OD is not necessarily copper-catalysed. Over time, the [IMesH][OCD_3] undergoes copper-catalysed aerobic oxidation[1-7] to the related hemi-acetal;[Φ] evidenced by the growth of the ^{1}H-NMR resonances

[¥] ^{1}H-NMR (400 MHz, CH_3OH/CD_3OD capillary): δ 2.14 (12H, s, IMes-H *ortho*-C*H*$_3$), 2.35 (6H, s, IMes-H *para*-C*H*$_3$), 7.14 (4H, s, IMes-H *meta*-*H*), 8.00 (2H, s, IMes-H C(4/5)*H*).

[Φ] In CD_3OD solution, due to the prevalence of exchange, the hemi-acetal is best thought of as the related 2-hydroxy-imidazolium species. Further oxidation of this salt to the related ketone is a possibility; indeed, the copper-catalysed aerobic oxidation of imidazolium cations to cyclic urea derivatives has been reported by Begtrup.[45] However, if the corresponding ketone compound is generated under these conditions, then it is readily converted into the related hemi-acetal species.

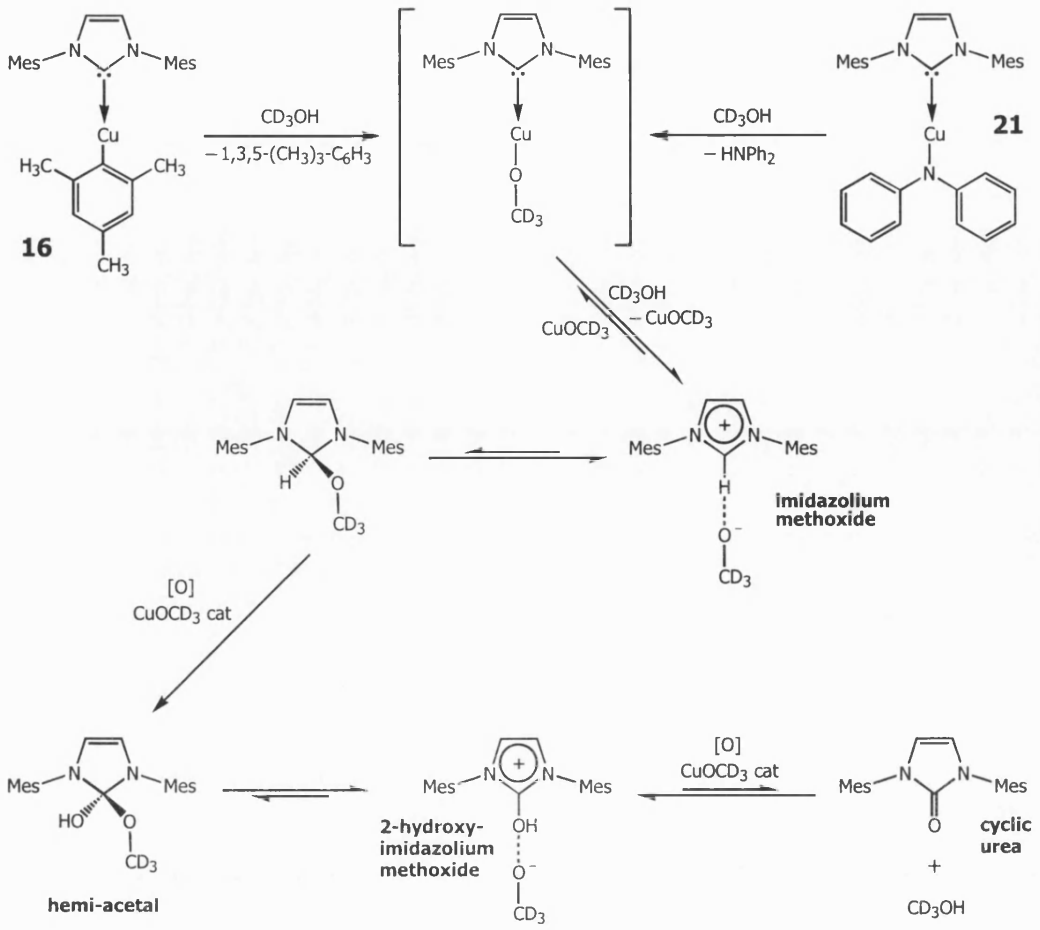

Scheme 3.9: Reaction of *N*-heterocyclic carbene-copper(I) species **16** and **21** with excess CD_3OD in the presence of water and molecular oxygen

observed at 1.73 ppm, 2.44 ppm, 6.99 ppm and 7.30 ppm; at the expense of those at chemical shifts of 2.14 ppm, 2.35 ppm, 7.07 ppm and 7.42 ppm (Figure 3.2).

As a result of the poor solubility of compound **21** (Scheme 3.8) in C_6D_6 solution we decided to characterise this product indirectly, by means of the identification of the individual components present in solution following the dissolution of this species in CD_3OD. ^{1}H-NMR spectroscopic analysis reveals that **21** undergoes an analogous reaction with excess CD_3OD, in the presence of water and molecular oxygen, to that of the *N*-heterocyclic carbene-copper(I)-aryl adduct **16**; generating diphenylamine, the methoxide salt of the *N*-heterocyclic carbene ligand - which is, over time, oxidised to the corresponding 2-hydroxy-imidazolium species (Figure 3.3) - and, presumably, copper(I)-methoxide (Scheme 3.9). The chemical shifts of

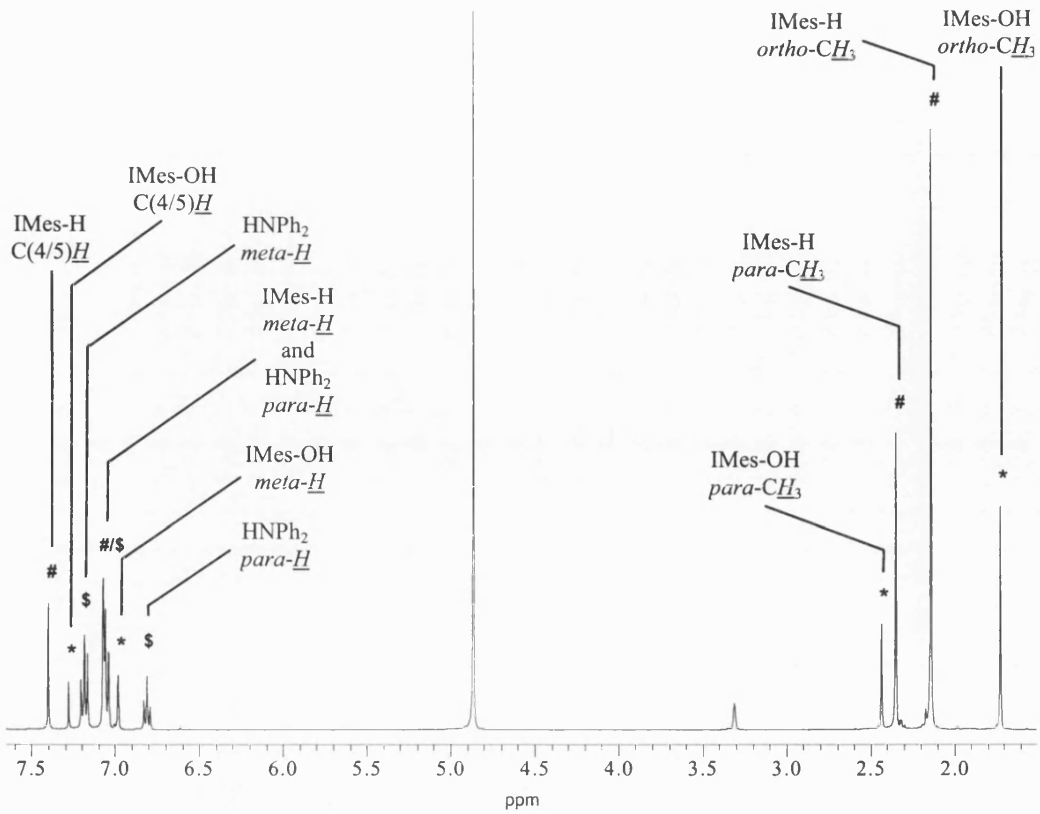

Figure 3.3: ^{1}H-NMR spectrum recorded at 400 MHz during the course of the reaction of compound **21** with CD_3OD showing the three components: **(s)** diphenylamine; **(#)** 1,3-bis-(2,4,6-trimethylphenyl)-imidazolium methoxide; **(*)** 1,3-bis-(2,4,6-trimethylphenyl)-2-hydroxy-imidazolium methoxide

the resonances assigned to the imidazolium salt and the 2-hydroxy-imidazolium species are consistent with those observed on treatment of **16** with excess CD_3OD (Figure 3.2). In addition, the multiplets at 6.76–6.86 ppm, 7.02–7.06 ppm and 7.12–7.21 ppm (Figure 3.3) are reminiscent of the signals corresponding to the aromatic ring hydrogen substituents observed within the ^{1}H-NMR spectrum of diphenylamine recorded in CH_3OH solution.[f] The olefinic C(4/5)-H backbone hydrogen atoms of the two imidazolium species are observed upfield of those of the 1,3-bis-(2,4,6-trimethylphenyl)-imidazolium cation of the related chloride salt ([IMesH][Cl]) - 7.28 ppm and 7.40 ppm versus 8.07 ppm in CD_3OD solution

[f] ^{1}H-NMR (400 MHz, CH_3OH/CD_3OD capillary): δ 6.70–6.80 (2H, t, $J_{(H-H)}$ = 7.2 Hz, $HNPh_2$ *para-H*), 6.94–7.04 (4H, d, $J_{(H-H)}$ = 7.6 Hz, $HNPh_2$ *ortho-H*), 7.07–7.18 (4H, t, $J_{(H-H)}$ = 7.6 Hz, $HNPh_2$ *meta-H*), 7.37 (1H, br s, $HNPh_2$ N*H*).

(Table 3.1) - which suggests that the cations generated as a result of the reaction of compound **21** with CD_3OD possess more imidazol-2-ylidene character than that of the imidazolium chloride salt. In the case of the imidazolium methoxide salt, the lower than anticipated ^{1}H-NMR chemical shift of the C(4/5)-H hydrogen atom resonance probably results from the reversible *in situ* deprotonation of this species in CD_3OD solution by copper(I)-methoxide; whereas in the case of its oxidation product, the 2-hydroxy-imidazolium species, a cyclic urea resonance structure is likely to account for this observation. The absence of signals corresponding to the acidic protons suggests that exchange processes are in operation within this protic solvent medium (Figure 3.3). Nonetheless, it should be noted that, despite the prevalence of exchange, the acidic imidazolium C(2)-H proton is apparent in the ^{1}H-NMR spectrum of the related [IMesH][Cl] salt recorded in CD_3OD solution.[3]

$^{13}C\{^1H\}$-NMR spectra recorded during the course of the reaction of compound **21** with excess CD_3OD provide further corroboration that two distinct imidazolium species are present in solution; as two resonances, corresponding to the olefinic C(4/5) carbon atoms of electronically different heterocyclic cores, are observed at 124.1 ppm and 124.2 ppm (Table 3.2). These spectra display resonances assigned as the C(2) carbon atoms of the two related imidazolium species at chemical shifts of 136.0 ppm and 136.7 ppm (Table 3.2), which perhaps better demonstrate the electronic differences of these two five-membered heterocycles.

The individual components present in solution following the dissolution of **21** in CD_3OD are identified as diphenylamine, [IMesH][OCD_3], and [IMesOH][OCD_3], via the comparison of the ^{1}H- and $^{13}C\{^1H\}$-NMR data available for this compound (Figure 3.3 and Tables 3.1 and 3.2) with that of *N*-heterocyclic carbene-copper(I)-aryl adduct **16** (Figure 3.2), diphenylamine, IMes and [IMesH][Cl], all recorded in CD_3OD solution (Tables 3.1 and 3.2). By extrapolation, product **21** is established as (1,3-bis-(2,4,6-trimethylphenyl)-imidazol-2-ylidene)-copper(I)-diphenylamide (Scheme 3.8).

[3] ^{1}H-NMR (300 MHz, CD_3OD): δ 2.20 (12H, s, IMes-H *ortho*-C<u>*H*</u>$_3$), 2.40 (6H, s, IMes-H *para*-C<u>*H*</u>$_3$), 7.20 (4H, s, IMes-H *meta*-<u>*H*</u>), 8.07 (2H, s, IMes-H C(4/5)<u>*H*</u>), 9.53 (1H, s, IMes-H C(2)<u>*H*</u>).

Determination of the solid state molecular structure of compounds **16-21** by single crystal x-ray diffraction reveals that these products are indeed discrete monomeric imidazol-2-ylidene-copper(I) complexes bearing a solitary *N*-heterocyclic carbene ligand (Scheme 3.8). In addition, as might be expected from steric considerations, all of these two-coordinate *N*-heterocyclic carbene ligated copper(I) coordination compounds possess a near linear geometry about the central metal atom. Another feature common to the solid state structures of products **16-21** - briefly described in turn in the remainder of this section - is the participation of at least one of the olefinic C(4/5)-H backbone hydrogen atoms of the individual molecules in an intermolecular electrostatic interaction with their neighbours that results in their association into an extended supramolecular array.

The asymmetric unit of the discrete imidazol-2-ylidene-copper(I)-aryl species **16** incorporates two crystallographically independent molecules (Figure 3.4). The C(2)–Cu bond lengths C1–Cu1 and C101–Cu2 (Figure 3.4), at 1.900(2) Å and 1.891(2) Å respectively, lie towards the short end of the range reported in the scientific literature;[13, 30-35, 46] the shortest published C(2)–Cu bond length within an imidazol-2-ylidene-copper species being 1.850(5) Å observed within the *N*-heterocyclic carbene-copper(I)-acetate complex synthesised by Sadighi *et al.*,[32] while the longest such contact is 1.993(2) Å within a dimeric compound isolated and structurally characterised by Meyer *et al.*, in which two tris-*N*-heterocyclic carbene ligands bridge two copper(I) ions.[46] With the angles C1–Cu1–C31 and C101–Cu2–C131 equalling 173.46(8)° and 176.76(8)°, respectively, the geometry about the copper centres of the two crystallographically independent molecules within the asymmetric unit approaches linearity (Figure 3.4). The separations between central metal atoms Cu1 and Cu2 and the *ipso*-carbons of their respective aryl ring substituents, Cu1–C31 and Cu2–C131 (Figure 3.4), at 1.922(2) Å and 1.916(2) Å respectively, are larger than the corresponding distance of 1.890(6) Å in the monomeric univalent copper(I)-aryl complex prepared by Strähle *et al.*[47] The two crystallographically independent molecules of compound **16** within the asymmetric unit are associated via an intermolecular C–H·····π(arene) interaction (D = 3.603 Å, d = 2.662 Å and θ = 170.82°), [C102–H102·····centroid(C31-C36)] (Figure 3.4).

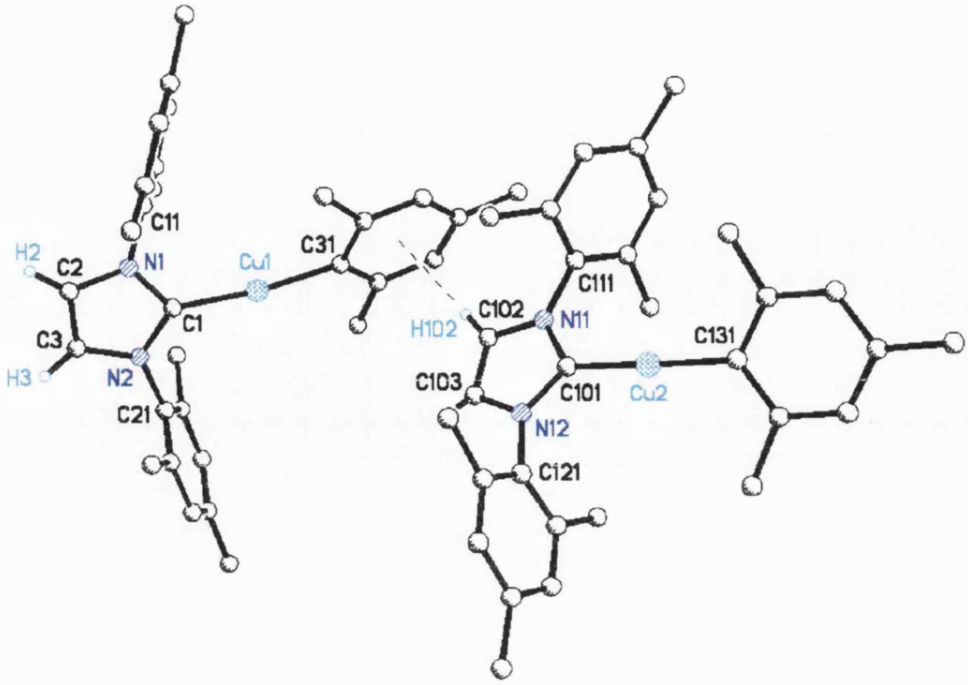

Figure 3.4: Graphical representation of the two crystallographically independent molecules within the asymmetric unit of *N*-heterocyclic carbene-copper(I)-aryl species **16** as determined by single crystal x-ray diffraction analysis

Imidazol-2-ylidene-copper(I) chloride complex **17** crystallises from dilute toluene solution in the space group *Fdd*2 yielding a batch of colourless blocks. Analysis of a suitable single crystal via x-ray diffraction reveals that, consistent with the C_2-symmetry through the molecule - about the C1-Cl1 (Figure 3.5) vector - the asymmetric unit contains only half a molecule of **17**. The geometry about the two-coordinate copper centre can be described as linear; the C1–Cu1–Cl1 angle (Figure 3.5) equals 180.000(1)° as is the case in 1,3-bis-(2,4,6-trimethylphenyl)-imidazol-2-ylidene-silver(I) chloride, the analogous monomeric silver(I) complex recently prepared by Abernethy *et al.*[48] The C1–Cu1 bond length (Figure 3.5), at 1.888(6) Å, lies towards the short end of the range of imidazol-2-ylidene-copper C(2)–Cu connectivities reported within the literature; shorter indeed than within the 1,3-bis-(2,6-diisopropylphenyl)-imidazol-2-ylidene-copper(I) chloride isolated by Nolan *et al.*,[13] in which the C(2)–Cu bond distance measures 1.953 Å, and comparable with the values of 1.868(6) Å and 1.888(6) Å in the *N*-heterocyclic carbene-copper(I) chloride complexes isolated by Raubenheimer *et al.*[30, 31] The Cu1–Cl1 bond length (Figure 3.5) of 2.098(1) Å is shorter than the shortest Cu–Cl

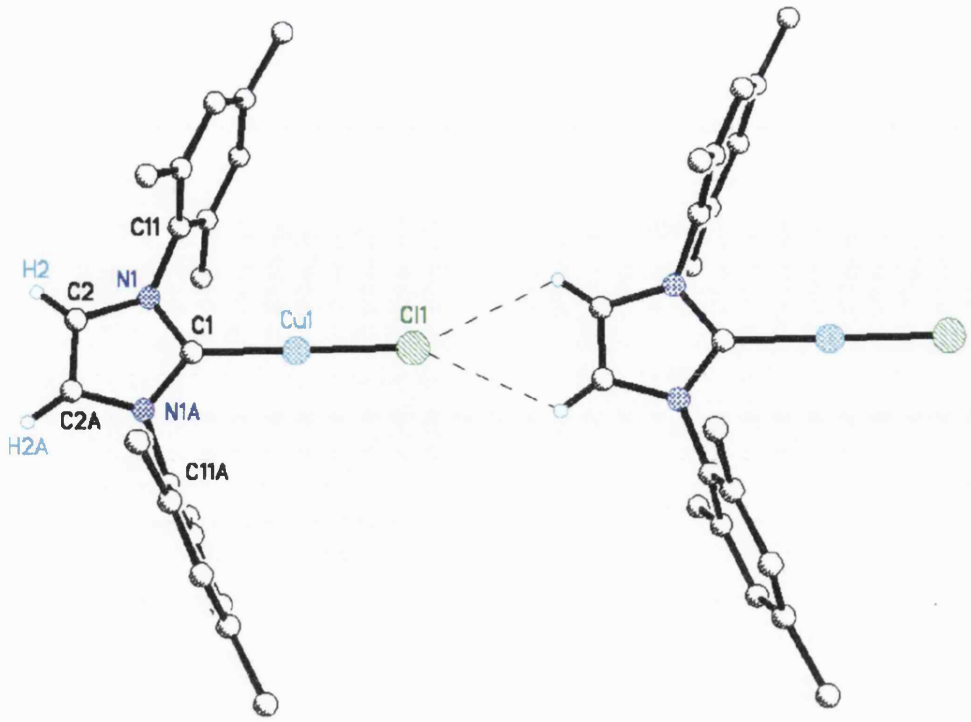

Figure 3.5: Supramolecular structure of imidazol-2-ylidene-copper(I) chloride complex **17** as determined by single crystal x-ray diffraction analysis (H2A, C2A, N1A and C11A are symmetry generated equivalents of H2, C2, N1 and C11, respectively)

distance (2.122(2) Å) in the thiazol-2-ylidene-copper(I) chloride dimer isolated by Raubenheimer *et al.*,[30] typical of that observed in the closely related monomeric *N*-heterocyclic carbene-copper(I) chloride (2.099(2) Å),[31] and longer than that in the imidazol-2-ylidene-copper(I) chloride reported by Nolan *et al.* (2.089 Å).[13] The C(4/5)-H hydrogens of each individual molecule of **17** participate in tandem intermolecular C–H·····Cl interactions (D = 3.424 Å, d = 2.887 Å and θ = 118.05°) with the Cl ligand of the neighbouring molecule (Figure 3.5), which results in a situation reminiscent of that observed by Abernethy *et al.*[48] for the isostructural 1,3-bis-(2,4,6-trimethylphenyl)-imidazol-2-ylidene-silver(I) chloride,[α] whereby individual molecules of **17** are associated into straight polymeric chains.

[α] Compound **17** and 1,3-bis-(2,4,6-trimethylphenyl)-imidazol-2-ylidene-silver(I) chloride possess, within experimental error, identical unit cell parameters. However, the C(2)–Cu and Cu–Cl bonds in **17** are shorter than the C(2)–Ag and Ag–Cl bonds in the analogous silver(I) complex; the weak C–H·····Cl interactions are able to breathe in order to accommodate such differences in bond length.

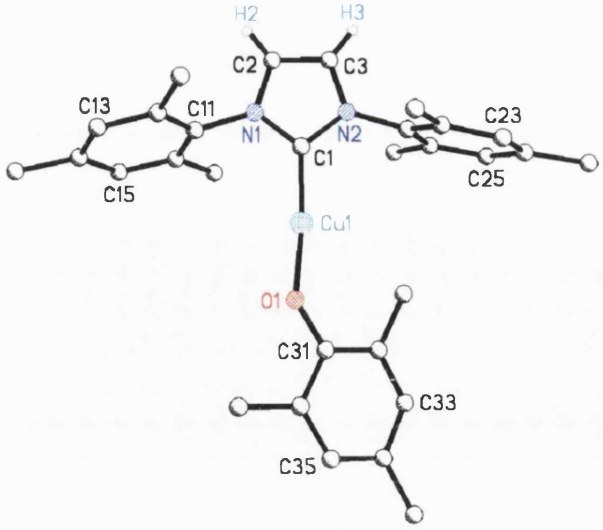

Figure 3.6: Molecular structure of the imidazol-2-ylidene-copper(I)-phenoxide complex **18** in the solid state as determined by single crystal x-ray diffraction

Single crystal x-ray diffraction analysis of discrete imidazol-2-ylidene-copper(I)-phenoxide **18** reveals that this species crystallises in the space group $P2_1/c$. To the best of our knowledge, this is the first structurally characterised *N*-heterocyclic carbene-copper(I)-phenoxide species. The asymmetric unit contains one complete molecule of this discrete monomeric *N*-heterocyclic carbene-copper(I) terminal phenoxide complex (Figure 3.6). At 1.853(2) Å, the C1–Cu1 bond (Figure 3.6) does not differ significantly in length from the shortest C(2)–Cu distance reported in the literature; 1.850(5) Å in the imidazol-2-ylidene-copper(I)-acetate species prepared by Sadighi *et al.*[32] With a C1–Cu1–O1 angle (Figure 3.6) equal to 174.33(8)°, the geometry about the two-coordinate copper centre Cu1 approaches linearity, as is the case in the two crystallographically independent molecules of the imidazol-2-ylidene-copper(I)-aryl species **16** (Figure 3.4). The Cu1–O1 bond length (Figure 3.6), measuring 1.812(2) Å, is shorter than that observed within the neutral monomeric three-coordinate copper(I) terminal phenoxide species bearing ancillary isocyanide ligation structurally characterised by Floriani *et al.*,[49] which exhibits a Cu–O distance of 1.917(3) Å, and comparable with the Cu–O lengths of 1.806(6) Å and 1.798(8) Å observed in the two-coordinate bisphenoxide cuprate anion reported in the same publication.[49] The Cu1–O1–C31 angle (Figure 3.6) of 134.3(1)° is reminiscent of that of 134.3(2)° within the trigonal planar three-

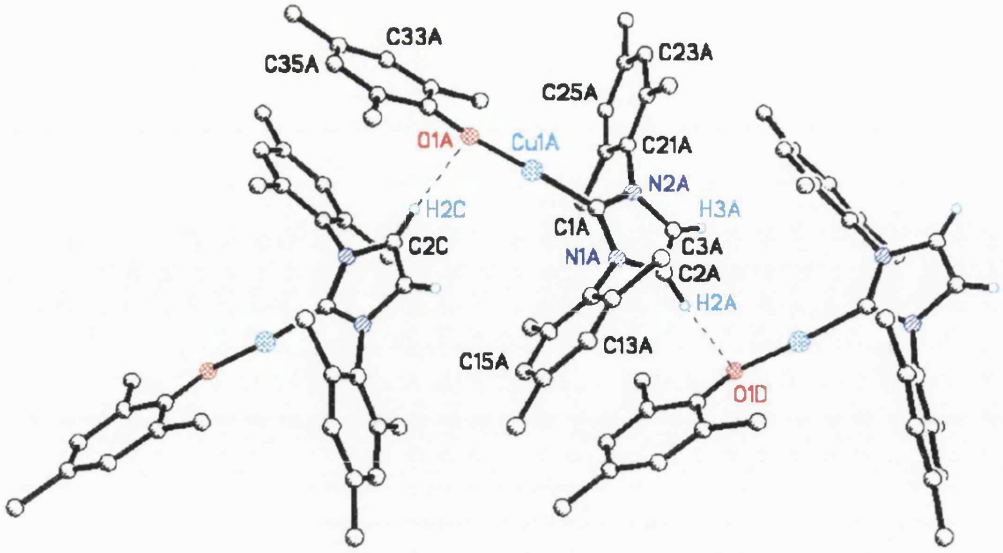

Figure 3.7: Intermolecular C–H·····O interactions between neighbouring molecules of compound **18** within a section of a zig-zagging polymeric chain

coordinate copper(I) terminal phenoxide complex prepared by Floriani *et al.*;[49] the corresponding angles within the bisphenoxide cuprate anion equal 137.0(5)° and 135.2(5)°.[49] The individual molecules of *N*-heterocyclic carbene-copper(I) terminal phenoxide complex **18** are associated into zig-zagging polymeric chains through intermolecular C–H·····O interactions (D = 3.295 Å, d = 2.486 Å and θ = 143.08°), [C2C–H2C·····O1A] and [C2A–H2A·····O1D] (Figure 3.7).

The asymmetric unit of compound **19** incorporates a molecule of 1,3-bis-(2,4,6-trimethylphenyl)-imidazol-2-ylidene-copper(I)-2,4,6-trimethylphenoxide and one equivalent of 2,4,6-trimethylphenol. The phenol moiety and the oxygen atom of the terminally bound phenoxide ligand participate in an O–H·····O hydrogen bond (D = 2.658 Å, d = 1.662 Å and θ = 160.25°), [O2A–H1A·····O1A] (Figure 3.10). The molecular structure of imidazol-2-ylidene-copper(I)-phenoxide:phenol adduct **19** is, in this respect, analogous to that of the corresponding hydrogen-bonded metal-*N*-heterocyclic carbene complex organic precursor compound imidazolium phenoxide:phenol **3** (Figure 3.8). The stoichiometric reaction of the imidazolium phenoxide:phenol adduct **3** with a single equivalent of the metal source compound

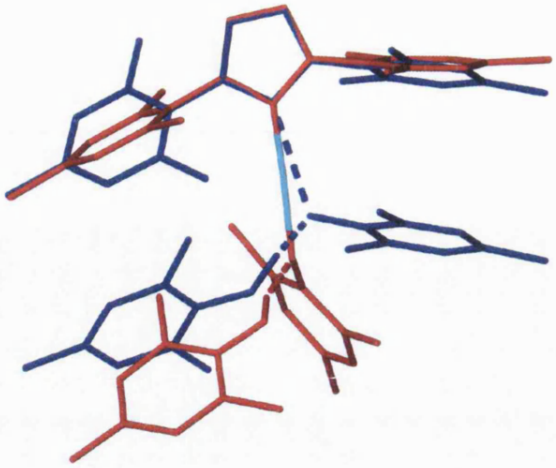

Figure 3.8: Overlay of the molecular structures of compound **19** (red) and the imidazolium phenoxide:phenol adduct **3** (blue)

2,4,6-trimethylphenyl-copper(I) (Scheme 3.8) represents an isolobal replacement of the imidazolium C(2)-H proton of the hydrogen-bonded metal-*N*-heterocyclic carbene complex organic precursor species by a Cu(I) cation (Figure 3.8). The C1A–Cu1A bond length (Figure 3.10), Cu1A–O1A distance (Figure 3.10), and C1A–Cu1A–O1A and Cu1A–O1A–C31A angles (Figure 3.10) observed within the imidazol-2-ylidene-copper(I)-phenoxide:phenol adduct **19** are not significantly different from the corresponding distances and angles within the related discrete imidazol-2-ylidene-copper(I)-phenoxide coordination compound **18** (Figure 3.9); 1.859(2) Å, 1.820(2) Å, and 174.2(1)° and 132.6(1)° respectively, while those in

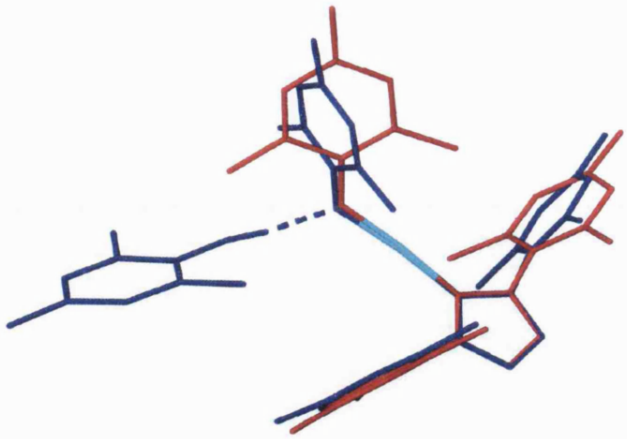

Figure 3.9: Overlay of the molecular structures of compound **19** (blue) and the imidazol-2-ylidene-copper(I) phenoxide complex **18** (red)

18 equal 1.853(2) Å, 1.812(2) Å, 174.33(8)° and 134.3(1)° respectively. This suggests that the electronic attributes of the copper centre are unaffected by the O–H·····O hydrogen bond between the phenol moiety and the terminal phenoxide; which is not unexpected since, in addition to two bonding pairs of electrons, the oxygen atom of the phenoxide ligand bears two lone pairs available to participate in hydrogen-bonding. However, the orientation of the terminal phenoxide ligand relative to the *N*-heterocyclic carbene functionality within adduct **19** differs from that observed in the discrete imidazol-2-ylidene-copper(I)-phenoxide complex **18**, in that the aromatic ring of the phenoxide ligand and the heterocyclic core of the imidazol-2-ylidene are closer to coplanarity in compound **18** (Figure 3.9); this is presumably a crystal packing effect - in order to accommodate the phenol moiety in a pocket beneath one of the *N*-heterocyclic carbene aryl ring substituents (Figure 3.10) the phenoxide ligand in **19** adopts an alternate orientation, relative to the imidazol-2-ylidene, to that observed in compound **18** (Figure 3.9). Calderazzo *et al.* reported a similar O–H·····O hydrogen-bonding interaction (D = 2.572(5) Å, d = 1.76(7) Å and θ = 164.7°) between the terminal phenoxide ligands and phenol solvent molecules in the dimeric complex $[Cu(NH_2CHCHNH_2)(OPh)_2.HOPh]_2$.[50] Neighbouring molecules of the hydrogen-bonded imidazol-2-ylidene-copper(I)-phenoxide:phenol adduct **19** associate head-to-tail into a polymeric extended array through C–H·····π(arene) interactions (D = 3.739 Å, d = 2.848 Å and θ = 176.45°), [C2A–H2A·····centroid(C41A'-C46A')] (Figure 3.10).

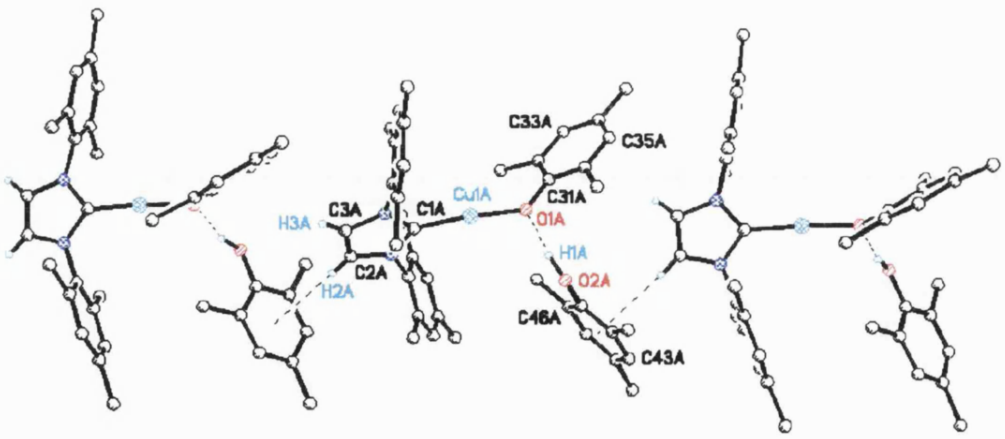

Figure 3.10: Intramolecular O–H·····O and intermolecular C–H·····π(arene) interactions within a section of the polymeric supramolecular structure of compound **19**

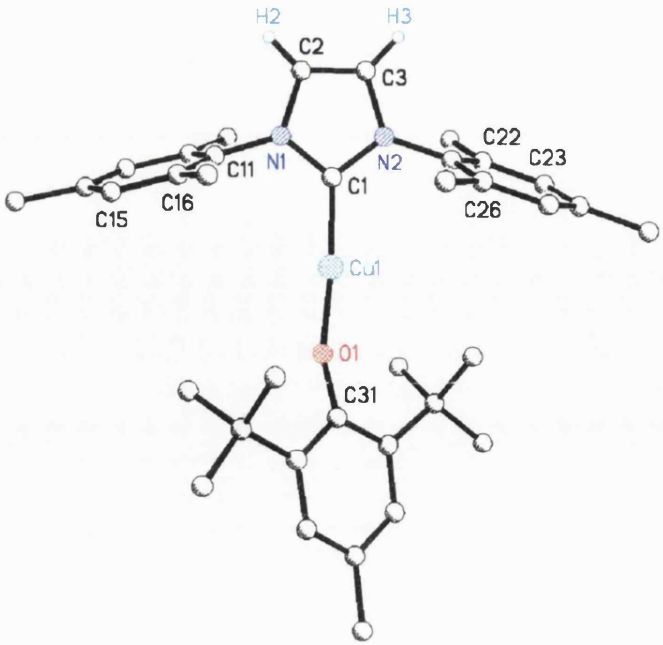

Figure 3.11: Graphical representation of the molecular structure of the discrete imidazol-2-ylidene-copper(I) terminal phenoxide complex **20** in the solid state

Structural characterisation of imidazol-2-ylidene-copper(I)-phenoxide complex **20** by single crystal x-ray diffraction reveals the asymmetric unit to be comprised of a single molecule of this discrete two-coordinate *N*-heterocyclic carbene ligated copper(I) terminal phenoxide (Figure 3.11). The solid state molecular structure of the imidazol-2-ylidene-copper(I)-phenoxide complex **20** closely resembles that of the corresponding hydrogen-bonded organic precursor compound **9** (Figures 3.12 and 3.13). The treatment of one equivalent of the imidazolium phenoxide **9** with a single equivalent of the metal source compound 2,4,6-trimethylphenyl-copper(I) to yield the imidazol-2-ylidene-copper(I) terminal phenoxide complex **20** can be viewed as an isolobal replacement of the acidic imidazolium C(2)-H proton within the hydrogen-bonded organic metal-*N*-heterocyclic carbene complex precursor species by a Cu(I) ion. The C1–Cu1 bond distance (Figure 3.11), at 1.848(3) Å, compares well with the corresponding imidazol-2-ylidene-copper C(2)–Cu bond lengths within compound **18**, hydrogen-bonded adduct **19**, and the *N*-heterocyclic carbene-copper(I)-acetate species synthesised by Sadighi *et al.*;[32] 1.853(2) Å, 1.859(2) Å, and 1.850(5) Å, respectively. The geometry about the two-coordinate central metal atom once again approaches linearity, indeed the C1–Cu1–O1 angle

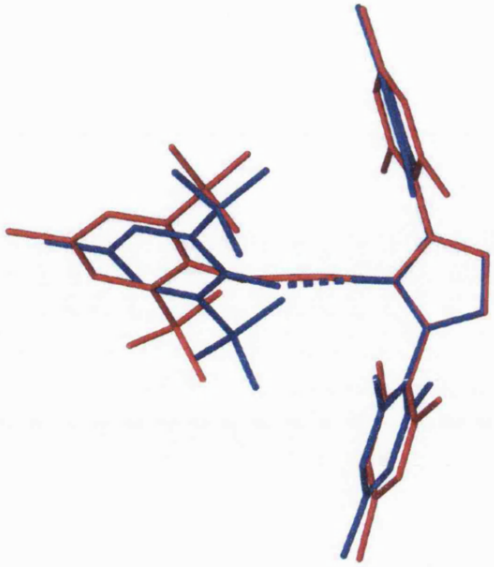

Figure 3.12: Molecular structure of *N*-heterocyclic carbene-copper(I) terminal phenoxide complex **20** (red) superimposed over that of one of the crystallographically independent molecules of the corresponding imidazolium phenoxide salt **9** (**blue**)

(Figure 3.11) measures 174.0(1)°. At 1.780(2) Å, the Cu1–O1 bond (Figure 3.11) is shorter than the corresponding length within the monomeric copper(I) terminal phenoxide bearing ancillary isocyanide ligation prepared by Floriani *et al.*,[49] with a Cu–O distance of 1.917(3) Å, and comparable with those of 1.806(6) Å and 1.798(8) Å within the two-coordinate bisphenoxide cuprate anion reported in the same publication;[49] similar Cu–O bond lengths are also apparent within the solid state molecular structures of the discrete monomeric complex **18** (Figure 3.6) and the related hydrogen-bonded adduct **19** (Figure 3.10), 1.812(2) Å and 1.820(2) Å respectively. The significant increase in the Cu1–O1–C31 angle observed within

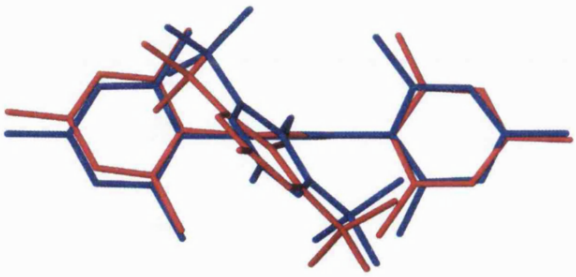

Figure 3.13: Overlay of the molecular structures of copper(I)-phenoxide species **20** (red) and one of the crystallographically independent contact ion pairs of the hydrogen-bonded imidazolium phenoxide precursor salt **9** (**blue**)

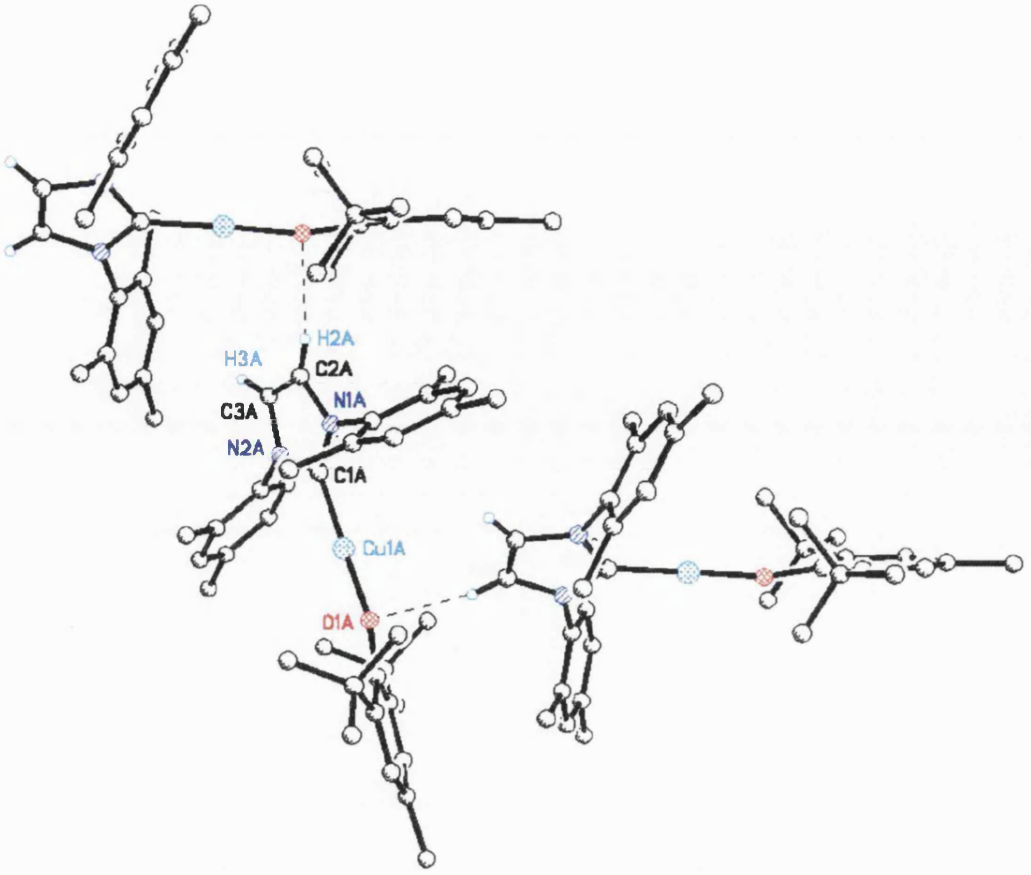

Figure 3.14: Intermolecular C–H·····O interactions in a section of zig-zagging polymeric chain within the extended structure of the imidazol-2-ylidene-copper(I)-phenoxide **20**

the discrete monomeric imidazol-2-ylidene ligated copper(I) terminal phenoxide complex **20** (Figure 3.11) relative to that of the analogous coordination compound **18** (Figure 3.6), 161.0(2)° compared with 134.3(1)°, is attributed to the increased steric bulk of the *ortho*-substituents of the terminally bound phenoxide ligand. Individual molecules of imidazol-2-ylidene-copper(I) terminal phenoxide **20** form zig-zagging polymeric chains through intermolecular C–H·····O interactions (D = 3.265 Å, d = 2.389 Å and θ = 151.63°), [C2A–H2A·····O1A'] (Figure 3.14); similar interactions (D = 3.295 Å, d = 2.486 Å and θ = 143.08°) are observed between neighbouring molecules of the analogous imidazol-2-ylidene-copper(I)-phenoxide complex **18** (Figure 3.7).

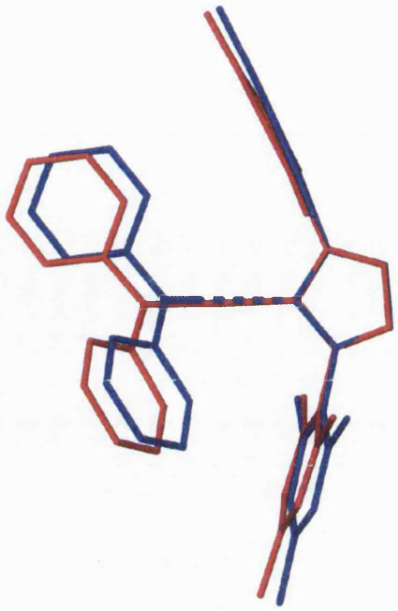

Figure 3.15: Molecular structure of the discrete *N*-heterocyclic carbene-copper(I)-amide complex **21** (red) superimposed over that of the corresponding hydrogen-bonded organic precursor compound imidazol-2-ylidene:amine adduct **15** (blue)

Single crystal x-ray diffraction analysis of the imidazol-2-ylidene-copper(I)-amide complex **21** reveals that the asymmetric unit incorporates one complete molecule of this monomeric two-coordinate *N*-heterocyclic carbene ligated copper species. To the best of our knowledge, this is the first structurally characterised example of an *N*-heterocyclic carbene-copper(I)-amide species. The unit cell parameters of compound **21** are identical, within experimental error, to those of the isostructural neutral hydrogen-bonded imidazol-2-ylidene:amine adduct **15** (Figures 3.15 and 3.16). The stoichiometric reaction of the organic precursor **15** with one equivalent of the basic metal source compound 2,4,6-trimethylphenyl-copper(I), to yield the isomorphous metal-amide complex **21** (Scheme 3.8), may formally be considered as isolobal displacement of the central hydrogen atom within the neutral organic imidazol-2-ylidene:amine adduct **15** by a Cu atom.

The imidazol-2-ylidene-copper C(2)–Cu bond length (C1–Cu1), at 1.856(2) Å, lies at the short end of the range reported in the literature.[13, 30-35, 46] The angle between the imidazol-2-ylidene-copper C(2)–Cu and copper-diphenylamide Cu–N bonds (C1–Cu1–N3) equals 175.76(9)°; the geometry about the central metal ion

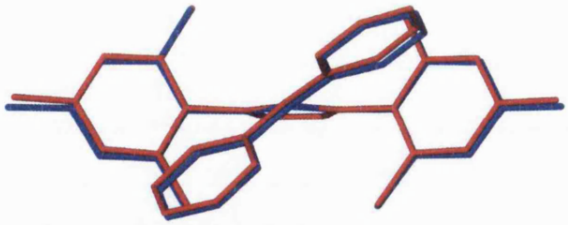

Figure 3.16: Overlay of the molecular structures of imidazol-2-ylidene-copper(I)-amide species **21** (red) and the hydrogen-bonded imidazol-2-ylidene:amine adduct **15** (blue)

can therefore be described as near linear (Figures 3.15 and 3.16). At 1.867(2) Å, the copper-amide Cu–N bond length (Cu1–N3) is shorter than that of 2.030(4) Å observed in the copper(I)-amide complex $[Cu(CO)_2(N(SO_2CF_3)_2)]$ structurally characterised by Strauss *et al.*[51] The heavy atom separation (*D*) in the neutral organic hydrogen-bonded imidazol-2-ylidene:amine adduct **15** equals 3.196(2) Å, while the analogous imidazol-2-ylidene C(2) carbon-diphenylamide nitrogen atom distance within *N*-heterocyclic carbene-copper(I)-amide complex **21** is 3.720 Å (Figures 3.15 and 3.16). The intramolecular C–H·····π(arene) interactions observed in the solid state structure of product **21**, [C38B–H38B·····centroid(C11B-C16B)]

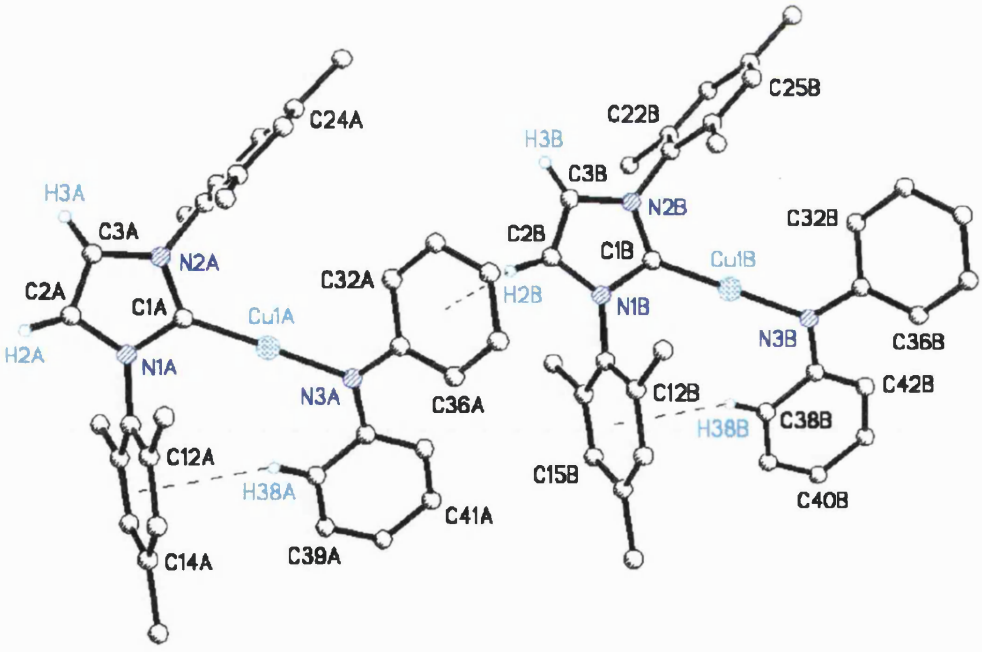

Figure 3.17: C–H·····π(arene) interactions within the extended supramolecular structure of the discrete imidazol-2-ylidene-copper(I)-amide **21**

(D = 3.875 Å, d = 2.969 Å and θ = 160.00°) and [C32B–H32B·····centroid(C21B-C26B)] (D = 4.102 Å, d = 3.190 Å and θ = 161.60°) (Figure 3.17), compare more favourably with the longer of the two intramolecular C–H·····π(arene) interactions observed within the hydrogen-bonded adduct **15**, [C42–H42·····centroid(C11-C16)] (D = 3.808(4) Å, d = 2.90(2) Å and θ = 156(2)°) (Figure 2.28). The differences in the molecular structures of these two isomorphous species (Figures 3.15 and 3.16) are negated by the deformation of the intermolecular C–H·····π(arene) interactions; the intermolecular C–H·····π(arene) interaction within the *N*-heterocyclic carbene-copper(I)-amide complex **21**, [C2B–H2B·····centroid(C31A-C36A)] (D = 3.578 Å, d = 2.817 Å and θ = 137.83°) (Figure 3.17), is therefore shorter than that observed in the extended solid state structure of the imidazol-2-ylidene:amine adduct **15**, [C2–H2·····centroid(C31A-C36A)] (D = 3.725(4) Å, d = 2.95(2) Å and θ = 140(2)°) (Figure 2.30).

3.3: Copper-*N*-Heterocyclic Carbene Salt Complexes

In the light of reports from Arduengo *et al.* concerning the preparation, isolation and characterisation of a cationic bis-*N*-heterocyclic carbene-copper(I) species[28] and an isostructural biscarbene-proton complex;[29] we decided to investigate the formation of bisimidazol-2-ylidene-copper coordination compounds via the *in situ* deprotonation of the organic metal-*N*-heterocyclic carbene precursors described in Chapter Two (Schemes 3.10 and 3.11). The bis-*N*-heterocyclic carbene-copper(I) triflate salt $[(IMes)_2Cu][O_3SCF_3]$ prepared by Arduengo *et al.* was formed via the addition of two equivalents of 1,3-bis-(2,4,6-trimethylphenyl)-imidazol-2-ylidene (IMes) to the benzene solvate of copper(I) triflate.[28] Unfortunately, single crystal x-ray diffraction did not provide satisfactory structural data for this compound.[28] We decided to prepare the bisimidazol-2-ylidene-copper(I) hexafluorophosphate salt $[(IMes)_2Cu][PF_6]$ in order to acquire single crystal x-ray diffraction data for this species.[29] Given the success of the substitution of *N*-heterocyclic carbenes for coordinated solvent in the preparation of $[(IMes)_2Cu][O_3SCF_3]$, we decided to synthesise bisimidazol-2-ylidene-copper(I) hexafluorophosphate compound **22** via the reaction of $[Cu(NCCH_3)_4][PF_6]$ with two equivalents of IMes (Scheme 3.10).

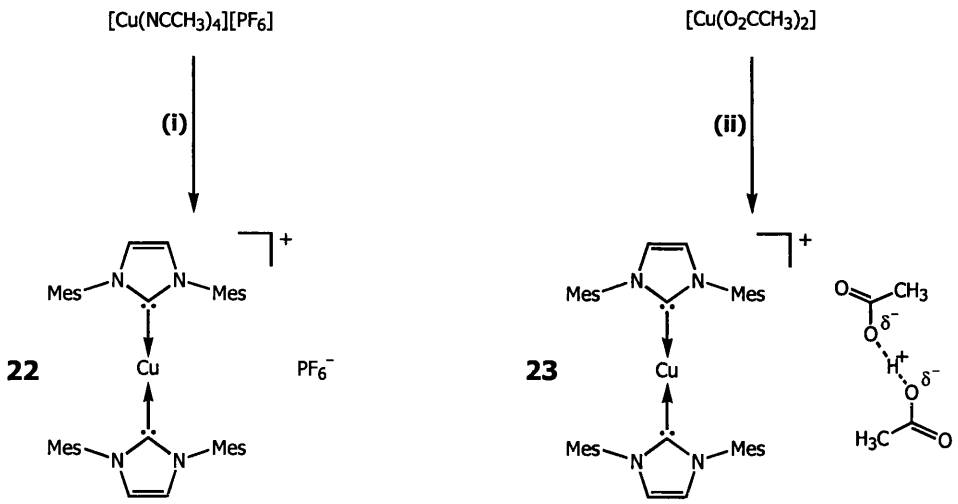

Scheme 3.10: Reaction of $[Cu(NCCH_3)_4][PF_6]$ with 1,3-bis-(2,4,6-trimethylphenyl)-imidazol-2-ylidene and $[Cu(O_2CCH_3)_2]$ with a related *in situ* generated imidazolium precursor to metal-*N*-heterocyclic carbene complexes
(i) 1,3-bis-(2,4,6-trimethylphenyl)-imidazol-2-ylidene, acetonitrile and toluene;
(ii) 1,3-bis-(2,4,6-trimethylphenyl)-imidazol-2-ylidene and imidazolium phenoxide:phenol adduct **3**, toluene

NMR spectroscopic analysis of compound **22** was performed in CD_3CN solution. The ^1H- and $^{13}C\{^1H\}$-NMR data compares favourably with that of the analogous bisimidazol-2-ylidene-copper(I) triflate species $[(IMes)_2Cu][O_3SCF_3]$ recorded in d_8-tetrahydrofuran.[28] The ^1H-NMR spectrum of compound **22** exhibits a singlet at a chemical shift of 7.15 ppm, consistent with the C(4/5)-H backbone hydrogen substituents of a metal-imidazol-2-ylidene species. Furthermore, the resonances observed at 178.4 ppm and 123.7 ppm within the $^{13}C\{^1H\}$-NMR spectrum of this species are also consistent with the C(2) and C(4/5) carbon atoms, respectively, of a metal-imidazol-2-ylidene complex. ^{31}P- and ^{19}F-NMR spectroscopy confirm the presence of a hexafluorophosphate anion.

Recrystallisation of bisimidazol-2-ylidene-copper(I) hexafluorophosphate salt **22** from toluene provided colourless blocks suitable for study by single crystal x-ray diffraction. The asymmetric unit of copper-*N*-heterocyclic carbene salt complex **22** consists of a bisimidazol-2-ylidene-copper(I) cation and a hexafluorophosphate anion (Figure 3.18) disordered over two positions. Compound **22** is isostructural with the related biscarbene-proton complex reported by Arduengo *et al.*[29] The

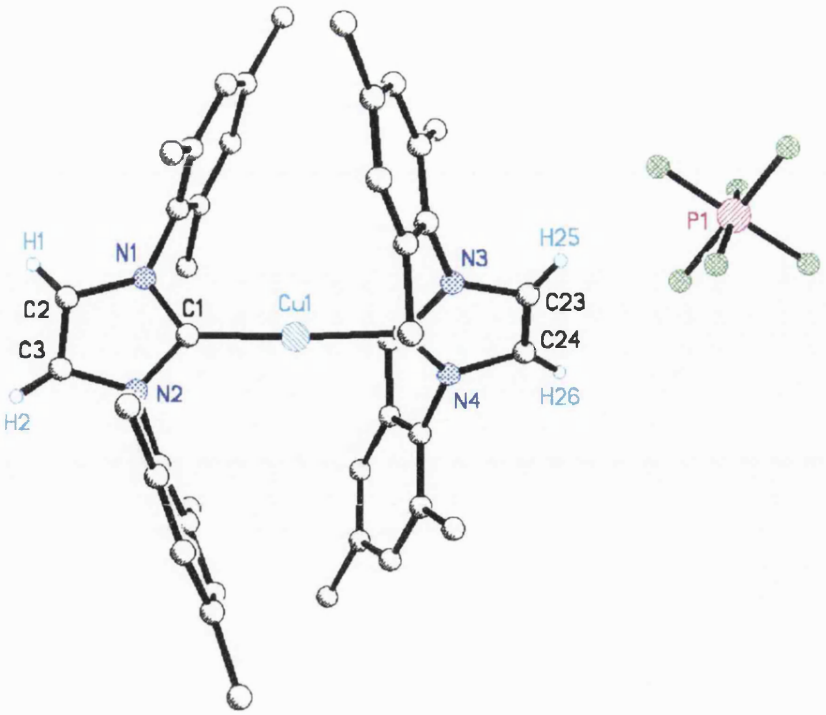

Figure 3.18: Representation of the molecular structure of the copper-*N*-heterocyclic carbene salt complex **22** as determined by single crystal x-ray diffraction

imidazol-2-ylidene-copper C(2)–Cu bonds C1–Cu1 and C4–Cu1 (Figure 3.18), at 1.885(4) Å and 1.882(3) Å respectively, are at the short end of the range reported within the chemical literature.[13, 30-35, 46] The two *N*-heterocyclic carbene ligands within the cation are in a staggered conformation; however, since the geometry about the central copper(I) ion is not linear - the C1–Cu1–C4 angle (Figure 3.18) equals 176.0(2)° - a single torsion angle does not adequately describe the twist of these ligands relative to one another. As observed in the analogous biscarbene-proton complex, studied crystallographically by Arduengo *et al.*,[29] the extended solid state structure of compound **22** consists of ribbons of individual molecules associated by means of intermolecular C–H·····F interactions.

In an effort to prepare a bisimidazol-2-ylidene-copper salt complex, we decided to investigate the reaction of two equivalents of the organic precursor salt 1,3-bis-(2,4,6-trimethylphenyl)-imidazolium 2,4,6-trimethylphenoxide ([IMesH][OMes]), generated *in situ* via the addition of IMes to the imidazolium phenoxide:phenol adduct 3, with a single equivalent of the basic metal source compound copper(II)

acetate (Scheme 3.10). As the reaction proceeds, a dramatic colour change from blue-green, through yellow, to deep red is observed. The product isolated from this reaction has been identified as the bisimidazol-2-ylidene-copper(I) species **23** (Scheme 3.10). The addition of [IMesH][OMes] to copper(II) acetate, therefore, induces the reduction of the copper centre.[52] This would seem to suggest that the basic metal source compound copper(II) acetate deprotonates the *in situ* generated organic metal-*N*-heterocyclic carbene complex precursor [IMesH][OMes] to form an *N*-heterocyclic carbene-copper(II)-phenoxide intermediate; thus mirroring the preparation of complexes **18-21** via the *in situ* deprotonation of the corresponding organic precursors by 2,4,6-trimethylphenyl-copper(I) (Scheme 3.8).

Copper(II)-phenoxide Cu–O bonds have been shown to possess some copper(I)-phenoxyl radical character.[52-56] The greater the stability of the phenoxyl radical the larger the contribution of the copper(I)-phenoxyl radical resonance form to the ground-state structure of the copper(II)-phenoxide complex; indeed, the copper-phenoxide Cu–O bonds within copper(II) complexes bearing phenoxide ligands that possess *ortho*- and *para*-substituents exhibit significant copper(I)-phenoxyl radical character.[52, 53, 57] Furthermore, Tolman *et al.* have previously reported the decomposition of a three-coordinate β-diketiminate-copper(II) terminal phenoxide complex prepared from the corresponding β-diketiminate-copper(II)-chloride via a salt metathesis reaction involving a sodium phenoxide salt; the decomposition products were isolated, and their identity established that decomposition proceeds via the homolytic fission of the copper(II)-phenoxide Cu–O bond.[52]

NMR spectroscopic characterisation of the product obtained from the reaction of two equivalents of the *in situ* generated metal-*N*-heterocyclic carbene precursor salt [IMesH][OMes] with a single equivalent of the basic metal source compound copper(II) acetate (Scheme 3.10) was performed in CD_2Cl_2 solution. On the basis of the comparison of the ^1H- and $^{13}C\{^1H\}$-NMR data for this species with that of product **22**; compound **23** is identified as a bisimidazol-2-ylidene-copper(I) salt complex incorporating the $[(IMes)_2Cu]^+$ cation. Further inspection of the ^1H- and $^{13}C\{^1H\}$-NMR spectra of bisimidazol-2-ylidene-copper(I) salt complex **23** reveals that the $CH_3CO_2^-$ ion is the anionic component; and also that a molecule of acetic

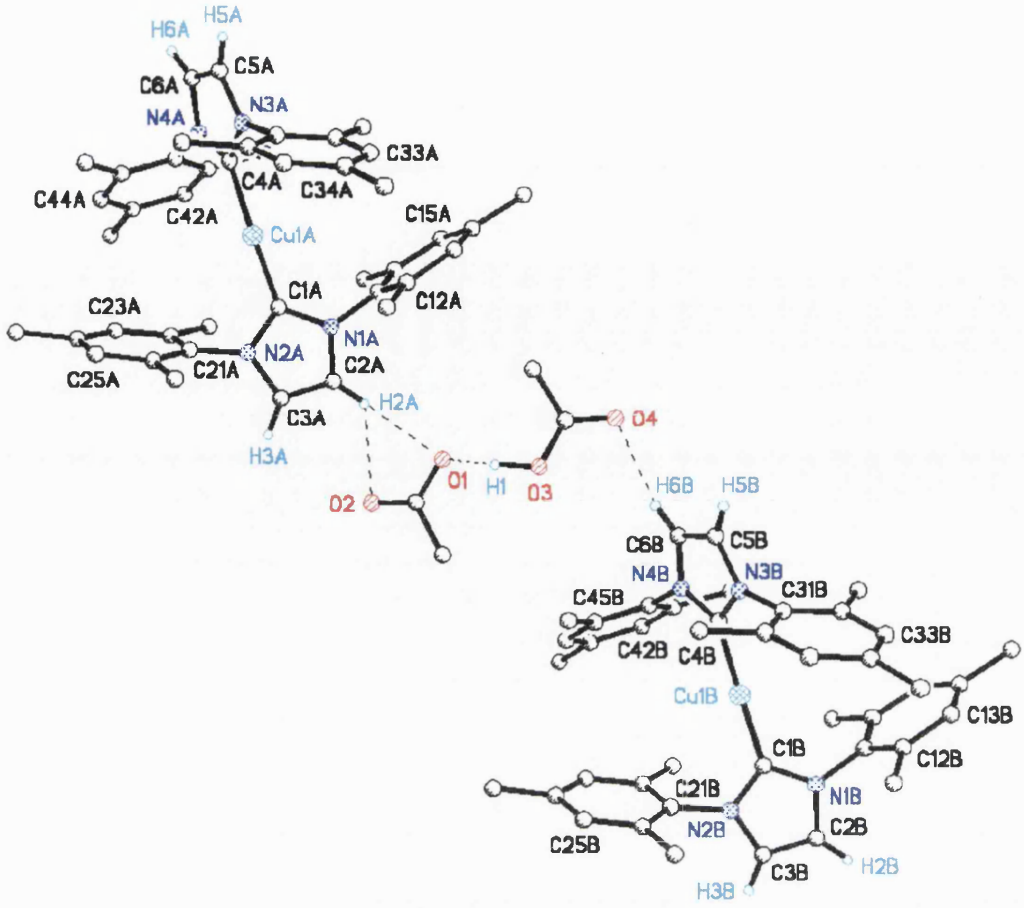

Figure 3.19: Role of O–H·····O^- and C–H·····O interactions within the solid state structure of the bisimidazol-2-ylidene-copper(I) salt complex **23**

acid solvent is present. The broad low-field resonance observed at 16.08 ppm in the ^{1}H-NMR spectrum of compound **23** suggests that rapid acetic acid-to-acetate proton transfer occurs in solution; such exchange of acidic protons is indicative of the existence of a hydrogen-bonding interaction in solution (Chapter Two).[58]

Single crystal x-ray diffraction reveals that the asymmetric unit of compound **23** incorporates a single $[(IMes)_2Cu]^+$ cation and acetate anion associated via tandem C–H·····O hydrogen-bonding interactions: (D = 3.180 Å, d = 2.497 Å and θ = 128.78°), [C2A–H2A·····O2], and (D = 3.316 Å, d = 2.397 Å and θ = 162.84°), [C2A–H2A·····$O1^-$] (Figure 3.19). The asymmetric unit also contains a molecule of acetic acid, which participates in an O–H·····O^- interaction with the $CH_3CO_2^-$

anion (D = 2.448 Å, d = 1.345 Å and θ = 175.35°), [O3–H1·····O1$^-$] (Figure 3.19). The metrical parameters of the $[(IMes)_2Cu]^+$ cation are reminiscent of those of the bisimidazol-2-ylidene-copper(I) salt complex **22**: indeed, the imidazol-2-ylidene-copper C(2)–Cu bonds C1–Cu1 and C4–Cu1 measure 1.888(1) Å and 1.889(1) Å, respectively; and the C1–Cu1–C4 angle equals 178.30(6)° - the geometry about the copper centre can therefore be described as near linear. Individual molecules of the bisimidazol-2-ylidene-copper(I) salt $[(IMes)_2Cu][CH_3CO_2][HO_2CCH_3]$ are associated into a polymeric extended solid state structure through intermolecular C–H·····O hydrogen-bonding interactions (D = 3.291 Å, d = 2.368 Å and θ = 163.97°), [C6B–H6B·····O4] (Figure 3.19).

Compound **23** is exceptionally stable to air and moisture; a crystalline sample of this bis-*N*-heterocyclic carbene-copper(I) salt complex product stored in air for a period of eighteen months showed no sign of degradation or decomposition. In an attempt to prepare further examples of bis-*N*-heterocyclic carbene-copper(I) salt complexes incorporating hydrogen-bonded anions, we decided to investigate the reaction of two equivalents of the hydrogen-bonded organic metal-*N*-heterocyclic carbene precursor salts discussed in Chapter Two with one equivalent of the basic metal source compound 2,4,6-trimethylphenyl-copper(I) (Scheme 3.11).

The reaction of two equivalents of the metal-*N*-heterocyclic carbene precursor salt [IMesH][OMes], generated *in situ* via the addition of one equivalent of IMes to the imidazolium phenoxide:phenol adduct **3**, with a single equivalent of the basic metal source compound CuMes provides the bisimidazol-2-ylidene-copper(I) salt complex **24** (Scheme 3.11). It is envisaged that the initial stage in the formation of product **24** is the *in situ* deprotonation of one equivalent of the [IMesH][OMes] salt by 2,4,6-trimethylphenyl-copper(I) to yield the imidazol-2-ylidene-copper(I) terminal phenoxide species **18**. The basic phenoxide ligand subsequently effects the deprotonation of the second equivalent of the *in situ* generated imidazolium phenoxide species. Similarly, the reaction of two equivalents of the imidazolium benzoate salt **11** with a single equivalent of CuMes to yield the analogous bis-*N*-heterocyclic carbene-copper(I) salt complex **25** (Scheme 3.11) proceeds via two

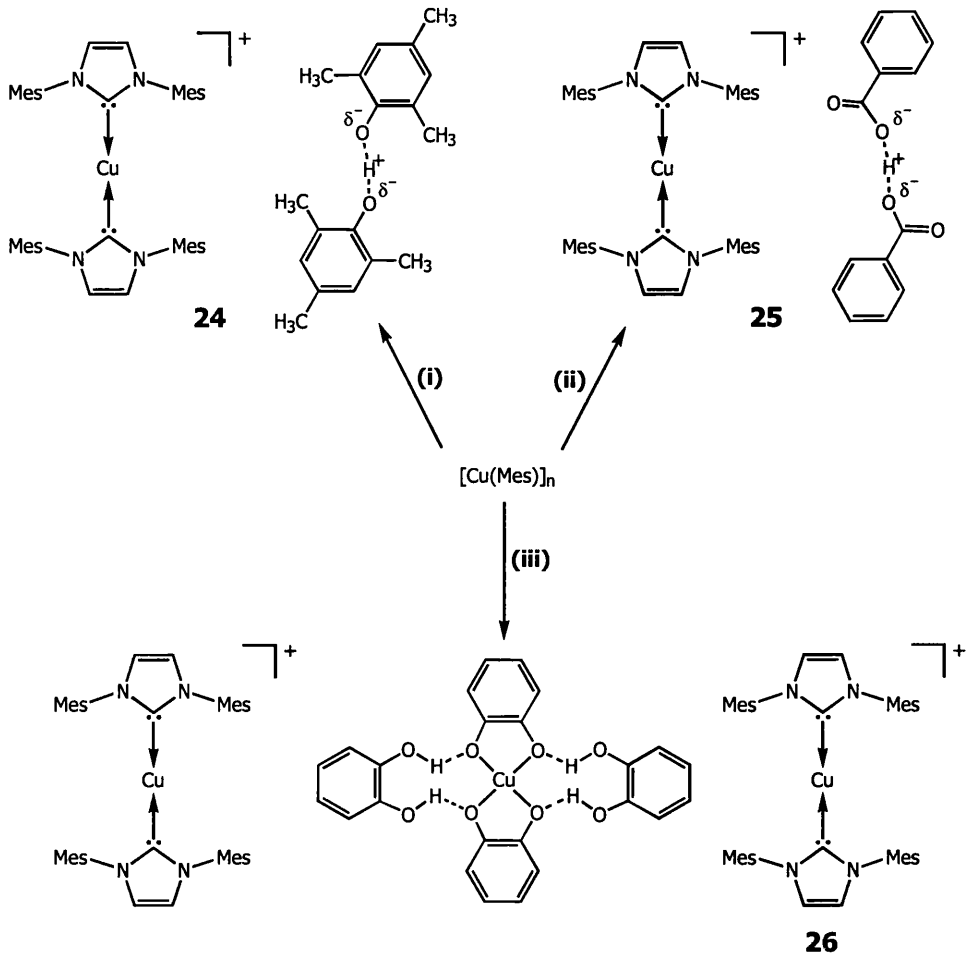

Scheme 3.11: Reaction of 2,4,6-trimethylphenyl-copper(I) with imidazolium precursors to metal-*N*-heterocyclic carbene complexes **(i)** 1,3-bis-(2,4,6-trimethylphenyl)-imidazol-2-ylidene and imidazolium phenoxide:phenol adduct **3**, toluene; **(ii)** imidazolium benzoate salt **11**, toluene; **(iii)** imidazolium catecholate **5**, toluene

successive *in situ* deprotonation steps: initial *in situ* deprotonation of the organic metal-*N*-heterocyclic carbene precursor salt **11** by basic metal source compound CuMes generates the related imidazol-2-ylidene-copper(I)-benzoate species; this intermediate then deprotonates the second equivalent of the hydrogen-bonded imidazolium benzoate salt **11**.

NMR spectroscopic analysis of compounds **24** and **25** was performed in CD_3CN solution. On the basis of the comparison of the ^1H- and $^{13}C\{^1H\}$-NMR data for these products with that of $[(IMes)_2Cu][PF_6]$ salt complex **22** recorded in the same solvent; compounds **24** and **25** are identified as bisimidazol-2-ylidene-copper(I)

salt complexes incorporating the $[(IMes)_2Cu]^+$ cation. The signals corresponding to the C(4/5)-H backbone hydrogen atom substituents are observed at chemical shifts of 7.13 ppm and 7.15 ppm in the ^{1}H-NMR spectra of products **24** and **25**, respectively. The $^{13}C\{^1H\}$-NMR spectrum of compound **24** exhibits resonances corresponding to the C(2) and C(4/5) carbon atoms of the heterocyclic core of a metal-imidazol-2-ylidene species at 178.3 ppm and 123.8 ppm, respectively. The C(4/5) carbon atom resonance is observed within the $^{13}C\{^1H\}$-NMR spectrum of **25** at a chemical shift of 123.7 ppm. The anionic components of these species are identified as the 2,4,6-trimethylphenoxide ion and the benzoate ion, respectively. Further inspection of the ^{1}H- and $^{13}C\{^1H\}$-NMR spectra of bisimidazol-2-ylidene-copper(I) salt complexes **24** and **25** reveals them to be 2,4,6-trimethylphenol and benzoic acid solvates, respectively.

Single crystal x-ray diffraction analysis reveals the asymmetric unit of product **24** to incorporate a single $[(IMes)_2Cu]^+$ cation and a phenoxide anion participating in an O–H·····O$^-$ hydrogen-bonding interaction with a molecule of solvating phenol (D = 2.451 Å, d = 1.427 Å and θ = 179.10°), [O1A–H1A·····O2A$^-$] (Figure 3.20). The cations and anions associate through C–H·····O$^-$ contacts (D = 3.220 Å, d =

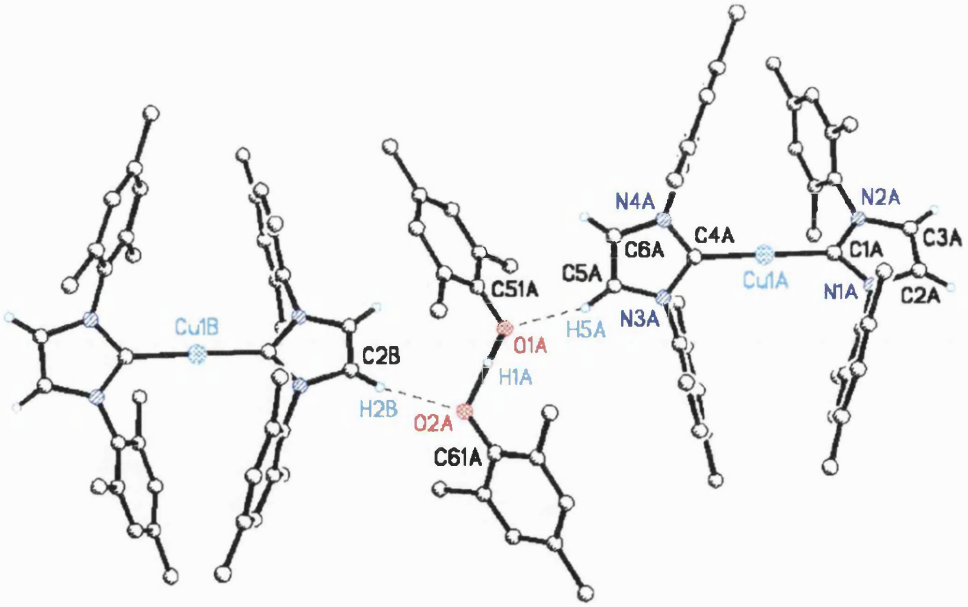

Figure 3.20: Role of O–H·····O$^-$ and C–H·····O interactions within the solid state structure of the bisimidazol-2-ylidene-copper(I) salt complex **24**

2.303 Å and θ = 161.85°), [C2B–H2B·····O2A$^-$] (Figure 3.20). The [(IMes)$_2$Cu]$^+$ cation metrical parameters are reminiscent of those of compounds **22** and **23**: the imidazol-2-ylidene-copper C(2)–Cu bonds C1–Cu1 and C4–Cu1 equal 1.878(4) Å and 1.882(4) Å, respectively; and the C1–Cu1–C4 angle measures 179.4(2)° - the geometry about the copper centre can therefore be described as near linear. The individual molecules of [(IMes)$_2$Cu][MesO][HOMes] associate into a polymeric extended array through intermolecular C–H·····O interactions (*D* = 3.116 Å, *d* = 2.223 Å and θ = 154.26°), [C5A–H5A·····O1A] (Figure 3.20).

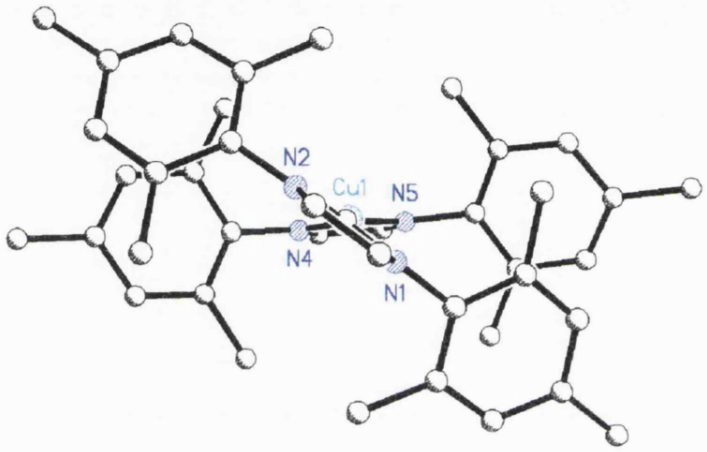

Figure 3.21: Graphical representation of the cation within the bisimidazol-2-ylidene-copper(I) salt complex **25**

The asymmetric unit of compound **25** incorporates a single [(IMes)$_2$Cu]$^+$ cation, a benzoate anion, and a molecule of benzoic acid. The metrical parameters of the cation are consistent with those of the cations in bisimidazol-2-ylidene-copper(I) salt complexes **22-24**: the imidazol-2-ylidene-copper C(2)–Cu bonds C1–Cu1 and C4–Cu1 (Figure 3.21) are 1.879(2) Å and 1.881(2) Å in length, respectively; and the C1–Cu1–C4 angle (Figure 3.21) measures 176.43(7)°. The benzoate anion participates in an O–H·····O$^-$ interaction with the molecule of benzoic acid (*D* = 2.497 Å, *d* = 1.317 Å and θ = 169.96°), [O1–H1·····O3$^-$] (Figure 3.22); which is comparable with the O–H·····O$^-$ contacts within the imidazolium phenoxide:phenol adducts **1-3**, the tetra-*n*-butyl ammonium phenoxide:phenol adduct synthesised by Reetz *et al.*,[59] and, the bisimidazol-2-ylidene-copper(I) salt complexes **23** and **24**.

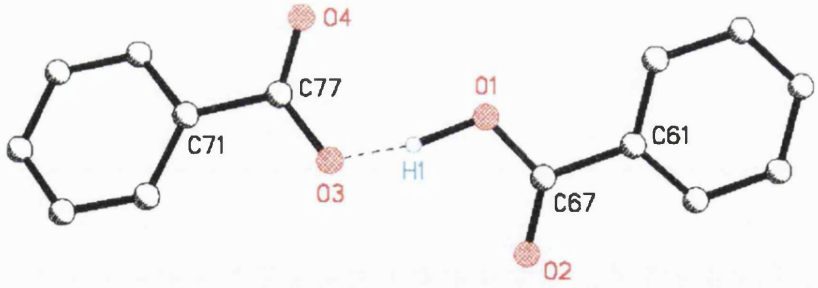

Figure 3.22: Graphical representation of the anion within the bisimidazol-2-ylidene-copper(I) salt complex **25**

We have also prepared another example of a bisimidazol-2-ylidene-copper(I) salt complex via the stoichiometric reaction of a single equivalent of the imidazolium catecholate **5** with one equivalent of the basic metal source compound CuMes (Scheme 3.11). A fine suspension of copper(0) metal, most probably the result of a disproportionation reaction, developed within the green toluene solution during the course of the reaction. Following filtration to remove the suspended material, the product crystallised as a batch of green blocks and was subsequently identified as the bisimidazol-2-ylidene-copper(I) salt complex **26** rather than the anticipated neutral *N*-heterocyclic carbene-copper(I)-catecholate species.

NMR spectroscopic analysis of compound **26** was performed in CD_3CN solution. On the basis of the comparison of the ^1H- and $^{13}C\{^1H\}$-NMR data for this species with that of compounds **22**, **24** and **25** recorded in the same solvent; compound **26** is identified as a bisimidazol-2-ylidene-copper(I) salt complex that incorporates the $[(IMes)_2Cu]^+$ cation. The ^1H-NMR resonance corresponding to the C(4/5)-H backbone hydrogen atom substituents is observed at a chemical shift of 7.15 ppm, which is indicative of an imidazol-2-ylidene-metal adduct. The $^{13}C\{^1H\}$-NMR spectrum exhibits resonances consistent with the C(2) and C(4/5) carbon atoms of the planar heterocyclic core of an imidazol-2-ylidene-metal species at 178.4 ppm and 123.7 ppm, respectively. Integration of the ^1H-NMR spectrum of compound **26** suggests that this bisimidazol-2-ylidene-copper(I) salt complex possesses two IMes ligands per catechol residue; this product composition is inconsistent with the stoichiometry of the reaction (Scheme 3.11).

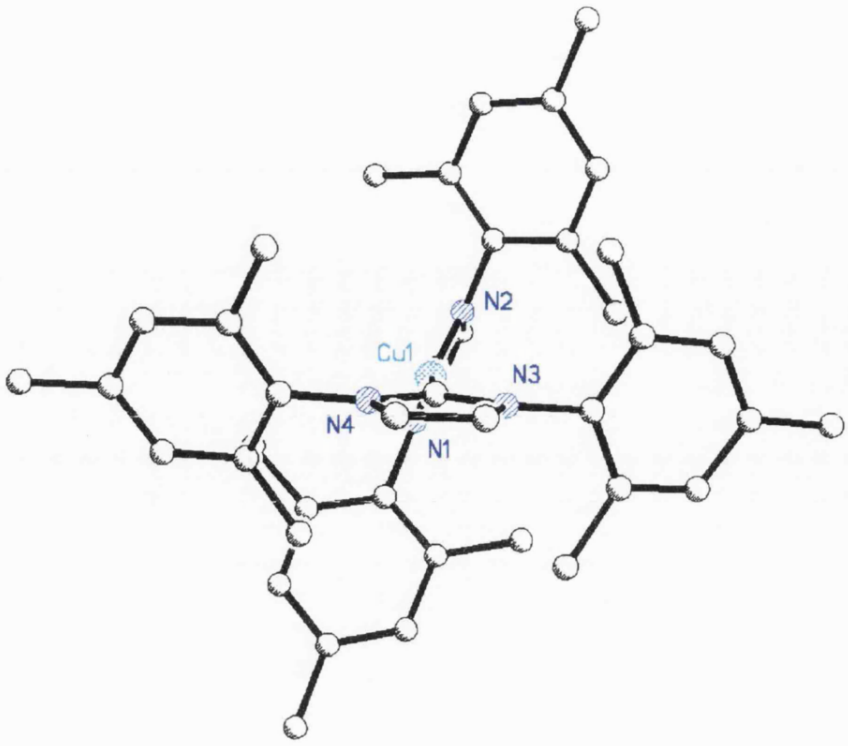

Figure 3.23: Graphical representation of the single cation within the asymmetric unit of the bisimidazol-2-ylidene-copper(I) salt complex **26**

Single crystal x-ray diffraction analysis of a green block isolated from the reaction mixture reveals the asymmetric unit of product **26** to contain only half a molecule of this copper salt complex. Compound **26** consists of two bisimidazol-2-ylidene-copper(I) cations, a planar copper(II) dianion bearing two doubly-deprotonated catechol residues, and two molecules of catechol. The metrical parameters of the cation within the asymmetric unit of compound **26** are consistent with those of bisimidazol-2-ylidene-copper(I) salt complexes **22-25**: the imidazol-2-ylidene-copper C(2)–Cu bonds C1–Cu1 and C4–Cu1 (Figure 3.23) measure 1.886(5) Å and 1.880(4) Å in length, respectively; and the C1–Cu1–C4 (Figure 3.23) angle is found to measure 175.1(2)° - the geometry about the copper centre of the cation can therefore be described as near linear. The greater stagger between the two IMes ligands within the bisimidazol-2-ylidene-copper(I) cations of compound **26** (Figure 3.23) relative to that observed within the cation of bisimidazol-2-ylidene-copper(I) salt complex **25** (Figure 3.21) is thought to be a result of crystal packing effects.

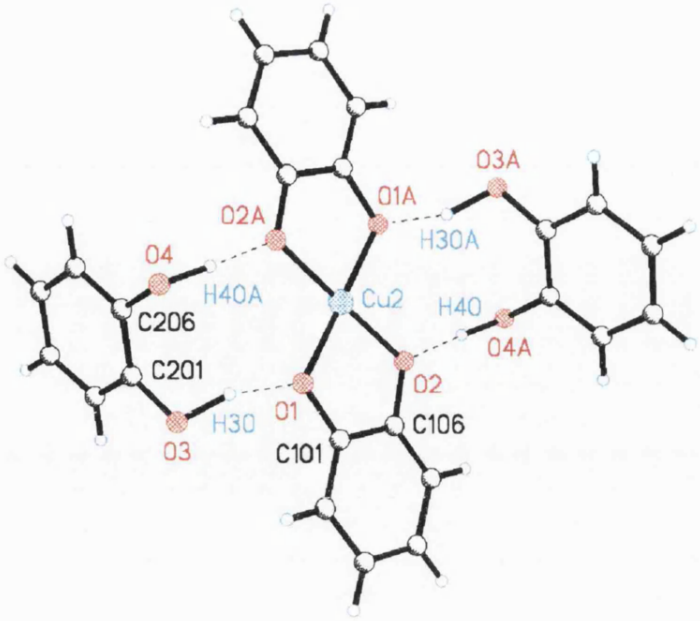

Figure 3.24: O–H·····O$^-$ hydrogen-bonding between the solvating catechol molecules and the planar dianion within bisimidazol-2-ylidene-copper(I) salt complex **26** (O1A, O2A, O3A, O4A, H30A and H40A are symmetry generated equivalents of O1, O2, O3, O4, H30 and H40, respectively)

Catechol solvent molecules bridge the two doubly-deprotonated catechol residues within the planar dianion via O–H·····O$^-$ hydrogen-bonded contacts: (D = 2.574 Å, d = 1.448 Å and θ = 160.92°), [O3–H30·····O1$^-$], and (D = 2.566 Å, d = 1.451 Å and θ = 175.78°), [O4A–H40·····O2$^-$] (Figure 3.24). The chelating deprotonated catechol residues coordinate the copper(II) centre through a fairly representative O–Cu bond equal to 1.897(3) Å, [O1–Cu2] (Figure 3.24), and one longer O–Cu contact measuring 1.924(3) Å, [O2–Cu2] (Figure 3.24). The chelating donor ligands are unequivocally indentified as doubly-deprotonated catechol residues, rather than singly-deprotonated semiquinones or quinones, on the basis of their C101–O1 and C106–O2 bond lengths (Figure 3.24), which equal 1.365(6) Å and 1.345(6) Å, respectively; since the C–O bonds within semiquinones and quinones are significantly shorter.[60, 61]

3.4: Conclusions

The *in situ* deprotonation of the hydrogen-bonded organic metal-*N*-heterocyclic carbene precursor species described in Chapter Two by the basic metal source compound 2,4,6-trimethylphenyl-copper(I) represents a convenient route to both neutral imidazol-2-ylidene-copper(I) complexes **18-21** and bisimidazol-2-ylidene-copper(I) salt complexes **24-26**.

The solid state molecular structures of neutral *N*-heterocyclic carbene-copper(I) species **19-21** are remarkably similar to those of their hydrogen-bonded organic metal-*N*-heterocyclic carbene precursor compounds **3, 9** and **15**. Compounds **16** and **21** undergo a reaction with excess CD_3OD to provide the methoxide salt of the *N*-heterocyclic carbene ligand; in the presence of trace quantities of water and molecular oxygen, this species is converted to the related 2-hydroxy-imidazolium methoxide salt via a copper-catalysed oxidation reaction. This demonstrates that protonation of *N*-heterocyclic carbene ligands from metal centres is an important aspect of the reactivity of these species and may occur in the presence of acidic solvents or reagents.

The robust nature of the bisimidazol-2-ylidene-copper(I) cation in salts prepared via the reaction of two equivalents of an organic metal-*N*-heterocyclic carbene complex precursor with the basic metal source compound 2,4,6-trimethylphenyl-copper(I) allows the O–H·····O^- hydrogen-bonding interaction between the anion and the acidic solvent molecule present to be structurally characterised by single crystal x-ray diffraction. The stability of the bisimidazol-2-ylidene-copper(I) salt complexes coupled with the prevalence of rapid solvent-to-anion proton transfer suggests that these species may find utility in anionic polymerisation processes such as the ring-opening polymerisation of cyclic esters, which is discussed in some detail in Chapter Four. The decomposition observed in the preparation of **23** and **26** demonstrates that some *N*-heterocyclic carbene-metal complexes are inaccessible via the *in situ* deprotonation of organic metal-*N*-heterocyclic carbene precursor compounds; since some hydrogen-bonded organic precursor species are incompatible with some basic metal source compounds.

3.5: References

[1] P. Gamez, P. G. Aubel, W. L. Driessen, J. Reedijk, *Chem. Soc. Rev.*, **2001**, *30*, 376.

[2] N. Komiya, T. Naota, S. I. Murahashi, *Tetrahedron Lett.*, **1996**, *37*, 1633.

[3] B. Phillips, F. C. Frostick Jr., P. S. Starcher, *J. Am. Chem. Soc.*, **1957**, *79*, 5982.

[4] N. Kitajima, T. Koda, Y. Iwata, Y. Moro-oka, *J. Am. Chem. Soc.*, **1990**, *112*, 8833.

[5] S. I. Murahashi, Y. Oda, T. Naota, N. Komiya, *J. Chem. Soc.-Chem. Commun.*, **1993**, 139.

[6] I. E. Marko, P. R. Giles, M. Tsukazaki, I. Chelle-Regnaut, A. Gautier, S. M. Brown, C. J. Urch, *J. Org. Chem.*, **1999**, *64*, 2433.

[7] B. Betzemeier, M. Cavazzini, S. Quici, P. Knochel, *Tetrahedron Lett.*, **2000**, *41*, 4343.

[8] R. Gupta, R. Mukherjee, *Tetrahedron Lett.*, **2000**, *41*, 7763.

[9] J. Kruger, E. M. Carreira, *J. Am. Chem. Soc.*, **1998**, *120*, 837.

[10] B. L. Pagenkopf, J. Kruger, A. Stojanovic, E. M. Carreira, *Angew. Chem.-Int. Ed. Engl.*, **1998**, *37*, 3124.

[11] T. Rovis, D. A. Evans, *"Structural and mechanistic investigations in asymmetric copper(I) and copper(II) catalyzed reactions"*, in *Progress in Inorganic Chemistry*, John Wiley & Sons Inc, New York, **2001**. 1-150.

[12] V. Jurkauskas, J. P. Sadighi, S. L. Buchwald, *Org. Lett.*, **2003**, *5*, 2417.

[13] H. Kaur, F. K. Zinn, E. D. Stevens, S. P. Nolan, *Organometallics*, **2004**, *23*, 1157.

[14] H. O. House, M. J. Umen, *J. Org. Chem.*, **1973**, *38*, 3893.

[15] D. A. Evans, M. M. Faul, M. T. Bilodeau, *J. Org. Chem.*, **1991**, *56*, 6744.

[16] D. A. Evans, M. M. Faul, M. T. Bilodeau, B. A. Anderson, D. M. Barnes, *J. Am. Chem. Soc.*, **1993**, *115*, 5328.

[17] W. Kirmse, *Angew. Chem.-Int. Ed. Engl.*, **2003**, *42*, 1088.

[18] O. W. Webster, *Science*, **1991**, *251*, 887.

[19] J. S. Wang, K. Matyjaszewski, *J. Am. Chem. Soc.*, **1995**, *117*, 5614.

[20] J. S. Wang, K. Matyjaszewski, *Macromolecules*, **1995**, *28*, 7572.

[21] J. S. Wang, K. Matyjaszewski, *Macromolecules*, **1995**, *28*, 7901.

[22] T. E. Patten, J. H. Xia, T. Abernathy, K. Matyjaszewski, *Science*, **1996**, *272*, 866.

[23] D. M. Haddleton, C. B. Jasieczek, M. J. Hannon, A. J. Shooter, *Macromolecules*, **1997**, *30*, 2190.

[24] D. M. Haddleton, A. J. Clark, M. C. Crossman, D. J. Duncalf, A. M. Heming, S. R. Morsley, A. J. Shooter, *J. Chem. Soc.-Chem. Commun.*, **1997**, 1173.

[25] K. Matyjaszewski, *Macromolecules*, **1998**, *31*, 4710.

[26] K. Matyjaszewski, B. E. Woodworth, *Macromolecules*, **1998**, *31*, 4718.

[27] K. Matyjaszewski, *Chem.-Eur. J.*, **1999**, *5*, 3095.

[28] A. J. Arduengo, H. V. R. Dias, J. C. Calabrese, F. Davidson, *Organometallics*, **1993**, *12*, 3405.
[29] A. J. Arduengo, S. F. Gamper, M. Tamm, J. C. Calabrese, F. Davidson, H. A. Craig, *J. Am. Chem. Soc.*, **1995**, *117*, 572.
[30] H. G. Raubenheimer, S. Cronje, P. H. Vanrooyen, P. J. Olivier, J. G. Toerien, *Angew. Chem.-Int. Ed. Engl.*, **1994**, *33*, 672.
[31] H. G. Raubenheimer, S. Cronje, P. J. Olivier, *J. Chem. Soc.-Dalton Trans.*, **1995**, 313.
[32] N. P. Mankad, T. G. Gray, D. S. Laitar, J. P. Sadighi, *Organometallics*, **2004**, *23*, 1191.
[33] A. A. D. Tulloch, A. A. Danopoulos, S. Kleinhenz, M. E. Light, M. B. Hursthouse, G. Eastham, *Organometallics*, **2001**, *20*, 2027.
[34] P. L. Arnold, A. C. Scarisbrick, A. J. Blake, C. Wilson, *J. Chem. Soc.-Chem. Commun.*, **2001**, 2340.
[35] X. L. Hu, I. Castro-Rodriguez, K. Meyer, *J. Am. Chem. Soc.*, **2003**, *125*, 12237.
[36] E. M. Meyer, S. Gambarotta, C. Floriani, A. Chiesi-Villa, C. Guastini, *Organometallics*, **1989**, *8*, 1067.
[37] H. Eriksson, M. Hakansson, *Organometallics*, **1997**, *16*, 4243.
[38] T. Tsuda, K. Watanabe, K. Miyata, H. Yamamoto, T. Saegusa, *Inorg. Chem.*, **1981**, *20*, 2728.
[39] H. L. Aalten, G. van Koten, K. Goubitz, C. H. Stam, *J. Chem. Soc.-Chem. Commun.*, **1985**, 1252.
[40] A. J. Arduengo, H. V. R. Dias, J. C. Calabrese, F. Davidson, *J. Am. Chem. Soc.*, **1992**, *114*, 9724.
[41] A. J. Arduengo, R. Krafczyk, R. Schmutzler, H. A. Craig, J. R. Goerlich, W. J. Marshall, M. Unverzagt, *Tetrahedron*, **1999**, *55*, 14523.
[42] M. Tafipolsky, W. Scherer, K. Ofele, G. Artus, B. Pedersen, W. A. Herrmann, G. S. McGrady, *J. Am. Chem. Soc.*, **2002**, *124*, 5865.
[43] R. W. Alder, P. R. Allen, S. J. Williams, *J. Chem. Soc.-Chem. Commun.*, **1995**, 1267.
[44] Y. J. Kim, A. Streitwieser, *J. Am. Chem. Soc.*, **2002**, *124*, 5757.
[45] M. Begtrup, *J. Chem. Soc.-Chem. Commun.*, **1975**, 334.
[46] X. Hu, I. Castro-Rodriguez, K. Meyer, *Organometallics*, **2003**, *22*, 3016.
[47] R. Lingnau, J. Strahle, *Angew. Chem.-Int. Ed. Engl.*, **1988**, *27*, 436.
[48] T. Ramnial, C. D. Abernethy, M. D. Spicer, I. D. McKenzie, I. D. Gay, J. A. C. Clyburne, *Inorg. Chem.*, **2003**, *42*, 1391.
[49] P. Fiaschi, C. Floriani, M. Pasquali, A. Chiesi-Villa, C. Guastini, *J. Chem. Soc.-Chem. Commun.*, **1984**, 888.
[50] F. Calderazzo, F. Marchetti, G. Dell'Amico, *J. Chem. Soc.-Dalton Trans.*, **1980**, 1419.
[51] O. G. Polyakov, S. M. Ivanova, C. M. Gaudinski, S. M. Miller, O. P. Anderson, S. H. Strauss, *Organometallics*, **1999**, *18*, 3769.
[52] B. A. Jazdzewski, P. L. Holland, M. Pink, V. G. Young, D. J. E. Spencer, W. B. Tolman, *Inorg. Chem.*, **2001**, *40*, 6097.

[53] K. Fujisawa, Y. Iwata, N. Kitajima, H. Higashimura, M. Kubota, Y. Miyashita, Y. Yamada, K. Okamoto, Y. Moro-oka, *Chem. Lett.*, **1999**, 739.
[54] S. Itoh, M. Taki, S. Takayama, S. Nagatomo, T. Kitagawa, N. Sakurada, R. Arakawa, S. Fukuzumi, *Angew. Chem.-Int. Ed. Engl.*, **1999**, *38*, 2774.
[55] L. Benisvy, A. J. Blake, D. Collison, E. S. Davies, C. D. Garner, E. J. L. McInnes, J. McMaster, G. Whittaker, C. Wilson, *J. Chem. Soc.-Chem. Commun.*, **2001**, 1824.
[56] L. Benisvy, A. J. Blake, D. Collison, E. S. Davies, C. D. Garner, E. J. L. McInnes, J. McMaster, G. Whittaker, C. Wilson, *J. Chem. Soc.-Dalton Trans.*, **2003**, 1975.
[57] P. Chaudhuri, K. Wieghardt, *"Phenoxyl radical complexes"*, in *Progress in Inorganic Chemistry*, John Wiley & Sons Inc, New York, **2001**. 151-216.
[58] G. A. Jeffrey, *An Introduction to Hydrogen Bonding*, Oxford University Press, Oxford, **1997**.
[59] R. Goddard, H. M. Herzog, M. T. Reetz, *Tetrahedron*, **2002**, *58*, 7847.
[60] J. S. Thompson, J. C. Calabrese, *J. Am. Chem. Soc.*, **1986**, *108*, 1903.
[61] L. M. Berreau, S. Mahapatra, J. A. Halfen, R. P. Houser, V. G. Young, W. B. Tolman, *Angew. Chem.-Int. Ed. Engl.*, **1999**, *38*, 207.

Zinc-*N*-Heterocyclic Carbene Complexes

4.1: Introduction

This chapter reports on the preparation, characterisation and reactivity of zinc(II) species obtained via the *in situ* deprotonation of related hydrogen-bonded organic precursors as a result of reaction with dimethylzinc. An *N*-heterocyclic carbene-zinc(II) bisphenoxide complex synthesised employing this methodology has been evaluated as a catalyst and pre-catalyst in the ring-opening polymerisation of the cyclic ester ε-caprolactone. This introduction briefly reviews the exploitation of zinc compounds in the catalysis of polymerisation and copolymerisation reactions, and summarises previous research into zinc-*N*-heterocyclic carbene complexes.

4.1.1: Zinc Compounds in Polymerisation Catalysis

Zinc compounds are employed in the catalysis of a number of polymerisation and copolymerisation reactions, examples that will be briefly discussed here include: the ring-opening polymerisation of epoxides; the copolymerisation of epoxides with carbon dioxide; and the ring-opening polymerisation of cyclic esters such as dilactide and ε-caprolactone.

Bruce *et al.* reported that zinc alkoxide species generated via addition of alcohols to organozinc reagents initiate the ring-opening homopolymerisation of epoxides to provide polyethers.[1, 2] The driving-force for polymerisation is release of the ring-strain within the three-membered cyclic monomer.[3, 4] It has been proposed that polymerisation proceeds via a coordination-insertion mechanism: in which coordination of a molecule of Lewis basic epoxide monomer to the Lewis acidic zinc alkoxide species is followed by transfer of an anionic alkoxide functionality to, and concomitant ring-opening of, the coordinated monomer (Scheme 4.1).[5] Subsequent ring-opening events involve transfer of a propagating chain from the active Lewis acidic zinc centre to successive molecules of coordinated epoxide (Scheme 4.1).[5] Supporting evidence for this postulated coordination-insertion mechanism is provided via the NMR spectroscopic analysis of the homopolymer,

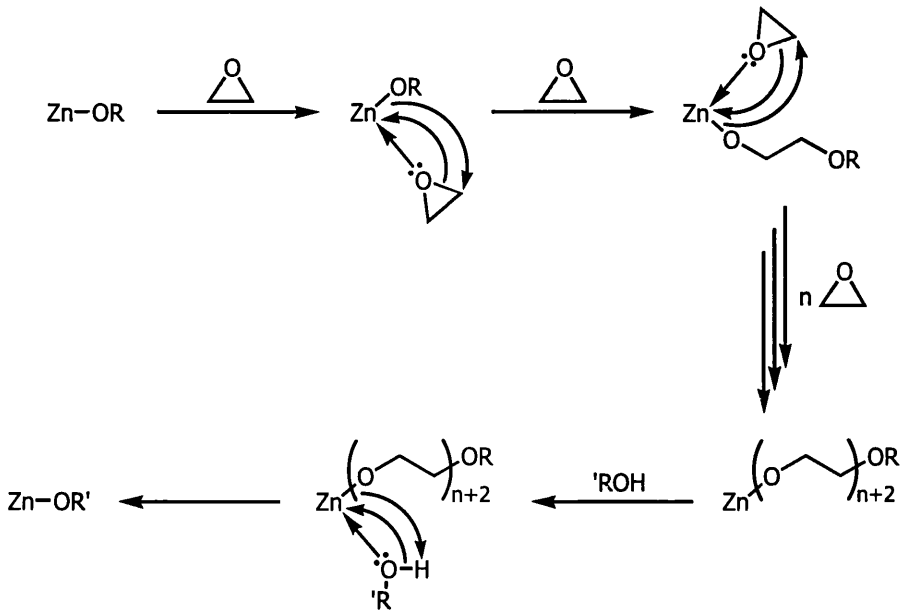

Scheme 4.1: Ring-opening polymerisation of epoxides catalysed by zinc alkoxide species

which reveals that the alkoxy group at the chain terminus originates from the zinc alkoxide initiator (Scheme 4.1).[1, 2] Polymerisation continues until all available monomer has been consumed or the catalyst is deactivated. It has been suggested more recently that the monomer is activated on coordination to one Lewis acidic metal centre and ring-opened as a result of transfer of an alkoxide functionality from a neighbouring metal centre.[6-8] This back-side attack hypothesis is gaining acceptance as it seems to account for the observed stereochemistry in polymers prepared via the ring-opening homopolymerisation of propylene oxide.[9]

Zinc alkoxide species prepared via the methodology employed by Bruce *et al.*[1, 2] inevitably incorporate trace quantities of the corresponding alcohol, which may be removed by heating the compound under dynamic vacuum.[1] The presence of alcohol is reported to adversely affect the activity of the zinc alkoxide initiator and also reduce the yield and molecular weight of the polyether produced.[1, 2] These observations suggest that the alcohol coordinates to the Lewis acidic zinc alkoxide initiator, which would interfere with the coordination of the Lewis basic epoxide monomer and therefore impede propagation.[2] Bruce *et al.* have proposed that the coordination of the alcohol to the catalytically active zinc centre may result in the termination of the growing chain and regeneration of the zinc alkoxide initiator

(Scheme 4.1).[2] It is interesting to note that, when all the available monomer has been consumed, the polyether homopolymer may be recovered by the addition of alcohol to the system.[2] Under a carbon dioxide atmosphere; zinc alkoxides also effect the copolymerisation of epoxides and carbon dioxide.[10]

Darensbourg *et al.* have recently embarked on the development of analogous zinc phenoxide species as carbon dioxide/epoxide copolymerisation catalysts.[11-15] In such systems, the carbon dioxide/epoxide copolymerisation is accompanied by the homopolymerisation of the epoxide.[13, 15-17] The ratio of carbonate:ether linkages within the polymer backbone is found to be greatly increased in copolymerisation reactions initiated by phosphine:zinc bisphenoxide adducts.[12, 15-17]

Back-coordination of growing polymer chains to metal initiator species is a major problem in zinc catalysed polyoxygenate formations via both homopolymerisation and copolymerisation reactions.[2, 18, 19] Bruce *et al.* reported fast propagation in the early stages of diphenylzinc initiated ring-opening polymerisation of epoxides and attributed the subsequent decline in catalytic activity to problematic epoxide monomer coordination as a result of back-coordination of the growing polyether chain.[2] Darensbourg *et al.* have implicated the back-coordination of the growing polycarbonate chain, in the zinc catalysed copolymerisation of carbon dioxide and epoxides, in the formation of cyclic carbonate side products.[20]

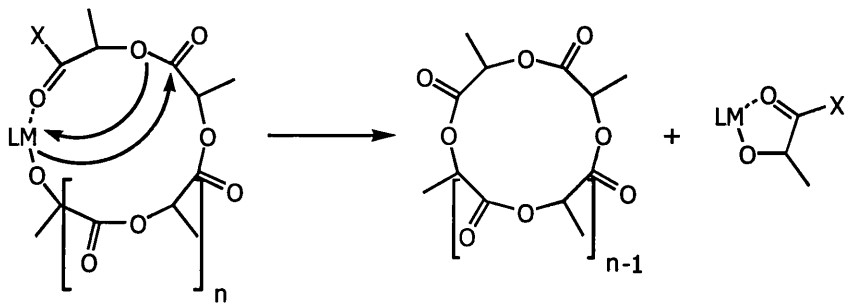

Scheme 4.2: Back-coordination of polylactide chain to metal initiator and subsequent intrachain transesterification

Due to properties such as biocompatibility, biodegradability and permeability to drugs; polyoxygenates such as polylactide and poly(caprolactone) are well suited to biomedical applications; including use as biodegradable sutures, artificial skins

and drug-delivery implants.[21, 22] Zinc species have been identified as appropriate catalysts for biomedical polymer production.[22] A recent report published in the literature demonstrates that the back-coordination of the growing polymer chain also represents a problem in polyester formation: this brings the chain ends into close proximity and leads to intrachain transesterification (Scheme 4.2).[23]

4.1.2: Zinc-*N*-Heterocyclic Carbene Complexes

Only a few examples of zinc-*N*-heterocyclic carbene species have been reported in the literature to date.[24-26] The first zinc-*N*-heterocyclic carbene species reported within the literature were the imidazol-2-ylidene:dialkylzinc adducts prepared and isolated by Arduengo *et al.*[24] The very first zinc-*N*-heterocyclic carbene species crystallographically characterised by x-ray diffraction was the adduct prepared via addition of 1,3-bis-(1-adamantyl)-imidazol-2-ylidene, which was the first stable crystalline carbene to be isolated and studied,[27] to diethylzinc.[24]

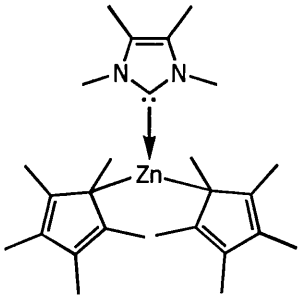

Figure 4.1: An imidazol-2-ylidene:zincocene adduct

Arduengo *et al.* have crystallographically characterised another example of an *N*-heterocyclic-carbene:diorganozinc adduct; prepared by means of the complexation of 1,3,4,5-tetramethyl-imidazol-2-ylidene to zincocene (Figure 4.1).[25] The zinc-*N*-heterocyclic carbene bond within this species is short for Zn–C connectivities; illustrating that imidazol-2-ylidenes form strong bonds to zinc centres.[25]

The preparation and single crystal x-ray structural characterisation of a number of zinc-*N*-heterocyclic carbene complexes has recently been reported by Buchmeiser *et al.*[26] These species were subsequently investigated as polymerisation catalysts in reactions including the ring-opening homopolymerisation of propylene oxide,

cyclohexene oxide and ε-caprolactone, and, the copolymerisation of cyclohexene oxide and carbon dioxide (Scheme 4.3).[26] These zinc-*N*-heterocyclic carbene species were discovered to be inactive in the ring-opening homopolymerisation of propylene oxide, extremely inefficient for the production of poly(caprolactone), and of limited use in the ring-opening homopolymerisation of cyclohexene oxide. A number of the zinc-*N*-heterocyclic carbenes examined were demonstrated to be effective catalysts in the cyclohexene oxide and carbon dioxide copolymerisation reaction (Scheme 4.3). Perhaps more importantly, Buchmeiser *et al.* were able to demonstrate that zinc-*N*-heterocyclic carbene coordination compounds suppress polyether formation in the copolymerisation of carbon dioxide and epoxides,[26] just like the analogous phosphine species pioneered by Darensbourg *et al.*[12, 15-17]

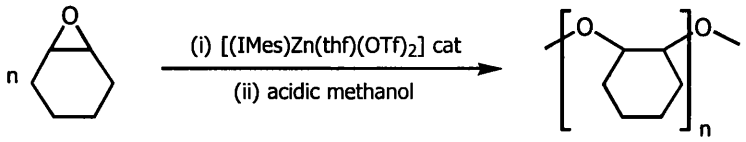

Scheme 4.3: Zinc-*N*-heterocyclic carbene complex catalysed ring-opening homopolymerisation of cyclohexene oxide

One further example of a zinc-*N*-heterocyclic carbene coordination compound has recently emerged in the literature.[28] This complex was examined as a catalyst for polylactide production via the ring-opening polymerisation of D,L-lactide and was determined to exhibit notable polymerisation activity. The decoordination of the *N*-heterocyclic carbene ligand from the metal centre, allowing polymerisation to proceed in an organocatalytic fashion as recently described by Hedrick *et al.*,[29-32] is considered as a explanation for the high polymerisation activity displayed by this zinc-*N*-heterocyclic carbene complex, but ultimately rejected on the grounds of the fact that the polymer produced employing the zinc-*N*-heterocyclic carbene catalyst is heterotactic in nature - a test reaction revealed that isotactic enriched polymer is produced from D,L-lactide when the polymerisation is effected by the free *N*-heterocyclic carbene in the presence of benzyl alcohol initiator.

4.2: Phenoxide and Amide Supported Zinc Species

We decided to conduct an investigation into the reaction of dimethylzinc with a series of related imidazolium phenoxide species prepared via the reaction of 1,3-bis-(2,4,6-trimethylphenyl)-imidazol-2-ylidene (IMes) with one, two, and three equivalents of 2,4,6-trimethylphenol (MesOH). The reaction of the organozinc reagent with a single equivalent of 1,3-bis-(2,4,6-trimethylphenyl)-imidazolium 2,4,6-trimethylphenoxide ([IMesH][OMes]), generated *in situ* via the treatment of the imidazolium phenoxide:phenol adduct **3** with IMes, provides the monomeric

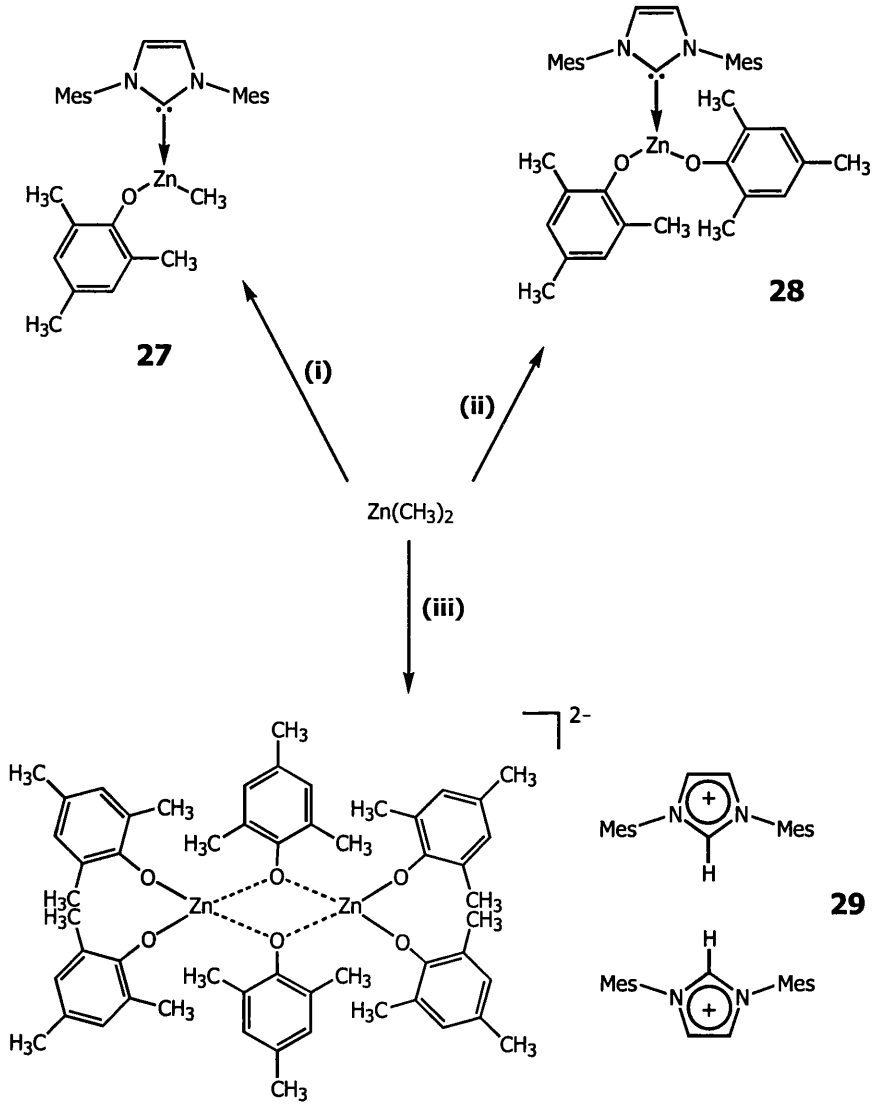

Scheme 4.4: Reaction of dimethylzinc with a series of imidazolium phenoxide species **(i)** 1,3-bis-(2,4,6-trimethylphenyl)-imidazol-2-ylidene and imidazolium phenoxide:phenol adduct **3**, toluene; **(ii)** imidazolium phenoxide:phenol adduct **3**, toluene; **(iii)** imidazolium phenoxide:phenol adduct **3** and 2,4,6-trimethylphenol, toluene

N-heterocyclic carbene-zinc(II)-phenoxide metal-alkyl species **27** (Scheme 4.4). The analogous reaction between the basic organometallic metal source compound and the imidazolium phenoxide:phenol adduct **3** yields the *N*-heterocyclic carbene ligated zinc(II)-bisphenoxide compound **28** (Scheme 4.4). Stoichiometric reaction of the organozinc reagent with a single equivalent of [IMesH][OMes].2 HOMes, generated *in situ* via the treatment of the imidazolium phenoxide:phenol adduct **3** with MesOH, results in the phenoxide-bridged dimer **29** (Scheme 4.4).[iii]

NMR spectroscopic characterisation of **27** in C_6D_6 solution reveals this compound to be an imidazol-2-ylidene ligated methylzinc-phenoxide complex (Scheme 4.4). The ^{1}H-NMR resonance corresponding to the C(4/5)-H backbone hydrogen atoms of the imidazol-2-ylidene ligand is observed further upfield than anticipated, at a chemical shift of 5.99 ppm. The $^{13}C\{^1H\}$-NMR spectrum exhibits resonances consistent with the C(2) and C(4/5) carbon atoms of the heterocyclic core of an imidazol-2-ylidene-metal adduct at chemical shifts of 181.7 ppm and 122.0 ppm, respectively. The organometallic methyl substituent is observed within the ^{1}H- and $^{13}C\{^1H\}$-NMR spectra at -0.70 ppm and -13.5 ppm, respectively.

NMR spectroscopic analysis of compound **28** was performed in CD_2Cl_2 solution. A singlet consistent with the C(4/5)-H backbone hydrogen atom substituents of an imidazol-2-ylidene-metal species is observed within the ^{1}H-NMR spectrum at a chemical shift of 7.22 ppm. Furthermore, the $^{13}C\{^1H\}$-NMR spectrum exhibits resonances corresponding to the C(2) and C(4/5) carbons of an imidazol-2-ylidene ligand at 172.5 ppm and 124.1 ppm, respectively. The absence of acidic proton signals within the ^{1}H-NMR spectrum suggests that the organometallic reagent has doubly-deprotonated the imidazolium phenoxide:phenol adduct **3** (Scheme 4.4).

NMR spectroscopic characterisation of compound **29** was undertaken in CD_3OD solution. This product is identified as an imidazolium salt species on the basis of the chemical shifts of its C(2) and C(4/5) carbon atom $^{13}C\{^1H\}$-NMR resonances;

[iii] We have isolated crystals of the imidazolium trisphenoxide-zincate(II) phenoxide-bridged dimer **29** from the reaction of *N*-heterocyclic carbene-zinc(II)-bisphenoxide **28** with propylene carbonate.

which are observed at 139.3 ppm and 130.2 ppm respectively. Most notably, the ^{1}H-NMR spectrum of this product lacks a resonance corresponding to C(4/5)-H backbone hydrogen atoms of the imidazolium cation. Denk *et al.* have observed H/D exchange of the C(4/5)-H backbone hydrogen atoms of imidazol-2-ylidenes in d_6-DMSO solution.[33] The ^{1}H-NMR spectrum of product **29** was subsequently recorded in CH_3OH solution in order to eliminate H/D exchange; the C(4/5)-H backbone hydrogen atom resonance is then clearly visible at 7.97 ppm.[ℵ]

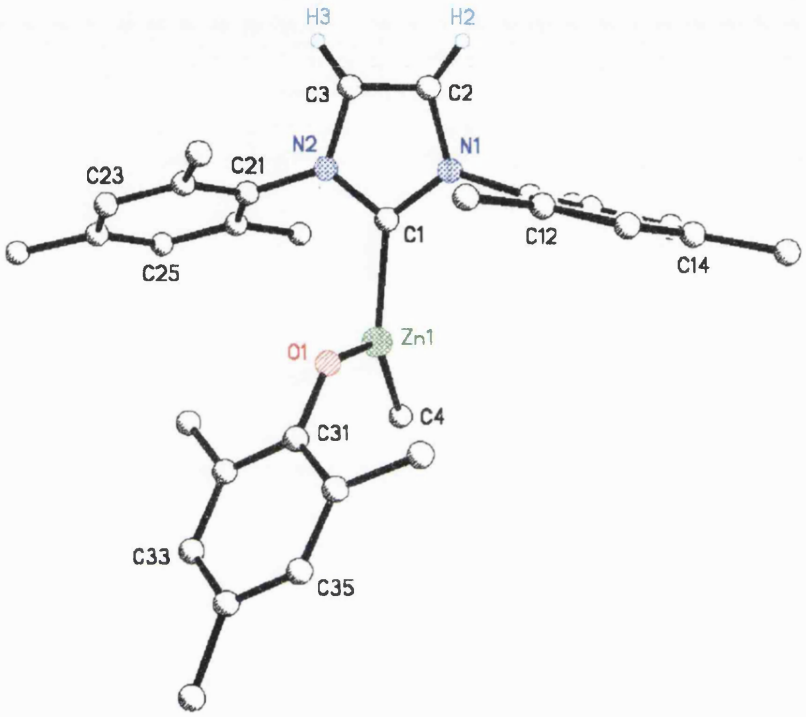

Figure 4.2: Molecular structure of the imidazol-2-ylidene-zinc(II)-phenoxide methyl species **27** as determined by single crystal x-ray diffraction

Determination of the solid state molecular structure of compound **27** by single crystal x-ray diffraction analysis reveals this product to be an imidazol-2-ylidene-zinc(II)-phenoxide methyl species (Figure 4.2). The asymmetric unit incorporates a single molecule of this discrete monomeric coordination compound (Figure 4.2). The three-coordinate pseudo trigonal-planar zinc centre bears one IMes ligand, a

[ℵ] ^{1}H-NMR (400 MHz, CH_3OH/CD_3OD capillary): δ 2.10 (18H, s, IMes-H *ortho*- and *para*-C$\underline{H}_3$), 2.13 (18H, s, OMes *ortho*-C$\underline{H}_3$), 2.34 (9H, s, OMes *para*-C$\underline{H}_3$), 6.62 (4H, s, IMes-H *meta*-$\underline{H}$), 7.13 (6H, s, MesOH *meta*-$\underline{H}$), 7.97 (2H, s, IMes-H C(4/5)$\underline{H}$).

terminally bound phenoxide functionality and a methyl substituent (Figure 4.2). The imidazol-2-ylidene-zinc C(2)–Zn bond C1–Zn1 (Figure 4.2), at 2.035(2) Å, is shorter than that of 2.096(3) Å within the imidazol-2-ylidene:diethylzinc adduct crystallographically characterised by Arduengo *et al.*;[24] and comparable with that observed in the imidazol-2-ylidene:bis(pentamethylcyclopentadienyl)-zinc adduct prepared in the same laboratory (2.022(3) Å).[25] The zinc-terminal phenoxide Zn–O bond Zn1–O1 (Figure 4.2) measures 1.910(1) Å; and the zinc-methyl Zn–C bond Zn1–C4 (Figure 4.2) is determined to be 1.958(2) Å in length.

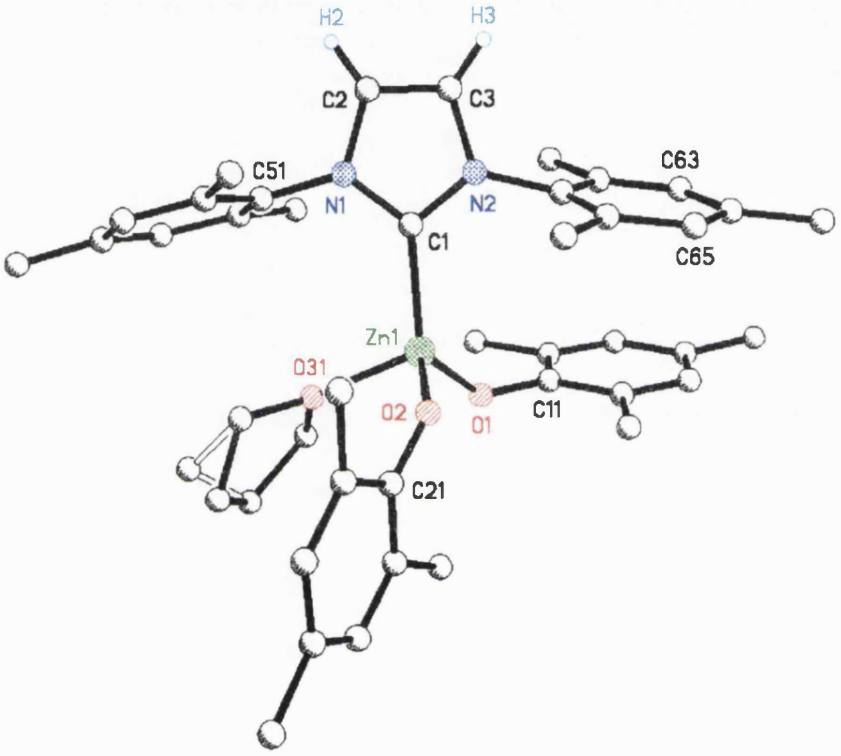

Figure 4.3: Molecular structure of the tetrahydrofuran solvate of imidazol-2-ylidene-zinc(II)-bisphenoxide species **28** as determined by single crystal x-ray diffraction

Crystals of compound **28** suitable for single crystal x-ray diffraction studies could not be obtained. However, the tetrahydrofuran solvate of this species crystallised from toluene solution to provide crystals suitable for x-ray diffraction analysis. The asymmetric unit is found to contain a single *N*-heterocyclic carbene-zinc(II) bisphenoxide tetrahydrofuran complex molecule and, additionally, two molecules of uncoordinated tetrahydrofuran solvent. The pseudo tetrahedral zinc atom bears one imidazol-2-ylidene ligand, two terminally bound phenoxides and a molecule

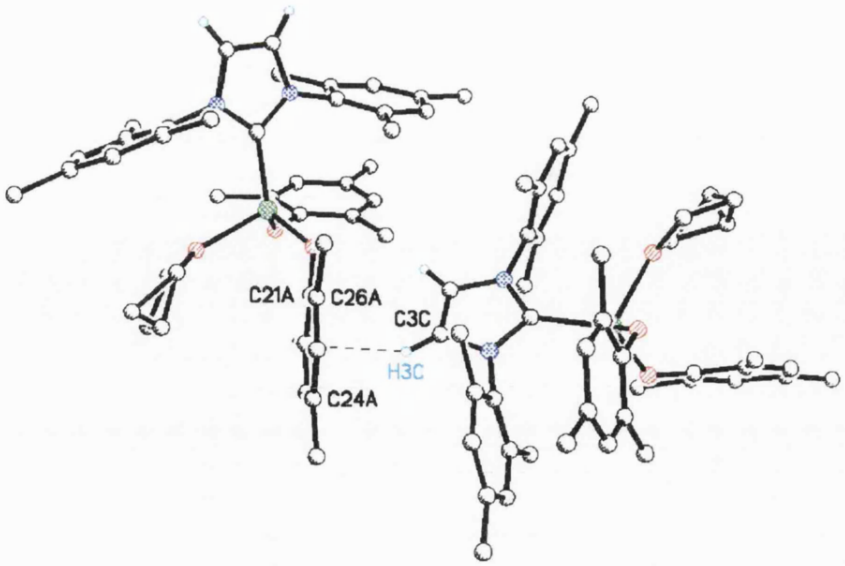

Figure 4.4: C–H·····π(arene) interactions in the supramolecular structure of the tetrahydrofuran solvate of imidazol-2-ylidene-zinc(II)-bisphenoxide species **28**

of coordinated tetrahydrofuran disordered over two positions. At 2.044(3) Å, the imidazol-2-ylidene-zinc C(2)–Zn bond C1–Zn1 (Figure 4.3) is shorter than that in 1,3-bis-(2,4,6-trimethylphenyl)-imidazol-2-ylidene:diethylzinc (2.096(3) Å),[24] and reminiscent of that within 1,3,4,5-tetramethyl-imidazol-2-ylidene:bis(pentamethylcyclopentadienyl)-zinc (2.022(3) Å);[25] which were crystallographically characterised by Arduengo *et al.* The zinc-phenoxide Zn–O bonds Zn1–O1 and Zn1–O2 (Figure 4.3) measure 1.895(2) Å and 1.914(2) Å, respectively. The zinc-coordinated tetrahydrofuran contact Zn1–O31 (Figure 4.3) is slightly longer, at 2.114(2) Å. The individual molecules of the tetrahydrofuran solvate of compound **28** associate via C–H·····π(arene) interactions (D = 3.184 Å, d = 2.327 Å and θ = 149.93°), [C3C–H3C·····centroid(C21A-C26A)] (Figure 4.4).

Single crystal x-ray diffraction analysis of compound **29** reveals this product is an imidazolium zincate dimer possessing a phenoxide-bridged dianion (Figure 4.5). The zinc centres within the dianion are pseudo tetrahedral and bear two terminal and two bridging phenoxide ligands. Purdy *et al.* have structurally characterised two related dimeric species $Na_2[Zn(O^tBu)_3]_2$ and $K_2[Zn(O^tBu)_3]_2$ incorporating an analogous alkoxide-bridged dianion.[34] The imidazolium cations are observed to

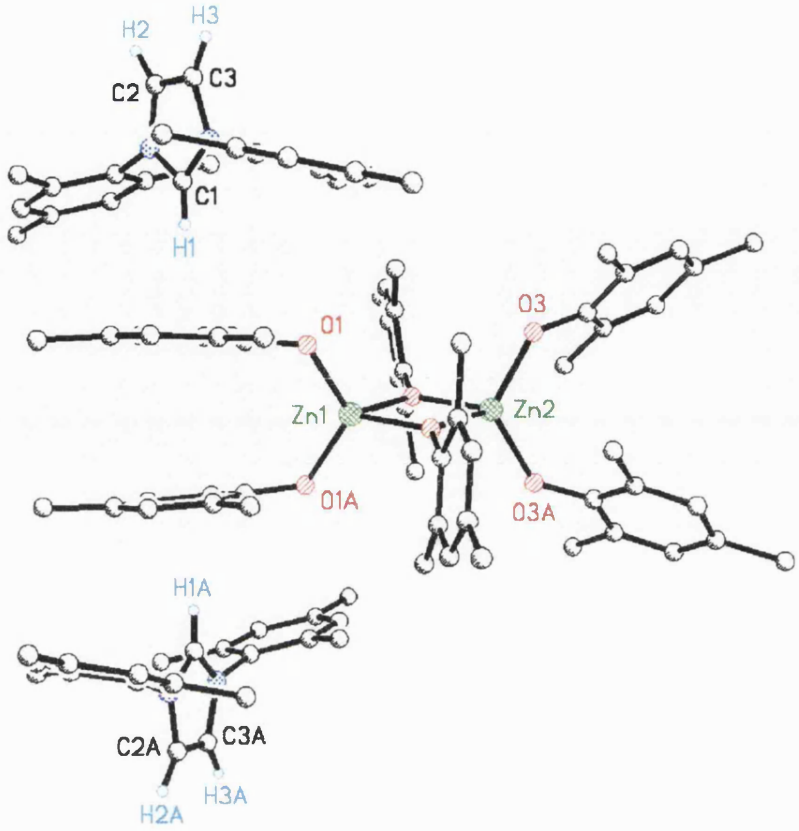

Figure 4.5: Solid state molecular structure of the dimeric imidazolium zincate species **29** as determined by x-ray diffraction (O1A, O3A, C2A, C3A, H1A, H2A and H3A are symmetry generated equivalents of O1, O3, C2, C3, H1, H2 and H3, respectively)

participate in C–H·····π(arene) interactions (*D* = 3.225 Å, *d* = 2.356 Å and *θ* = 172.83°) with the aromatic rings of two of the four terminal phenoxide ligands, [C1–H1·····centroid(C11-C16)] (Figure 4.5). Cowley *et al.* have recently reported the structural characterisation of a number of C–H·····π(arene) interactions between imidazolium cations and aromatic cyclic hydrocarbon anions:[35, 36] the shortest of which are the charge assisted C–H·····π(arene) interactions observed within the bisimidazolium cyclopentadienide cation (*D* = 3.086(8) Å, *d* = 2.295(9) Å and *θ* = 162.4(5)°).[35] There is some disorder in the two terminal phenoxide ligands in **29** that do not participate in C–H·····π(arene) interactions. The metrical parameters of the cations are consistent with those found for other imidazolium species:[27, 37-39] with N(1)–C(2)–N(3) angles of 108.8(4)°, and N–C(2) bonds of 1.320(6) Å and 1.326(6) Å (c.f. [IMesH][Cl][40] and compounds **1-5**, **8** and **9** in Chapter Two).

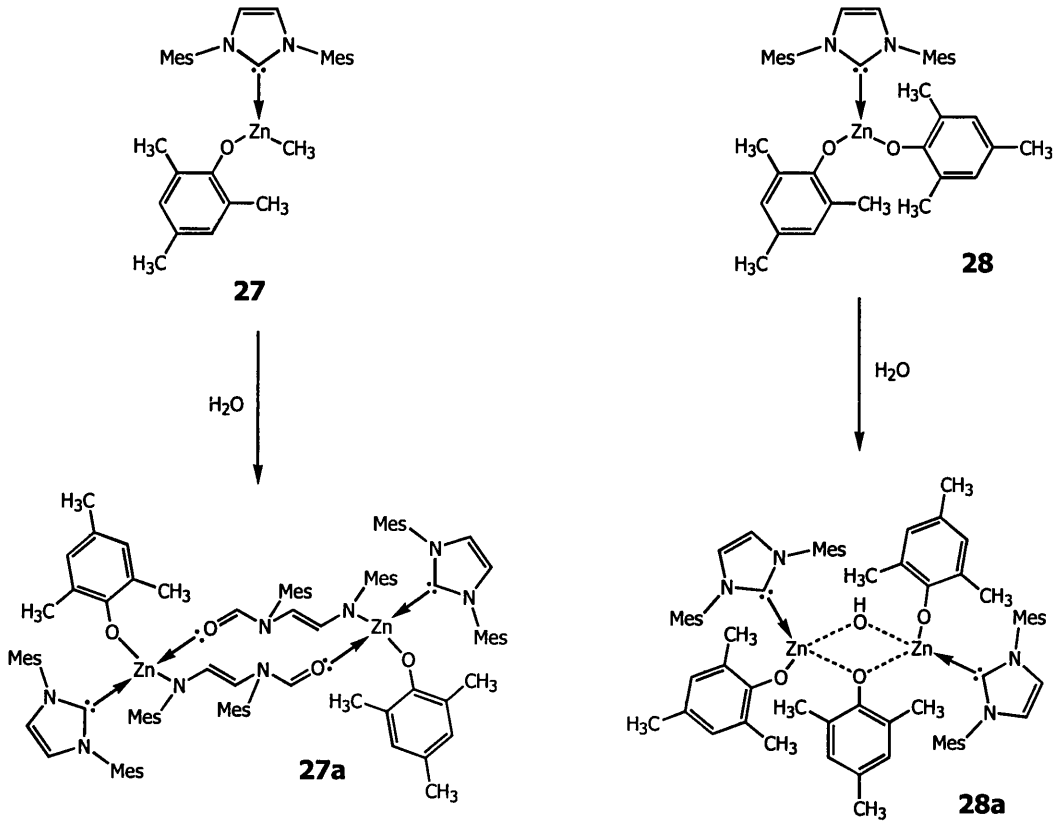

Scheme 4.5: Hydrolysis of *N*-heterocyclic carbene-zinc(II) terminal phenoxide species **27** and **28** to provide the dimeric compounds **27a** and **28a**, respectively

Crystalline samples of hydrolysis products **27a** and **28a** have been isolated from dilute toluene solutions of compounds **27** and **28**, respectively (Scheme 4.5). The imidazol-2-ylidene ligated methylzinc-phenoxide **27** seems to be more susceptible to hydrolysis than the *N*-heterocyclic carbene-zinc(II)-bisphenoxide complex **28**: significant quantities of **27a** were isolated, while only a few crystals of **28a** were recovered. The ring-opened imidazol-2-ylidene-bridged dimer **27a** could not be characterised via NMR spectroscopy since it is insoluble in both C_6D_6 and d_8-tetrahydrofuran, and reacts with $CDCl_3$, CD_2Cl_2 and d_5-pyridine. The absence of a molecular ion (M^+) peak in the mass spectrum of **27a** reveals that this species disintegrates under fast-atom bombardment - a fragment originating from the ring-opened imidazol-2-ylidene ligand is, however, observed at a mass/charge (*m/z*) ratio of 322.2. This species was unambiguously identified via single crystal x-ray diffraction. The hydroxy-bridged species **28a** is not readily soluble in C_6D_6 and decomposes on gentle warming: insufficient sample remained for further attempts at NMR analysis - **28a** was therefore also identified by single crystal diffraction.

The reaction of compound **27** with water presumably results in the evolution of methane and formation of the related *N*-heterocyclic carbene-zinc(II)-phenoxide hydroxy intermediate. The hydroxide functionality could then be delivered to the imidazol-2-ylidene and attack the out-of-plane p-orbital at the carbene centre in much the same way as recently reported for alkyl and carbonyl substituents.[41-43] This is consistent with the formulation of the ring-opened *N*-heterocyclic carbene ligand (Scheme 4.5 and Figure 4.6). The vacant coordination site is subsequently occupied by an imidazol-2-ylidene ligand scavenged from another zinc centre. We have subsequently isolated compound **27a** from the reaction of dimethylzinc with two equivalents of 1,3-bis-(2,4,6-trimethylphenyl)-imidazol-2-ylidene and a single equivalent of 2,4,6-trimethylphenol.

On the reaction of compound **28** with water, one of the phenoxide ligands within this species is exchanged for a hydroxide functionality to yield **28a**. We suggest that compound **28** is analogous in structure to this hydroxy-bridged dimer. The observed decomposition of this product on gentle warming in C_6D_6 is attributed to the ring-opening of one of the imidazol-2-ylidene ligands within this compound by the bridging hydroxide substituent.

Single crystal x-ray diffraction analysis reveals that both of the zinc centres in the ring-opened imidazol-2-ylidene-bridged *N*-heterocyclic carbene-zinc-phenoxide dimer **27a** possess pseudo tetrahedral geometries (Figure 4.6). At 2.040(2) Å, the imidazol-2-ylidene-zinc C(2)–Zn bond C1–Zn1 is comparable in length to those within **27** and **28**; 2.035(2) Å and 2.044(3) Å, respectively. The zinc-terminal phenoxide Zn–O bond Zn1–O1 (Figure 4.6) measures 1.914(2) Å; comparable with the zinc-terminal phenoxide Zn–O lengths in **27** and **28**. At 2.155(2) Å, the zinc-carbonyl Zn–O distance Zn1–O2A (Figure 4.6) is longer than the covalent zinc-phenoxide Zn–O bond Zn1–O1 (1.914(2) Å). At 1.245(3) Å, consistent with the double bond character of the aldehyde C–O bond, C6–O2 (Figure 4.6) is much shorter than the O–C(ipso) bond of the phenoxide ligand, O1–C101 (Figure 4.6), which measures 1.326(3) Å. In line with conservation of the C(4)=C(5) double bond, C4 and C5 (Figure 4.6) are sp^2 hybridised; the N3–C4–C5 and C4–C5–N4 angles (Figure 4.6) equal 129.9(2)° and 119.1(2)° respectively, and furthermore

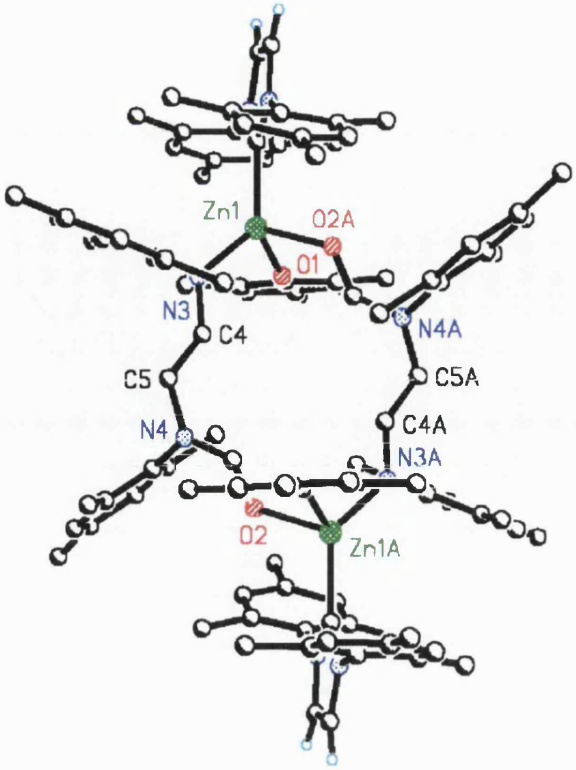

Figure 4.6: Molecular structure of the dimeric species **27a** as determined by x-ray diffraction (Zn1A, N3A, C4A, C5A, N4A and O2A are symmetry generated equivalents of Zn1, N3, C4, C5, N4 and O2, respectively)

the C4–C5 distance (Figure 4.6) measures 1.351(3) Å. The zinc-amide Zn–N bond Zn1–N3 (Figure 4.6) is determined to be 1.963(2) Å in length.

Single crystal x-ray structural characterisation of the dimeric hydrolysis product **28a** reveals that both of its zinc centres are pseudo tetrahedral in geometry. The imidazol-2-ylidene-zinc C(2)–Zn bonds C1–Zn1 and C101–Zn2, at 2.047(3) Å and 2.053(3) Å respectively, are shorter than that observed within the imidazol-2-ylidene:diethylzinc adduct (2.096(3) Å) structurally characterised by Arduengo *et al.*[24] One of the imidazol-2-ylidene aryl ring substituents is disordered over two positions; and the hydrogen of the bridging hydroxide is disordered 50:50 over two positions H1A and H1B (Figure 4.7). In line with the greater steric demands of the bridging phenoxide relative to the hydroxide; the Zn1–O2 and Zn2–O2 distances (Figure 4.7), at 2.086(2) Å and 2.058(2) Å respectively, are longer than Zn1–O4 and Zn2–O4 (Figure 4.7) - 1.935(2) Å and 1.958(2) Å, respectively.

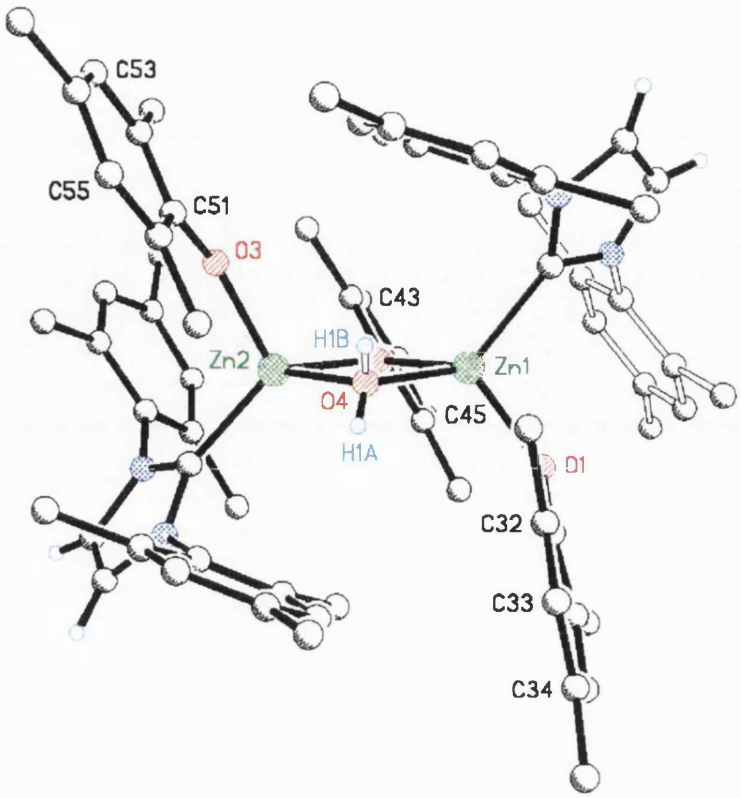

Figure 4.7: Molecular structure of the hydroxy-bridged dimeric hydrolysis product **28a** as determined by single crystal x-ray diffraction

In order to further evaluate the synthetic utility of the hydrogen-bonded organic metal-*N*-heterocyclic carbene complex precursors described in Chapter Two in the preparation of imidazol-2-ylidene ligated zinc(II) coordination compounds; we decided to investigate the *in situ* deprotonation of imidazolium phenoxide salt **9** and the imidazol-2-ylidene:amine adduct **15** by dimethylzinc. The stoichiometric reaction of the imidazolium phenoxide salt **9** with one equivalent of dimethylzinc provides the *N*-heterocyclic carbene ligated methylzinc(II)-phenoxide species **30** (Scheme 4.6). The reaction of a single equivalent of the neutral hydrogen-bonded imidazol-2-ylidene:amine adduct **15** with one equivalent of dimethylzinc yields the imidazol-2-ylidene ligated methylzinc(II)-amide **31** (Scheme 4.6).

NMR spectroscopic analysis of the *N*-heterocyclic carbene ligated methylzinc(II)-phenoxide complex **30** was undertaken in C_6D_6 solution. The imidazol-2-ylidene C(4/5)-H backbone hydrogen atom resonance is observed at a chemical shift of

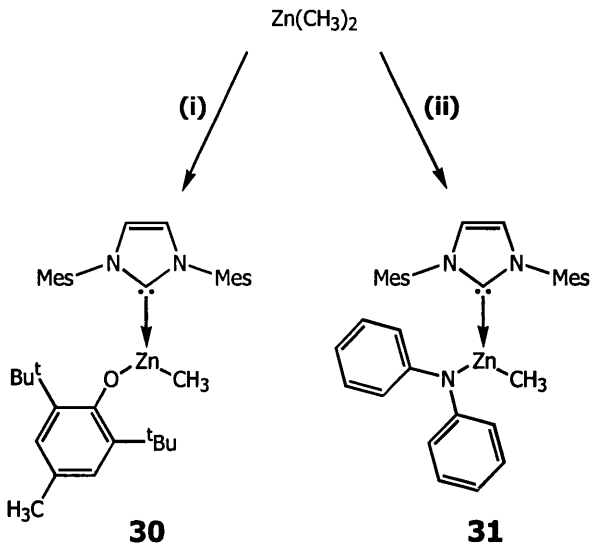

Scheme 4.6: Reaction of dimethylzinc with hydrogen-bonded organic metal-*N*-heterocyclic carbene complex precursor species
(i) imidazolium phenoxide salt **9**, toluene;
(ii) imidazol-2-ylidene:amine adduct **15**, toluene

5.98 ppm in the ^{1}H-NMR spectrum of compound **30**: the ^{1}H-NMR spectrum of the analogous terminal phenoxide **27** displays a singlet corresponding to the C(4/5)-H backbone hydrogen atoms of the imidazol-2-ylidene ligand at 5.99 ppm. As is the case in the ^{13}C{^{1}H}-NMR spectrum of compound **27**; the C(2) and C(4/5) carbon atom resonances are observed at chemical shifts indicative of the heterocyclic core of an imidazol-2-ylidene-metal adduct, at 180.3 ppm and 122.6 ppm respectively. The organometallic methyl substituent is observed within the ^{1}H- and ^{13}C{^{1}H}-NMR spectra at -0.78 ppm and -11.1 ppm, respectively.

NMR spectroscopic analysis of compound **31** was undertaken in CD_3OD solution. Vigorous methane evolution was observed on the addition of CD_3OD to **31**, which accounts for the absence of signals corresponding to the organometallic methyl substituent in the ^{1}H- and ^{13}C{^{1}H}-NMR spectra. The ^{1}H-NMR spectrum lacks a C(4/5)-H backbone hydrogen atom resonance: the absence of such a resonance is attributed to H/D exchange such as that observed in compound **29**. Furthermore, the ^{13}C{^{1}H}-NMR spectrum does not include a C(4/5) carbon atom signal. The ^{1}H-NMR spectrum recorded in CH_3OH solution at 400 MHz displays a singlet assigned as the C(4/5)-H backbone hydrogen atom resonance at a chemical shift

of 7.98 ppm. The $^{13}C\{^{1}H\}$-NMR spectrum recorded in CD_3OD incorporates a resonance corresponding to the C(2) carbon of a cationic imidazolium species at a chemical shift of 139.6 ppm. On closer inspection, the available ^{1}H- and $^{13}C\{^{1}H\}$-NMR data bears a remarkable resemblance to that obtained from the spectroscopic analysis of compound **21** in CD_3OD. On this basis, we suggest that the reaction of **31** with CD_3OD generates methane, diphenylamine, the methoxide salt of the *N*-heterocyclic carbene ligand, and $Zn(OCD_3)_2$. Indeed, the components present in solution can be identified as diphenylamine and the methoxide salt of the *N*-heterocyclic carbene via comparison of the available NMR data with that obtained from CH_3OH solutions of diphenylamine[∂] and the free imidazol-2-ylidene.[§]

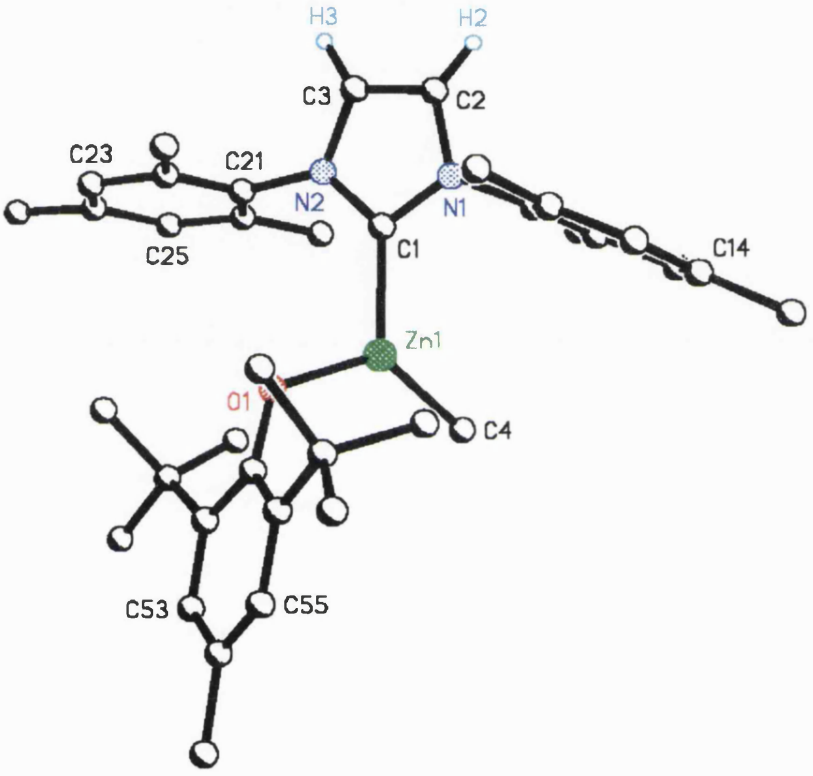

Figure 4.8: Representation of the molecular structure of the imidazol-2-ylidene-zinc(II)-phenoxide methyl species **30** as determined by single crystal x-ray diffraction

[∂] ^{1}H-NMR (400 MHz, CH_3OH/CD_3OD capillary): δ 6.70–6.80 (2H, t, $J_{(H-H)}$ = 7.2 Hz, $HNPh_2$ *para*-H), 6.94–7.04 (4H, d, $J_{(H-H)}$ = 7.6 Hz, $HNPh_2$ *ortho*-H), 7.07–7.18 (4H, t, $J_{(H-H)}$ = 7.6 Hz, $HNPh_2$ *meta*-H), 7.37 (1H, br s, $HNPh_2$ NH).

[§] ^{1}H-NMR (400 MHz, CH_3OH/CD_3OD capillary): δ 2.14 (12H, s, IMes-H *ortho*-CH_3), 2.35 (6H, s, IMes-H *para*-CH_3), 7.14 (4H, s, IMes-H *meta*-H), 8.00 (2H, s, IMes-H C(4/5)H).

Single crystal x-ray diffraction analysis confirms that compound **30** is indeed an imidazol-2-ylidene-zinc(II)-terminal phenoxide methyl species (Figure 4.8). The asymmetric unit contains one complete molecule of this three-coordinate zinc complex. The zinc centre Zn1 (Figure 4.8) is pseudo trigonal-planar in geometry. The imidazol-2-ylidene-zinc C(2)–Zn bond C1–Zn1 (Figure 4.8) is determined to be 2.041(2) Å in length, and compares well with that observed in the analogous *N*-heterocyclic carbene-zinc(II)-terminal phenoxide methyl species **27** (2.035(2) Å). The zinc-terminal phenoxide Zn–O bond Zn1–O1 (Figure 4.8) is 1.917(2) Å in length, which is comparable with the zinc-phenoxide Zn–O bond within **27**.

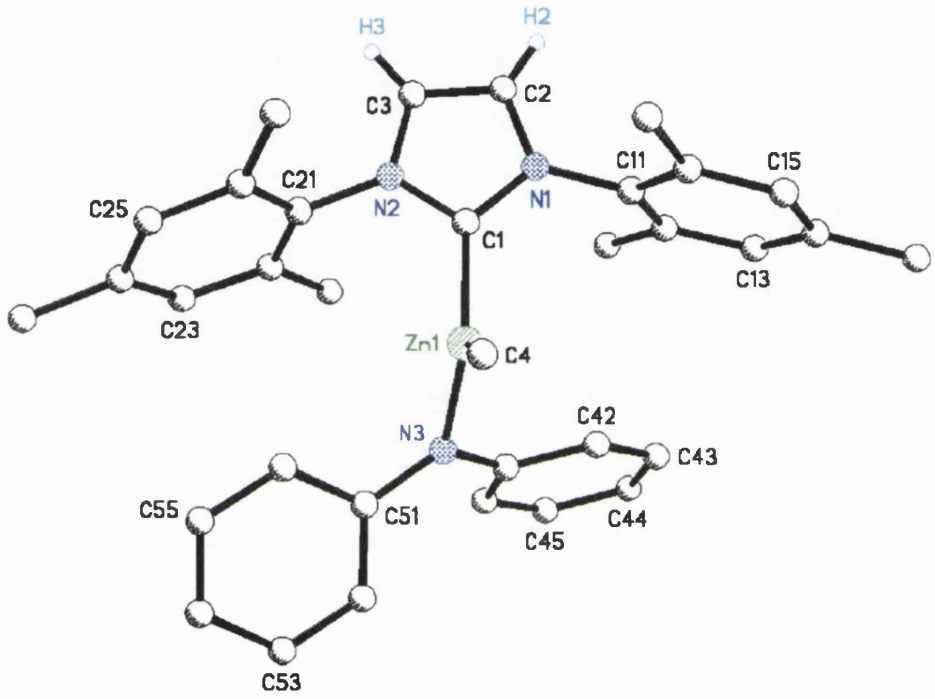

Figure 4.9: Representation of the molecular structure of the imidazol-2-ylidene-zinc(II)-amide methyl species **31** as determined by single crystal x-ray diffraction

Single crystal x-ray diffraction unambiguously identifies **31** as an *N*-heterocyclic carbene-zinc(II)-amide methyl species (Figure 4.9), in which the pseudo trigonal-planar three-coordinate zinc centre possesses an IMes ligand, a diphenylamide functionality and a methyl substituent (Figure 4.9). The imidazol-2-ylidene-zinc C(2)–Zn bond C1–Zn1 (Figure 4.9) is equal to 2.061(2) Å. The diphenylamide-zinc N–Zn bond N3–Zn1 (Figure 4.9) measures 1.971(2) Å, and is comparable in length to the zinc-amide N–Zn bond observed within **27a** (1.963(2) Å).

4.3: ε-Caprolactone Polymerisation

The formation of the hydrolysis product **28a** from the *N*-heterocyclic carbene-zinc(II)-bisphenoxide complex **28** seemed to imply that insertion into the zinc(II)-phenoxide bond is a possibility, and, along with the quite significant Lewis acidity of zinc centres,[24, 25] this prompted us to turn our attention towards the catalysis of coordination-insertion reactions such as ring-opening polymerisations.[5] It should be noted than zinc(II)-phenoxide species have previously been exploited in the catalysis of a number of ring-opening polymerisation processes.[11-13, 16, 17, 26, 44]

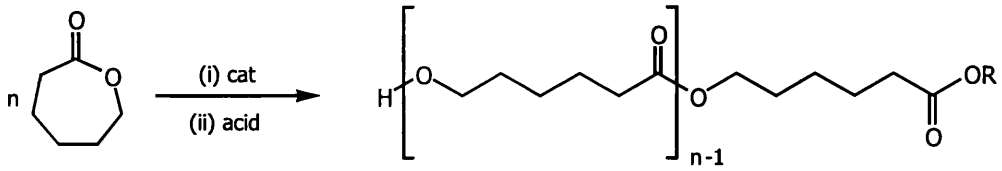

Scheme 4.7: Ring-opening polymerisation of ε-caprolactone

We decided to evaluate the *N*-heterocyclic carbene-zinc(II)-bisphenoxide complex **28**, [(IMes)Zn(OMes)$_2$], as an initiator in the ring-opening polymerisation of the cyclic ester ε-caprolactone (Scheme 4.7). The reaction conditions employed were adapted from those utilised in the aluminium alkoxide initiated polymerisation of ε-caprolactone, as reported by Lin *et al.*[45]

Our results indicate that compound **28** initiates the ring-opening polymerisation of ε-caprolactone (Scheme 4.7). At 50 °C, [(IMes)Zn(OMes)$_2$] converts all of the available monomer into poly(caprolactone) within 100 minutes (Table 4.1). NMR spectroscopic analysis of the polymer in $CDCl_3$ solution reveals that the chains are 2,4,6-trimethylphenoxy-terminated; confirming that polymerisation proceeds via insertion into the zinc(II)-phenoxide bond (Scheme 4.8).[1] The average number of repeat units per chain can be determined via the integration of the most acidic methylene protons within the polymer backbone relative to those at the hydroxy terminus [45] The number average molecular weight (M_n) of the isolated polymer was determined to be 25590 g mol^{-1} by means of this NMR end-group analysis methodology:[45] in this case, M_n (^{1}H-NMR) should equal 11516 g mol^{-1} if both zinc(II)-phenoxide sites are active and a living polymerisation mechanism is in

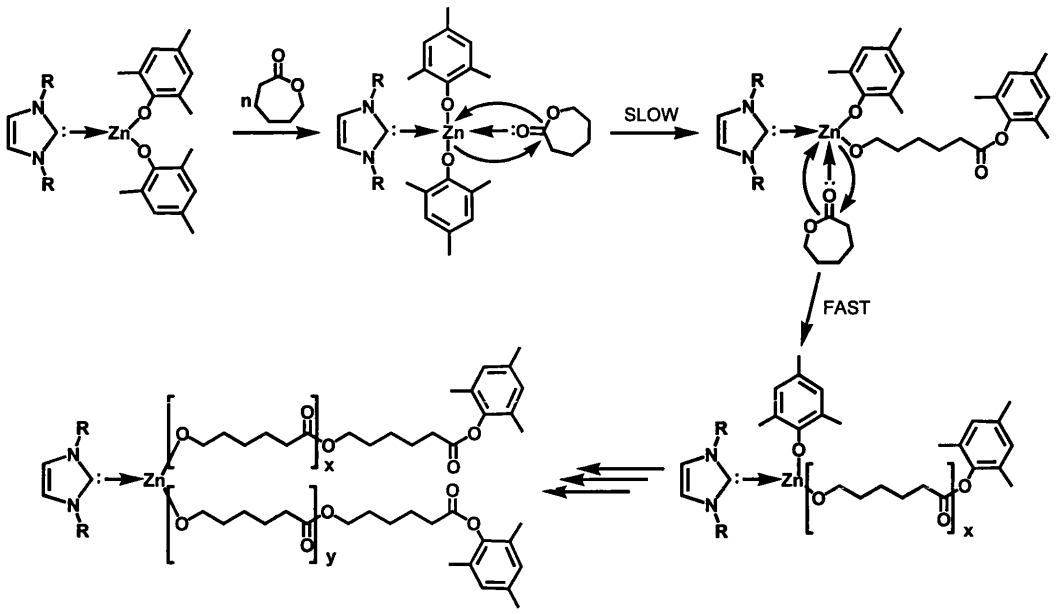

Scheme 4.8: Proposed mechanism for the ring-opening polymerisation of ε-caprolactone initiated by [(IMes)Zn(OMes)$_2$]

operation. GPC analysis of the polymer was undertaken in tetrahydrofuran and provided values of M_w (GPC) and M_n (GPC), relative to polystyrene standards, of 80307 g mol^{-1} and 32589 g mol^{-1}, respectively; from which a Polydispersity Index (PDI) of 2.464 was calculated. We attribute the observed higher than anticipated average molecular weight and broad molecular weight distribution to slow initial catalyst activation and rapid subsequent propagation (Scheme 4.8). The difficult initial insertion of the monomer into the zinc(II)-phenoxide bond, consistent with slow hydrolysis of **28** to yield **28a**, provides an active zinc(II)-alkoxide bond into which all subsequent insertions are rapid (Scheme 4.8).

In an effort to obtain polymers with narrower molecular weight distributions, we decided to attempt to activate the pre-catalyst species [(IMes)Zn(OMes)$_2$] prior to addition of the monomer. Alcohol was added to the pre-catalyst with the aim of substituting one or more of the phenoxide ligands for an alkoxide functionality (Scheme 4.9 - Pathway A). Toluene solutions of the pre-catalyst **28** and one, two and eight equivalents of the alcohol initiator isopropanol were maintained at 50 °C for 900 minutes, 900 minutes and 1530 minutes, respectively (Table 4.1), in order to accelerate the rate of alcoholysis. Addition of ε-caprolactone to these activated

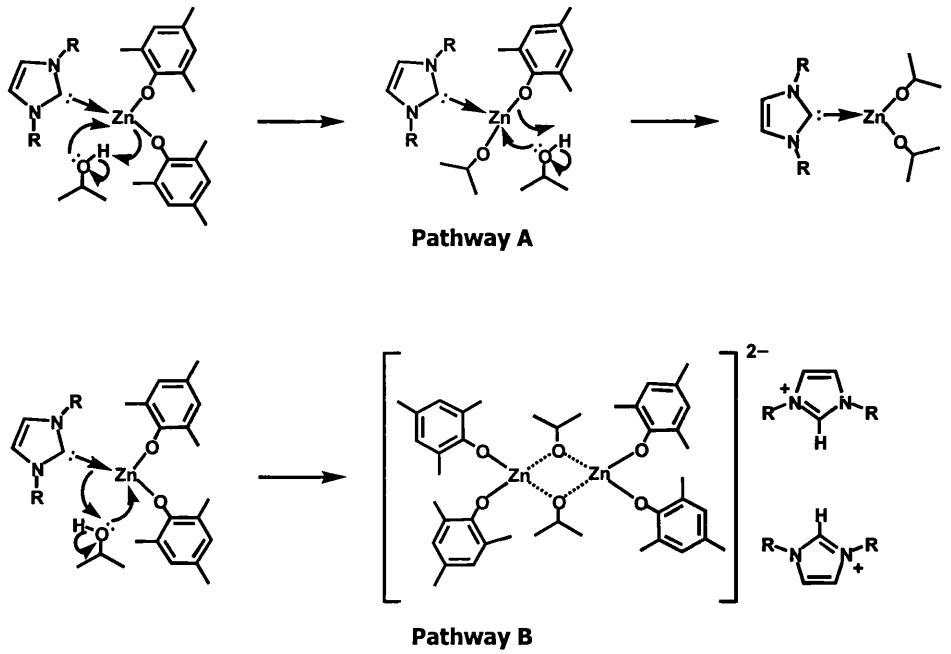

Scheme 4.9: Proposed pathways for the activation of the [(IMes)Zn(OMes)$_2$] pre-catalyst via isopropanol alcoholysis

pre-catalyst solutions subsequently resulted in the complete consumption of all the available monomer within a period of 100 minutes. The polymers isolated from these reactions indeed display narrower molecular weight distributions than is the case in the absence of isopropanol (Table 4.1). The number average molecular weights of these polymers determined by NMR end-group analysis M_n (^{1}H-NMR) equal 19350 g mol^{-1}, 10447 g mol^{-1}, and 2685 g mol^{-1}, respectively; which more closely resemble the values of 22860 g mol^{-1}, 11460 g mol^{-1}, and 2910 g mol^{-1}, respectively (Table 4.1), predicted assuming a living polymerisation mechanism.

The fact that the activation of the pre-catalyst does not require an induction period and occurs at room temperature suggests that the alcoholysis reaction proceeds via Pathway B rather than Pathway A (Scheme 4.9). Compounds **16** and **21** (Chapter Three), and **31**, display similar reactivity with CD_3OD. The addition of alcohol initiator to the pre-catalyst [(IMes)Zn(OMes)$_2$] generates an imidazolium zincate dimer, which incorporates an alkoxide-bridged dianion: this structural analogue to compound **29** deaggregates in the presence of ε-caprolactone monomer to provide the catalytically active monomeric imidazolium alkoxide ligated zincate species (Scheme 4.10). The subsequent insertion of the monomer into the zinc alkoxide

Temperature	Alcohol Initiator	Activation Time	Reaction Time	Isolated Yield (% of Theoretical)	Mn (^{1}H-NMR)	Mw (GPC)	Mn (GPC)	PDI
323K	——	——	100 mins	2.71 g (100%)	25590	80307	32589	2.464
323K	1 eq	900 mins	100 mins	2.68 g (100%)	19350	45017	26260	1.714
323K	2 eq	900 mins	100 mins	2.59 g (96%)	10447	22014	14596	1.508
323K	8 eq	1530 mins	100 mins	2.48 g (92%)	2685	5199	4018	1.294
323K	2 eq	——	100 mins	2.61 g (97%)	10219	22411	12416	1.805
323K	2 eq	——	30 mins	2.69 g (100%)	9306	19678	15804	1.245
323K	8 eq	——	30 mins	1.47 g (55%)	2155	3866	3201	1.208
323K	2 eq	——	2.5 mins	1.75 g (65%)	6566	14171	12442	1.139
323K	2 eq	——	4 mins	2.01 g (75%)	8050	18268	15406	1.186
323K	2 eq	——	10 mins	2.60 g (97%)	7479	21380	16940	1.262
298K	2 eq	——	100 mins	2.28 g (85%)	6566	13408	10971	1.222
298K	2 eq	——	120 mins	2.55 g (95%)	11588	20603	17257	1.194
298K	8 eq	——	50 mins	2.35 g (87%)	2685	5159	4212	1.225
298K	8 eq	——	60 mins	2.41 g (90%)	973	4778	3849	1.241

Table 4.1: Summary of the various catalytic runs completed exploiting [(IMes)Zn(OMes)$_2$] as the catalyst or pre-catalyst

bond of this species is confirmed by NMR spectroscopic analysis of the polymers produced; all of which are isopropoxy-terminated. The number of equivalents of alcohol initiator added to [(IMes)Zn(OMes)$_2$] during catalyst pre-activation has an influence on the length of the polymer chain, and therefore the average molecular

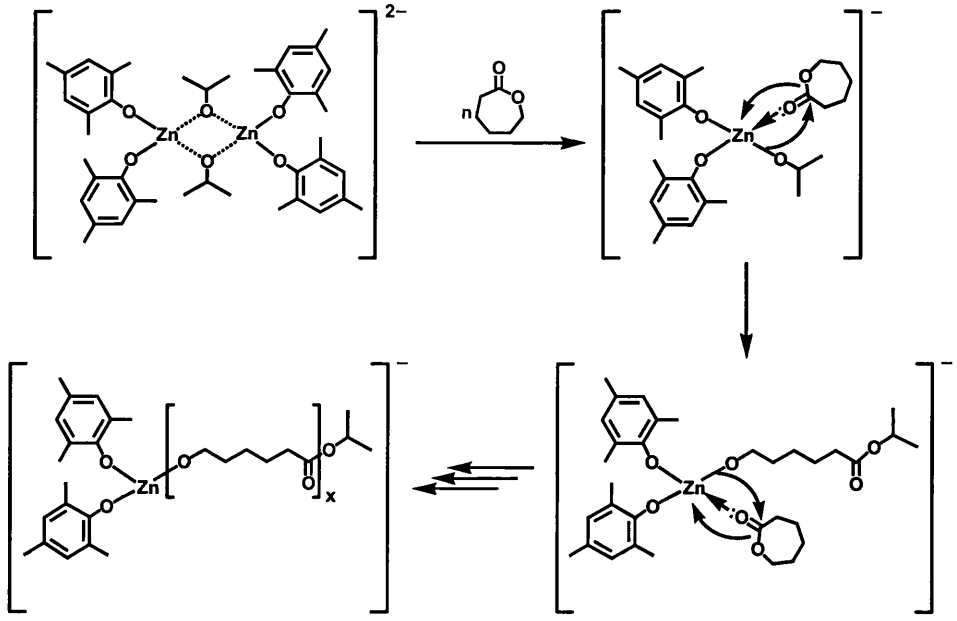

Scheme 4.10: Proposed mechanism for the ring-opening polymerisation of ε-caprolactone initiated by an *in situ* generated zinc-alkoxide catalyst

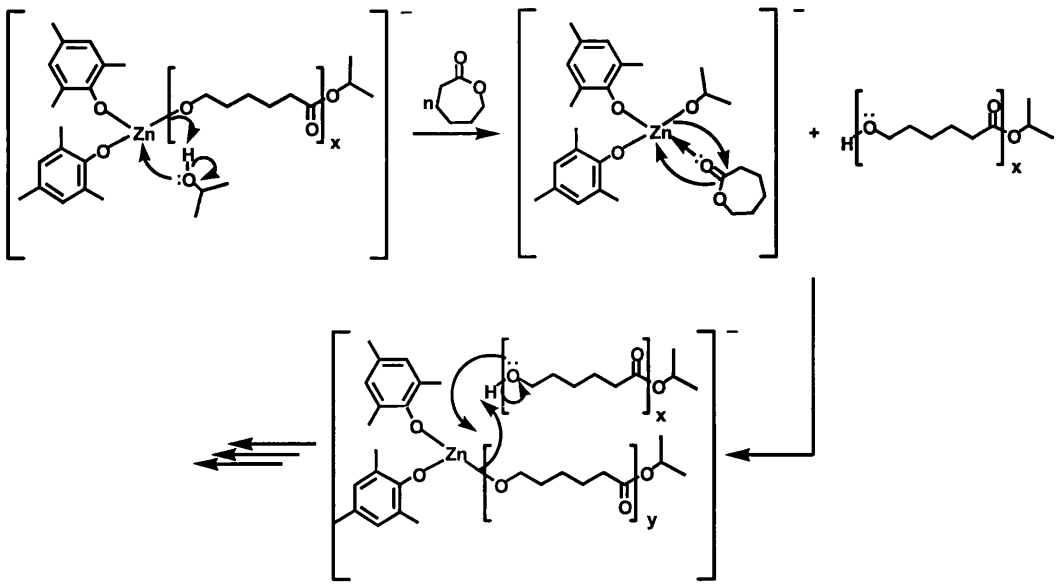

Scheme 4.11: Reversible chain-transfer during the ring-opening polymerisation of ε-caprolactone initiated by an *in situ* generated zinc-alkoxide catalyst

weights of the poly(caprolactone) produced (Table 4.1). In polymerisations that have reached completion; the polymer chain length and average molecular weight of the isolated polymer is directly proportional to the number of equivalents of alcohol present in solution. This is consistent with an immortal polymerisation process:[45-47] the growing chains are reversibly terminated as a result of their reaction with alcohol or a dormant chain (Scheme 4.11). The molecular weight of the poly(caprolactone) isolated depends on the relative concentrations of the ε-caprolactone monomer and the alcohol initiator; and therefore a greater number of chains can be propagated than would be anticipated from a consideration of the relative concentrations of the monomer and the zinc initiator. In order for narrow molecular weight polymers to be produced via immortal polymerisation reactions the rate of chain transfer must exceed the rate of propagation.[48-55]

The activity of the *in situ* generated catalytically active species $[Zn(OMes)_2(OR)]^-$ in the ring-opening homopolymerisation of ε-caprolactone is attributed to the high concentration of electron density at the zinc centre. Even though this would not assist the coordination of monomer to the zinc centre, it has been suggested that it leads to an enhancement in the rate of the insertion step.[56-58] Furthermore, we propose that increased electron density at the zinc centre, and the rapid exchange

of growing polymer chains at the metal centre, reduces the likelihood of back-coordination of the growing polymer chain to the initiator species. Breakdown of the polymer via macrocycle formation is therefore not a problem associated with this system. However, we recognise that since the number of propagating chains present can exceed the number of metal initiator molecules present - depending on the quantity of alcohol introduced into the system in the catalyst pre-activation stage - interchain transesterification may be prevalent.

4.4: Conclusions

We have prepared a series of phenoxide and amide supported zinc species by the *in situ* deprotonation of hydrogen-bonded organic metal-*N*-heterocyclic carbene complex precursors described in Chapter Two. Compounds **27** and **28** undergo hydrolysis to **27a** and **28a**, respectively, in toluene solution. NMR spectroscopic characterisation of **29** is complicated by H/D exchange of the C(4/5)-H backbone hydrogen atoms of the imidazolium cation. *N*-heterocyclic carbene-zinc-amide methyl species **31** reacts with CD_3OD to provide diphenylamine, the methoxide salt of the imidazol-2-ylidene ligand, and, presumably, $Zn(OCD_3)_2$.

Compound **28** has been exploited as both a catalyst and pre-catalyst in the ring-opening polymerisation of ε-caprolactone. Polymerisation reactions conducted in the presence of alcohol yield polymers with narrow molecular weight distributions and chain lengths proportional to the amount of alcohol introduced into the system during the pre-catalyst activation step. Catalyst pre-activation occurs immediately at room temperature suggesting that the catalytically active species is in fact an imidazolium zincate salt - compound **31** undergoes a similar rapid reaction with CD_3OD. The increased electron density at the zinc centre probably precludes the back-coordination of the growing polymer chain and subsequent degradation of the polymer via macrocycle formation. However, at high alcohol concentrations the degradation of the poly(caprolactone) polymer by interchain transesterification may represent a significant problem. We suggest that further research to ascertain the extent of these transesterification processes is warranted.

4.5: References

[1] J. M. Bruce, D. W. Farren, *Polymer*, **1965**, *6*, 509.
[2] J. M. Bruce, F. M. Rabagliati, *Polymer*, **1967**, *8*, 361.
[3] J. McMurry, *Organic Chemistry*, 4th, Brooks/Cole, London, **1996**,
[4] M. B. Smith, J. March, *March's Advanced Organic Chemistry: Reactions, Mechanisms, and Structure*, 5th, John Wiley & Sons, Inc, Chichester, **2001**,
[5] J. M. Bruce, S. J. Hurst, *Polymer*, **1966**, *7*, 1.
[6] K. Shimasaki, T. Aida, S. Inoue, *Macromolecules*, **1987**, *20*, 3076.
[7] M. H. Chisholm, J. K. Crandall, D. G. McCollum, M. Pagel, *Macromolecules*, **1999**, *32*, 5744.
[8] C. Billouard, S. Carlotti, P. Desbois, A. Deffieux, *Macromolecules*, **2004**, *37*, 4038.
[9] Y. Watanabe, T. Yasuda, T. Aida, S. Inoue, *Macromolecules*, **1992**, *25*, 1396.
[10] T. Sarbu, E. J. Beekman, *Macromolecules*, **1999**, *32*, 6904.
[11] D. J. Darensbourg, M. W. Holtcamp, *Macromolecules*, **1995**, *28*, 7577.
[12] D. J. Darensbourg, M. S. Zimmer, P. Rainey, D. L. Larkins, *Inorg. Chem.*, **1998**, *37*, 2852.
[13] D. J. Darensbourg, M. W. Holtcamp, G. E. Struck, M. S. Zimmer, S. A. Niezgoda, P. Rainey, J. B. Robertson, J. D. Draper, J. H. Reibenspies, *J. Am. Chem. Soc.*, **1999**, *121*, 107.
[14] D. J. Darensbourg, S. A. Niezgoda, J. D. Draper, J. H. Reibenspies, *Inorg. Chem.*, **1999**, *38*, 1356.
[15] D. J. Darensbourg, J. R. Wildeson, J. C. Yarbrough, J. H. Reibenspies, *J. Am. Chem. Soc.*, **2000**, *122*, 12487.
[16] D. J. Darensbourg, S. A. Niezgoda, J. D. Draper, J. H. Reibenspies, *J. Am. Chem. Soc.*, **1998**, *120*, 4690.
[17] D. J. Darensbourg, M. S. Zimmer, P. Rainey, D. L. Larkins, *Inorg. Chem.*, **2000**, *39*, 1578.
[18] D. J. Darensbourg, M. W. Holtcamp, *Coord. Chem. Rev.*, **1996**, *153*, 155.
[19] B. J. O'Keefe, M. A. Hillmyer, W. B. Tolman, *J. Chem. Soc.-Dalton Trans.*, **2001**, 2215.
[20] D. J. Darensbourg, J. R. Wildeson, J. C. Yarbrough, *Inorg. Chem.*, **2002**, *41*, 973.
[21] N. Yui, P. J. Dijkstra, J. Feijen, *J. Makromol. Chem.*, **1990**, *191*, 481.
[22] I. Barakat, P. Dubois, R. Jerome, P. Teyssie, *Macromolecules*, **1991**, *24*, 6542.
[23] M. H. Chisholm, E. E. Delbridge, *New J. Chem.*, **2003**, *27*, 1177.
[24] A. J. Arduengo, H. V. R. Dias, F. Davidson, R. L. Harlow, *J. Organomet. Chem.*, **1993**, *462*, 13.
[25] A. J. Arduengo, F. Davidson, R. Krafczyk, W. J. Marshall, M. Tamm, *Organometallics*, **1998**, *17*, 3375.

[26] D. Wang, K. Wurst, M. R. Buchmeiser, *J. Organomet. Chem.*, **2004**, *689*, 2123.
[27] A. J. Arduengo, R. L. Harlow, M. Kline, *J. Am. Chem. Soc.*, **1991**, *113*, 361.
[28] T. R. Jensen, L. E. Breyfogle, M. A. Hillmyer, W. B. Tolman, *J. Chem. Soc.-Chem. Commun.*, **2004**, 2504.
[29] E. F. Connor, G. W. Nyce, M. Myers, A. Mock, J. L. Hedrick, *J. Am. Chem. Soc.*, **2002**, *124*, 914.
[30] G. W. Nyce, T. Glauser, E. F. Connor, A. Mock, R. M. Waymouth, J. L. Hedrick, *J. Am. Chem. Soc.*, **2003**, *125*, 3046.
[31] G. W. Nyce, S. Csihony, R. M. Waymouth, J. L. Hedrick, *Chem.-Eur. J.*, **2004**, *10*, 4073.
[32] A. C. Sentman, S. Csihony, R. M. Waymouth, J. L. Hedrick, *J. Org. Chem.*, **2005**, *70*, 2391.
[33] M. K. Denk, J. M. Rodezno, *J. Organomet. Chem.*, **2001**, *617*, 737.
[34] A. P. Purdy, C. F. George, *Polyhedron*, **1994**, *13*, 709.
[35] C. D. Abernethy, C. L. B. Macdonald, J. A. C. Clyburne, A. H. Cowley, *J. Chem. Soc.-Chem. Commun.*, **2001**, 61.
[36] S. Filipponi, J. N. Jones, J. A. Johnson, A. H. Cowley, F. Grepioni, D. Braga, *J. Chem. Soc.-Chem. Commun.*, **2003**, 2716.
[37] A. J. Arduengo, H. V. R. Dias, R. L. Harlow, M. Kline, *J. Am. Chem. Soc.*, **1992**, *114*, 5530.
[38] V. Langer, K. Huml, G. Reck, *Acta Crystallogr. Sect. B-Struct. Commun.*, **1982**, *38*, 298.
[39] A. K. Abdulsada, A. M. Greenway, P. B. Hitchcock, T. J. Mohammed, K. R. Seddon, J. A. Zora, *J. Chem. Soc.-Chem. Commun.*, **1986**, 1753.
[40] A. J. Arduengo, S. F. Gamper, M. Tamm, J. C. Calabrese, F. Davidson, H. A. Craig, *J. Am. Chem. Soc.*, **1995**, *117*, 572.
[41] D. S. McGuinness, K. J. Cavell, *Organometallics*, **2000**, *19*, 4918.
[42] D. S. McGuinness, N. Saendig, B. F. Yates, K. J. Cavell, *J. Am. Chem. Soc.*, **2001**, *123*, 4029.
[43] D. S. McGuinness, B. F. Yates, K. L. J. Cavell, *Organometallics*, **2002**, *21*, 5408.
[44] M. H. Chisholm, J. C. Gallucci, H. H. Zhen, J. C. Huffman, *Inorg. Chem.*, **2001**, *40*, 5051.
[45] H. L. Chen, B. T. Ko, B. H. Huang, C. C. Lin, *Organometallics*, **2001**, *20*, 5076.
[46] M. Endo, T. Aida, S. Inoue, *Macromolecules*, **1987**, *20*, 2982.
[47] M. Akatsuka, T. Aida, S. Inoue, *Macromolecules*, **1995**, *28*, 1320.
[48] G. Odian, *Principles of Polymerization*, John Wiley & Sons, New York, **1991**, 538-540.
[49] A. Duda, *Macromolecules*, **1996**, *29*, 1399.
[50] J. Baran, A. Duda, A. Kowalski, R. Szymanski, S. Penczek, *Macromol. Rapid Commun.*, **1997**, *18*, 325.

[51] A. Kowalski, J. Libiszowski, A. Duda, S. Penczek, *Macromolecules*, **2000**, *33*, 1964.
[52] S. Penczek, T. Biela, A. Duda, *Macromol. Rapid Commun.*, **2000**, *21*, 941.
[53] T. M. Ovitt, G. W. Coates, *J. Polym. Sci. Pol. Chem.*, **2000**, *38*, 4686.
[54] Z. Zhong, S. Schneiderbauer, P. J. Dijkstra, M. Westerhausen, J. Feijen, *J. Polym. Environ.*, **2001**, *9*, 31.
[55] C. K. Williams, L. E. Breyfogle, S. K. Choi, W. Nam, V. G. Young, M. A. Hillmyer, W. B. Tolman, *J. Am. Chem. Soc.*, **2003**, *125*, 11350.
[56] T. Aida, M. Ishikawa, S. Inoue, *Macromolecules*, **1986**, *19*, 8.
[57] D. J. Darensbourg, J. C. Yarbrough, *J. Am. Chem. Soc.*, **2002**, *124*, 6335.
[58] D. A. Walker, T. J. Woodman, M. Schormann, D. L. Hughes, M. Bochmann, *Organometallics*, **2002**, *22*, 797.

Experimental Section

General Information

All manipulations were performed under a dry argon atmosphere using standard Schlenk-line and glovebox techniques.[1] Glassware was dried for several hours prior to use in an oven maintained at 130 °C. All solvents were distilled from the appropriate drying-agents under a nitrogen atmosphere, degassed and then stored under argon. Solid starting materials were dried *in vacuo* prior to subsequent reaction. 1,3-bis-(2,4,6-trimethylphenyl)-imidazol-2-ylidene (IMes) was prepared via a procedure adapted from the synthesis of a related imidazol-2-ylidene, as reported by Nolan *et al.*[2] 2,4,6-trimethylphenyl-copper(I) (CuMes) was obtained according to a published literature method.[3] 2,4,6-trimethylphenol (MesOH) was purchased from Lancaster and recrystallised from hexane prior to use. All other chemicals were used as supplied by Acros, Aldrich, Avocado, Fluka or Lancaster. Deuterated NMR solvents were purchased from Goss Scientific Ltd. and, where appropriate, dried before use.[4]

Characterisation Details

All NMR spectra were recorded at 293K. Chemical shifts are reported in units of ppm downfield of TMS. ^{1}H-NMR spectra were recorded on a Bruker Avance 300 MHz spectrometer or a Varian Mercury 400 MHz spectrometer. $^{13}C\{^{1}H\}$-NMR spectra were recorded on the same spectrometers at 75.5 MHz and 100 MHz, respectively. ^{19}F-NMR spectra were recorded on the Varian Mercury 400 MHz spectrometer at 376 MHz, or a Bruker WP 100 MHz Spectrometer at 94.2 MHz, and referenced to external $CFCl_3$ (δ 0.00). ^{31}P-NMR spectra were recorded on the Bruker Avance 300 MHz spectrometer at 122 MHz and referenced externally to 85% H_3PO_4 (δ 0.00). ^{1}H-NMR spectra were referenced to the chemical shifts of the residual protio solvent resonances (δ CD_3CN, 1.94; C_6D_6, 7.16; $CDCl_3$, 7.26; CD_2Cl_2, 5.32; d_6-DMSO, 2.50; CD_3OD, 3.31).[5] $^{13}C\{^{1}H\}$-NMR spectra were referenced to the chemical shifts of the residual solvent peaks (δ CD_3CN, 1.32; C_6D_6, 128.06; $CDCl_3$, 77.16; CD_2Cl_2, 53.80; d_6-DMSO, 39.52; CD_3OD, 49.00).[5]

Melting points were determined using an Electrothermal IA9200 Digital Melting Point Apparatus. Elemental analyses were performed by the University of Bath Microanalysis Service on an Exeter Analytical Inc. CE-440 Elemental Analyser. Results obtained for organic compounds were in good agreement with anticipated values when crystalline samples were submitted for analysis and in satisfactory agreement when microcrystalline samples or powders were examined. Elemental analyses for the metal complexes are generally within acceptable tolerances of the expected values considering many of these species are highly reactive and also extremely sensitive to oxygen and moisture; although in a few cases discrepancies between the calculated and observed values are considerable. Mass spectra were recorded by the University of Bath Mass Spectrometry Service on a Micromass Autospec spectrometer (FAB) and a Finnigan MAT 8340 spectrometer (CI/EI). A peak corresponding to the fragment IMes-Cu-IMes$^+$ is observed within the spectra of the neutral copper(I)-*N*-heterocyclic carbene species **16, 17** and **19-21**; a similar fragment has been observed by Danopoulos *et al.* in the mass spectrum (ES) of a pyridyl-sidearm functionalised *N*-heterocyclic carbene-silver(I) bromide.[6]

Solid-State Structure Determination

Single crystal x-ray diffraction data collection was carried out on an Enraf Nonius Kappa CCD diffractometer equipped with an Oxford Cryosystems cooling device. Crystals coated in perfluorinated ether oil were mounted on gas fibres and placed in a stream of cold nitrogen gas, with diffraction of the graphite-monochromated Mo-Kα radiation (λ=0.71073 Å) detected by means of an xyz area detector. Data acquisition was controlled by the Nonius COLLECT[7] software package. Unit cell determination and refinement were subsequently performed using DENZO[8] and SCALEPACK.[8] Structures were solved by direct methods, generally in sir92, sir97 or SHELXS-86,[9] and full-matrix least squares refinement performed using SHELXL-97.[10]

ε-Caprolactone Polymerisation

ε-Caprolactone polymerisation reactions were performed according to a published procedure.[11] ε-Caprolactone was distilled from calcium hydride and stored under argon over 4 Å molecular sieves. Glassware was rigorously flame dried prior to use. M_n of the polymers was ascertained by end-group analysis; the integration of the ^{1}H-NMR resonances corresponding to the repeat units relative to those of the polymer end-group, which provides the mean number of monomer units of known molecular weight that comprise each chain. The molecular weight distributions of the polymers were determined by Gel Permeation Chromatography; samples of the polymers were dissolved in tetrahydrofuran (0.01 g of polymer in 5.0 ml) and injected into a column of styrene divinylbenzene beads, maintained at 35 °C in a VE2585 Column Oven, via a Viscotek GPCMax VE2001 Control Module, elution was monitored with a VE3580 Refractive Index Detector.

Preparation of [IMes-H][OC_6H_5][HOC_6H_5] (1)

A warm toluene (30 mL) solution of phenol (0.21 g, 2.2 mmol) and IMes (0.30 g, 1.0 mmol) was filtered and allowed to cool slowly to room temperature. The product crystallised as yellow blocks suitable for x-ray diffraction, which were isolated by filtration, washed with hexane and dried *in vacuo*. Yield 0.18 g, 37% w.r.t. IMes. m.p. 168–172 °C. Elemental analysis: Calcd for $C_{33}H_{36}N_2O_2$: C, 80.45; H, 7.37; N, 5.69%. Found: C, 80.20; H, 7.36; N, 5.69%. ^{1}H-NMR (300 MHz, d_6-DMSO): δ 2.11 (12H, s, IMes-H *ortho*-C$\underline{H}_3$), 2.35 (6H, s, IMes-H *para*-C$\underline{H}_3$), 6.24–6.33 (2H, t, $^3J_{(H\text{-}H)}$=7.2 Hz, PhOH *para*-$\underline{H}$), 6.42–6.51 (4H, d, $^3J_{(H\text{-}H)}$= 8.4 Hz, PhOH *ortho*-$\underline{H}$), 6.84–6.94 (4H, dd, $^3J_{(H\text{-}H)}$=8.4 Hz, $^3J_{(H\text{-}H)}$=7.2 Hz, PhOH *meta*-$\underline{H}$), 7.20 (4H, s, IMes-H *meta*-$\underline{H}$), 8.26 (2H, s, IMes-H C(4/5)$\underline{H}$), 9.75 (1H, br s, IMes-H C(2)$\underline{H}$). ^{13}C-NMR (75.5 MHz, d_6-DMSO): δ 16.9 (IMes-H *ortho*-$\underline{C}$H$_3$), 20.7 (IMes-H *para*-$\underline{C}$H$_3$), 112.7 (PhOH *para*-$\underline{C}_{(arom)}$H), 117.1 (PhOH *ortho*-$\underline{C}_{(arom)}$H), 124.7 (IMes-H $\underline{C}$(4/5)H), 128.7 (PhOH *meta*-$\underline{C}_{(arom)}$H), 129.4 (IMes-H *meta*-$\underline{C}_{(arom)}$H), 131.1 (IMes-H *ipso*-$\underline{C}_{(arom)}$), 134.3 (IMes-H *para*-$\underline{C}_{(arom)}$), 140.6 (IMes-H *ortho*-$\underline{C}_{(arom)}$), 165.0 (PhOH *ipso*-$\underline{C}_{(arom)}$).

Preparation of [IMes-H][OC_6F_5][HOC_6F_5] (2)

Pentafluorophenol (0.30 g, 1.6 mmol) was dissolved in toluene (5 mL) by gentle warming and subsequently added to a warm toluene (10 mL) solution of IMes (0.25 g, 0.8 mmol). The reaction mixture was allowed to cool slowly to room temperature to yield a crop of colourless needles suitable for x-ray diffraction, which were isolated by filtration, washed with hexane and dried *in vacuo*. Yield 0.32 g, 58% w.r.t. IMes. m.p. 192–194 °C. Elemental analysis: Calcd for $C_{33}H_{26}N_2O_2F_{10}$: C, 58.93; H, 3.90; N, 4.17%. Found: C, 58.61; H, 3.90; N, 4.07%. ^{1}H-NMR (400 MHz, CD_2Cl_2): δ 2.11 (12H, s, IMes-H *ortho*-C*H*$_3$), 2.31 (6H, s, IMes-H *para*-C*H*$_3$), 6.98 (4H, s, IMes-H *meta*-*H*), 7.47 (2H, d, $^3J_{(H-H)}$=1.3 Hz, IMes-H C(4/5)*H*), 10.32 (1H, br s, IMes-H C(2)*H*). ^{13}C-NMR (100 MHz, CD_2Cl_2): δ 17.3 (IMes-H *ortho*-*C*H$_3$), 21.1 (IMes-H *para*-*C*H$_3$), 124.5 (IMes-H *C*(4/5)H), 129.9 (IMes-H *meta*-*C*$_{(arom)}$H), 134.5 (IMes-H *para*-*C*$_{(arom)}$). ^{19}F-NMR (94.2 MHz, CD_2Cl_2): δ -88.30—88.70 (dd, $^3J_{(F-F)}$ = 19.0 Hz, $^4J_{(F-F)}$ = 9.0 Hz, F_5C_6OH *ortho*-*F*), -91.68—92.32 (dd, $^3J_{(F-F)}$=22.0 Hz, $^3J_{(F-F)}$=19.0 Hz, F_5C_6OH *meta*-*F*), -103.57—104.23 (tt, $^3J_{(F-F)}$=22.0 Hz, $^4J_{(F-F)}$=9.0 Hz, F_5C_6OH *para*-*F*).

Preparation of [IMes-H][OMes][HOMes] (3)

A toluene (30 mL) solution of 2,4,6-trimethylphenol (0.27 g, 2.0 mmol) and IMes (0.30 g, 1.0 mmol) was heated to reflux, filtered and allowed to cool slowly to room temperature. The product crystallised as a crop of yellow needles suitable for x-ray diffraction, which were isolated by filtration, washed with hexane and dried *in vacuo*. Yield 0.29 g, 50% w.r.t. IMes. m.p. 197–200 °C. Elemental analysis: Calcd for $C_{39}H_{48}N_2O_2$: C, 81.21; H, 8.39; N, 4.86%. Found: C, 80.80; H, 8.36; N, 4.91%. ^{1}H-NMR (300 MHz, d_6-DMSO): δ 2.00 (12H, s, MesOH *ortho*-C*H*$_3$), 2.05 (6H, s, MesOH *para*-C*H*$_3$), 2.11 (12H, s, IMes-H *ortho*-C*H*$_3$), 2.35 (6H, s, IMes-H *para*-C*H*$_3$), 6.51 (4H, s, MesOH *meta*-*H*), 7.18 (4H, s, IMes-H *meta*-*H*), 8.22 (2H, s, IMes-H C(4/5)*H*). ^{1}H-NMR (300 MHz, CD_2Cl_2): δ 1.79 (12H, s, MesOH *ortho*-C*H*$_3$), 1.96 (12H, s, IMes-H *ortho*-C*H*$_3$), 2.04 (6H, s, MesOH *para*-C*H*$_3$), 2.37 (6H, s, IMes-H *para*-C*H*$_3$), 6.41 (4H, s, MesOH *meta*-*H*), 6.96 (4H, s, IMes-H *meta*-*H*), 7.21 (2H, s, IMes-H C(4/5)*H*), 11.32 (2H, br s, IMes-H C(2)*H* and MesOH O*H*). ^{13}C-NMR (100 MHz, d_6-DMSO): δ 17.0 (IMes-

H *ortho*-$\underline{C}H_3$), 17.4 (MesOH *ortho*-$\underline{C}H_3$), 20.3 (MesOH *para*-$\underline{C}H_3$), 20.7 (IMes-H *para*-$\underline{C}H_3$), 122.1 (MesOH *ortho*-$\underline{C}_{(arom)}$), 124.1 (MesOH *para*-$\underline{C}_{(arom)}$), 124.4 (IMes-H $\underline{C}$(4/5)H), 128.0 (MesOH *meta*-$\underline{C}_{(arom)}$H), 129.1 (IMes-H *meta*-$\underline{C}_{(arom)}$H), 131.0 (IMes-H *ipso*-$\underline{C}_{(arom)}$), 134.1 (IMes-H *para*-$\underline{C}_{(arom)}$), 140.2 (IMes-H *ortho*-$\underline{C}_{(arom)}$), 155.9 (MesOH *ipso*-$\underline{C}_{(arom)}$). ^{13}C-NMR (75.5 MHz, CD_2Cl_2): δ 17.3 (MesOH *ortho*-$\underline{C}H_3$), 17.4 (IMes-H *ortho*-$\underline{C}H_3$), 20.4 (MesOH *para*-$\underline{C}H_3$), 21.2 (IMes-H *para*-$\underline{C}H_3$), 124.4 (IMes-H $\underline{C}$(4/5)H), 125.9 (MesOH *ortho*-$\underline{C}_{(arom)}$), 128.3 (MesOH *para*-$\underline{C}_{(arom)}$), 129.6 (MesOH *meta*-$\underline{C}_{(arom)}$H), 129.9 (IMes-H *meta*-$\underline{C}_{(arom)}$H), 131.2 (IMes-H *ipso*-$\underline{C}_{(arom)}$), 134.5 (IMes-H *para*-$\underline{C}_{(arom)}$), 141.3 (IMes-H *ortho*-$\underline{C}_{(arom)}$).

Preparation of [IMes-H][OC_6Cl_5] (4)

A warm toluene (50 mL) solution of pentachlorophenol (0.27 g, 1.0 mmol) and IMes (0.30 g, 1.0 mmol) was filtered and subsequently allowed to cool to room temperature. The product precipitated as a white microcrystalline solid and was collected by filtration, washed with hexane and subsequently dried *in vacuo*. Yield 0.47 g, 82% w.r.t. IMes. m.p. 223–226 °C. Elemental analysis: Calcd for $C_{27}H_{25}N_2O_1Cl_5(C_7H_8)_{0.4}$: C, 58.91; H, 4.68; N, 4.61%. Found: C, 58.60; H, 4.68; N, 4.60%. ^{1}H-NMR (300 MHz, d_6-DMSO): δ 2.11 (12H, s, IMes-H *ortho*-C$\underline{H}_3$), 2.35 (6H, s, IMes-H *para*-C$\underline{H}_3$), 7.19 (4H, s, IMes-H *meta*-$\underline{H}$), 8.28 (2H, s, IMes-H C(4/5)$\underline{H}$), 9.69 (1H, br s, IMes-H C(2)$\underline{H}$). ^{13}C-NMR (100 MHz, d_6-DMSO): δ 17.0 (IMes-H *ortho*-$\underline{C}H_3$), 20.7 (IMes-H *para*-$\underline{C}H_3$), 124.6 (IMes-H $\underline{C}$(4/5)H), 125.1 (Cl_5C_6OH *para*-$\underline{C}_{(arom)}$), 128.0 (Cl_5C_6OH *ortho*-$\underline{C}_{(arom)}$), 128.7 (Cl_5C_6OH *meta*-$\underline{C}_{(arom)}$), 129.1 (IMes-H *meta*-$\underline{C}_{(arom)}$H), 130.8 (IMes-H *ipso*-$\underline{C}_{(arom)}$), 134.0 (IMes-H *para*-$\underline{C}_{(arom)}$), 137.1 (Cl_5C_6OH *ipso*-$\underline{C}_{(arom)}$), 138.4 (IMes-H $\underline{C}$(2)H), 140.3 (IMes-H *ortho*-$\underline{C}_{(arom)}$). Colourless needles suitable for single crystal x-ray diffraction were obtained by allowing a warm tetrahydrofuran (5 mL) solution of pentachlorophenol (0.17 g, 0.6 mmol) and IMes (0.20 g, 0.7 mmol) to cool slowly to room temperature.

Preparation of [IMes-H][O(HO)C_6H_4] (5)

Catechol (1.00 g, 9.4 mmol) and IMes (2.87 g, 9.4 mmol) were gently warmed into tetrahydrofuran (60 mL). The resulting yellow solution was heated to reflux, filtered and allowed to cool slowly to room temperature. The product crystallised as large colourless blocks suitable for x-ray diffraction, which were subsequently isolated by filtration, washed with hexane and dried *in vacuo*. Yield 3.07 g, 79% w.r.t. IMes. m.p. 178–186 °C (dec). Elemental analysis: Calcd for $C_{27}H_{30}N_2O_2$: C, 78.23; H, 7.29; N, 6.76%. Found: C, 78.30; H, 7.39; N, 6.72%. ^{1}H-NMR (300 MHz, d_6-DMSO): δ 2.10 (12H, s, IMes-H *ortho*-C$\underline{H}_3$), 2.35 (6H, s, IMes-H *para*-C$\underline{H}_3$), 6.00–6.12 (2H, m, catechol C$_{(arom)}\underline{H}$), 6.12–6.24 (2H, m, catechol C$_{(arom)}\underline{H}$), 7.18 (4H, s, IMes-H *meta*-$\underline{H}$), 8.24 (2H, s, IMes-H C(4/5)$\underline{H}$), 8.73 (2H, br s, IMes-H C(2)$\underline{H}$ and catechol O$\underline{H}$). ^{13}C-NMR (75.5 MHz, d_6-DMSO): δ 17.0 (IMes-H *ortho*-$\underline{C}$H$_3$), 20.7 (IMes-H *para*-$\underline{C}$H$_3$), 110.8 (catechol $\underline{C}_{(arom)}$H), 113.7 (catechol $\underline{C}_{(arom)}$H), 124.6 (IMes-H $\underline{C}$(4/5)H), 129.3 (IMes-H *meta*-$\underline{C}_{(arom)}$H), 131.5 (IMes-H *ipso*-$\underline{C}_{(arom)}$), 134.3 (IMes-H *para*-$\underline{C}_{(arom)}$), 140.3 (IMes-H *ortho*-$\underline{C}_{(arom)}$), 153.2 (catechol $\underline{C}_{(arom)}$OH).

Preparation of [IMes-H][OC_6(OH)H_4] (6)

A warm tetrahydrofuran (30 mL) solution of resorcinol (0.13 g, 1.2 mmol) and IMes (0.36 g, 1.2 mmol) was heated to reflux, filtered and allowed to cool slowly to room temperature. On standing overnight at 5 °C, the product precipitated as a light brown coloured microcrystalline solid, which was isolated by filtration, washed with hexane and dried *in vacuo*. Yield 0.20 g, 41% w.r.t. IMes. m.p. 208–224 °C (dec). Elemental analysis: Calcd for $C_{27}H_{30}N_2O_2$: C, 78.23; H, 7.29; N, 6.76%. Found: C, 74.80; H, 6.98; N, 5.62%. ^{1}H-NMR (300 MHz, d_6-DMSO) major component: δ 2.11 (12H, s, IMes-H *ortho*-C$\underline{H}_3$), 2.35 (6H, s, IMes-H *para*-C$\underline{H}_3$), 5.78–5.88 (2H, dd, $^3J_{(H\text{-}H)}$ = 7.9 Hz, $^4J_{(H\text{-}H)}$ = 2.2 Hz, resorcinol C$_{(arom)}\underline{H}$), 5.97–5.99 (1H, t, $^4J_{(H\text{-}H)}$=2.2 Hz, resorcinol C$_{(arom)}\underline{H}$), 6.57–6.67 (1H, t, $^3J_{(H\text{-}H)}$ = 8.0 Hz, resorcinol C$_{(arom)}\underline{H}$), 7.20 (4H, s, IMes-H *meta*-$\underline{H}$), 8.26 (2H, s, IMes-H C(4/5)$\underline{H}$), 9.94 ($^1/_2$H, br s, IMes-H C(2)$\underline{H}$). ^{13}C-NMR (100 MHz, d_6-DMSO) major component: δ 17.0 (IMes-H *ortho*-$\underline{C}$H$_3$), 20.7 (IMes-H *para*-$\underline{C}$H$_3$), 103.8 (resorcinol $\underline{C}_{(arom)}$H), 104.6 (resorcinol $\underline{C}_{(arom)}$H), 124.5 (IMes-H

$\underline{C}$(4/5)H), 128.4 (resorcinol $\underline{C}_{(arom)}$H), 129.1 (IMes-H *meta*-$\underline{C}_{(arom)}$H), 130.8 (IMes-H *ipso*-$\underline{C}_{(arom)}$), 134.1 (IMes-H *para*-$\underline{C}_{(arom)}$), 140.3 (IMes-H *ortho*-$\underline{C}_{(arom)}$), 161.7 (resorcinol $\underline{C}_{(arom)}$OH).

Preparation of [IMes-H][$OC_6H_4(OH)$] (7)

A suspension of hydroquinone (0.13 g, 1.2 mmol) and IMes (0.36 g, 1.2 mmol) in toluene (30 mL) was heated to reflux, filtered and allowed to cool slowly to room temperature. The product precipitated as a white powder, and was isolated by filtration, washed with hexane and dried *in vacuo*. Yield 0.48 g, 98% w.r.t. IMes. m.p. 242–244 °C. Elemental analysis: Calcd for $C_{27}H_{30}N_2O_2$: C, 78.23; H, 7.29; N, 6.76%. Found: C, 74.00; H, 6.85; N, 5.60%. ^{1}H-NMR (300 MHz, d_6-DMSO): δ 2.11 (12H, s, IMes-H *ortho*-C$\underline{H}_3$), 2.35 (6H, s, IMes-H *para*-C$\underline{H}_3$), 6.34 (6H, br s, hydroquinone C$_{(arom)}\underline{H}$ and hydroquinone O$\underline{H}$), 7.19 (4H, s, IMes-H *meta*-$\underline{H}$), 8.23 (2H, s, IMes-H C(4/5)$\underline{H}$). ^{13}C-NMR (100 MHz, d_6-DMSO): δ 17.0 (IMes-H *ortho*-$\underline{C}$H$_3$), 20.7 (IMes-H *para*-$\underline{C}$H$_3$), 115.7 (hydroquinone $\underline{C}_{(arom)}$H), 124.5 (IMes-H $\underline{C}$(4/5)H), 129.1 (IMes-H *meta*-$\underline{C}_{(arom)}$H), 130.9 (IMes-H *ipso*-$\underline{C}_{(arom)}$), 134.1 (IMes-H *para*-$\underline{C}_{(arom)}$), 139.2 (IMes-H $\underline{C}$(2)H), 140.3 (IMes-H *ortho*-$\underline{C}_{(arom)}$), 150.5 (hydroquinone $\underline{C}_{(arom)}$OH).

Preparation of [IMes-H][OC_6H_4-2-$\overline{CN(C_6H_4)O}$] (8)

A suspension of 2-(2-hydroxyphenyl)benzoxazole (0.21 g, 1.0 mmol) and IMes (0.30 g, 1.0 mmol) in toluene (45 mL) was heated to reflux. The resulting yellow solution was filtered immediately and allowed to cool slowly to room temperature to yield a crop of yellow needles, which were subsequently isolated by filtration, washed with hexane and dried *in vacuo*. Yield 0.40 g, 78% w.r.t. IMes. m.p. 207–209 °C. Elemental analysis: Calcd for $C_{34}H_{33}N_3O_2$: C, 79.20; H, 6.45; N, 8.15%. Found: C, 79.20; H, 6.54; N, 8.32%. ^{1}H-NMR (300 MHz, d_6-DMSO): δ 2.09 (12H, s, IMes-H *ortho*-C$\underline{H}_3$), 2.33 (6H, s, IMes-H *para*-C$\underline{H}_3$), 5.83–5.92 (1H, dd, $^3J_{(H-H)}$=7.2 Hz, $^3J_{(H-H)}$=6.7 Hz, benzoxazole C$_{(arom)}\underline{H}$), 6.07–6.14 (1H, d, $^3J_{(H-H)}$=8.6 Hz, benzoxazole C$_{(arom)}\underline{H}$), 6.75–6.85 (1H, ddd, $^3J_{(H-H)}$=8.6 Hz, $^3J_{(H-H)}$=6.6 Hz, $^4J_{(H-H)}$ = 2.1 Hz, benzoxazole C$_{(arom)}\underline{H}$), 7.10–7.24 (2H, m, benzoxazole C$_{(arom)}\underline{H}$), 7.15 (4H, s, IMes-H *meta*-$\underline{H}$), 7.45–7.52 (2H, d, $^3J_{(H-H)}$ = 7.3 Hz,

benzoxazole $C_{(arom)}\underline{H}$), 7.57–7.63 (1H, dd, $^{3}J_{(H\text{-}H)}$ = 7.9 Hz, $^{4}J_{(H\text{-}H)}$ = 2.0 Hz, benzoxazole $C_{(arom)}\underline{H}$), 8.27 (2H, s, IMes-H C(4/5)$\underline{H}$), 9.91 (1H, br s, IMes-H C(2)$\underline{H}$). ^{13}C-NMR (75.5 MHz, d_6-DMSO): δ 16.9 (IMes-H *ortho*-$\underline{C}H_3$), 20.6 (IMes-H *para*-$\underline{C}H_3$), 106.3 (benzoxazole $\underline{C}_{(arom)}H$), 109.6 (benzoxazole $\underline{C}_{(arom)}H$), 112.3 (benzoxazole $\underline{C}_{(arom)}$), 117.4 (benzoxazole $\underline{C}_{(arom)}H$), 122.1 (benzoxazole $\underline{C}_{(arom)}H$), 123.2 (benzoxazole $\underline{C}_{(arom)}H$), 124.1 (benzoxazole $\underline{C}_{(arom)}H$), 124.7 (IMes-H $\underline{C}$(4/5)H), 129.3 (IMes-H *meta*-$\underline{C}_{(arom)}H$), 130.9 (benzoxazole $\underline{C}_{(arom)}H$), 131.0 (IMes-H *ipso*-$\underline{C}_{(arom)}$), 131.8 (benzoxazole $\underline{C}_{(arom)}H$), 134.3 (IMes-H *para*-$\underline{C}_{(arom)}$), 139.1 (IMes-H $\underline{C}$(2)H), 140.5 (IMes-H *ortho*-$\underline{C}_{(arom)}$), 142.5 (benzoxazole $\underline{C}_{(arom)}$), 149.7 (benzoxazole $\underline{C}_{(arom)}$), 167.5 (benzoxazole $\underline{C}_{(arom)}$), 172.2 (benzoxazole $\underline{C}_{(arom)}$). Recrystallisation from acetonitrile yielded crystals suitable for study by x-ray diffraction.

Preparation of [IMes-H][$OC_6{}^tBu_2H_2CH_3$] (9)

A warm toluene (5 mL) solution of 2,6-di-*tert*-butyl-4-methylphenol (0.42 g, 1.9 mmol) and IMes (0.58 g, 1.9 mmol) was filtered and allowed to cool slowly to room temperature. The product crystallised as a crop of yellow needles suitable for x-ray diffraction, which were isolated by filtration, washed with hexane and dried *in vacuo*. Yield 0.91 g, 91% w.r.t. IMes. m.p. 186–191 °C. Elemental analysis: Calcd for $C_{36}H_{48}N_2O_1$: C, 82.39; H, 9.22; N, 5.34%. Found: C, 82.10; H, 9.23; N, 5.36%. ^{1}H-NMR (300 MHz, d_6-DMSO): δ 1.23 (18H, s, BHT C($C\underline{H}_3$)$_3$), 2.00 (3H, s, BHT *para*-$C\underline{H}_3$), 2.11 (12H, s, IMes-H *ortho*-$C\underline{H}_3$), 2.33 (6H, s, IMes-H *para*-$C\underline{H}_3$), 6.43 (2H, s, BHT *meta*-$\underline{H}$), 7.17 (4H, s, IMes-H *meta*-$\underline{H}$), 8.22 (2H, s, IMes-H C(4/5)$\underline{H}$). ^{13}C-NMR (75.5 MHz, d_6-DMSO): δ 17.0 (IMes-H *ortho*-$\underline{C}H_3$), 20.7 (IMes-H *para*-$\underline{C}H_3$), 21.6 (BHT *para*-$\underline{C}H_3$), 30.0 (BHT C($\underline{C}H_3$)$_3$), 34.5 (BHT $\underline{C}(CH_3)_3$), 123.7 (BHT *meta*-$\underline{C}_{(arom)}H$), 124.6 (IMes-H $\underline{C}$(4/5)H), 129.3 (IMes-H *meta*-$\underline{C}_{(arom)}H$), 131.4 (IMes-H *ipso*-$\underline{C}_{(arom)}$), 134.3 (IMes-H *para*-$\underline{C}_{(arom)}$), 135.2 (BHT *ortho*-$\underline{C}_{(arom)}$), 140.3 (IMes-H *ortho*-$\underline{C}_{(arom)}$).

Preparation of [IMes-H]$_2$[(OC$_6$^{t}Bu$_2$H$_2$)$_2$CH$_2$] (10)

4,4'-methylene-bis-(2,6-di-*tert*-butylphenol) (0.21 g, 0.5 mmol) and IMes (0.30 g, 1.0 mmol) were dissolved in toluene (30 mL). The resulting solution was heated to reflux, filtered and allowed to cool slowly to room temperature. On standing overnight at -20 °C, the product precipitated from solution as a light pink coloured microcrystalline solid, which was collected by filtration, washed with hexane and dried *in vacuo*. Yield 0.32 g, 62% w.r.t. IMes. m.p. 169–177 °C. Elemental analysis: Calcd for $C_{71}H_{92}N_4O_2$: C, 82.51; H, 8.97; N, 5.42%. Found: C, 79.40; H, 8.73; N, 4.23%. ^{1}H-NMR (300 MHz, d$_6$-DMSO): δ 1.25 (36H, s, bis(BHT) C(C$\underline{H}_3$)$_3$), 2.11 (24H, s, IMes-H *ortho*-C$\underline{H}_3$), 2.33 (12H, s, IMes-H *para*-C$\underline{H}_3$), 6.63 (4H, s, bis(BHT) *meta*-$\underline{H}$), 7.17 (10H, s, IMes-H *meta*-$\underline{H}$ and bis(BHT) -C$\underline{H}_2$-), 8.21 (4H, s, IMes-H C(4/5)$\underline{H}$). ^{13}C-NMR (100 MHz, d$_6$-DMSO): δ 17.0 (IMes-H *ortho*-$\underline{C}$H$_3$), 20.7 (IMes-H *para*-$\underline{C}$H$_3$), 29.5 (bis(BHT) -$\underline{C}$H$_2$-), 30.2 (bis(BHT) C($\underline{C}$H$_3$)$_3$), 34.5 (bis(BHT) $\underline{C}$(CH$_3$)$_3$), 123.5 (bis(BHT) *meta*-$\underline{C}_{(arom)}$H), 124.6 (IMes-H $\underline{C}$(4/5)H), 129.1 (IMes-H *meta*-$\underline{C}_{(arom)}$H), 129.4 (bis(BHT) *para*-$\underline{C}_{(arom)}$), 131.0 (IMes-H *ipso*-$\underline{C}_{(arom)}$), 134.0 (IMes-H *para*-$\underline{C}_{(arom)}$), 134.4 (bis(BHT) *ortho*-$\underline{C}_{(arom)}$), 134.9 (bis(BHT) *ipso*-$\underline{C}_{(arom)}$), 140.2 (IMes-H *ortho*-$\underline{C}_{(arom)}$).

Preparation of [IMes-H][O$_2$CC$_6$H$_5$] (11)

A toluene (30 mL) solution of benzoic acid (0.12 g, 1.0 mmol) and IMes (0.30 g, 1.0 mmol) was heated to reflux, filtered and allowed to cool slowly to room temperature. On standing overnight at 5 °C, the product precipitated as a yellow microcrystalline solid, which was isolated by filtration, washed with hexane and dried *in vacuo*. Yield 0.32 g, 75% w.r.t. IMes. m.p. 182–184 °C. Elemental analysis: Calcd for $C_{28}H_{30}N_2O_2$: C, 78.84; H, 7.09; N, 6.57%. Found: C, 78.40; H, 7.04; N, 6.26%. ^{1}H-NMR (300 MHz, d$_6$-DMSO): δ 2.12 (12H, s, IMes-H *ortho*-C$\underline{H}_3$), 2.34 (6H, s, IMes-H *para*-C$\underline{H}_3$), 7.19 (7H, s, IMes-H *meta*-$\underline{H}$ and benzoic acid C$_{(arom)}\underline{H}$), 7.70–7.80 (2H, m, benzoic acid C$_{(arom)}\underline{H}$), 8.29 (2H, s, IMes-H C(4/5)$\underline{H}$), 9.78 (1H, s, IMes-H C(2)$\underline{H}$). ^{13}C-NMR (100 MHz, d$_6$-DMSO): δ 17.0 (IMes-H *ortho*-$\underline{C}$H$_3$), 20.7 (IMes-H *para*-$\underline{C}$H$_3$), 124.6 (IMes-H $\underline{C}$(4/5)H), 126.5 (benzoic acid $\underline{C}_{(arom)}$H), 127.4 (benzoic acid $\underline{C}_{(arom)}$H), 128.6 (benzoic acid

$\underline{C}_{(arom)}H$), 129.1 (IMes-H *meta*-$\underline{C}_{(arom)}H$), 130.8 (IMes-H *ipso*-$\underline{C}_{(arom)}$), 134.1 (IMes-H *para*-$\underline{C}_{(arom)}$), 138.4 (IMes-H $\underline{C}(2)H$), 140.3 (IMes-H *ortho*-$\underline{C}_{(arom)}$), 142.0 (benzoic acid *ipso*-$\underline{C}_{(arom)}$), 167.6 (benzoic acid $\underline{C}O_2H$).

Preparation of [IMes-H][$(C_6H_5C(O))_2CH$] (12)

A suspension of dibenzoylmethane (1.00 g, 4.6 mmol) and IMes (1.60 g, 5.3 mmol) in toluene (30 mL) was heated to reflux and taken into solution by the addition of tetrahydrofuran (30 mL). The yellow solution was allowed to cool slowly to room temperature to yield the product as a crop of fine yellow needles, which were isolated by filtration, washed with hexane and dried *in vacuo*. Yield 1.98 g, 81% w.r.t. dibenzoylmethane. m.p. 207–209 °C. Elemental analysis: Calcd for $C_{36}H_{36}N_2O_2$: C, 81.79; H, 6.86; N, 5.30%. Found: C, 81.00; H, 6.81; N, 5.22%. ^{1}H-NMR (300 MHz, d_6-DMSO): δ 2.11 (12H, s, IMes-H *ortho*-C$\underline{H}_3$), 2.32 (6H, s, IMes-H *para*-C$\underline{H}_3$), 5.95 (1H, br s, dibenzoylmethane Ph-C(O)-C$\underline{H}$-(O)C-Ph), 7.15 (4H, s, IMes-H *meta*-$\underline{H}$), 7.18–7.34 (6H, m, dibenzoylmethane $C_{(arom)}\underline{H}$), 7.58–7.76 (4H, m, dibenzoylmethane $C_{(arom)}\underline{H}$), 8.25 (2H, s, IMes-H C(4/5)$\underline{H}$), 10.14 (1H, s, IMes-H C(2)$\underline{H}$). ^{13}C-NMR (100 MHz, d_6-DMSO): δ 17.0 (IMes-H *ortho*-$\underline{C}H_3$), 20.7 (IMes-H *para*-$\underline{C}H_3$), 90.0 (dibenzoylmethane Ph-C(O)-$\underline{C}$H-(O)C-Ph), 124.4 (IMes-H $\underline{C}(4/5)H$), 126.3 (dibenzoylmethane $\underline{C}_{(arom)}H$), 127.1 (dibenzoylmethane $\underline{C}_{(arom)}H$), 127.8 (dibenzoylmethane $\underline{C}_{(arom)}H$), 129.0 (IMes-H *meta*-$\underline{C}_{(arom)}H$), 130.9 (IMes-H *ipso*-$\underline{C}_{(arom)}$), 134.1 (IMes-H *para*-$\underline{C}_{(arom)}$), 139.3 (IMes-H $\underline{C}(2)H$), 140.1 (IMes-H *ortho*-$\underline{C}_{(arom)}$), 144.9 (dibenzoylmethane *ipso*-$\underline{C}_{(arom)}$).

Preparation of [IMes-H][$OC_6H_2(C_6H_4)$-$C_6(C_6H_4)H_2OH$] (13)

Binaphthol (1.22 g, 4.3 mmol) and IMes (1.31 g, 4.3 mmol) were gently warmed into tetrahydrofuran (60 mL). The resulting yellow solution was heated to reflux, filtered and allowed to cool slowly to room temperature. The product crystallised as a crop of fine yellow needles, which were isolated by filtration, washed with hexane and subsequently dried *in vacuo*. Yield 2.35 g, 93% w.r.t. IMes. m.p. 240–242 °C. Elemental analysis: Calcd for $C_{41}H_{38}N_2O_2$: C, 83.36; H, 6.48; N,

4.74%. Found: C, 83.40; H, 6.48; N, 4.47%. ^{1}H-NMR (300 MHz, d_6-DMSO): δ 2.11 (12H, s, IMes-H *ortho*-C$\underline{H}_3$), 2.35 (6H, s, IMes-H *para*-C$\underline{H}_3$), 6.80–7.05 (8H, m, binaphthol C$_{(arom)}\underline{H}$), 7.20 (4H, s, IMes-H *meta*-$\underline{H}$), 7.45–7.70 (4H, m, binaphthol C$_{(arom)}\underline{H}$), 8.27 (2H, s, IMes-H C(4/5)$\underline{H}$), 9.64 (1H, s, IMes-H C(2)$\underline{H}$). ^{13}C-NMR (100 MHz, d_6-DMSO): δ 17.0 (IMes-H *ortho*-$\underline{C}$H$_3$), 20.7 (IMes-H *para*-$\underline{C}$H$_3$), 117.8 (binaphthol $\underline{C}_{(arom)}$), 119.2 (binaphthol $\underline{C}_{(arom)}$H), 123.5 (binaphthol $\underline{C}_{(arom)}$H), 123.7 (binaphthol $\underline{C}_{(arom)}$H), 124.6 (IMes-H $\underline{C}$(4/5)H), 125.5 (binaphthol $\underline{C}_{(arom)}$H), 125.9 (binaphthol $\underline{C}_{(arom)}$), 127.0 (binaphthol $\underline{C}_{(arom)}$H), 127.4 (binaphthol $\underline{C}_{(arom)}$H), 129.1 (IMes-H *meta*-$\underline{C}_{(arom)}$H), 130.8 (IMes-H *ipso*-$\underline{C}_{(arom)}$), 134.1 (IMes-H *para*-$\underline{C}_{(arom)}$), 134.2 (binaphthol $\underline{C}_{(arom)}$), 138.3 (IMes-H $\underline{C}$(2)H), 140.3 (IMes-H *ortho*-$\underline{C}_{(arom)}$), 162.1 (binaphthol $\underline{C}_{(arom)}$OH).

Preparation of [IMes-H][O_3SCF_3] (14)

A suspension of silver(I) triflate (0.51 g, 2.0 mmol) and [IMes-H][Cl] (0.68 g, 2.0 mmol) in dichloromethane (60 mL) was stirred at room temperature for 60 hours. After which time, the reaction mixture was heated to reflux and filtered through Celite. The solvent was removed and the solid residue dissolved in toluene (30 mL). The toluene solution was heated to reflux and allowed to cool slowly to room temperature to yield the product as a crop of off-white needles, which were subsequently isolated by filtration, washed with hexane and dried *in vacuo*. Yield 0.60 g, 66% w.r.t. [IMes-H][Cl]. m.p. 196–198 °C. Elemental analysis: Calcd for $C_{22}H_{25}N_2O_3S_1F_3$: C, 58.14; H, 5.54; N, 6.16%. Found: C, 57.80; H, 5.50; N, 6.18%. ^{1}H-NMR (300 MHz, d_6-DMSO): δ 2.12 (12H, s, IMes-H *ortho*-C$\underline{H}_3$), 2.35 (6H, s, IMes-H *para*-C$\underline{H}_3$), 7.21 (4H, s, IMes-H *meta*-$\underline{H}$), 8.28 (2H, s, IMes-H C(4/5)$\underline{H}$), 9.64 (1H, s, IMes-H C(2)$\underline{H}$). ^{13}C-NMR (75.5 MHz, d_6-DMSO): δ 16.9 (IMes-H *ortho*-$\underline{C}$H$_3$), 20.7 (IMes-H *para*-$\underline{C}$H$_3$), 124.8 (IMes-H $\underline{C}$(4/5)H), 129.4 (IMes-H *meta*-$\underline{C}_{(arom)}$H), 131.0 (IMes-H *ipso*-$\underline{C}_{(arom)}$), 134.4 (IMes-H *para*-$\underline{C}_{(arom)}$), 138.5 (IMes-H $\underline{C}$(2)H), 140.7 (IMes-H *ortho*-$\underline{C}_{(arom)}$). ^{19}F-NMR (376 MHz, d_6-DMSO): δ -78.24 (s, $O_3SC\underline{F}_3$).

Preparation of [IMes][$HNPh_2$] (15)

Diphenylamine (0.17 g, 1.0 mmol) and IMes (0.30 g, 1.0 mmol) were dissolved in toluene (5 mL) by gentle warming. The solution was filtered and allowed to cool slowly to room temperature to yield the product as a crop of colourless needles suitable for x-ray diffraction. The product was isolated by filtration, washed with hexane and dried *in vacuo*. Yield 0.18 g, 38% w.r.t. IMes. m.p. 155–159 °C. Elemental analysis: Calcd for $C_{33}H_{35}N_3$: C, 83.68; H, 7.45; N, 8.87%. Found: C, 82.60; H, 7.45; N, 8.71%. ^{1}H-NMR (400 MHz, d_6-DMSO): δ 2.01 (12H, s, IMes *ortho*-C$\underline{H}_3$), 2.31 (6H, s, IMes *para*-C$\underline{H}_3$), 6.77–6.82 (2H, tt, $^3J_{(H\text{-}H)}$=7.2 Hz, $^4J_{(H\text{-}H)}$ =1.2 Hz, $HNPh_2$ *para*-$\underline{H}$), 7.02 (4H, s, IMes *meta*-$\underline{H}$), 7.03–7.08 (4H, dd, $^3J_{(H\text{-}H)}$= 8.8 Hz, $^4J_{(H\text{-}H)}$=1.2 Hz, $HNPh_2$ *ortho*-$\underline{H}$), 7.17–7.23 (4H, dd, $^3J_{(H\text{-}H)}$=8.8 Hz, $^3J_{(H\text{-}H)}$=7.2 Hz, $HNPh_2$ *meta*-$\underline{H}$), 7.38 (2H, s, IMes C(4/5)$\underline{H}$). ^{13}C-NMR (100 MHz, d_6-DMSO): δ 17.3 (IMes *ortho*-$\underline{C}H_3$), 20.7 (IMes *para*-$\underline{C}H_3$), 116.5 ($HNPh_2$ *ortho*-$\underline{C}_{(arom)}H$), 119.4 ($HNPh_2$ *para*-$\underline{C}_{(arom)}H$), 121.5 (IMes $\underline{C}$(4/5)H), 128.4 (IMes *meta*-$\underline{C}_{(arom)}H$), 128.9 ($HNPh_2$ *meta*-$\underline{C}_{(arom)}H$), 134.3 (IMes *ipso*-$\underline{C}_{(arom)}$), 136.7 (IMes *para*-$\underline{C}_{(arom)}$), 137.2 (IMes *ortho*-$\underline{C}_{(arom)}$), 143.2 ($HNPh_2$ *ipso*-$\underline{C}_{(arom)}$).

Preparation of [(IMes)Cu(Mes)] (16)

A toluene (30 mL) solution of 2,4,6-trimethylphenyl-copper(I) (0.18 g, 1.0 mmol) and IMes (0.30 g, 1.0 mmol) was heated to reflux, filtered through Celite and allowed to cool slowly to room temperature. The solution was then placed in a freezer at -20 °C to yield the product as a batch of colourless blocks suitable for study by x-ray diffraction, which were isolated by filtration, washed with hexane and dried *in vacuo*. Yield 0.15 g, 31% w.r.t. IMes. m.p. 126–140 °C. Elemental analysis: Calcd for $C_{30}H_{35}N_2Cu_1$: C, 73.96; H, 7.24; N, 5.75%. Found: C, 73.10; H, 6.88; N, 6.64%. ^{1}H-NMR (300 MHz, C_6D_6): δ 2.01 (12H, s, IMes *ortho*-C$\underline{H}_3$), 2.12 (6H, s, IMes *para*-C$\underline{H}_3$), 2.30 (6H, s, CuMes *ortho*-C$\underline{H}_3$), 2.32 (3H, s, CuMes *para*-C$\underline{H}_3$), 6.02 (2H, s, IMes C(4/5)$\underline{H}$), 6.74 (4H, s, IMes *meta*-$\underline{H}$), 6.95 (2H, s, CuMes *meta*-$\underline{H}$). ^{13}C-NMR (75.5 MHz, C_6D_6): δ 17.8 (IMes *ortho*-$\underline{C}H_3$), 21.0 (IMes *para*-$\underline{C}H_3$), 21.7 (CuMes *para*-$\underline{C}H_3$), 28.3 (CuMes *ortho*-$\underline{C}H_3$), 121.1 (IMes $\underline{C}$(4/5)H), 124.6 (CuMes *meta*-$\underline{C}_{(arom)}H$), 129.4 (IMes *meta*-$\underline{C}_{(arom)}H$), 132.8 (CuMes *ortho*-$\underline{C}_{(arom)}$), 135.1 (IMes *para*-$\underline{C}_{(arom)}$), 136.2 (IMes *ipso*-$\underline{C}_{(arom)}$), 139.1

(IMes *ortho*-$\underline{C}_{(arom)}$), 147.2 (CuMes *para*-$\underline{C}_{(arom)}$), 164.0 (CuMes *ipso*-$\underline{C}_{(arom)}$). MS (FAB): *m/z* 671.4 (78%, IMes-Cu-IMes$^+$), 486.2 (M^+), 367.2 (100%, IMes-Cu$^+$), 303.3 (76%, IMes$^+$).

Preparation of [(IMes)Cu(Cl)] (17)

A suspension of [IMes-H][Cl] (0.34 g, 1.0 mmol) and 2,4,6-trimethylphenyl-copper(I) (0.18 g, 1.0 mmol) in toluene (30 mL) was heated to reflux, filtered through Celite and allowed to cool slowly to room temperature. The solution was then placed in a fridge at 5 °C to yield the product as a batch of colourless blocks suitable for x-ray diffraction, which were subsequently isolated by filtration, washed with hexane and dried *in vacuo*. Yield 0.18 g, 45% w.r.t. [IMes-H][Cl]. m.p. 277–278 °C. Elemental analysis: Calcd for $C_{21}H_{24}N_2Cl_1Cu_1$: C, 62.52; H, 6.00; N, 6.94%. Found: C, 61.70; H, 5.97; N, 6.85%. ^{1}H-NMR (300 MHz, $CDCl_3$): δ 2.10 (12H, s, IMes *ortho*-C$\underline{H}_3$), 2.34 (6H, s, IMes *para*-C$\underline{H}_3$), 6.99 (4H, s, IMes *meta*-$\underline{H}$), 7.05 (2H, s, IMes C(4/5)$\underline{H}$). ^{13}C-NMR (100 MHz, $CDCl_3$): δ 18.0 (IMes *ortho*-$\underline{C}H_3$), 21.4 (IMes *para*-$\underline{C}H_3$), 122.2 (IMes $\underline{C}$(4/5)H), 129.4 (IMes *meta*-$\underline{C}_{(arom)}$H), 134.5 (IMes *para*-$\underline{C}_{(arom)}$), 135.0 (IMes *ipso*-$\underline{C}_{(arom)}$), 139.4 (IMes *ortho*-$\underline{C}_{(arom)}$), 178.8 (IMes $\underline{C}$(2)). MS (FAB): *m/z* 671.4 (100%, IMes-Cu-IMes$^+$), 367.2 (15%, IMes-Cu$^+$), 303.3 (14%, IMes$^+$).

Preparation of [(IMes)Cu(OMes)] (18)

[IMes-H][OMes][HOMes] (0.29 g, 0.5 mmol), IMes (0.15 g, 0.5 mmol) and 2,4,6-trimethylphenyl-copper(I) (0.18 g, 1.0 mmol) were dissolved in toluene (30 mL). The resulting solution was heated to reflux, filtered through Celite and allowed to cool slowly to room temperature, at which point the solution was placed in a fridge at 5 °C. The product subsequently crystallised as a crop of pink needles suitable for x-ray diffraction, which were isolated by filtration, washed with hexane and dried *in vacuo*. Yield 0.10 g, 20% w.r.t. [IMes-H][OMes][HOMes]. m.p. 163–167 °C. Elemental analysis: Calcd for $C_{30}H_{35}N_2O_1Cu_1$: C, 71.61; H, 7.01; N, 5.57%. Found: C, 67.20; H, 6.49; N, 4.73%. ^{1}H-NMR (400 MHz, C_6D_6): δ 1.88 (12H, s, IMes *ortho*-C$\underline{H}_3$), 2.10 (6H, s, IMes *para*-C$\underline{H}_3$), 2.28 (6H, s, MesOH *ortho*-C$\underline{H}_3$), 2.38 (3H, s, MesOH *para*-C$\underline{H}_3$), 5.93 (2H, s, IMes

C(4/5)*H*), 6.65 (4H, s, IMes *meta*-*H*), 6.96 (2H, s, MesOH *meta*-*H*). ^{13}C-NMR (100 MHz, C_6D_6): δ 17.9 (IMes *ortho*-*C*H_3), 19.6 (MesOH *ortho*-*C*H_3), 21.3 (IMes *para*-*C*H_3), 21.4 (MesOH *para*-*C*H_3), 121.5 (IMes *C*(4/5)H), 124.9 (MesOH *para*-$C_{(arom)}$), 129.0 (MesOH *meta*-$C_{(arom)}$H), 129.6 (IMes *meta*-$C_{(arom)}$H), 134.7 (IMes *para*-$C_{(arom)}$), 135.7 (IMes *ipso*-$C_{(arom)}$), 139.2 (IMes *ortho*-$C_{(arom)}$).

Preparation of [(IMes)Cu(OMes)][HOMes] (19)

A toluene (10 mL) solution of [IMes-H][OMes][HOMes] (0.58 g, 1.0 mmol) and 2,4,6-trimethylphenyl-copper(I) (0.18 g, 1.0 mmol) was heated to reflux, filtered through Celite and allowed to cool slowly to room temperature. The solution was then placed in a fridge at 5 °C. The product crystallised as a batch of red blocks suitable for x-ray diffraction, which were isolated by filtration, washed with hexane and dried *in vacuo*. Yield 0.46 g, 72% w.r.t. [IMes-H][OMes][HOMes]. m.p. 159–161 °C. Elemental analysis: Calcd for $C_{39}H_{47}N_2O_2Cu_1$: C, 73.27; H, 7.41; N, 4.38%. Found: C, 71.20; H, 6.94; N, 3.98%. ^{1}H-NMR (400 MHz, C_6D_6): δ 1.87 (12H, s, IMes *ortho*-C*H*$_3$), 2.12 (6H, s, IMes *para*-C*H*$_3$), 2.17 (12H, s, MesOH *ortho*-C*H*$_3$), 2.27 (6H, s, MesOH *para*-C*H*$_3$), 5.93 (2H, s, IMes C(4/5)*H*), 6.37 (1H, br s, MesOH O*H*), 6.66 (4H, s, IMes *meta*-*H*), 6.80 (2H, s, MesOH *meta*-*H*). ^{13}C-NMR (100 MHz, C_6D_6): δ 17.9 (IMes *ortho*-*C*H_3), 18.1 (MesOH *ortho*-*C*H_3), 21.2 (MesOH *para*-*C*H_3), 21.4 (IMes *para*-*C*H_3), 121.5 (IMes *C*(4/5)H), 124.7 (MesOH *para*-$C_{(arom)}$), 129.2 (MesOH *meta*-$C_{(arom)}$H), 129.6 (IMes *meta*-$C_{(arom)}$H), 134.8 (IMes *para*-$C_{(arom)}$), 135.7 (IMes *ipso*-$C_{(arom)}$), 139.2 (IMes *ortho*-$C_{(arom)}$). MS (FAB): *m/z* 671.3 (26%, IMes-Cu-IMes$^+$), 367.2 (27%, IMes-Cu$^+$), 303.3 (23%, IMes$^+$).

Preparation of [(IMes)Cu($OC_6{}^tBu_2H_2CH_3$)] (20)

A toluene (60 mL) solution of [IMes-H][$OC_6{}^tBu_2H_2CH_3$] (0.52 g, 1.0 mmol) and 2,4,6-trimethylphenyl-copper(I) (0.18 g, 1.0 mmol) was heated to reflux, filtered through Celite and allowed to cool slowly to room temperature. The solution was then placed in a fridge at 5 °C to yield the product as a crop of yellow needles suitable for x-ray diffraction, which were isolated by filtration, washed with hexane and dried *in vacuo*. Yield 0.42 g, 71% w.r.t. [IMes-H][$OC_6{}^tBu_2H_2CH_3$].

m.p. 211–215 °C (dec). Elemental analysis: Calcd for $C_{36}H_{47}N_2O_1Cu_1$: C, 73.62; H, 8.07; N, 4.77%. Found: C, 73.50; H, 8.03; N, 4.74%. ^{1}H-NMR (400 MHz, C_6D_6): δ 1.59 (18H, s, BHT C(C*H*$_3$)$_3$), 1.92 (12H, s, IMes *ortho*-C*H*$_3$), 2.13 (6H, s, IMes *para*-C*H*$_3$), 2.44 (3H, s, BHT *para*-C*H*$_3$), 5.95 (2H, s, IMes C(4/5)*H*), 6.72 (4H, s, IMes *meta*-*H*), 7.20 (2H, s, BHT *meta*-*H*). ^{13}C-NMR (100 MHz, C_6D_6): δ 17.9 (IMes *ortho*-*C*H$_3$), 21.3 (IMes *para*-*C*H$_3$), 22.2 (BHT *para*-*C*H$_3$), 31.4 (BHT C(*C*H$_3$)$_3$), 35.7 (BHT *C*(CH$_3$)$_3$), 120.4 (BHT *para*-*C*$_{(arom)}$), 121.6 (IMes *C*(4/5)H), 125.4 (BHT *meta*-*C*$_{(arom)}$H), 129.6 (IMes *meta*-*C*$_{(arom)}$H), 134.8 (IMes *para*-*C*$_{(arom)}$), 135.7 (IMes *ipso*-*C*$_{(arom)}$), 137.8 (BHT *ortho*-*C*$_{(arom)}$), 139.4 (IMes *ortho*-*C*$_{(arom)}$), 164.1 (BHT *ipso*-*C*$_{(arom)}$). MS (FAB): *m/z* 671.3 (100%, IMes-Cu-IMes$^+$), 520.2 (6%, M$^+$), 367.2 (30%, IMes-Cu$^+$), 303.3 (20%, IMes$^+$).

Preparation of [(IMes)Cu(NPh$_2$)] (21)

A toluene (30 mL) solution of [IMes][HNPh$_2$] (0.47 g, 1.0 mmol) and 2,4,6-trimethylphenyl-copper(I) (0.18 g, 1.0 mmol) was heated to reflux and filtered through Celite. The solution was allowed to cool to room temperature and placed in a fridge at 5 °C. The product crystallised as a batch of light brown coloured blocks suitable for x-ray diffraction, and was subsequently isolated by filtration, washed with hexane and dried *in vacuo*. Yield 0.36 g, 67% w.r.t. [IMes][HNPh$_2$]. m.p. 243–246 °C (dec). Elemental analysis: Calcd for $C_{33}H_{34}N_3Cu_1$: C, 73.92; H, 6.39; N, 7.84%. Found: C, 73.10; H, 6.32; N, 7.99%. ^{1}H-NMR (400 MHz, CD_3OD): δ 1.73* and 2.14$^{\#}$ (12H, s, IMes-OH and IMes-H *ortho*-C*H*$_3$), 2.35$^{\#}$ and 2.44* (6H, s, IMes-H and IMes-OH *para*-C*H*$_3$), 6.76–6.86$^{\$}$ (2H, tt, $^3J_{(H\text{-}H)}$ = 7.2 Hz, $^4J_{(H\text{-}H)}$ = 1.2 Hz, HNPh$_2$ *para*-*H*), 6.98* and 7.07$^{\#}$ (4H, s, IMes-OH and IMes-H *meta*-*H*), 7.02–7.06$^{\$}$ (4H, dd, $^3J_{(H\text{-}H)}$ = 8.4 Hz, $^4J_{(H\text{-}H)}$ = 1.2 Hz, HNPh$_2$ *ortho*-*H*), 7.12–7.21$^{\$}$ (4H, dd, $^3J_{(H\text{-}H)}$ = 8.4 Hz, $^3J_{(H\text{-}H)}$ = 7.2 Hz, HNPh$_2$ *meta*-*H*), 7.28* and 7.40$^{\#}$ (2H, s, IMes-OH and IMes-H C(4/5)*H*). ^{13}C-NMR (100 MHz, CD_3OD): δ 17.5* and 18.0$^{\#}$ (IMes-OH and IMes-H *ortho*-*C*H$_3$), 21.2$^{\#}$ and 21.3* (IMes-H and IMes-OH *para*-*C*H$_3$), 118.1$^{\$}$ (HNPh$_2$ *ortho*-*C*$_{(arom)}$H), 120.9$^{\$}$ (HNPh$_2$ *para*-*C*$_{(arom)}$H), 124.1* and 124.2$^{\#}$ (IMes-OH and IMes-H *C*(4/5)H), 129.9$^{\$}$ (HNPh$_2$ *meta*-*C*$_{(arom)}$H), 130.1*$^{/\#}$ (IMes-OH and IMes-H *meta*-*C*$_{(arom)}$H), 135.6*$^{/\#}$ (IMes-OH and IMes-H *para*-*C*$_{(arom)}$), 135.8*$^{/\#}$ (IMes-OH and IMes-H *ipso*-*C*$_{(arom)}$), 136.0* and 136.7$^{\#}$ (IMes-OH and IMes-H *C*(2)), 140.6*$^{/\#}$ (IMes-OH and IMes-H

ortho-$\underline{C}_{(arom)}$), 145.0$^{\$}$ ($HNPh_2$ *ipso*-$\underline{C}_{(arom)}$). *[IMes-OH]$^+$, $^{\#}$[IMes-H]$^+$, $^{\$}$[$HNPh_2$]. MS (FAB): *m/z* 671.3 (100%, IMes-Cu-IMes$^+$), 367.2 (46%, IMes-Cu$^+$), 303.3 (27%, IMes$^+$).

Preparation of $[(IMes)_2Cu][PF_6]$ (22)

A suspension of $[Cu(NCCH_3)_4][PF_6]$ (0.37 g, 1.0 mmol) and IMes (0.61 g, 2.0 mmol) in toluene (60 mL) was heated to reflux and taken into solution with the addition of acetonitrile (40 mL). The solution was filtered through Celite, allowed to cool slowly to room temperature and subsequently placed in a fridge at 5 °C. The product precipitated as a white microcrystalline solid, which was isolated by filtration, washed with hexane and dried *in vacuo*. Yield 0.46 g, 56% w.r.t. IMes. m.p. 349–355 °C. Elemental analysis: Calcd for $C_{42}H_{48}N_4P_1F_6Cu_1$: C, 61.72; H, 5.92; N, 6.85%. Found: C, 61.30; H, 5.86; N, 7.04%. ^{1}H-NMR (300 MHz, CD_3CN): δ 1.67 (24H, s, IMes *ortho*-C$\underline{H}_3$), 2.41 (12H, s, IMes *para*-C$\underline{H}_3$), 6.97 (8H, s, IMes *meta*-$\underline{H}$), 7.15 (4H, s, IMes C(4/5)$\underline{H}$). ^{13}C-NMR (75.5 MHz, CD_3CN): δ 17.2 (IMes *ortho*-$\underline{C}H_3$), 21.1 (IMes *para*-$\underline{C}H_3$), 123.7 (IMes $\underline{C}$(4/5)H), 129.9 (IMes *meta*-$\underline{C}_{(arom)}$H), 135.5 (IMes *para*-$\underline{C}_{(arom)}$), 135.7 (IMes *ipso*-$\underline{C}_{(arom)}$), 140.3 (IMes *ortho*-$\underline{C}_{(arom)}$), 178.4 (IMes $\underline{C}$(2)). ^{31}P-NMR (122 MHz, CD_3CN): δ -126.0—160.9 (sept, $^1J_{(P\text{-}F)}$ = 700 Hz, $\underline{P}F_6$). ^{19}F-NMR (376 MHz, CD_3CN): δ -72.50—74.36 (d, $^1J_{(F\text{-}P)}$ = 700 Hz, P$\underline{F}_6$). Colourless blocks suitable for x-ray diffraction study were obtained by recrystallisation from toluene.

Preparation of $[(IMes)_2Cu][O_2CCH_3][HO_2CCH_3]$ (23)

A stirred suspension of copper(II) acetate (0.36 g, 2.0 mmol) in tetrahydrofuran (40 mL) was maintained at -78 °C while a warm tetrahydrofuran (40 mL) solution of [IMes-H][OMes][HOMes] (1.16 g, 2.0 mmol) and IMes (0.61 g, 2.0 mmol) was added via cannula. The reaction mixture was subsequently allowed to warm to room temperature and stirred for 60 hours, during which time a colour change from blue-green, through yellow, to deep red was observed. The reaction mixture was heated to reflux for 2 hours, filtered through Celite and subsequently allowed to cool slowly to room temperature. The resulting solution was concentrated with the removal of solvent under reduced pressure. The product crystallised as a

batch of large colourless blocks suitable for study by x-ray diffraction, which were isolated from the supernatant solution by filtration, washed with toluene and dried *in vacuo*. The solvent was removed from the filtrate and the solid residue dissolved in toluene (20 mL). The solution was heated to reflux and allowed to cool slowly to room temperature before being cooled to 5 °C to yield a second batch of colourless blocks, which were isolated by filtration, washed with hexane and dried *in vacuo*. Combined yield 0.99 g, 63% w.r.t. copper(II) acetate. m.p. 192–196 °C. Elemental analysis: Calcd for $C_{46}H_{55}N_4O_4Cu_1$: C, 69.80; H, 7.00; N, 7.08%. Found: C, 69.80; H, 6.97; N, 7.11%. ^{1}H-NMR (300 MHz, CD_2Cl_2): δ 1.68 (24H, s, IMes *ortho*-C$\underline{H}_3$), 1.85 (6H, s, C$\underline{H}_3CO_2H$), 2.42 (12H, s, IMes *para*-C$\underline{H}_3$), 6.92 (8H, s, IMes *meta*-$\underline{H}$), 7.04 (4H, s, IMes C(4/5)$\underline{H}$), 16.08 (1H, br s, $CH_3CO_2\underline{H}$). ^{13}C-NMR (75.5 MHz, CD_2Cl_2): δ 17.1 (IMes *ortho*-$\underline{C}H_3$), 21.3 (IMes *para*-$\underline{C}H_3$), 23.4 ($\underline{C}H_3CO_2H$), 123.0 (IMes $\underline{C}$(4/5)H), 129.4 (IMes *meta*-$\underline{C}_{(arom)}$H), 134.8 (IMes *para*-$\underline{C}_{(arom)}$), 134.9 (IMes *ipso*-$\underline{C}_{(arom)}$), 139.8 (IMes *ortho*-$\underline{C}_{(arom)}$), 175.3 ($CH_3\underline{C}O_2H$), 177.9 (IMes $\underline{C}$(2)). MS (FAB): *m/z* 671.2 (100%, IMes-Cu-IMes$^+$), 365.1 (19%, IMes-Cu$^+$), 303.2 (17%, IMes$^+$).

Preparation of [(IMes)$_2$Cu][OMes][HOMes] (24)

[IMes-H][OMes][HOMes] (0.58 g, 1.0 mmol), IMes (0.30 g, 1.0 mmol) and 2,4,6-trimethylphenyl-copper(I) (0.18 g, 1.0 mmol) were dissolved in toluene (30 mL). The resulting red solution was heated to reflux, filtered through Celite, allowed to cool slowly to room temperature and then placed in a fridge at 5 °C. The product crystallised as a batch of colourless blocks suitable for study by x-ray diffraction, which were isolated by filtration, washed with hexane and dried *in vacuo*. Yield 0.41 g, 44% w.r.t. [IMes-H][OMes][HOMes]. m.p. 129–135 °C (dec). Elemental analysis: Calcd for $C_{60}H_{71}N_4O_2Cu_1$: C, 76.36; H, 7.58; N, 5.94%. Found: C, 75.10; H, 6.98; N, 5.72%. ^{1}H-NMR (400 MHz, CD_3CN): δ 1.67 (24H, s, IMes *ortho*-C$\underline{H}_3$), 2.05 (12H, s, MesOH *ortho*-C$\underline{H}_3$), 2.09 (6H, s, MesOH *para*-C$\underline{H}_3$), 2.41 (12H, s, IMes *para*-C$\underline{H}_3$), 6.07 (1H, br s, MesOH O$\underline{H}$), 6.55 (4H, s, MesOH *meta*-$\underline{H}$), 6.96 (8H, s, IMes *meta*-$\underline{H}$), 7.13 (4H, s, IMes C(4/5)$\underline{H}$). ^{13}C-NMR (100 MHz, CD_3CN): δ 17.5 (IMes *ortho*-$\underline{C}H_3$), 18.2 (MesOH *ortho*-$\underline{C}H_3$), 20.9 (MesOH *para*-$\underline{C}H_3$), 21.5 (IMes *para*-$\underline{C}H_3$), 122.4 (MesOH *ortho*-$\underline{C}_{(arom)}$), 123.8 (IMes $\underline{C}$(4/5)H), 126.1 (MesOH *para*-$\underline{C}_{(arom)}$), 129.0 (MesOH *meta*-$\underline{C}_{(arom)}$H),

129.9 (IMes *meta*-$\underline{C}_{(arom)}H$), 135.5 (IMes *para*-$\underline{C}_{(arom)}$), 135.7 (IMes *ipso*-$\underline{C}_{(arom)}$), 140.3 (IMes *ortho*-$\underline{C}_{(arom)}$), 178.3 (IMes $\underline{C}(2)$).

Preparation of $[(IMes)_2Cu][O_2CC_6H_5][HO_2CC_6H_5]$ (25)

A toluene (30 mL) solution of $[IMes\text{-}H][O_2CC_6H_5]$ (0.85 g, 2.0 mmol) and 2,4,6-trimethylphenyl-copper(I) (0.18 g, 1.0 mmol) was heated to reflux, immediately filtered through Celite, and then allowed to cool slowly to room temperature. The solution was placed in a fridge at 5 °C and the product crystallised as a crop of light brown coloured needles suitable for study by x-ray diffraction, which were subsequently isolated by filtration, washed with hexane and dried *in vacuo*. Yield 0.44 g, 48% w.r.t. $[IMes\text{-}H][O_2CC_6H_5]$. m.p. 169–170 °C. Elemental analysis: Calcd for $C_{56}H_{59}N_4O_4Cu_1$: C, 73.46; H, 6.50; N, 6.12%. Found: C, 66.90; H, 6.10; N, 5.22%. ^{1}H-NMR (300 MHz, CD_3CN): δ 1.66 (24H, s, IMes *ortho*-C$\underline{H}_3$), 2.40 (12H, s, IMes *para*-C$\underline{H}_3$), 6.96 (8H, s, IMes *meta*-$\underline{H}$), 7.15 (4H, s, IMes C(4/5)$\underline{H}$), 7.25–7.47 (6H, br m, benzoic acid $C_{(arom)}\underline{H}$), 7.86–8.08 (4H, br m, benzoic acid $C_{(arom)}\underline{H}$). ^{13}C-NMR (75.5 MHz, CD_3CN): δ 17.2 (IMes *ortho*-$\underline{C}H_3$), 21.2 (IMes *para*-$\underline{C}H_3$), 123.7 (IMes $\underline{C}$(4/5)H), 128.7 (benzoic acid $\underline{C}_{(arom)}$H), 129.9 (IMes *meta*-$\underline{C}_{(arom)}$H), 130.5 (benzoic acid $\underline{C}_{(arom)}$H), 131.1 (benzoic acid $\underline{C}_{(arom)}$H), 135.5 (IMes *para*-$\underline{C}_{(arom)}$), 135.7 (IMes *ipso*-$\underline{C}_{(arom)}$), 140.3 (IMes *ortho*-$\underline{C}_{(arom)}$).

Preparation of $[(IMes)_2Cu]_2[(O(O)C_6H_4)_2Cu]$ $[(O(HO)C_6H_4)]_2$ (26)

A toluene (20 mL) solution of $[IMes\text{-}H][O(HO)C_6H_4]$ (0.41 g, 1.0 mmol) and 2,4,6-trimethylphenyl-copper(I) (0.18 g, 1.0 mmol) was heated to reflux, filtered through Celite and allowed to cool slowly to room temperature. The solution was placed in a fridge at 5 °C, and the product subsequently crystallised as a batch of green blocks suitable for study by x-ray diffraction, which were isolated by filtration, washed with hexane and dried *in vacuo*. Yield 0.10 g, 22% w.r.t. $[IMes\text{-}H][O(HO)C_6H_4]$. m.p. 190–195 °C (dec). Elemental analysis: Calcd for $C_{108}H_{114}N_8O_8Cu_3$: C, 70.39; H, 6.24; N, 6.08%. Found: C, 68.60; H, 6.40; N,

5.59%. ^{1}H-NMR (400 MHz, CD_3CN): δ 1.68 (48H, s, IMes *ortho*-C$\underline{H}_3$), 2.41 (24H, s, IMes *para*-C$\underline{H}_3$), 6.45–6.52 (4H, m, catechol $C_{(arom)}\underline{H}$), 6.52–6.59 (4H, m, catechol $C_{(arom)}\underline{H}$), 6.96 (16H, s, IMes *meta*-$\underline{H}$), 7.15 (8H, s, IMes C(4/5)$\underline{H}$). ^{13}C-NMR (75.5 MHz, CD_3CN): δ 17.2 (IMes *ortho*-$\underline{C}H_3$), 21.1 (IMes *para*-$\underline{C}H_3$), 110.7 (catechol $\underline{C}_{(arom)}H$), 123.7 (IMes $\underline{C}$(4/5)H), 129.9 (IMes *meta*-$\underline{C}_{(arom)}H$), 135.5 (IMes *para*-$\underline{C}_{(arom)}$), 135.7 (IMes *ipso*-$\underline{C}_{(arom)}$), 140.3 (IMes *ortho*-$\underline{C}_{(arom)}$), 151.7 (catechol $\underline{C}_{(arom)}OH$), 178.4 (IMes $\underline{C}$(2)). MS (FAB): *m/z* 671.4 (100%, IMes-Cu-IMes$^+$), 367.2 (16%, IMes-Cu$^+$), 303.3 (14%, IMes$^+$).

Preparation of [(IMes)Zn(OMes)(CH_3)] (27)

A suspension of [IMes-H][OMes][HOMes] (0.29 g, 0.5 mmol) and IMes (0.15 g, 0.5 mmol) in toluene (20 mL) was maintained at -78 °C over the course of the dropwise addition of a 2M toluene solution of dimethylzinc (0.5 mL, 1.0 mmol). The reaction mixture was allowed to warm to room temperature, heated to reflux and filtered. The hot filtrate was subsequently allowed to cool slowly to room temperature and placed in a fridge at 5 °C for 1 hour before being transferred to a freezer at -20 °C. The product crystallised as a batch of yellow blocks suitable for study by x-ray diffraction, which were isolated by filtration, washed with hexane and dried *in vacuo*. Yield 0.30 g, 57% w.r.t. [IMes-H][OMes][HOMes]. m.p. 154–158 °C. Elemental analysis: Calcd for $C_{31}H_{38}N_2O_1Zn_1$: C, 71.60; H, 7.37; N, 5.39%. Found: C, 71.40; H, 7.38; N, 5.41%. ^{1}H-NMR (400 MHz, C_6D_6): δ -0.70 (3H, s, Zn-C$\underline{H}_3$), 2.05 (12H, s, IMes *ortho*-C$\underline{H}_3$), 2.08 (6H, s, IMes *para*-C$\underline{H}_3$), 2.11 (6H, s, MesOH *ortho*-C$\underline{H}_3$), 2.36 (3H, s, MesOH *para*-C$\underline{H}_3$), 5.99 (2H, s, IMes C(4/5)$\underline{H}$), 6.71 (4H, s, IMes *meta*-$\underline{H}$), 6.97 (2H, s, MesOH *meta*-$\underline{H}$). ^{13}C-NMR (75.5 MHz, C_6D_6): δ -13.5 (Zn-$\underline{C}H_3$), 17.5 (IMes *ortho*-$\underline{C}H_3$), 18.1 (MesOH *ortho*-$\underline{C}H_3$), 21.0 (IMes *para*-$\underline{C}H_3$), 21.1 (MesOH *para*-$\underline{C}H_3$), 121.4 (MesOH *ortho*-$\underline{C}_{(arom)}$), 122.0 (IMes $\underline{C}$(4/5)H), 125.2 (MesOH *para*-$\underline{C}_{(arom)}$), 128.9 (MesOH *meta*-$\underline{C}_{(arom)}H$), 129.5 (IMes *meta*-$\underline{C}_{(arom)}H$), 134.8 (IMes *ipso*-$\underline{C}_{(arom)}$), 135.5 (IMes *para*-$\underline{C}_{(arom)}$), 139.8 (IMes *ortho*-$\underline{C}_{(arom)}$), 163.2 (MesOH *ipso*-$\underline{C}_{(arom)}$), 181.7 (IMes $\underline{C}$(2)). MS (FAB): *m/z* 520.2 (8%, M$^+$), 385.2 (10%, IMes-Zn-CH_3^+), 369.2 (34%, IMes-Zn$^+$), 305.3 (100%, IMes-H$^+$).

Preparation of [(IMes)Zn(OMes)$_2$] (28)

A stirred suspension of [IMes-H][OMes][HOMes] (1.16 g, 2.0 mmol) in toluene (80 mL) was maintained at -78 °C while a 2M toluene solution of dimethylzinc (1.0 mL, 2.0 mmol) was added dropwise. The reaction mixture was subsequently allowed to warm to room temperature, heated to reflux and the resulting solution filtered. The hot yellow filtrate was allowed to cool slowly to room temperature, placed in a fridge at 5 °C for 1 hour and then transferred to a freezer at -20 °C. The product precipitated as an off-white microcrystalline solid and was isolated by filtration, washed with hexane and dried *in vacuo*. Yield 0.83 g, 65% w.r.t. [IMes-H][OMes][HOMes]. m.p. 252–254 °C. Elemental analysis: Calcd for $C_{39}H_{46}N_2O_2Zn_1$: C, 73.17; H, 7.24; N, 4.38%. Found: C, 73.40; H, 7.27; N, 4.52%. ^{1}H-NMR (300 MHz, CD_2Cl_2): δ 1.66 (12H, s, MesOH *ortho*-C$\underline{H}_3$), 2.02 (12H, s, IMes *ortho*-C$\underline{H}_3$), 2.10 (6H, s, MesOH *para*-C$\underline{H}_3$), 2.40 (6H, s, IMes *para*-C$\underline{H}_3$), 6.52 (4H, s, MesOH *meta*-$\underline{H}$), 7.02 (4H, s, IMes *meta*-$\underline{H}$), 7.22 (2H, s, IMes C(4/5)$\underline{H}$). ^{13}C-NMR (75.5 MHz, CD_2Cl_2): δ 17.0 (MesOH *ortho*-$\underline{C}$H$_3$), 17.4 (IMes *ortho*-$\underline{C}$H$_3$), 20.5 (MesOH *para*-$\underline{C}$H$_3$), 21.3 (IMes *para*-$\underline{C}$H$_3$), 123.4 (MesOH *ortho*-$\underline{C}_{(arom)}$), 124.1 (IMes $\underline{C}$(4/5)H), 125.5 (MesOH *para*-$\underline{C}_{(arom)}$), 128.3 (MesOH *meta*-$\underline{C}_{(arom)}$H), 129.9 (IMes *meta*-$\underline{C}_{(arom)}$H), 134.1 (IMes *ipso*-$\underline{C}_{(arom)}$), 135.7 (IMes *para*-$\underline{C}_{(arom)}$), 140.9 (IMes *ortho*-$\underline{C}_{(arom)}$), 160.3 (MesOH *ipso*-$\underline{C}_{(arom)}$), 172.5 (IMes $\underline{C}$(2)). MS (FAB): *m/z* 638.3 (M^+), 504.3 (1%, IMes-Zn-OMes$^+$), 369.2 (58%, IMes-Zn$^+$), 305.3 (100%, IMes-H$^+$). An attempt to obtain crystals of [(IMes)Zn(OMes)$_2$] suitable for x-ray diffraction study resulted instead in the preparation of [(IMes)Zn(OMes)$_2$(thf)]. A 2M toluene solution of dimethylzinc (0.6 mL, 1.2 mmol) was added dropwise at -78 °C to a suspension of [IMes-H][OMes][HOMes] (0.71 g, 1.2 mmol) in toluene (40 mL). The reaction mixture was subsequently allowed to warm to room temperature, heated to reflux and the suspended solid taken into solution with the addition of tetrahydrofuran (10 mL). The resulting yellow solution was filtered, and the hot filtrate allowed to cool slowly to room temperature before being placed in a fridge at 5 °C. Colourless blocks of [(IMes)Zn(OMes)$_2$(thf)] formed on standing at -20 °C.

Preparation of [Zn(OMes)$_3$][IMes-H] (29)

A suspension of [(IMes)Zn(OMes)$_2$] (0.64 g, 1.0 mmol) in toluene (40 mL) was maintained at -78 °C while a toluene (20 mL) solution of 2,4,6-trimethylphenol (0.14 g, 1.0 mmol) was added via cannula. The reaction mixture was allowed to warm to room temperature and stirred for 60 hours, before being heated to reflux for a further 2 hours. After cooling slowly to room temperature, the reaction mixture was transferred to a freezer at -20 °C. The product, an off-white coloured solid, was isolated by filtration, washed with hexane and dried *in vacuo*. Yield 0.64 g, 82% w.r.t. [(IMes)Zn(OMes)$_2$]. m.p. 206–212 °C (dec). Elemental analysis: Calcd for $C_{48}H_{58}N_2O_3Zn_1$: C, 74.26; H, 7.53; N, 3.61%. Found: C, 69.90; H, 7.00; N, 4.19%. ^{1}H-NMR (400 MHz, CD_3OD): δ 2.14 (18H, s, IMes-H -C*H*$_3$), 2.18 (18H, s, MesOH *ortho*-C*H*$_3$), 2.40 (9H, s, MesOH *para*-C*H*$_3$), 6.65 (4H, s, IMes-H *meta*-*H*), 7.18 (6H, s, MesOH *meta*-*H*). ^{13}C-NMR (100 MHz, CD_3OD): δ 17.1 (IMes-H *ortho*-*C*H$_3$), 17.5 (MesOH *ortho*-*C*H$_3$), 20.7 (IMes-H *para*-*C*H$_3$), 21.2 (MesOH *para*-*C*H$_3$), 125.6 (IMes-H *para*-*C*$_{(arom)}$), 127.9 (IMes-H *ortho*-*C*$_{(arom)}$), 129.5 (IMes-H *meta*-*C*$_{(arom)}$H), 130.2 (IMes-H *C*(4/5)H), 130.7 (MesOH *meta*-*C*$_{(arom)}$H), 132.0 (MesOH *ipso*-*C*$_{(arom)}$), 135.4 (MesOH *para*-*C*$_{(arom)}$), 139.3 (IMes-H *C*(2)H), 142.7 (MesOH *ortho*-*C*$_{(arom)}$), 153.8 (IMes-H *ipso*-*C*$_{(arom)}$). Colourless blocks suitable for study by x-ray diffraction were obtained from the reaction of [(IMes)Zn(OMes)$_2$] with propylene carbonate. Propylene carbonate (0.08 mL, 1.0 mmol) was added to a suspension of [(IMes)Zn(OMes)$_2$] (0.64 g, 1.0 mmol) in toluene (30 mL) and the suspended solid gently warmed into solution. The resulting solution was filtered, allowed to cool slowly to room temperature and transferred to a freezer at -20 °C to yield [Zn(OMes)$_3$][IMes-H] as the only crystalline product.

Preparation of [(IMes)Zn(OC$_6$^{t}Bu$_2$H$_2$CH$_3$)(CH$_3$)] (30)

A suspension of [IMes-H][OC$_6$^{t}Bu$_2$H$_2$CH$_3$] (0.52 g, 1.0 mmol) in toluene (30 mL) was maintained at -78 °C while a 2M toluene solution of dimethylzinc (0.5 mL, 1.0 mmol) was added dropwise. The reaction mixture was allowed to warm to room temperature, and the resulting solution heated to reflux and filtered. The hot filtrate was allowed to cool slowly to room temperature and subsequently placed

in a fridge at 5 °C to yield the product as a batch of yellow blocks suitable for study by x-ray diffraction. The product was isolated by filtration, washed with hexane and dried *in vacuo*. Yield 0.35 g, 58% w.r.t. [IMes-H][$OC_6{}^tBu_2H_2CH_3$]. m.p. 237–241 °C. Elemental analysis: Calcd for $C_{37}H_{50}N_2O_1Zn_1$: C, 73.55; H, 8.34; N, 4.64%. Found: C, 73.90; H, 8.28; N, 4.63%. ^{1}H-NMR (400 MHz, C_6D_6): δ -0.78 (3H, s, Zn-C$\underline{H}_3$), 1.43 (18H, s, BHT C(C$\underline{H}_3$)$_3$), 2.04 (12H, s, IMes *ortho*-C$\underline{H}_3$), 2.13 (6H, s, IMes *para*-C$\underline{H}_3$), 2.42 (3H, s, BHT *para*-C$\underline{H}_3$), 5.98 (2H, s, IMes C(4/5)$\underline{H}$), 6.74 (4H, s, IMes *meta*-$\underline{H}$), 7.19 (2H, s, BHT *meta*-$\underline{H}$). ^{13}C-NMR (100 MHz, C_6D_6): δ -11.1 (Zn-$\underline{C}$H$_3$), 17.9 (IMes *ortho*-$\underline{C}$H$_3$), 21.3 (IMes *para*-$\underline{C}$H$_3$), 22.2 (BHT *para*-$\underline{C}$H$_3$), 31.9 (BHT C($\underline{C}$H$_3$)$_3$), 35.3 (BHT $\underline{C}$(CH$_3$)$_3$), 121.1 (BHT *para*-$\underline{C}_{(arom)}$), 122.6 (IMes $\underline{C}$(4/5)H), 125.3 (BHT *meta*-$\underline{C}_{(arom)}$H), 129.9 (IMes *meta*-$\underline{C}_{(arom)}$H), 135.0 (IMes *ipso*-$\underline{C}_{(arom)}$), 135.2 (IMes *para*-$\underline{C}_{(arom)}$), 138.3 (BHT *ortho*-$\underline{C}_{(arom)}$), 139.9 (IMes *ortho*-$\underline{C}_{(arom)}$), 165.9 (BHT *ipso*-$\underline{C}_{(arom)}$), 180.3 (IMes $\underline{C}$(2)). MS (FAB): *m/z* 385.2 (18%, IMes-Zn-CH_3^+), 369.2 (50%, IMes-Zn^+), 305.3 (100%, IMes-H^+).

Preparation of [(IMes)Zn(NPh_2)(CH_3)] (31)

A solution of [IMes][$HNPh_2$] (0.47 g, 1.0 mmol) in toluene (30 mL) was cooled to -78 °C and a 2M toluene solution of dimethylzinc (0.5 mL, 1.0 mmol) added in a dropwise fashion. The reaction mixture was subsequently allowed to warm to room temperature, heated to reflux and filtered. The hot filtrate was allowed to cool slowly to room temperature and placed in a fridge at 5 °C to yield the product as a batch of light brown blocks suitable for x-ray diffraction, which were isolated by filtration, washed with hexane and dried *in vacuo*. Yield 0.05 g, 9% w.r.t. [IMes][$HNPh_2$]. m.p. 200–216 °C (dec). Elemental analysis: Calcd for $C_{34}H_{37}N_3Zn_1$: C, 73.84; H, 6.74; N, 7.60%. Found: C, 60.20; H, 5.78; N, 6.02%. ^{1}H-NMR (400 MHz, CD_3OD): δ 2.18 (12H, s, IMes-H *ortho*-C$\underline{H}_3$), 2.39 (6H, s, IMes-H *para*-C$\underline{H}_3$), 6.76–6.84 (2H, tt, $^3J_{(H-H)}$ = 7.6 Hz, $^4J_{(H-H)}$ = 1.2 Hz, $HNPh_2$ *para*-$\underline{H}$), 7.01–7.08 (4H, dd, $^3J_{(H-H)}$ = 8.4 Hz, $^4J_{(H-H)}$ = 1.2 Hz, $HNPh_2$ *ortho*-$\underline{H}$), 7.13–7.23 (4H, dd, $^3J_{(H-H)}$ = 8.4 Hz, $^3J_{(H-H)}$ = 7.6 Hz, $HNPh_2$ *meta*-$\underline{H}$), 7.18 (4H, s, IMes-H *meta*-$\underline{H}$). ^{13}C-NMR (75.5 MHz, CD_3OD): δ 17.4 (IMes-H *ortho*-$\underline{C}$H$_3$), 21.2 (IMes-H *para*-$\underline{C}$H$_3$), 118.3 ($HNPh_2$ *ortho*-$\underline{C}_{(arom)}$H), 121.1 ($HNPh_2$ *para*-

$\underline{C}_{(arom)}H$), 130.1 ($HNPh_2$ *meta*-$\underline{C}_{(arom)}H$), 130.9 (IMes-H *meta*-$\underline{C}_{(arom)}H$), 132.3 (IMes-H *ipso*-$\underline{C}_{(arom)}$), 136.6 (IMes-H *para*-$\underline{C}_{(arom)}$), 139.6 (IMes-H $\underline{C}(2)$), 143.0 (IMes-H *ortho*-$\underline{C}_{(arom)}$), 145.3 ($HNPh_2$ *ipso*-$\underline{C}_{(arom)}$). MS (FAB): *m/z* 536.3 (6%, IMes-Zn-NPh_2^+), 385.2 (8%, IMes-Zn-CH_3^+), 369.2 (19%, IMes-Zn^+), 305.3 (100%, IMes-H^+).

General ε-Caprolactone Polymerisation Procedure[11]

A stirred toluene (30 mL) solution of [(IMes)Zn$(OMes)_2$] (0.08 g, 0.125 mmol) was maintained at the desired reaction temperature and anhydrous isopropanol initiator added via syringe as required. ε-Caprolactone (2.6 mL, 25 mmol) was added after the prescribed activation period had elapsed, and the polymerisation allowed to proceed for the designated reaction time. The reaction was quenched with 0.35M aqueous acetic acid (50 mL), and the polymer precipitated by addition of hexane. Following collection by filtration, the poly(caprolactone) produced was washed with water and hexane, and then dried. The polymer was analysed by ^{1}H-NMR (300 MHz, $CDCl_3$) and Gel Permeation Chromatography ($CHCl_3$).

References

[1] R. J. Errington, *Advanced Practical Inorganic and Metalorganic Chemistry*, 2nd, Blackie Academic and Professional, London, **1997**.

[2] L. Jafarpour, E. D. Stevens, S. P. Nolan, *J. Organomet. Chem.*, **2000**, *606*, 49.

[3] T. Tsuda, K. Watanabe, K. Miyata, H. Yamamoto, T. Saegusa, *Inorg. Chem.*, **1981**, *20*, 2728.

[4] W. L. F. Armarego, D. D. Perrin, *Purification of Laboratory Chemicals*, 4th, Butterworth-Heinemann, Oxford, **1997**.

[5] H. E. Gottlieb, V. Kotlyar, A. Nudelman, *J. Org. Chem.*, **1997**, *62*, 7512.

[6] A. A. D. Tulloch, A. A. Danopoulos, S. Winston, S. Kleinhenz, G. Eastham, *J. Chem. Soc.-Dalton Trans.*, **2000**, 4499.

[7] R. Hooft, B. V. Nonius, *COLLECT: Data Collection Software*, **1998**.

[8] Z. Otwinowski, W. Minor, *"Processing of X-ray Diffraction Data Collected in Oscillation Mode"*, in *Methods in Enzymology: Macromolecular Crystallography*, Academic Press, New York, **1997**. 307.

[9] G. M. Sheldrick, *SHELXS-86: Program for Crystal Structure Solution*, University of Gottingen, Gottingen, **1986**.

[10] G. M. Sheldrick, *SHELXL-97: Program for Crystal Structure Refinement*, University of Gottingen, Gottingen, **1997**.

[11] H. L. Chen, B. T. Ko, B. H. Huang, C. C. Lin, *Organometallics*, **2001**, *20*, 5076.

Crystal Data and Diffraction Experiment Details

Crystal data and structure refinement for **1**.		
Identification code	**1**	
Empirical formula	C33 H36 N2 O2	
Formula weight	492.64	
Temperature	150(2) K	
Wavelength	0.71073 Å	
Crystal system	Monoclinic	
Space group	$P2_1/n$	
Unit cell dimensions	a = 9.43600(10) Å	α= 90°.
	b = 18.7750(3) Å	β= 104.2830(10)°.
	c = 16.1460(3) Å	γ = 90°.
Volume	2772.02(7) $Å^3$	
Z	4	
Density (calculated)	1.180 Mg/m^3	
Absorption coefficient	0.073 mm^{-1}	
F(000)	1056	
Crystal size	0.30 x 0.25 x 0.08 mm^3	
Theta range for data collection	3.58 to 27.48°.	
Index ranges	-12<=h<=12, -24<=k<=24, -20<=l<=20	
Reflections collected	35886	
Independent reflections	6344 [R(int) = 0.0717]	
Completeness to theta = 27.48°	99.7 %	
Absorption correction	None	
Max. and min. transmission	0.9942 and 0.9784	
Refinement method	Full-matrix least-squares on F^2	
Data / restraints / parameters	6344 / 0 / 357	
Goodness-of-fit on F^2	1.027	
Final R indices [I>2sigma(I)]	R1 = 0.0509, wR2 = 0.1293	
R indices (all data)	R1 = 0.0754, wR2 = 0.1458	
Extinction coefficient	0.0091(15)	
Largest diff. peak and hole	0.387 and -0.259 $e.Å^{-3}$	

Crystal data and structure refinement for **2**.

Identification code	**2**	
Empirical formula	C33 H26 F10 N2 O2	
Formula weight	672.56	
Temperature	100(2) K	
Wavelength	0.71073 Å	
Crystal system	Monoclinic	
Space group	$P2_1/c$	
Unit cell dimensions	a = 8.159(2) Å	α= 90°.
	b = 14.293(4) Å	β= 93.191(4)°.
	c = 26.863(8) Å	γ = 90°.
Volume	3127.9(15) $Å^3$	
Z	4	
Density (calculated)	1.428 Mg/m^3	
Absorption coefficient	0.130 mm^{-1}	
F(000)	1376	
Crystal size	0.45 x 0.35 x 0.25 mm^3	
Theta range for data collection	3.23 to 26.60°.	
Index ranges	-9<=h<=9, -17<=k<=17, -33<=l<=33	
Reflections collected	22785	
Independent reflections	6014 [R(int) = 0.0499]	
Completeness to theta = 26.60°	91.8 %	
Absorption correction	None	
Refinement method	Full-matrix least-squares on F^2	
Data / restraints / parameters	6014 / 0 / 536	
Goodness-of-fit on F^2	1.059	
Final R indices [I>2sigma(I)]	R1 = 0.0445, wR2 = 0.1025	
R indices (all data)	R1 = 0.0572, wR2 = 0.1124	
Extinction coefficient	0.0066(7)	
Largest diff. peak and hole	0.336 and -0.363 $e.Å^{-3}$	

Crystal data and structure refinement for **3**.

Identification code	**3**	
Empirical formula	C39 H48 N2 O2	
Formula weight	576.79	
Temperature	150(2) K	
Wavelength	0.71070 Å	
Crystal system	Triclinic	
Space group	P-1	
Unit cell dimensions	a = 8.7830(4) Å	α= 75.042(3)°.
	b = 12.1050(6) Å	β= 80.144(2)°.
	c = 17.0090(8) Å	γ = 76.121(2)°.
Volume	1684.54(14) $Å^3$	
Z	2	
Density (calculated)	1.137 Mg/m^3	
Absorption coefficient	0.069 mm^{-1}	
F(000)	624	
Crystal size	0.20 x 0.10 x 0.10 mm^3	
Theta range for data collection	3.76 to 27.49°.	
Index ranges	0<=h<=11, -14<=k<=15, -21<=l<=22	
Reflections collected	18796	
Independent reflections	7598 [R(int) = 0.0865]	
Completeness to theta = 27.49°	98.1 %	
Absorption correction	None	
Max. and min. transmission	0.9931 and 0.9863	
Refinement method	Full-matrix least-squares on F^2	
Data / restraints / parameters	7598 / 0 / 409	
Goodness-of-fit on F^2	0.993	
Final R indices [I>2sigma(I)]	R1 = 0.0578, wR2 = 0.1375	
R indices (all data)	R1 = 0.1167, wR2 = 0.1635	
Extinction coefficient	0.007(2)	
Largest diff. peak and hole	0.223 and -0.242 $e.Å^{-3}$	

Crystal data and structure refinement for **4**.

Identification code	**4**	
Empirical formula	C31 H33 Cl5 N2 O2	
Formula weight	642.84	
Temperature	100(2) K	
Wavelength	0.71073 Å	
Crystal system	Monoclinic	
Space group	$P2_1$	
Unit cell dimensions	a = 7.422(2) Å	α= 90°.
	b = 26.875(8) Å	β= 114.838(4)°.
	c = 8.567(3) Å	γ = 90°.
Volume	1550.9(8) Å^3	
Z	2	
Density (calculated)	1.377 Mg/m^3	
Absorption coefficient	0.499 mm^{-1}	
F(000)	668	
Crystal size	0.6 x 0.3 x 0.05 mm^3	
Theta range for data collection	1.52 to 30.49°.	
Index ranges	-10<=h<=10, -36<=k<=36, -12<=l<=12	
Reflections collected	19171	
Independent reflections	8426 [R(int) = 0.0590]	
Completeness to theta = 30.49°	92.4 %	
Absorption correction	Semi-empirical from equivalents	
Max. and min. transmission	1.0000 and 0.6745	
Refinement method	Full-matrix least-squares on F^2	
Data / restraints / parameters	8426 / 1 / 361	
Goodness-of-fit on F^2	1.099	
Final R indices [I>2sigma(I)]	R1 = 0.0552, wR2 = 0.1253	
R indices (all data)	R1 = 0.0701, wR2 = 0.1329	
Absolute structure parameter	0.00(6)	
Largest diff. peak and hole	0.720 and -0.493 e.Å^{-3}	

Crystal data and structure refinement for **5**.

Identification code	**5**	
Empirical formula	C27 H30 N2 O2	
Formula weight	414.53	
Temperature	150(2) K	
Wavelength	0.71073 Å	
Crystal system	Monoclinic	
Space group	$P2_1/c$	
Unit cell dimensions	a = 11.1540(2) Å	α= 90°.
	b = 13.9950(2) Å	β= 106.1220(10)°.
	c = 14.9080(2) Å	γ = 90°.
Volume	2235.62(6) $Å^3$	
Z	4	
Density (calculated)	1.232 Mg/m^3	
Absorption coefficient	0.078 mm^{-1}	
F(000)	888	
Crystal size	0.38 x 0.32 x 0.25 mm^3	
Theta range for data collection	3.48 to 27.48°.	
Index ranges	-14<=h<=14, -18<=k<=18, -18<=l<=19	
Reflections collected	41102	
Independent reflections	5099 [R(int) = 0.0554]	
Completeness to theta = 27.48°	99.4 %	
Absorption correction	None	
Max. and min. transmission	0.9809 and 0.9711	
Refinement method	Full-matrix least-squares on F^2	
Data / restraints / parameters	5099 / 0 / 295	
Goodness-of-fit on F^2	1.026	
Final R indices [I>2sigma(I)]	R1 = 0.0410, wR2 = 0.0980	
R indices (all data)	R1 = 0.0706, wR2 = 0.1114	
Extinction coefficient	0.0128(14)	
Largest diff. peak and hole	0.204 and -0.170 $e.Å^{-3}$	

Crystal data and structure refinement for **8**.

Identification code	**8**	
Empirical formula	C34 H33 N3 O2	
Formula weight	515.63	
Temperature	120(2) K	
Wavelength	0.71073 Å	
Crystal system	Monoclinic	
Space group	$P2_1/c$	
Unit cell dimensions	a = 20.443(3) Å	α= 90°.
	b = 6.9412(9) Å	β= 101.378(2)°.
	c = 19.742(3) Å	γ = 90°.
Volume	2746.3(6) $Å^3$	
Z	4	
Density (calculated)	1.247 Mg/m^3	
Absorption coefficient	0.078 mm^{-1}	
F(000)	1096	
Crystal size	0.9 x 0.75 x 0.5 mm^3	
Theta range for data collection	2.03 to 27.49°.	
Index ranges	-26<=h<=23, -9<=k<=8, -25<=l<=25	
Reflections collected	23906	
Independent reflections	6270 [R(int) = 0.0262]	
Completeness to theta = 27.49°	99.8 %	
Absorption correction	None	
Refinement method	Full-matrix least-squares on F^2	
Data / restraints / parameters	6270 / 0 / 484	
Goodness-of-fit on F^2	1.042	
Final R indices [I>2sigma(I)]	R1 = 0.0399, wR2 = 0.1012	
R indices (all data)	R1 = 0.0518, wR2 = 0.1080	
Largest diff. peak and hole	0.245 and -0.205 $e.Å^{-3}$	

Crystal data and structure refinement for **9**.

Identification code	**9**	
Empirical formula	C41.85 H57.38 N2 O	
Formula weight	604.52	
Temperature	100(2) K	
Wavelength	0.71073 Å	
Crystal system	Trigonal	
Space group	P-3	
Unit cell dimensions	a = 27.008(9) Å	α= 90°.
	b = 27.008(9) Å	β= 90°.
	c = 17.684(9) Å	γ = 120°.
Volume	11171(8) $Å^3$	
Z	12	
Density (calculated)	1.078 Mg/m^3	
Absorption coefficient	0.063 mm^{-1}	
F(000)	3966	
Crystal size	0.2 x 0.2 x 0.1 mm^3	
Theta range for data collection	0.87 to 27.48°.	
Index ranges	-35<=h<=35, -35<=k<=35, -22<=l<=22	
Reflections collected	121960	
Independent reflections	17079 [R(int) = 0.0557]	
Completeness to theta = 27.48°	100.0 %	
Absorption correction	None	
Refinement method	Full-matrix least-squares on F^2	
Data / restraints / parameters	17079 / 9 / 935	
Goodness-of-fit on F^2	1.011	
Final R indices [I>2sigma(I)]	R1 = 0.0597, wR2 = 0.1547	
R indices (all data)	R1 = 0.0967, wR2 = 0.1853	
Largest diff. peak and hole	0.762 and -0.526 $e.Å^{-3}$	

Crystal data and structure refinement for **11a**.

Identification code	**11a**	
Empirical formula	C34 H44 N2 O3	
Formula weight	528.71	
Temperature	150(2) K	
Wavelength	0.71073 Å	
Crystal system	Triclinic	
Space group	P-1	
Unit cell dimensions	a = 8.36000(10) Å	α= 86.7430(10)°.
	b = 8.9390(2) Å	β= 83.3870(10)°.
	c = 21.7110(5) Å	γ = 71.4450(10)°.
Volume	1527.54(5) $Å^3$	
Z	2	
Density (calculated)	1.149 Mg/m^3	
Absorption coefficient	0.073 mm^{-1}	
F(000)	572	
Crystal size	0.25 x 0.15 x 0.08 mm^3	
Theta range for data collection	2.56 to 27.53°.	
Index ranges	-10<=h<=10, -11<=k<=11, -28<=l<=27	
Reflections collected	32435	
Independent reflections	7001 [R(int) = 0.0656]	
Completeness to theta = 27.53°	99.4 %	
Absorption correction	None	
Max. and min. transmission	0.9942 and 0.9821	
Refinement method	Full-matrix least-squares on F^2	
Data / restraints / parameters	7001 / 0 / 365	
Goodness-of-fit on F^2	1.053	
Final R indices [I>2sigma(I)]	R1 = 0.0586, wR2 = 0.1505	
R indices (all data)	R1 = 0.1094, wR2 = 0.1752	
Extinction coefficient	0.041(5)	
Largest diff. peak and hole	0.665 and -0.456 $e.Å^{-3}$	

Crystal data and structure refinement for **15**.

Identification code	**15**	
Empirical formula	C33 H35 N3	
Formula weight	473.64	
Temperature	30(2) K	
Wavelength	0.71073 Å	
Crystal system	Triclinic	
Space group	P-1	
Unit cell dimensions	a = 9.6629(19) Å	α= 80.60(3)°.
	b = 10.578(2) Å	β= 71.68(3)°.
	c = 14.967(3) Å	γ = 67.72(3)°.
Volume	1342.3(5) $Å^3$	
Z	2	
Density (calculated)	1.172 Mg/m^3	
Absorption coefficient	0.069 mm^{-1}	
F(000)	508	
Crystal size	0.48 x 0.26 x 0.16 mm^3	
Theta range for data collection	3.46 to 27.17 °.	
Index ranges	-12<=h<=11, -13<=k<=13, -18<=l<=19	
Reflections collected	11025	
Independent reflections	5307 [R(int) = 0.0285]	
Completeness to theta = 27.17 °	88.7 %	
Max. and min. transmission	0.9942 and 0.9821	
Refinement method	Full-matrix least-squares on F^2	
Data / restraints / parameters	5307/ 0 / 465	
Goodness-of-fit on F^2	1.029	
Final R indices [I>2sigma(I)]	R1 = 0.0376, wR2 = 0.0935	
R indices (all data)	R1 = 0.0482, wR2 = 0.0991	
Largest diff. peak and hole	0.257 and -0.207 $e.Å^{-3}$	

Crystal data and structure refinement for **16**.

Identification code	**16**
Empirical formula	C30 H35 Cu N2
Formula weight	487.14
Temperature	150(2) K
Wavelength	0.71073 Å
Crystal system	Monoclinic
Space group	$P2_1/c$
Unit cell dimensions	a = 16.89600(10) Å α= 90°.
	b = 14.34600(10) Å β= 96.21°.
	c = 22.5490(2) Å γ = 90°.
Volume	5433.56(7) $Å^3$
Z	8
Density (calculated)	1.191 Mg/m^3
Absorption coefficient	0.822 mm^{-1}
F(000)	2064
Crystal size	0.3 x 0.25 x 0.125 mm^3
Theta range for data collection	2.98 to 26.01°.
Index ranges	-20<=h<=20, -17<=k<=17, -27<=l<=27
Reflections collected	101698
Independent reflections	10655 [R(int) = 0.0536]
Completeness to theta = 26.01°	99.6 %
Absorption correction	None
Refinement method	Full-matrix least-squares on F^2
Data / restraints / parameters	10655 / 0 / 614
Goodness-of-fit on F^2	1.031
Final R indices [I>2sigma(I)]	R1 = 0.0328, wR2 = 0.0871
R indices (all data)	R1 = 0.0456, wR2 = 0.0950
Extinction coefficient	0.0010(2)
Largest diff. peak and hole	0.335 and -0.364 $e.Å^{-3}$

Crystal data and structure refinement for **17**.

Identification code	**17**	
Empirical formula	C84 H96 Cl4 Cu4 N8 O0	
Formula weight	1613.65	
Temperature	150(2) K	
Wavelength	0.71073 Å	
Crystal system	Orthorhombic	
Space group	Fdd2	
Unit cell dimensions	a = 14.7060(2) Å	α= 90°.
	b = 29.0100(8) Å	β= 90.0000(10)°.
	c = 9.4840(3) Å	γ = 90°.
Volume	4046.07(18) $Å^3$	
Z	2	
Density (calculated)	1.325 Mg/m^3	
Absorption coefficient	1.217 mm^{-1}	
F(000)	1680	
Crystal size	0.2 x 0.2 x 0.3 mm^3	
Theta range for data collection	3.95 to 27.49°.	
Index ranges	-19<=h<=19, -37<=k<=35, -12<=l<=12	
Reflections collected	18929	
Independent reflections	2319 [R(int) = 0.0574]	
Completeness to theta = 27.49°	99.7 %	
Absorption correction	None	
Refinement method	Full-matrix least-squares on F^2	
Data / restraints / parameters	2319 / 1 / 119	
Goodness-of-fit on F^2	1.033	
Final R indices [I>2sigma(I)]	R1 = 0.0361, wR2 = 0.0852	
R indices (all data)	R1 = 0.0514, wR2 = 0.0905	
Absolute structure parameter	0.491(17)	
Extinction coefficient	0.00044(14)	
Largest diff. peak and hole	0.211 and -0.323 $e.Å^{-3}$	

Crystal data and structure refinement for **18**.

Identification code	**18**	
Empirical formula	C30 H35 Cu N2 O	
Formula weight	503.14	
Temperature	150(2) K	
Wavelength	0.71073 Å	
Crystal system	Monoclinic	
Space group	$P2_1/c$	
Unit cell dimensions	a = 13.0570(2) Å	α= 90°.
	b = 12.9450(3) Å	β= 90.1660(10)°.
	c = 16.0550(4) Å	γ = 90°.
Volume	2713.65(10) $Å^3$	
Z	4	
Density (calculated)	1.232 Mg/m^3	
Absorption coefficient	0.828 mm^{-1}	
F(000)	1064	
Crystal size	0.22 x 0.20 x 0.05 mm^3	
Theta range for data collection	3.72 to 27.52°.	
Index ranges	-16<=h<=16, -16<=k<=16, -20<=l<=20	
Reflections collected	49606	
Independent reflections	6190 [R(int) = 0.0880]	
Completeness to theta = 27.52°	99.5 %	
Absorption correction	None	
Max. and min. transmission	0.9598 and 0.8388	
Refinement method	Full-matrix least-squares on F^2	
Data / restraints / parameters	6190 / 0 / 317	
Goodness-of-fit on F^2	1.023	
Final R indices [I>2sigma(I)]	R1 = 0.0418, wR2 = 0.0904	
R indices (all data)	R1 = 0.0841, wR2 = 0.1040	
Extinction coefficient	0.0012(6)	
Largest diff. peak and hole	0.322 and -0.400 $e.Å^{-3}$	

Crystal data and structure refinement for **19**.

Identification code	**19**	
Empirical formula	C39 H47 Cu N2 O2	
Formula weight	639.33	
Temperature	150(2) K	
Wavelength	0.71073 Å	
Crystal system	Monoclinic	
Space group	$P2_1/n$	
Unit cell dimensions	a = 11.58300(10) Å	α= 90°.
	b = 15.2230(2) Å	β= 98.9430(10)°.
	c = 19.8360(3) Å	γ = 90°.
Volume	3455.12(8) $Å^3$	
Z	4	
Density (calculated)	1.229 Mg/m^3	
Absorption coefficient	0.667 mm^{-1}	
F(000)	1360	
Crystal size	0.25 x 0.13 x 0.13 mm^3	
Theta range for data collection	3.23 to 27.54°.	
Index ranges	-15<=h<=15, -19<=k<=19, -22<=l<=25	
Reflections collected	64740	
Independent reflections	7921 [R(int) = 0.0899]	
Completeness to theta = 27.54°	99.5 %	
Absorption correction	None	
Max. and min. transmission	0.9183 and 0.8510	
Refinement method	Full-matrix least-squares on F^2	
Data / restraints / parameters	7921 / 0 / 421	
Goodness-of-fit on F^2	1.014	
Final R indices [I>2sigma(I)]	R1 = 0.0453, wR2 = 0.1008	
R indices (all data)	R1 = 0.0943, wR2 = 0.1203	
Largest diff. peak and hole	0.287 and -0.502 $e.Å^{-3}$	

Crystal data and structure refinement for **20**.

Identification code	**20**	
Empirical formula	C36 H47 Cu N2 O	
Formula weight	587.30	
Temperature	150(2) K	
Wavelength	0.71073 Å	
Crystal system	Monoclinic	
Space group	$P2_1/n$	
Unit cell dimensions	a = 11.4860(2) Å	α= 90°.
	b = 13.0180(2) Å	β= 102.8640(10)°.
	c = 23.4820(4) Å	γ = 90°.
Volume	3423.01(10) $Å^3$	
Z	4	
Density (calculated)	1.140 Mg/m^3	
Absorption coefficient	0.665 mm^{-1}	
F(000)	1256	
Crystal size	0.22 x 0.08 x 0.05 mm^3	
Theta range for data collection	3.64 to 25.29°.	
Index ranges	-13<=h<=13, -15<=k<=13, -27<=l<=28	
Reflections collected	54909	
Independent reflections	6192 [R(int) = 0.0980]	
Completeness to theta = 25.29°	99.3 %	
Absorption correction	None	
Max. and min. transmission	0.9675 and 0.8674	
Refinement method	Full-matrix least-squares on F^2	
Data / restraints / parameters	6192 / 0 / 362	
Goodness-of-fit on F^2	1.022	
Final R indices [I>2sigma(I)]	R1 = 0.0452, wR2 = 0.1016	
R indices (all data)	R1 = 0.0814, wR2 = 0.1173	
Extinction coefficient	0.0027(7)	
Largest diff. peak and hole	0.368 and -0.442 $e.Å^{-3}$	

Crystal data and structure refinement for **21**.

Identification code	**21**	
Empirical formula	C33 H34 Cu N3	
Formula weight	536.17	
Temperature	150(2) K	
Wavelength	0.71073 Å	
Crystal system	Triclinic	
Space group	P-1	
Unit cell dimensions	a = 10.1490(2) Å	α= 81.3220(10)°.
	b = 10.5100(3) Å	β= 73.8770(10)°.
	c = 14.7950(4) Å	γ = 66.0820(10)°.
Volume	1384.55(6) $Å^3$	
Z	2	
Density (calculated)	1.286 Mg/m^3	
Absorption coefficient	0.815 mm^{-1}	
F(000)	564	
Crystal size	0.28 x 0.20 x 0.17 mm^3	
Theta range for data collection	3.97 to 27.47°.	
Index ranges	-13<=h<=13, -13<=k<=13, -19<=l<=19	
Reflections collected	30961	
Independent reflections	6309 [R(int) = 0.0788]	
Completeness to theta = 27.47°	99.4 %	
Absorption correction	None	
Max. and min. transmission	0.8739 and 0.8040	
Refinement method	Full-matrix least-squares on F^2	
Data / restraints / parameters	6309 / 0 / 341	
Goodness-of-fit on F^2	1.000	
Final R indices [I>2sigma(I)]	R1 = 0.0419, wR2 = 0.0837	
R indices (all data)	R1 = 0.0876, wR2 = 0.0962	
Extinction coefficient	0.0019(10)	
Largest diff. peak and hole	0.318 and -0.338 $e.Å^{-3}$	

Crystal data and structure refinement for **22**.

Identification code	**22**	
Empirical formula	C23 H27 Cu0.25 F1.50 N3 P0.25	
Formula weight	397.60	
Temperature	150(2) K	
Wavelength	0.71073 Å	
Crystal system	Triclinic	
Space group	P-1	
Unit cell dimensions	a = 11.0280(2) Å	α= 91.4590(10)°.
	b = 11.9140(3) Å	β= 94.2790(10)°.
	c = 15.8740(4) Å	γ = 92.5030(10)°.
Volume	2076.98(8) $Å^3$	
Z	4	
Density (calculated)	1.272 Mg/m^3	
Absorption coefficient	0.350 mm^{-1}	
F(000)	842	
Crystal size	0.50 x 0.20 x 0.17 mm^3	
Theta range for data collection	3.83 to 27.55°.	
Index ranges	-14<=h<=14, -15<=k<=15, -20<=l<=19	
Reflections collected	24250	
Independent reflections	9463 [R(int) = 0.0339]	
Completeness to theta = 27.55°	98.5 %	
Absorption correction	None	
Max. and min. transmission	0.9430 and 0.8446	
Refinement method	Full-matrix least-squares on F^2	
Data / restraints / parameters	9463 / 0 / 474	
Goodness-of-fit on F^2	1.042	
Final R indices [I>2sigma(I)]	R1 = 0.0771, wR2 = 0.2175	
R indices (all data)	R1 = 0.0881, wR2 = 0.2312	
Extinction coefficient	0.017(4)	
Largest diff. peak and hole	1.918 and -1.744 $e.Å^{-3}$	

Crystal data and structure refinement for **23**.

Identification code	**23**	
Empirical formula	C23 H27.50 Cu0.50 N2 O2	
Formula weight	395.74	
Temperature	150(2) K	
Wavelength	0.71073 Å	
Crystal system	Triclinic	
Space group	P-1	
Unit cell dimensions	a = 10.62400(10) Å	α= 81.8100(10)°.
	b = 14.2250(2) Å	β= 73.7100(10)°.
	c = 15.6130(2) Å	γ = 76.1700(10)°.
Volume	2191.94(5) $Å^3$	
Z	4	
Density (calculated)	1.199 Mg/m^3	
Absorption coefficient	0.543 mm^{-1}	
F(000)	840	
Crystal size	0.30 x 0.25 x 0.20 mm^3	
Theta range for data collection	4.05 to 27.53°.	
Index ranges	-13<=h<=13, -18<=k<=18, -20<=l<=20	
Reflections collected	31419	
Independent reflections	10024 [R(int) = 0.0363]	
Completeness to theta = 27.53°	99.1 %	
Absorption correction	None	
Max. and min. transmission	0.8992 and 0.8540	
Refinement method	Full-matrix least-squares on F^2	
Data / restraints / parameters	10024 / 0 / 515	
Goodness-of-fit on F^2	1.003	
Final R indices [I>2sigma(I)]	R1 = 0.0326, wR2 = 0.0896	
R indices (all data)	R1 = 0.0373, wR2 = 0.0941	
Extinction coefficient	0.0013(10)	
Largest diff. peak and hole	0.341 and -0.615 $e.Å^{-3}$	

Crystal data and structure refinement for **24**.

Identification code	**24**	
Empirical formula	C40 H47.33 Cu0.67 N2.67 O1.33	
Formula weight	629.17	
Temperature	150(2) K	
Wavelength	0.71073 Å	
Crystal system	Monoclinic	
Space group	$P2_1/c$	
Unit cell dimensions	a = 13.7080(3) Å	α= 90°.
	b = 15.2870(3) Å	β= 93.5470(10)°.
	c = 25.3070(6) Å	γ = 90°.
Volume	5293.0(2) $Å^3$	
Z	6	
Density (calculated)	1.184 Mg/m^3	
Absorption coefficient	0.458 mm^{-1}	
F(000)	2016	
Crystal size	0.15 x 0.13 x 0.05 mm^3	
Theta range for data collection	3.72 to 21.25°.	
Index ranges	-13<=h<=13, -15<=k<=15, -25<=l<=25	
Reflections collected	26226	
Independent reflections	5779 [R(int) = 0.0998]	
Completeness to theta = 21.25°	98.5 %	
Absorption correction	None	
Max. and min. transmission	0.9775 and 0.9345	
Refinement method	Full-matrix least-squares on F^2	
Data / restraints / parameters	5779 / 0 / 627	
Goodness-of-fit on F^2	1.040	
Final R indices [I>2sigma(I)]	R1 = 0.0466, wR2 = 0.0921	
R indices (all data)	R1 = 0.0810, wR2 = 0.1077	
Extinction coefficient	0.0010(2)	
Largest diff. peak and hole	0.241 and -0.233 $e.Å^{-3}$	

Crystal data and structure refinement for **25**.

Identification code	**25**	
Empirical formula	C56 H59 Cu N4 O4	
Formula weight	915.61	
Temperature	150(2) K	
Wavelength	0.71073 Å	
Crystal system	Triclinic	
Space group	P-1	
Unit cell dimensions	a = 11.7340(2) Å	α= 103.2630(10)°.
	b = 14.7860(2) Å	β= 96.5090(10)°.
	c = 14.9730(3) Å	γ = 92.8070(10)°.
Volume	2504.65(7) $Å^3$	
Z	2	
Density (calculated)	1.214 Mg/m^3	
Absorption coefficient	0.485 mm^{-1}	
F(000)	968	
Crystal size	0.15 x 0.13 x 0.08 mm^3	
Theta range for data collection	3.85 to 27.54°.	
Index ranges	-15<=h<=14, -19<=k<=19, -19<=l<=19	
Reflections collected	47917	
Independent reflections	11425 [R(int) = 0.0465]	
Completeness to theta = 27.54°	98.9 %	
Absorption correction	None	
Max. and min. transmission	0.9646 and 0.9309	
Refinement method	Full-matrix least-squares on F^2	
Data / restraints / parameters	11425 / 0 / 603	
Goodness-of-fit on F^2	1.000	
Final R indices [I>2sigma(I)]	R1 = 0.0398, wR2 = 0.0942	
R indices (all data)	R1 = 0.0696, wR2 = 0.1061	
Extinction coefficient	0.0044(8)	
Largest diff. peak and hole	0.257 and -0.309 $e.Å^{-3}$	

Crystal data and structure refinement for **26**.

Identification code	**26**	
Empirical formula	C28.75 H31 Cu0.75 N2 O2	
Formula weight	484.21	
Temperature	150(2) K	
Wavelength	0.71073 Å	
Crystal system	Triclinic	
Space group	P-1	
Unit cell dimensions	a = 13.0960(6) Å	α= 73.066(2)°.
	b = 14.7430(5) Å	β= 81.951(2)°.
	c = 14.8660(7) Å	γ = 69.599(2)°.
Volume	2571.19(19) $Å^3$	
Z	4	
Density (calculated)	1.251 Mg/m^3	
Absorption coefficient	0.675 mm^{-1}	
F(000)	1021	
Crystal size	0.25 x 0.20 x 0.15 mm^3	
Theta range for data collection	3.12 to 27.47°.	
Index ranges	-16<=h<=16, -19<=k<=19, -19<=l<=19	
Reflections collected	37404	
Independent reflections	11629 [R(int) = 0.1520]	
Completeness to theta = 27.47°	98.9 %	
Absorption correction	None	
Max. and min. transmission	0.9055 and 0.8494	
Refinement method	Full-matrix least-squares on F^2	
Data / restraints / parameters	11629 / 0 / 648	
Goodness-of-fit on F^2	1.010	
Final R indices [I>2sigma(I)]	R1 = 0.0729, wR2 = 0.1390	
R indices (all data)	R1 = 0.1683, wR2 = 0.1816	
Extinction coefficient	0.0000(7)	
Largest diff. peak and hole	0.549 and -0.822 $e.Å^{-3}$	

Crystal data and structure refinement for **27**.

Identification code	**27**	
Empirical formula	C62 H76 N4 O2 Zn2	
Formula weight	1040.01	
Temperature	150(2) K	
Wavelength	0.71073 Å	
Crystal system	Monoclinic	
Space group	$P2_1/c$	
Unit cell dimensions	a = 11.4600(2) Å	α= 90°.
	b = 15.0970(3) Å	β= 104.9680(10)°.
	c = 16.7920(3) Å	γ = 90°.
Volume	2806.64(9) $Å^3$	
Z	2	
Density (calculated)	1.231 Mg/m^3	
Absorption coefficient	0.900 mm^{-1}	
F(000)	1104	
Crystal size	0.30 x 0.25 x 0.20 mm^3	
Theta range for data collection	3.67 to 29.37°.	
Index ranges	-15<=h<=14, -19<=k<=20, -20<=l<=22	
Reflections collected	27545	
Independent reflections	6759 [R(int) = 0.0443]	
Completeness to theta = 29.37°	87.6 %	
Max. and min. transmission	0.8406 and 0.7741	
Refinement method	Full-matrix least-squares on F^2	
Data / restraints / parameters	6759 / 0 / 327	
Goodness-of-fit on F^2	1.020	
Final R indices [I>2sigma(I)]	R1 = 0.0348, wR2 = 0.0830	
R indices (all data)	R1 = 0.0555, wR2 = 0.0924	
Extinction coefficient	0.0055(8)	
Largest diff. peak and hole	0.327 and -0.405 $e.Å^{-3}$	

Crystal data and structure refinement for **27a**.

Identification code	**27a**	
Empirical formula	C58 H68 N4 O2 Zn	
Formula weight	918.53	
Temperature	150(2) K	
Wavelength	0.71073 Å	
Crystal system	Monoclinic	
Space group	$P2_1/a$	
Unit cell dimensions	a = 14.44800(10) Å	α= 90°.
	b = 24.9880(3) Å	β= 114.7300(10)°.
	c = 15.3840(2) Å	γ = 90°.
Volume	5044.67(10) $Å^3$	
Z	4	
Density (calculated)	1.209 Mg/m^3	
Absorption coefficient	0.532 mm^{-1}	
F(000)	1960	
Crystal size	0.25 x 0.20 x 0.17 mm^3	
Theta range for data collection	3.52 to 25.04°.	
Index ranges	-17<=h<=17, -26<=k<=29, -18<=l<=18	
Reflections collected	58375	
Independent reflections	8886 [R(int) = 0.0642]	
Completeness to theta = 25.04°	99.5 %	
Absorption correction	None	
Max. and min. transmission	0.9150 and 0.8784	
Refinement method	Full-matrix least-squares on F^2	
Data / restraints / parameters	8886 / 0 / 599	
Goodness-of-fit on F^2	1.045	
Final R indices [I>2sigma(I)]	R1 = 0.0422, wR2 = 0.1004	
R indices (all data)	R1 = 0.0578, wR2 = 0.1091	
Extinction coefficient	0.0008(2)	
Largest diff. peak and hole	0.356 and -0.361 $e.Å^{-3}$	

Crystal data and structure refinement for **28 thf solvate**.

Identification code	**28 thf solvate**	
Empirical formula	C49 H66 N2 O4.50 Zn	
Formula weight	820.41	
Temperature	150(2) K	
Wavelength	0.71073 Å	
Crystal system	Monoclinic	
Space group	$P2_1/c$	
Unit cell dimensions	a = 9.3960(2) Å	α= 90°.
	b = 16.2850(3) Å	β= 92.5730(10)°.
	c = 29.4520(6) Å	γ = 90°.
Volume	4502.02(16) $Å^3$	
Z	4	
Density (calculated)	1.210 Mg/m^3	
Absorption coefficient	0.591 mm^{-1}	
F(000)	1760	
Crystal size	0.20 x 0.10 x 0.08 mm^3	
Theta range for data collection	3.66 to 24.70°.	
Index ranges	-11<=h<=10, -19<=k<=19, -34<=l<=34	
Reflections collected	48616	
Independent reflections	7613 [R(int) = 0.1110]	
Completeness to theta = 24.70°	99.4 %	
Max. and min. transmission	0.9570 and 0.8910	
Refinement method	Full-matrix least-squares on F^2	
Data / restraints / parameters	7613 / 0 / 548	
Goodness-of-fit on F^2	1.066	
Final R indices [I>2sigma(I)]	R1 = 0.0520, wR2 = 0.0944	
R indices (all data)	R1 = 0.0965, wR2 = 0.1090	
Largest diff. peak and hole	0.315 and -0.431 $e.Å^{-3}$	

Crystal data and structure refinement for **28a**.

Identification code	**28a**	
Empirical formula	C76 H90 N4 O4 Zn2	
Formula weight	1254.26	
Temperature	150(2) K	
Wavelength	0.71073 Å	
Crystal system	Monoclinic	
Space group	$P2_1/c$	
Unit cell dimensions	a = 21.1510(2) Å	α= 90°.
	b = 10.91400(10) Å	β= 90.7770(10)°.
	c = 29.5950(3) Å	γ = 90°.
Volume	6831.14(11) $Å^3$	
Z	4	
Density (calculated)	1.220 Mg/m^3	
Absorption coefficient	0.753 mm^{-1}	
F(000)	2664	
Crystal size	0.30 x 0.25 x 0.20 mm^3	
Theta range for data collection	3.69 to 24.71°.	
Index ranges	-24<=h<=24, -10<=k<=12, -33<=l<=34	
Reflections collected	43049	
Independent reflections	11463 [R(int) = 0.0538]	
Completeness to theta = 24.71°	98.5 %	
Absorption correction	None	
Max. and min. transmission	0.8640 and 0.8056	
Refinement method	Full-matrix least-squares on F^2	
Data / restraints / parameters	11463 / 0 / 778	
Goodness-of-fit on F^2	1.024	
Final R indices [I>2sigma(I)]	R1 = 0.0470, wR2 = 0.1170	
R indices (all data)	R1 = 0.0729, wR2 = 0.1322	
Extinction coefficient	0.0006(2)	
Largest diff. peak and hole	0.892 and -0.363 $e.Å^{-3}$	

Crystal data and structure refinement for **29**.

Identification code	**29**	
Empirical formula	C55 H66 N2 O3 Zn	
Formula weight	868.47	
Temperature	150(2) K	
Wavelength	0.71073 Å	
Crystal system	Monoclinic	
Space group	$C2_1/c$	
Unit cell dimensions	a = 18.5260(5) Å	α= 90°.
	b = 26.7620(8) Å	β= 106.238(2)°.
	c = 21.0670(6) Å	γ = 90°.
Volume	10028.2(5) $Å^3$	
Z	8	
Density (calculated)	1.150 Mg/m^3	
Absorption coefficient	0.532 mm^{-1}	
F(000)	3712	
Crystal size	0.38 x 0.25 x 0.22 mm^3	
Theta range for data collection	3.55 to 20.84°.	
Index ranges	-18<=h<=18, -26<=k<=26, -21<=l<=21	
Reflections collected	24659	
Independent reflections	5231 [R(int) = 0.0522]	
Completeness to theta = 20.84°	99.0 %	
Max. and min. transmission	0.8896 and 0.8254	
Refinement method	Full-matrix least-squares on F^2	
Data / restraints / parameters	5231 / 0 / 536	
Goodness-of-fit on F^2	1.069	
Final R indices [I>2sigma(I)]	R1 = 0.0486, wR2 = 0.1241	
R indices (all data)	R1 = 0.0635, wR2 = 0.1405	
Largest diff. peak and hole	0.577 and -0.405 $e.Å^{-3}$	

Crystal data and structure refinement for **30**.

Identification code	**30**	
Empirical formula	C37 H50 N2 O Zn	
Formula weight	604.16	
Temperature	150(2) K	
Wavelength	0.71073 Å	
Crystal system	Orthorhombic	
Space group	Pbca	
Unit cell dimensions	a = 18.1470(2) Å	α= 90°.
	b = 18.2170(2) Å	β= 90°.
	c = 21.2560(3) Å	γ = 90°.
Volume	7026.89(15) $Å^3$	
Z	8	
Density (calculated)	1.142 Mg/m^3	
Absorption coefficient	0.727 mm^{-1}	
F(000)	2592	
Crystal size	0.25 x 0.17 x 0.10 mm^3	
Theta range for data collection	3.68 to 27.49°.	
Index ranges	-23<=h<=23, -23<=k<=23, -27<=l<=27	
Reflections collected	96875	
Independent reflections	8045 [R(int) = 0.1487]	
Completeness to theta = 27.49°	99.7 %	
Absorption correction	None	
Max. and min. transmission	0.9308 and 0.8391	
Refinement method	Full-matrix least-squares on F^2	
Data / restraints / parameters	8045 / 0 / 385	
Goodness-of-fit on F^2	1.029	
Final R indices [I>2sigma(I)]	R1 = 0.0447, wR2 = 0.0887	
R indices (all data)	R1 = 0.0920, wR2 = 0.1072	
Extinction coefficient	0.0011(2)	
Largest diff. peak and hole	0.417 and -0.399 $e.Å^{-3}$	

Crystal data and structure refinement for **31**.

Identification code	**31**	
Empirical formula	C41 H45 N3 Zn	
Formula weight	645.17	
Temperature	150(2) K	
Wavelength	0.71073 Å	
Crystal system	Monoclinic	
Space group	$P2_1/a$	
Unit cell dimensions	a = 15.17400(10) Å	α= 90°.
	b = 11.47200(10) Å	β= 97.16°.
	c = 20.4770(2) Å	γ = 90°.
Volume	3536.76(5) $Å^3$	
Z	4	
Density (calculated)	1.212 Mg/m^3	
Absorption coefficient	0.726 mm^{-1}	
F(000)	1368	
Crystal size	0.25 x 0.20 x 0.17 mm^3	
Theta range for data collection	3.69 to 27.50°.	
Index ranges	-19<=h<=19, -14<=k<=14, -26<=l<=26	
Reflections collected	58972	
Independent reflections	8089 [R(int) = 0.0566]	
Completeness to theta = 27.50°	99.7 %	
Absorption correction	None	
Max. and min. transmission	0.8835 and 0.8394	
Refinement method	Full-matrix least-squares on F^2	
Data / restraints / parameters	8089 / 0 / 415	
Goodness-of-fit on F^2	1.038	
Final R indices [I>2sigma(I)]	R1 = 0.0384, wR2 = 0.0993	
R indices (all data)	R1 = 0.0493, wR2 = 0.1080	
Extinction coefficient	0.0012(6)	
Largest diff. peak and hole	0.820 and -0.433 $e.Å^{-3}$	